INTERRELATIONS BETWEEN BID AND CYCLOPHILINS IN THE MITOCHONDRIAL APOPTOTIC PATHWAY

A thesis submitted for the degree of

Doctor of Philosophy

By

Kieran Gillick

Department of Biochemistry and Molecular Biology

University College London

ProQuest LLC
789 East Eisenhower Parkway
P.O. Box 1346
Ann Arbor, MI 48106-1346

DECLARATION

I, Kieran Gillick, confirm that the work presented in this thesis is my own. Where information has been derived from other sources, I confirm that this has been indicated in the thesis.

Signed .....

ACKNOWLEDGEMENTS

Many thanks to my supervisor, Professor Martin Crompton, for all his help and advice, both regarding my practical work and during preparation of this thesis. His knowledge and motivation have been invaluable.

Many thanks also to Dr Mina Edwards for all her help with B50 cell culturing.

Thanks also to Michela Capano for her help in the lab and to my mentor, Professor David Saggerson, for his support.

Thanks to Becci Taylor for her help with some of the harder calculus, and elsewhere.

Thanks to the Under Cover Lovers, the UCLU Ultimate Frisbee Club, for keeping me sane through flying plastic.

And finally, thanks to my parents, Jim and Lesley, without whom none of this would have been possible.

ABSTRACT

The BH3-only BCL-2 protein BID is thought, in some cases, to be responsible for the initiation of cytochrome c release from mitochondria during apoptosis. In order to study this process in an *in vitro* system, the rat Bid gene was cloned, recombinant BID purified, and truncated BID (tBID) produced. Additionally, reliable procedures were developed for the isolation of intact mitochondria from a rat neuroblastoma cell line and for assay of cytochrome c release from the isolated mitochondria.

The involvement of the permeability transition (widely regarded as a mechanism for mitochondrial permeabilisation and/or remodelling during cytochrome c release) was investigated. However, using mitochondrially entrapped fluorophores and agents that promote the transition (Ca^{2+}, overexpression of mitochondrial cyclophilin D), BID-induced cytochrome c release was in fact found to be independent of permeability transition. Nevertheless, CSA, a potent inhibitor of cyclophilins and the permeability transition, did inhibit cytochrome c release.

To resolve the action of CSA, a kinetic model of tBID-induced cytochrome c release was formulated from first principles. This considered tBID-induced oligomerisation and auto-oligomerisation of the BAK protein into BAK pores and efflux of cytochrome c via these pores. The model was based on previously published data and the presence of BAK, but not BAX, in the isolated mitochondria. Analysis according to this model indicated that the formation of pores, rather than efflux through pores, was inhibited by CSA. Direct measurements of tBID-induced change in BAK conformation (an essential step in oligomerisation) by trypsin cleavage confirmed that CSA inhibited this step.

As potential targets of CSA, the isolated mitochondria contained both cyclophilin D (mitochondrial matrix) and residual cyclophilin A (a cytosolic enzyme). However neither cyclophilin D (overexpression) nor cyclophilin A (addition of recombinant enzyme) stimulated cytochrome c release. Moreover, DB25, a CSA analogue that inhibits the catalytic activity of both cyclophilins, but does not allow interaction with downstream targets such as calcineurin, was ineffective, and instead had a stimulatory effect on cytochrome c release. It appeared therefore that the cyclophilin-CSA complex may be the inhibitory species. However inhibition was not attributable to calcineurin inhibition, as judged by ^{32}P labelling and the effects of Ca^{2+}. It is concluded that the cyclophilin-CSA complex may inhibit BAK conformational change by a novel mechanism.

Two other novel findings arose in the course of the study, namely a 54 kD proline-rich cyclophilin D binding protein (identified by pull-downs and mass spectrometry) and phosphorylation of a (non-identified) 17 kD protein in cyclophilin D overexpressing mitochondria.

TABLE OF CONTENTS

DECLARATION 2
ACKNOWLEDGEMENTS 3
ABSTRACT 4
TABLE OF CONTENTS 5
LIST OF FIGURES 9
LIST OF TABLES 13
ABBREVIATIONS 14
CHAPTER 1 : BACKGROUND 16
[1.1] OVERVIEW 16
[1.2] APOPTOSIS 16
[1.3] THE PERMEABILITY TRANSITION PORE (PT PORE) 19
[1.4] BCL-2 PROTEINS 22
[1.5] RELATIONSHIPS BETWEEN BCL2 PROTEINS, MITOCHONDRIAL MEMBRANE PROTEINS AND APOPTOSIS 27
[1.6] ROLE OF TBID 29
[1.7] ROLE OF CYCLOPHILINS 31
[1.8] THE ACTIONS OF CSA 33
[1.9] MITOCHONDRIAL FISSION AND FUSION 34
[1.10] PHOSPHORYLATION 35
CHAPTER 2 : MATERIALS AND METHODS 37
[2.1] CHEMICALS 37
[2.2] POLYMERASE CHAIN REACTION (PCR) 37
[2.3] AGAROSE GEL ELECTROPHORESIS 37
[2.4] DNA PURIFICATION FROM AGAROSE GELS 38
[2.5] DNA QUANTITATION 38
[2.6] PLASMID GENERATION 38
[2.7] GENERATION OF BACTERIAL CELL LINES 39
[2.8] GENE CLONING USING THE PPCR-SCRIPT VECTOR 40
[2.9] PREPARATION OF PLASMID DNA FROM BACTERIA 40
[2.10] DNA SEQUENCING 40
[2.11] PREPARATION OF GLYCEROL STOCKS 42
[2.12] FAST PROTEIN LIQUID CHROMATOGRAPHY (FPLC) 42
[2.13] SODIUM DODECYL SULPHATE POLYACRYLAMIDE GEL ELECTROPHORESIS (SDS-PAGE) 42
[2.14] COOMASSIE STAINING 45
[2.15] SILVER STAINING 45
[2.16] WESTERN BLOTTING 46
[2.17] PROTEIN ASSAYS 46
[2.18] GST AFFINITY PRECIPITATION 47

[2.19] PROTEIN SEQUENCING 48
[2.20] ^{32}P LABELLING 48
[2.21] IMMUNOPRECIPITATION USING PROTEIN G-AGAROSE BEADS 49
[2.22] COUPLING ANTIBODY TO CARBOLINK RESIN (PIERCE) 49
[2.23] PULL-DOWN USING CARBOLINK-COUPLED ANTIBODY 49
[2.24] CROSS-LINKING 50
[2.25] ISOLATION OF MITOCHONDRIA FROM RAT LIVER OR HEART 50
[2.26] ISOLATION OF MITOCHONDRIA FROM B50 CELLS 50
[2.27] PREPARATION OF MITOCHONDRIAL AND CELL EXTRACTS 53
[2.28] CALCEIN RELEASE ASSAY 53
[2.29] MEMBRANE POTENTIAL MEASUREMENTS 55
[2.30] MITOCHONDRIAL SWELLING ASSAY 57
[2.31] PROTOCOL FOR ASSAYING BID-INDUCED CYTOCHROME C RELEASE 57
[2.32] PREINCUBATION WITH CYTOCHROME C 57
[2.33] PEPTIDYL- PROLYL- CIS-TRANS ISOMERASE (PPIASE) ASSAY 59
[2.34] MONOAMINE OXIDASE (MAO) ASSAY 60
[2.35] CASPASE ASSAYS 60
[2.36] BAK DIGESTION ASSAY 61
[2.37] PREPARATION OF COVER-SLIPS 61
[2.38] B50 CELL CULTURE 61
[2.39] TRANSIENT TRANSFECTION 61
[2.40] CELL FIXING AND PERMEABILISATION 62
[2.41] CELL STAINING AND IMAGING 62
[2.42] GENERATION OF CYCLOPHILIN D(+) CELL LINE 62
[2.43] EXTRACTION OF TOTAL RNA FROM RAT LIVER 64
[2.44] FIRST-STRAND CDNA SYNTHESIS 64
[2.45] EXPRESSION OF BID 64
[2.46] NICKEL AFFINITY CHROMATOGRAPHY 64
[2.47] REMOVAL OF POLY-HISTIDINE TAG FROM RECOMBINANT BID 65
[2.48] BUFFER EXCHANGE OF BID 65
[2.49] GENERATION OF TBID 65
[2.50] EXPRESSION OF RECOMBINANT CYCLOPHILIN A 65
[2.51] GENERATING EPITOPE-TAGGED CYCLOPHILIN D CONSTRUCTS 66
[2.52] CALCULATING THE FREE CALCIUM CONCENTRATION IN EGTA BUFFERS 72

CHAPTER 3 : CLONING AND EXPRESSION OF BID 74
[3.1] INTRODUCTION 74
[3.2] GENERATION OF EXPRESSION PLASMID 74
[3.3] EXPRESSION 78
[3.4] PURIFICATION 82
[3.5] CHARACTERISATION OF RECOMBINANT BID BY ION EXCHANGE CHROMATOGRAPHY 82

[3.6] CHARACTERISATION OF RECOMBINANT BID BY GEL FILTRATION 82
[3.7] GENERATING MONOMERIC BID 89
[3.8] GENERATION OF TBID 89
[3.9] DISCUSSION 89

CHAPTER 4 : BID-INDUCED CYTOCHROME C RELEASE FROM ISOLATED MITOCHONDRIA – DEVELOPMENT OF A REPRODUCIBLE PROTOCOL 95
[4.1] INTRODUCTION 95
[4.2] DEVELOPMENT OF MITOCHONDRIAL ISOLATION PROCEDURE FOR CELL LINES 95
[4.3] CYTOCHROME C RELEASE ASSAY 99
[4.4] EFFECT OF BID ON MITOCHONDRIA FROM DIFFERENT TISSUES 101
[4.5] EFFECT OF CONCENTRATION OF MITOCHONDRIA ON TBID-INDUCED CYTOCHROME C RELEASE 104
[4.6] BID-INDUCED AIF RELEASE 104
[4.7] EFFECT OF ENERGY STATE ON BID-INDUCED CYTOCHROME C RELEASE 104
[4.8] EFFECT OF EXOGENOUS CYTOCHROME C ON BID-INDUCED CYTOCHROME C RELEASE 110
[4.9] EQUIVALENCE OF COMMERCIAL AND IN-HOUSE GENERATED TBID 110
[4.10] DISCUSSION 110

CHAPTER 5 : ON THE INVOLVEMENT OF THE PERMEABILITY TRANSITION PORE IN BID ACTION 114
[5.1] INTRODUCTION 114
[5.2] EFFECT OF CALCIUM ON TBID ACTION 114
[5.3] CALCEIN RELEASE DURING TBID-INDUCED CYTOCHROME C RELEASE 114
[5.4] THE EFFECT OF CYCLOPHILIN D ON APOPTOSIS AND MITOCHONDRIAL CYTOCHROME C RELEASE 116
[5.5] DISCUSSION 119

CHAPTER 6 : KINETICS OF BID-INDUCED CYTOCHROME C RELEASE 125
[6.1] INTRODUCTION 125
[6.2] TIME-COURSE OF TBID-INDUCED CYTOCHROME C RELEASE 125
[6.3] FITTING THE MODEL TO EXPERIMENTAL DATA 133
[6.4] DISCUSSION 137

CHAPTER 7 : THE EFFECT OF CYCLOSPORIN A ON CYTOCHROME C RELEASE 139
[7.1] INTRODUCTION 139
[7.2] EFFECT OF CSA ON MITOCHONDRIAL RESPIRATION 139
[7.3] THE EFFECT OF CSA ON TBID- INDUCED CYTOCHROME C RELEASE 141
[7.4] ASSAY FOR BAK CONFORMATIONAL CHANGE 146
[7.5] EFFECT OF CYCLOPHILIN A 150
[7.6] DISCUSSION 154

CHAPTER 8 : THE EFFECTS OF DB25 157
[8.1] INTRODUCTION 157
[8.2] THE EFFECTS OF CSA AND DB25 157
[8.3] DISCUSSION 167

CHAPTER 9 : CYCLOPHILIN D INTERACTION PARTNERS 168

[9.1] INTRODUCTION 168
[9.2] PULL-DOWNS FROM CYCLOPHILIN D(+) CELLS 168
[9.3] PRODUCTION OF EPITOPE-TAGGED CYCLOPHILIN D IN B50 CELLS 168
[9.4] FLAG PULL-DOWN FROM TRANSIENTLY TRANSFECTED B50 CELLS 172
[9.5] GST-CYCLOPHILIN D PULL-DOWN FROM B50 CELLS 176
[9.6] GST-CYCLOPHILIN D PULL-DOWN FROM RAT HEART MITOCHONDRIAL MATRIX EXTRACTS 176
[9.7] GST-CYCLOPHILIN D PULL-DOWN FROM RAT HEART SMPS 184
[9.8] DISCUSSION 184

CHAPTER 10 : PHOSPHORYLATION CHANGES IN ISOLATED MITOCHONDRIA 187
[10.1] INTRODUCTION 187
[10.2] ^{32}P LABELLING OF MITOCHONDRIAL PROTEINS 187
[10.3] THE EFFECT OF CSA, DB25, TBID AND CYCLOPHILIN D ON PHOSPHORYLATION LEVELS 187
[10.4] DISCUSSION 189

CHAPTER 11 : DISCUSSION 194
[11.1] OVERVIEW OF THE PROJECT 194
[11.2] THE PATHWAY OF BID- AND TBID- INDUCED CYTOCHROME C RELEASE 195
[11.3] IMPORTANCE OF THE KINETIC MODEL 197
[11.4] THE EXISTENCE OF DISTINCT INTERNAL POOLS OF CYTOCHROME C 197
[11.5] THE EFFECT OF CSA AT THE OUTER MEMBRANE 200
[11.6] THE EFFECT OF DB25 203
[11.7] IDENTIFICATION OF A NOVEL CYCLOPHILIN D INTERACTION PARTNER 205
[11.8] BINDING PARTNERS OF MITOCHONDRIAL CYCLOPHILIN D 206
[11.9] PHOSPHORYLATION OF MITOCHONDRIAL PROTEINS 206

CHAPTER 12 :APPENDIX 209
[12.1] MOLECULAR WEIGHT STANDARDS 209
[12.2] MASS SPECTROMETRY DATA 211
[12.3] DERIVATION OF KINETIC ANALYSIS EQUATIONS 216
[12.4] DERIVATION OF EQUATIONS FOR PPIASE INHIBITION 218

CHAPTER 13 : REFERENCES 220

LIST OF FIGURES

Figure 1 - The intrinsic and extrinsic apoptotic pathways 18
Figure 2 - The BCL-2 protein family. 24
Figure 3 - The pPCR-script cloning strategy (Stratagene). 41
Figure 4 - Gel filtration of protein standards. 43
Figure 5 - Calibration graph deriving from gel filtration of protein standards. 44
Figure 6 - Apparatus for disrupting B50 cells. 51
Figure 7 - Strategy for isolating mitochondria from B50 cells. 52
Figure 8 - Calcein acetoxymethyl ester (Calcein-AM). 54
Figure 9 - The tetra-phenyl phosphonium (TPP^+). 56
Figure 10 - Set-up of TPP^+ electrode 56
Figure 11 - Procedure for assaying BID-induced cytochrome c release. 58
Figure 12 - The pcDNA 3.1 (+) plasmid. 63
Figure 13 - The translation start site of the cyclophilin D gene does not conform to the Kozak consensus sequence. 63
Figure 14 - Cyclophilin A elution profile. 67
Figure 15 - Purification of cyclophilin A. 68
Figure 16 - The cyclophilin D gene was successfully amplified by PCR. 70
Figure 17 - The cyclophilin D constructs were ligated into pcDNA 3.1 (+). 70
Figure 18 - An insert of the expected size can be excised from the plasmid constructs 71
Figure 19 - Multiple sequence alignment of rat, mouse and human BID proteins by the ClustalW tool. 75
Figure 20 - Extraction of rat liver total RNA. 75
Figure 21 - Production of *Bid* first-strand cDNA. 77
Figure 22 - Generation of BID cDNA by PCR. 77
Figure 23 - Excising BID DNA from the pPCR-Script vector. 79
Figure 24 - Ligation of BID DNA into pET-15b. 80
Figure 25 - Expression of recombinant BID. 81
Figure 26 - Time-course of Bid expression. 83
Figure 27 - Purification of BID by nickel affinity chromatography. 84
Figure 28 - Removal of the polyhistidine tag from recombinant BID by digestion with thrombin. 85
Figure 29 - Anion exchange chromatography of thrombin-digest of recombinant BID. 87
Figure 30 - SDS-PAGE analysis of FPLC peaks. 87
Figure 31 - Anion exchange chromatography of thrombin-digest of recombinant BID purified in the presence of 1 mM DTT. 90
Figure 32 - Gel filtration of BID, purified in the presence of 1 mM DTT. 91
Figure 33 – Hydrophobic column chromatography elution profile of BID. 91
Figure 34 - SDS-PAGE analysis of the BID fraction eluted from the phenyl Superose column. 92
Figure 35 - Cleavage of recombinant p22 BID by caspase 8 *in vitro*. 92

Figure 36 - Gel filtration of stored BID protein. 93
Figure 37 - Comparison of cytochrome c levels in six different mitochondrial preparations, made on different days. 100
Figure 38 - Linearity of the assay for cytochrome c in samples taken from cytochrome c release assays. 102
Figure 39 - BID-induced cytochrome c release, using mitochondria isolated from different tissues... 103
Figure 40 - BID- and tBID- induced cytochrome c release from B50 mitochondria. 105
Figure 41 - tBID-induced cytochrome c release from preparations containing different amounts of mitochondrial protein. 106
Figure 42 - Effect of [mitochondria] on BID-induced cytochrome c release. 107
Figure 43 - Comparison of cytochrome c and AIF release induced by full-length BID and by tBID.. 108
Figure 44 - The release of cytochrome c from isolated mitochondria in response to tBID occurs at different [tBID] in respiring and non-respiring mitochondria. 109
Figure 45 - Neither mitochondrial cytochrome c content nor tBID action is affected by preincubation with exogenous cytochrome c. 111
Figure 46 – A commercial tBID preparation has a cytochrome c releasing activity equivalent to that of the tBID preparation used above. 112
Figure 47 - Ca^{2+} does not stimulate BID or tBID -induced cytochrome c release from isolated mitochondria. 115
Figure 48 - Release of matrix-entrapped calcein from mitochondria is induced by Ca^{2+} but not by tBID. 117
Figure 49 - tBID, but not Ca^{2+}, induces cytochrome c release from calcein-loaded mitochondria. 117
Figure 50 - Proposed structure of the PT pore. 118
Figure 51 - Cyclophilin D overexpression in B50 cells carrying the pcDNA 3.1–cyclophilin D plasmid. 118
Figure 52 - Caspase activation is inhibited in cells overexpressing cyclophilin D compared to control B50 cells. 120
Figure 53 - Cyclophilin D overexpression inhibits BID- and tBID- induced cytochrome c release. ... 121
Figure 54 - Cyclophilin D overexpression raises the EC_{50} for cytochrome c release. 122
Figure 55 - Comparison of MAO, ANT and cytochrome c levels in mitochondria isolated from control and cyclophilin D(+) cells. 123
Figure 56 - Time-course of tBID-induced cytochrome c release at seven different tBID concentrations. 126
Figure 57 - Determination of the value of the constant *a*. 128
Figure 58 - Theoretical release of cytochrome c from mitochondria with fully open channels. 129
Figure 59 - Model for release of mitochondrial cytochrome c though BAK channels 131
Figure 60 - Appearance of open BAK channels with time 132
Figure 61 - Determination of the value of the constant *f*. 134
Figure 62 - Comparison of experimental data on tBID-induced cytochrome c release and predicted release data from the model developed above. 135

Figure 63 - Values of *c* for the seven different tBID concentrations, derived by fitting the model to the experimental data points of Figure 56. 136
Figure 64 - The structure of Cyclosporin A (CSA). 140
Figure 65 - Neither CSA nor cyclophilin D overexpression affects mitochondrial inner membrane potential. 142
Figure 66 - CSA inhibits tBID-induced cytochrome c release from isolated mitochondria. 143
Figure 67 - CSA inhibits tBID- but not BID- induced cytochrome c release. 144
Figure 68 - CSA inhibition of tBID-induced cytochrome c release; analyses according to the kinetic model. 145
Figure 69 - Development of a BAK conformation assay : trypsin concentration and incubation time. 147
Figure 70 - Development of a BAK conformation assay : does incubation on ice (during trypsin digestion) stop both BAK conformational change and cytochrome c release? 148
Figure 71 - BAK, but not BAX, associates with the mitochondrial fraction. 148
Figure 72 - Development of a BAK conformation assay : correspondence between BAK conformational change and cytochrome c release. 149
Figure 73 - CSA inhibits tBID-induced conformational change of BAK. 151
Figure 74 - Cyclophilin A is present in mitochondrial preparations. 151
Figure 75 - Physiological cyclophilin A levels have no effect on tBID-induced cytochrome c release. 152
Figure 76 - CSA and a high concentration of cyclophilin A inhibit tBID-induced cytochrome c release to a similar extent, and in a non-additive fashion. 153
Figure 77 - Cyclophilin A does not stimulate BID-induced cytochrome c release. 155
Figure 78 - DB25 (D-MeAla-3-EtVal-4-cyclosporin A) 158
Figure 79 - The effect of DB25 on tBID-induced cytochrome c release is markedly different to that of CSA. 159
Figure 80 - The stimulation of tBID-induced cytochrome c release by DB25 is paralleled by a stimulation of BAK conformational change 160
Figure 81 - Neither CSA nor DB25 cause cytochrome c release from isolated mitochondria during a 1-hr incubation 161
Figure 82 - DB25 inhibits mitochondrial PPIase activity with a lower K_d than CSA. 163
Figure 83 - Both DB25 and CSA inhibit mitochondrial permeability transition induced by Ca^{2+}. 165
Figure 84 - Cyclosporin A and DB25 both adsorb to the surface of plastic tubes. 166
Figure 85 - Cyclophilin D antibody was efficiently conjugated to Carbolink™ beads. 169
Figure 86 - Mitochondrial cyclophilin D was not efficiently pulled down by the anti-cyclophilin D resin. 170
Figure 87 - Expression of epitope-tagged cyclophilin D proteins in B50 cells. 171
Figure 88 - The 3xFLAG-tagged fusion protein was correctly localised to mitochondria following transient transfection of B50 cells. 173
Figure 89 - The cyclophilin D-HA protein oligomerises to form cross-linkable multimers that are stable during SDS-PAGE. 174

Figure 90 - The cyclophilin D-3xFLAG protein oligomerises to form cross-linkable multimers that are stable during SDS-PAGE and are not disrupted in the presence of CSA. 175
Figure 91 - GST-cyclophilin D specifically pulled down two proteins from a B50 cell mitochondrial extract. 177
Figure 92 - GST-cyclophilin D pulled down three proteins from a rat heart mitochondrial extract. ... 178
Figure 93 - Amino acid sequence of the 54 kD cyclophilin D interaction partner, coded for by the uncharacterised rat gene RGD1305387. 180
Figure 94 - Disorder prediction based on the primary structure of the 54 kD protein, as calculated by the DISOPRED algorithm [291]. 182
Figure 95 - Strand slippage during DNA replication can lead to extension of codon repeats with the potential to form stable hairpins. 183
Figure 96 - CSA/DB25-sensitive removal of the 54 kD cyclophilin D interaction partner 185
Figure 97 - GST-cyclophilin D pulls down a 30 kD protein from a mitochondrial membrane extract. 186
Figure 98 - The interaction of GST-cyclophilin D with the VDAC-ANT complex is disrupted by CSA and DB25. 186
Figure 99 - Several mitochondrial proteins are labelled following incubation with $^{32}P_i$. 188
Figure 100 - tBID, CSA and DB25 do not affect the phosphorylation level of mitochondrial proteins. 190
Figure 101 - A 17 kD protein that is not cyclophilin D is phosphorylated in cyclophilin D overexpressing cells. 191
Figure 102 - Prediction of Cyclophilin D phosphorylation sites by the NetPhosII program 192
Figure 103 – Sequestration of mitochondrial cytochrome c stores within cristae. 198
Figure 104 - A change in the kinetics of redistribution of distinct cytochrome c stores is not necessarily reflected by a change in cytochrome c efflux kinetics. 201
Figure 105 - Cyclophilin D interaction partners 207

LIST OF TABLES

Table 1 - EGTA pK_a values for H^+ and Ca^{2+}. 73
Table 2 - Sequence comparison of rat and human BID, compared to vertebrate averages. 86
Table 3 - Gel filtration of BID protein. 88
Table 4 - Flow rates and fluid velocity at the three driving pressures used 97
Table 5 - Effect of driving pressure on the yield and intactness of mitochondria isolated from B50 cells. 97
Table 6 - Effect of passage number on the yield and intactness of mitochondria isolated from B50 cells. 98
Table 7 - Cytochrome c and MAO levels in unbroken cells and a mitochondrial preparation made from these cells. 100
Table 8 - Constants included in the model for tBID-induced cytochrome c release developed above. 134
Table 9 - There exist several Cyclosporin derivatives with differing patterns of interaction with cyclophilins. 158
Table 10 – Apparent K_d values for CSA and DB25 inhibition of recombinant cyclophilin A 166

ABBREVIATIONS

ACN	acetonitrile
AFC	7-amino-4-trifluoromethyl coumarin
AMPK	AMP-activated protein kinase
ANT	adenine nucleotide translocase
b.p.	base pair
BH	BCL-2 homology
BSA	bovine serum albumin
cDNA	complementary DNA
CSA	cyclosporin A
DMEM	Dulbecco's minimal essential medium
DMSO	dimethylsulphoxide
DNase	deoxyribonuclease
DPC	diethylpyrocarbonate
DSS	disuccinimidyl suberate
DTT	DL-dithiothreitol
FCS	foetal calf serum
FKBP	FK506-binding protein
FPLC	fast protein liquid chromatography
GSH	reduced glutathione
IPTG	isopropyl-β-D-thiogalactopyranoside
LC-MS-MS	liquid chromatography tandem mass spectrometry
MAC	mitochondrial apoptosis-induced channel
MAO	monoamine oxidase
MEF	mouse embryonic fibroblast
M_r	relative molecular mass
mRNA	messenger RNA
MST(E)	mannitol sucrose tris (+ EGTA)
NH	NaCl HEPES
OD	optical density
SDS-PAGE	sodium dodecyl sulphate polyacrylamide gel electrophoresis
PBS(-T)	phosphate buffered saline (+ tween-20)
PCR	polymerase chain reaction
PMSF	phenyl methyl sulphonyl fluoride
PPIase	peptidyl- prolyl- *cis-trans* isomerase
PT	permeability transition
RNase	ribonuclease
SDS	sodium dodecyl sulphate

SH-E	sucrose HEPES EGTA
SMP	sub-mitochondrial particle
tBuOOH	tert-butyl peroxide
TEMED	N, N, N', N' – tetramethylethylene-diamine
TMRM	tetramethylrhodamine methyl ester
TNF	tumour necrosis factor
TPP	tetra phenyl phosphonium
TRAIL	tumour necrosis factor-related apoptosis-inducing ligand
VDAC	voltage dependent anion channel
X-gal	5-bromo-4-chloro-3-indoyl-β-D-galactopyranosid

CHAPTER 1 : BACKGROUND

[1.1]Overview

The aim of this project was to investigate the process of cytochrome c release from mitochondria. Cytochrome c release is a key step in the progression of apoptosis, and as such there is considerable interest in the mechanisms by which it occurs, and also in the reasons why it either fails to occur, or occurs in a deregulated manner, in conditions such as neoplasias, ischaemic injury and neurodegenerative disease.

Specifically, this project considered the process of BID-induced release of cytochrome c from isolated mitochondria, and the effects on this process of cyclophilins and cyclosporin A. This introduction will first give some general background on the cellular mechanisms of apoptosis. Following this, some of the specifics of the process relevant to this study will be considered: the nature and role of the permeability transition pore; the role of BCL2 proteins; the structure and function of BID; the role of cyclophilins and cyclosporin A; the role of mitochondrial fission and fusion; and finally the role of protein phosphorylation.

[1.2]Apoptosis

[1.2.1]Definition

Apoptosis, or 'programmed cell death' is the process by which cells are induced, by intrinsic or extrinsic signals, actively to shut themselves down and remove themselves from the body. Apoptosis is an essential process in metazoans, playing a number of important physiological roles, including the removal of redundant cells during development, counterbalancing cell division in tissue homeostasis and the removal of diseased or damaged cells [1].

[1.2.2]Intrinsic and extrinsic pathways

Following its original description by Kerr and co-workers in 1972 [2], intensive research in this field over the last thirty years has defined many of the critical morphological and biochemical features of apoptosis. Two major signalling pathways have been delineated: firstly the extrinsic pathway, activated by ligation of death-domain-containing cell-surface receptors of the tumour necrosis factor receptor superfamily; and secondly the intrinsic pathway, induced by intracellular stimuli such as DNA damage or oxidative stress. The intrinsic pathway is characterised by the release of pro-apoptotic factors from the intermembrane space of mitochondria.

The two pathways converge on the activation of caspases, a family of intracellular proteases that make use of a catalytic cysteine residue to cleave a wide range of substrates after aspartate residues. Caspases exist as inactive zymogens in the cytosol, and upon induction of apoptosis are proteolytically cleaved to form active heterodimeric enzymes [3]. Active caspases can cleave other caspases, resulting in a proteolytic cascade with the executioner caspases-3, -6 and -7 at the distal end. These executioner caspases cleave cellular substrates, resulting in the typical biochemical and morphological hallmarks of apoptosis and ultimately leading to death and phagocytosis of the cell.

There is cross-talk between the two pathways – whilst some extrinsic signals are sufficient to activate the caspase cascade directly, in many cases activation of proximal caspases following death receptor ligation brings the mitochondrial loop into play in order to amplify the apoptotic signal. The intrinsic and extrinsic pathways are shown diagrammatically in Figure 1.

Scaffidi and co-workers [4] have identified two distinct cell types. Type 1 cells (e.g. SKW6.4 and H9 cells) rely exclusively on the extrinsic pathway to initiate apoptosis following death receptor ligation – there is a rapid, high level of caspase 8 processing, leading directly to caspase 3 activation and caspase cascade. In type 2 cells (e.g. Jurkat and CEM) there is very little immediate procaspase 8 processing. The small amount of active caspase 8 is, however, sufficient to initiate the mitochondrial pathway, and this leads to caspase 3 activation via cytochrome c release, thus amplifying the apoptotic signal. Overall there is no difference in susceptibility to apoptosis between the two cell types.

[1.2.3]Role of cytochrome c in the intrinsic pathway

One of the critical mitochondria-derived pro-apoptotic factors is cytochrome c, a 12-kD haem-containing redox carrier protein, normally responsible for transferring electrons between complexes III and IV of the respiratory chain. Upon activation of the mitochondrial (intrinsic) apoptotic pathway, cytochrome *c* is transported across the outer mitochondrial membrane into the cytosol. Once released into the cytosol, cytochrome *c* induces the formation of the apoptosome, consisting of caspase-9, Apaf-1 (apoptotic protease-activating factor-1), dATP or ATP and cytochrome c [5]. The apoptosome is highly active in processing and activating caspase-9 and other initiator caspases, thus propagating the apoptotic response.

[1.2.4]Loss of outer membrane integrity

As part of the intrinsic pathway of apoptosis, a number of proapoptotic factors are released from mitochondria along with cytochrome c [6]. These include AIF (a DNA cleavage factor), endonuclease G (responsible for nuclear DNA fragmentation), pro-caspase 3 (an effector caspase), Omi (a serine protease) and SMAC/DIABLO (a repressor of the IAP caspase inhibitor proteins, thereby potentiating caspase activation). These factors are normally located in the intermembrane space, and so a necessary step in their release is permeabilisation of the outer mitochondrial membrane.

Several competing theories, discussed in more detail below, have been proposed to account for the loss of outer membrane integrity. For example, BCL-2 family proteins may form channels in the outer membrane [7,8]; channels may form from resident mitochondrial proteins [9,10]; channels may form from mis-folded mitochondrial proteins [11]; impairment of ADP/ATP exchange may lead to matrix swelling and outer membrane rupture via an increase in inner membrane potential [12]; lipidic pores may be responsible for membrane permeabilisation [13]; or finally, opening of the permeability transition (PT) pore may lead to osmotic swelling of mitochondria and outer membrane rupture [14] (reviewed in [15]).

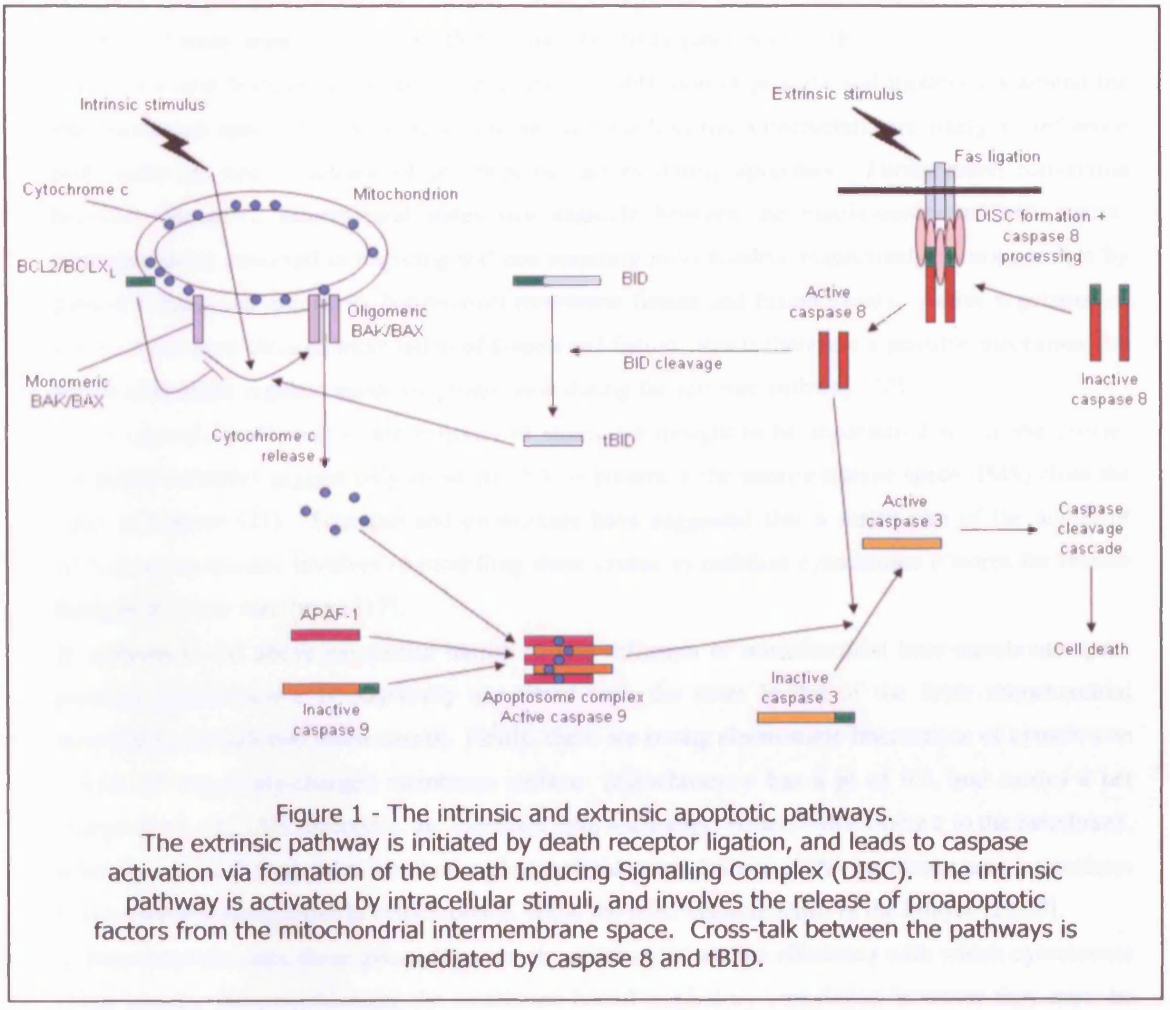

Figure 1 - The intrinsic and extrinsic apoptotic pathways.
The extrinsic pathway is initiated by death receptor ligation, and leads to caspase activation via formation of the Death Inducing Signalling Complex (DISC). The intrinsic pathway is activated by intracellular stimuli, and involves the release of proapoptotic factors from the mitochondrial intermembrane space. Cross-talk between the pathways is mediated by caspase 8 and tBID.

[1.2.5]Availability of inter-membrane space proteins for release through the outer membrane

It has been suggested that outer membrane permeabilisation *per se* is not sufficient to release some or all intermembrane space proteins to the cytosol during apoptosis. Electron tomography studies suggest that the traditional textbook view of mitochondrial substructure is incorrect. Rather than being composed of simple baffle-like folds, the inner membrane is distorted into complex tubular regions and extended internal compartments. Under some conditions, these compartments represent highly sequestered areas, separated from the IMS by narrow cristae junctions [17,18].

These structural features are predicted to inhibit free diffusion of proteins and metabolites around the intermembrane space [19], so that alterations in mitochondrial substructure are likely to influence profoundly the rate of release of proapoptotic factors during apoptosis. Furthermore, conversion between alternative substructural states (for example between the matrix-contracted and matrix-expanded states observed in respiring and non-respiring mitochondria, respectively) is not possible by passive folding and unfolding, but requires membrane fission and fusion events. Active regulation of substructural state through modulation of fission and fusion rates is therefore a possible mechanism by which cells might regulate apoptotic progression during the intrinsic pathway [20].

In the case of cytochrome *c*, the majority of stores are thought to be sequestered within the cristae; functional estimates suggest only about 10-15 % is present in the intermembrane space (IMS) close the outer membrane [21]. Scorrano and co-workers have suggested that a major part of the action of BCL-2 pro-apoptotics involves re-modelling these cristae to mobilise cytochrome c stores for release through the outer membrane [17].

In addition to the above-mentioned barrier to free diffusion of mitochondrial inter-membrane space proteins, cytochrome *c* is physically associated with the outer leaflet of the inner mitochondrial membrane, through two mechanisms. Firstly, there are strong electrostatic interactions of cytochrome c with the negatively-charged membrane surface (cytochrome *c* has a pI of 9.3, and carries a net charge of +8 [22,23]). Secondly, an 'extended lipid anchorage' tethers cytochrome c to the membrane, whereby one acyl chain of a membrane phospholipid protrudes out of the membrane and intercalates into a hydrophobic channel in cytochrome c, while the other chain remains in the bilayer [22,23].

In non-apoptotic cells, these associations are thought to increase the efficiency with which cytochrome *c* can transfer electrons between the membrane-bound respiratory complexes; however they must be breached during apoptosis. Ott and co-workers suggested that cytochrome c release during apoptosis proceeds by a two-step process; solubilisation of cytochrome c by breaching of the electrostatic and lipid-based interactions with the inner membrane is a necessary first step prior to release of cytochrome c across the outer membrane [24].

[1.3]The permeability transition pore (PT pore)

[1.3.1]Overview

Calcium- and inorganic phosphate- induced changes in the permeability characteristics of the inner mitochondrial membrane were first observed in the 1960s [25]. In the late 1970s, Haworth and Hunter further characterised this 'permeability transition' as a non-specific increase in membrane permeability,

uncoupling of oxidative phosphorylation and loss of respiratory control, and suggested that it may be due to a transmembrane channel [26]. Poly(ethylene glycol) permeability studies suggested that the mechanism was the induction of a large pore of discrete size, permeable to solutes up to around 1500 Da [27]. This observation was confirmed by direct measurement of the ratios of permeation of ^{14}C-labelled solutes of different sizes, and is consistent with a pore of 2 – 3 nm diameter [28].

[1.3.2]Structure

The minimal structure of the PT pore is generally accepted to comprise the voltage dependent anion channel (VDAC) in the outer membrane, the adenine nucleotide translocase (ANT) in the inner membrane and cyclophilin D in the matrix [29]. However ANT alone may also form the pore under extremely high [Ca^{2+}], as shown in reconstitutions with purified ANT [30]. It is certainly also the case that other proteins may be associated with the minimal pore components under some conditions. Notable among these other proteins are BCL-2, BAX, the peripheral benzodiazepine receptor and a number of kinases including hexokinase and glycerol kinase (reviewed in [31]). It has also been suggested from knockout studies that permeability transition is possible in the absence of ANT [32], and that other mitochondrial proteins may form the pore [11].

[1.3.3]Pore activity

Pore opening is dependent on several factors besides calcium. Magnesium ions were found to inhibit opening, presumably by competition with calcium for a binding site [26]. Pore opening requires the absence of adenine nucleotides and is stimulated by inorganic phosphate; the presence of exogenous adenine nucleotides prevents calcium-induced pore opening in isolated mitochondria [33]. Cellular redox state is also important, the oxidation state of intramitochondrial pyridine nucleotides apparently being a key indicator of this; as long as the pyridine nucleotide pool is maintained in a sufficiently reduced state, pore opening is inhibited. The cross-linking of Cys^{160} and Cys^{257} on the matrix side of ANT is thought to stabilize the 'c' conformation, enhance cyclophilin D binding, antagonise ADP binding, and strongly sensitise the PT pore to Ca^{2+}-induced opening [34,35]. Other pore effectors include the cyclophilin D inhibitors cyclosporin A (CSA) and sanglifehrin A [36], cGMP ([37]; via the action of protein kinase G) and the ANT ligands carboxyatractyloside and bongkrekate [38]. Interestingly, the F_1F_0 ATP synthase inhibitor oligomycin has also been shown to inhibit pore opening under certain conditions [39]. Finally, several ubiquinones have been shown to modulate pore activity [40]. Three classes have been defined, which either stimulate, inhibit or have no effect on the pore. Walter and co-workers suggest that quinines modulate pore activity through binding to a common site on a pore component, rather than through oxidation-reduction reactions [41].

Calcium-induced permeability transition is highly dependent on mitochondrial energy state and substrate utilisation [42]. Thus energisation with FADH-linked succinate results in increased susceptibility to PT pore opening compared to energisation with NADH-linked glutamate plus malate. Blocking of electron flow with inhibitors inhibits permeability transition, and susceptibility can be restored with artificial electron donors. Isenberg and co-workers report that rotenone inhibits the PT pore [43], and Chauvin and co-workers have confirmed this result [44], identifying electron flux through complex I as a key regulator of PT pore activity.

[1.3.4]Physiological and pathological function

Clearly, sustained PT pore opening is likely to be severely detrimental to cell viability, resulting as it does in dissipation of the proton motive force, ATP hydrolysis, loss of mitochondrial metabolites and deregulation of ion homeostasis in the mitochondria. On these grounds it was first proposed that the permeability transition is instrumental in necrotic cell death associated with oxidative stress and cellular calcium overload [45]. It has, however, been suggested that transient PT pore opening might play a useful physiological role, resulting in efflux from the mitochondria of excess metabolites, especially calcium [46]. Additionally, calcium-induced calcium release from mitochondria via transient PT pore opening has been suggested to be involved in intracellular signal propagation via electrical and/or calcium transients [47]. Pore opening does indeed tend to be transient at physiological calcium concentrations, with openings from a few milliseconds to seconds occurring with a frequency dependent on matrix free $[Ca^{2+}]$ [48,49]. Accordingly, mitochondria exposed to low levels of calcium will slowly accumulate sucrose whilst apparently maintaining an intact inner membrane potential as a population, due to transient pore flicker in a small proportion of mitochondria [50]. Nevertheless, it does seem unlikely for the cell to utilise PT pore opening physiologically. The basic function of matrix $[Ca^{2+}]$ regulation is to control the citric acid cycle and ATP production; but modulation of matrix $[Ca^{2+}]$ by pore opening (an event leading to disruption of the proton motive force and loss of mitochondrial metabolites) would disrupt the very process (ATP generation) that the cell is trying to control [50].

ROS induce PT pore opening [45]. Skulachev and co-workers propose a mechanism whereby transient pore opening acts as a protection mechanism following excessive ROS production [51]. In their model, pore opening would reduce ROS production by two mechanisms; firstly stimulation of respiration due to uncoupling would lower cellular $[O_2]$; and secondly dissipation of the membrane potential would ensure maximal oxidation of electron carriers such as coenzyme Q which can otherwise act as one-electron reducers of O_2 leading to ROS production. Following an adequate reduction in ROS levels, the pore would close.

[1.3.5]Involvement of the PT pore in apoptosis

Sustained opening of the PT pore allows free exchange of ions and metabolites across the mitochondrial membrane. *In vitro* at least, this results in osmotic swelling of the mitochondrion, and since the surface area of the convoluted inner membrane is far greater than that of the outer membrane, this rapidly leads to outer membrane rupture [52]. It is possible that this might be the mechanism of apoptotic cytochrome c release in some cases. For example, following transient cardiac ischaemia, in addition to the central core of necrosis, a surrounding region of cells is seen to die by apoptosis. In the necrotic region, PT pore opening on reperfusion has presumably led to uncontrolled metabolite exchange and ATP loss, thus causing cell death. A hypothetical model suggests that in the surrounding apoptotic region, a small amount of transient pore opening (insufficient to dissipate the proton motive force and exhaust ATP supplies) has led to cytochrome c release via outer membrane rupture which, in the presence of a maintained ATP supply, has initiated the cytosolic apoptotic pathway via apoptosome formation [28].

In addition to this involvement in "sub-necrotic" apoptosis, Kroemer has suggested that the PT pore might be involved more generally in apoptosis, being induced by multiple apoptotic stimuli and thus acting as a signal integrator at the level of the mitochondrion, leading to cytochrome c release [14].

[1.3.6]Evidence against permeability transition as the root mechanism of apoptosis

If cytochrome c release via swelling-induced rupture of the outer membrane following opening of the PT pore is a more general mechanism of apoptosis, then membrane potential loss should certainly occur prior to cytochrome c release. However Wigdal and co-workers showed in 2002 that, in mouse cerebellar granule neurons, cytochrome c release is in fact substantially complete prior to membrane potential loss. Furthermore they demonstrated by electron microscopy that mitochondria are not obviously swollen during cytochrome c release [53]. Similarly, von Ahsen and co-workers demonstrated that mitochondrial structure as well as protein import function is maintained even after complete cytochrome c loss induced by recombinant BID or BAX [54], and a number of other reports have placed cytochrome c release upstream of membrane potential loss and/or swelling [55-57]. In some cases, though, it seems that membrane potential loss does occur concurrent with, or prior to, cytochrome c release (e.g. BAX-induced cytochrome c release [56]). Also, Gogvadze and Distelhorst showed recently that small-amplitude swelling, sufficient to release cytochrome c, can leave mitochondria substantially intact and functionally active [58]. In summary, although the occurrence of transient PT pore opening during apoptosis is not ruled out, it seems that sustained opening of the pore and disruption of mitochondrial homeostasis is not a necessary step in the progression of apoptosis in all systems.

Evidence against PT pore involvement in apoptosis also comes from experiments with cyclophilin D knockouts. Nakagawa and co-workers generated knockout mice, and showed that, although mitochondria isolated from these animals were unable to undergo permeability transition, there was no difference in their response to apoptotic stimuli [59]. Baines and co-workers have obtained similar results [60], indicating that permeability transition is not required for apoptotic cell death.

[1.3.7]Organisation of cytochrome c by PT pore components

Several reports have suggested that cytochrome c is organised into localised clusters by PT pore components (e.g. [61]). Vyssokikh and co-workers showed that 10 - 20 % of cytochrome c was associated with contact sites, and that cytochrome c remained attached to VDAC-ANT complexes that were reconstituted in phospholipid vesicles [62].

[1.4]BCL-2 Proteins

[1.4.1]Overview

The key regulators of the mitochondrial steps in the apoptotic pathway are proteins of the BCL-2 family. BCL-2 itself was first described in follicular lymphoma, where the t(14;18) chromosomal translocation fuses the *bcl-2* gene to the immunoglobulin enhancer [63]; consequent over-expression of *bcl-2* protects the B lymphocyte from apoptosis. Subsequently, a total of sixteen BCL-2 family members have been described [15]. These fall into three categories, based on sequence homology

within the four conserved domains found in BCL-2, designated BCL-2 Homology (BH) 1 to BH4. Firstly, BH1-4 proteins such as BCL-2 and BCL-X_L, which share all four conserved domains with BCL-2, act predominantly as death inhibitors. Next, BH1-3 proteins such as BAX and BAK, which share only three domains with BCL-2, promote apoptosis in most cellular contexts. Finally BH3-only proteins such as BID and BIM, which share only the BH3 domain with BCL-2, function invariably as death agonists [64]. Figure 2 shows the domain arrangement in the sixteen BCL-2 family proteins.

[1.4.2]The pro-apoptotic BH1 – 3 domains

The first three BH domains (BH1 – 3) are thought to be involved in homo- and hetero-dimerisation of these proteins. BAX is capable of homo- and hetero- dimerisation with other BCL2 proteins even when the BH1 and BH2 domains are removed, revealing the BH3 domain as the only part of BAX critical for dimerisation [65,66]. BH3-mutants of BAX are inactive in promoting cell death in mammalian and yeast cells [65,66]. On the other hand it is the BH1 and BH2 domains of BCL-2 that are necessary for BAX-BCL-2 interaction [67].

[1.4.3]The BH4 domain

The amphipathic helical BH4 domain is found exclusively in BCL-2 family members displaying anti-apoptotic activity. It has been suggested that the BH4 domain is involved in protein-protein interactions with pro-apoptotic BCL-2 family members, thus neutralising their function.

The BH4 domain can be exchanged between the antiapoptotic proteins BCL-2 and BCL-X_L without loss of function, but residue substitution or deletion of all or part of BCL-2's BH4 domain impairs function [68]. This is despite the fact that the modified protein is still able to bind strongly to proapoptotic family members such as BAK, BIK, BIK, BAD and BIM, suggesting association with death agonists *per se* is not sufficient for cell survival function.

Although the primary function of the BCL-2 proteins is thought to be in regulating the mitochondrial pathways of apoptosis, Rosse and co-workers have shown that cells overexpressing BCL-2 can survive with significant amounts of cytochrome c in the cytoplasm [69], thus demonstrating that BCL-2 can also protect cells from apoptotic death downstream of mitochondrial involvement.

[1.4.4]The rheostat model

One model of apoptosis regulation by the BCL-2 family holds that, under normal circumstances, pro- and anti- apoptotic proteins titrate each other in roughly equal stoichiometry. A cell can set itself to a strongly 'pro-survival' state by up-regulating the amount of anti-apoptotic protein, so that a large increase in anti-apoptotic protein levels is required to tip the balance towards cell death. Conversely, a cell can render itself more sensitive to apoptosis by adjusting the balance closer to parity, so that only a small increase in pro-apoptotic protein level will lead to an excess of pro-apoptotic proteins and cell death [70].

By generating small-molecule inhibitors of BH3-domain interaction between BCL-2 family members, Degterev and co-workers confirmed that one of the key functions of anti-apoptotic BCL-2 proteins is to bind and sequester pro-apoptotic proteins, thus neutralising their activity [71].

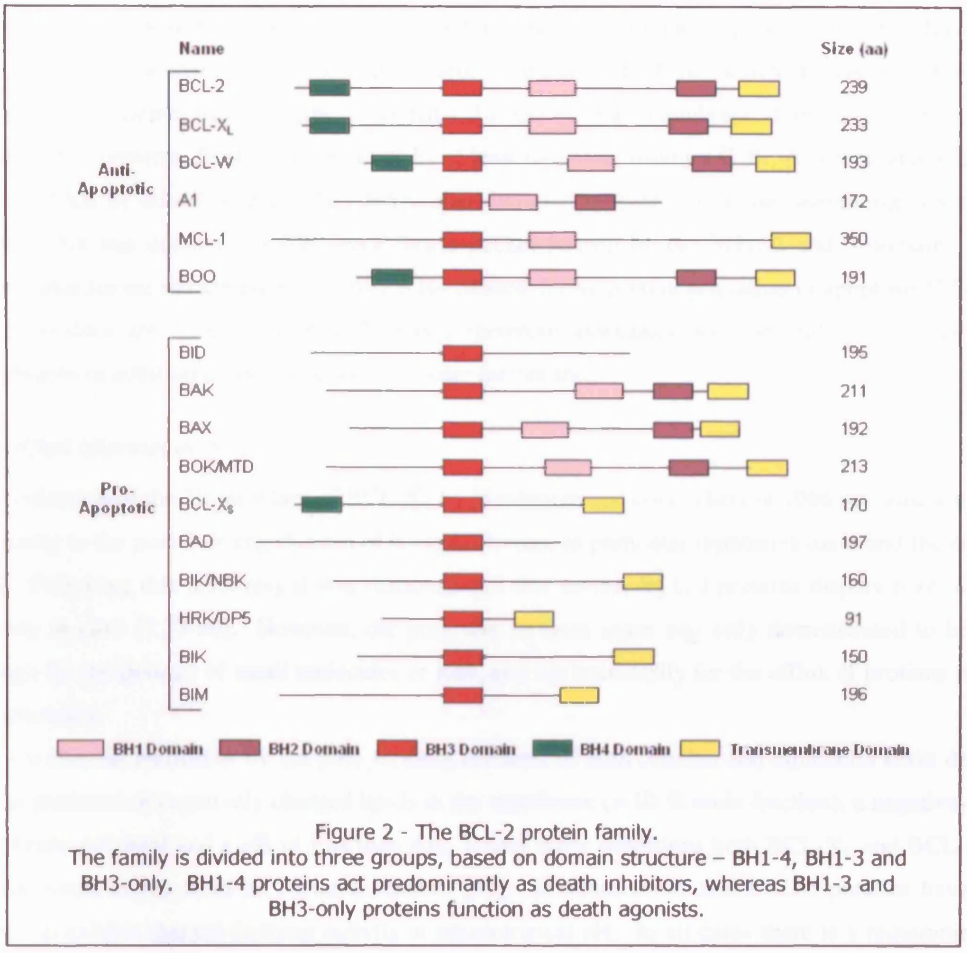

Figure 2 - The BCL-2 protein family.
The family is divided into three groups, based on domain structure – BH1-4, BH1-3 and BH3-only. BH1-4 proteins act predominantly as death inhibitors, whereas BH1-3 and BH3-only proteins function as death agonists.

This fits well with the observation that cell types which are inherently more sensitive to death by apoptosis tend to show a higher ratio of pro- to anti- apoptotic BCL-2 proteins than those which tend to be more resistant; for example non-progenitor cells in the adult mouse show a higher BAX / BCL-2 ratio than embryonic cells [72].

[1.4.5]Membrane association

The majority of BCL-2 family members are membrane-associated, either constitutively or following activation. Several of the proteins carry a trans-membrane domain (see Figure 2). In 2003, Kaufmann and co-workers described the targeting sequence present in BCL-X_L which directs it to the outer mitochondrial membrane to be the C-terminal 20-residue trans-membrane domain present in many other BCL-2 proteins, flanked at both ends by at least two basic residues [73]. A comparable sequence targets BAK to mitochondria [74]. BAX also carries a similar C-terminal membrane association domain, but this domain is folded back into a pocket formed by the BH1, 2 and 3 domains and is unavailable for membrane binding before it is released during protein activation in apoptosis [75]. The basic residues are lacking in BCL-2, which therefore associates with several other intracellular membranes in addition to the mitochondrial outer membrane.

[1.4.6]Ion channel activity

Determination of the 3D structure of BCL-X_L by Muchmore and co-workers in 1996 revealed a striking similarity to the pore-forming domain of bacterial toxins, in particular diphtheria toxin and the colicins [76]. Following this discovery it was demonstrated that several BCL-2 proteins display pore-forming activity *in vitro* [7,77-80]. However, the pore size in these cases was only demonstrated to be large enough for the passage of small molecules or ions, and not necessarily for the efflux of proteins such as cytochrome c.

In vitro channel formation by the pore forming domains of both colicins and diphtheria toxin depends on the presence of negatively charged lipids in the membrane (> 10 % mole fraction), a negative-inside membrane potential and a pH of less than 4.0. Under these conditions both BCL-X_L and BCL-2 also induce solute efflux from KCl-loaded vesicles [81]. In addition, several BCL-2 proteins have been shown to exhibit channel-forming activity at physiological pH. In all cases there is a requirement for acidic lipids in the membrane.

[1.4.7]A direct BAX / BAK pore

The direct involvement of BCL-2 proteins in outer membrane permeabilisation was first suggested as a result of the observation that pro-apoptotic BAX, BID and BAD translocate to mitochondria early in apoptosis [82]. Antonsson and co-workers showed that BAX is capable of forming BCL-2-inhibitable channels in lipid membranes through which liposome-entrapped carboxyfluorescein can be released [7]. Eskes went on to show that addition of BAX to isolated mitochondria resulted in cytochrome c release that could not be blocked by PT pore inhibitors [83], suggesting an autonomous BAX pore might be responsible for cytochrome c release during apoptosis. More recently, Pavlov and co-workers demonstrated by patch-clamping experiments a mitochondrial apoptosis-induced channel (MAC) of diameter (4 nm) sufficient to allow the passage of cytochrome c, whose existence correlated

with the presence of BAX in the outer membrane [84]. Guo and co-workers confirmed by electrophysiological methods that cytochrome c was able to interact with the pore [85].

A number of workers have confirmed in cell-free experiments the ability of BAX to form large channels. Kuwana and co-workers showed that tBID could activate monomeric BAX to form large openings in a vesicular membrane, sufficient to release dextran molecules of up to 2000 kDa [86]. Similarly Terrones and co-workers entrapped fluorescein isothiocyanate-labeled dextrans of various sizes in pure lipid vesicles, and showed that tBID and BAX were able to induce the release of molecules of sizes up to around 70 kD [87].

In 2005, Dejean and co-workers showed that MAC activity was blocked by immunodepletion of BAX [88]. They went on to show that MAC was associated with oligomeric rather than monomeric BAX; that MAC channel activity was modified by cytochrome c, consistent with entry of cytochrome c into the pore; that recombinant BAX channels and MAC isolated from apoptotic HeLa cells have similar single-channel electrical behaviour; and that MAC activity is absent in BAX/BAK double-knockout cells (but not in BAX single knockouts). The above results strongly suggest that BAX or BAK are capable of oligomerising to form a large pore in the mitochondrial outer membrane able to release cytochrome c during apoptosis. Several other groups have shown that the presence of either BAX or BAK is essential for mitochondrial apoptosis [89,90]. The specific region of BAX necessary for pore formation has been mapped to alpha helices 4 and 5; neither the transmembrane domain nor the BH3 domain are essential, these regions presumably being involved only in activation and targeting [91].

Chandra and co-workers investigated the effects of knocking out BAX and BAK proteins on apoptosis in HCT116 cells [92]. They observed that BAX and BAK are, to an extent, functionally redundant, although BAX(-) cells are less susceptible to apoptosis than BAK(-) cells (which are only slightly less susceptible than WT cells).

[1.4.8]BH3-only proteins as afferent receptors of apoptosis

The BH3-only family of BCL-2 proteins appear to act as the afferent receptors of apoptosis, integrating pro-apoptotic signals from a diverse range of stimuli and propagating the signal downstream via a single pathway – BAX/BAK-mediated mitochondrial cytochrome c release. Thus BID is activated downstream of the Fas/Fas-L pathway [93]; BAD is negatively regulated by the Akt/PKB survival pathway [94]; and BID, NOXA and PUMA are regulated by p53 [95-98].

[1.4.9]BH3-only proteins as activators of multi-domain proapoptotic proteins

Desagher and co-workers demonstrated a BID-induced conformational change in the pro-apoptotic BAX protein [99]. They suggested that, during apoptosis, BID translocates to mitochondria and activates BAX by this mechanism, this then being followed by cytochrome c release. Korsmeyer and co-workers confirmed this view, showing the induction by tBID of a 22 Å tetrameric BAX pore capable of translocating cytochrome c [8]. Ruffolo and co-workers identified the tBID-induced change to be the induction of an 'open' conformer of BAX or BAK, with the N-terminus exposed. This conformer induces conversion of other 'closed' BAX/BAK molecules to the 'open' conformation, thus initiating a cascade of BAX/BAK auto-activation into 'open' molecules capable of oligomerising to form the pore [100]. In this model, the primary role of anti-apoptotic BCL-2 proteins is to bind the

'open' BAX/BAK conformer, thus inhibiting the activation cascade, rather than inhibiting BH3-only action directly.

This 'BAX/BAK pore' model is supported by experiments with knock-out animals, in which it was shown that BID is incapable of inducing cytochrome c release in the absence of BAX or BAK [8,89,90,101,102]. There have, however, been some reports suggesting that tBID alone is capable of forming a pore for cytochrome c efflux [103].

[1.4.10]Release of sequestered multi-domain proapoptotic proteins by BH3-only proteins

Several other BH3-only proteins, however, are unable directly to activate multi-domain proapoptotic proteins to induce mitochondrial damage [104,105]. Moreau and co-workers have suggested a model wherein the primary function of the BH3-only family is to antagonise the anti-apoptotic effect of the BH1-4 proteins. These BH1-4 proteins are suggested constitutively to bind BH1-3 proteins, neutralising their function. BH3-only proteins compete for the same binding site on the BH1-4 proteins, thus releasing the proapoptotic factors [106]. Using a BAX-dependent membrane permeabilisation assay, Kuwana and co-workers showed that several peptides derived from the BH3 domain of BH3-only proteins relieved BAX inhibition caused by BCL-X_L or Mcl-1 [107]. This 'de-repression' function was accompanied by the ability of some peptides (derived from BID and BIM) to activate BAX directly [1.4.9].

[1.5]Relationships between BCL2 proteins, mitochondrial membrane proteins and apoptosis

[1.5.1]VDAC

Shimizu and co-workers showed in 1999 that cytochrome c release from mitochondria induced by BAX or BAK was completely inhibited in mitochondria isolated from a VDAC-1 deficient yeast strain [9]. They went on to show BAX/BAK-dependent, BCL-X_L-inhibitable release of cytochrome c from VDAC-1-containing liposomes, and hence suggested that VDAC itself was the cytochrome c release channel. Similarly, Sugiyama and co-workers demonstrated BIM-VDAC interaction and a BIM-dependent enhancement of VDAC activity, and showed VDAC-dependent apoptosis induced by BIM [108]. Capano and co-workers have demonstrated a BAX-VDAC interaction using a GFP-BAX pull-down assay [109]. Shimizu and co-workers have also observed that BAX interacts with VDAC, and that BAX-induced apoptosis is inhibited when this interaction is prevented by blocking antibodies [110]. However they observe no effect of these antibodies on BID-induced cell death or BID-induced cytochrome c release form isolated mitochondria. These findings have been challenged by Rostovtseva *et al*, who were unable to detect any interaction between BAX and VDAC. In contrast, these authors observed tBID-dependent *closure* of the VDAC channel, and suggested that disruption of mitochondrial metabolite exchange by this mechanism might lead to mitochondrial dysfunction and apoptosis [111]. Shimizu and co-workers were unable to detect any interaction between BID and VDAC, nor any effect of BID on liposome-incorporated VDAC [56].

Cheng and co-workers have identified a difference in role between the two VDAC isoforms present in mammals. VDAC-2-deficient cells were shown to be more susceptible to apoptotic death, and

VDAC-2 overexpression inhibited the mitochondrial apoptotic pathway [112]. The effect is suggested to be mediated by VDAC-2 sequestration of BAK in an inactive conformation, preventing activation. BH3-only molecules such as tBID, BIM and BAD were shown to displace VDAC2 from BAK, leading to homo- and hetero- oligomerisation of BAK and apoptosis. Loss of the more abundant VDAC-1 had no effect on apoptosis.

[1.5.2]ANT

ANT exists as two isoforms in the inner membrane. Peripheral inner membrane contains both isoforms, whereas the cristae membrane contains only ANT-2 [113]. ANT-1 has a higher affinity for cyclophilin D, consistent with the location of PT pore complexes exclusively in the peripheral inner membrane. Bauer and co-workers showed that overexpression of the ANT-1 isoform led cells to die by apoptosis [114]. The authors went on to show, by mutagenesis, that ADP/ATP transport activity was not necessary for this effect. Machida and co-workers showed in 2002 that the ANT inhibitor MT-21 was able to induce magnesium-dependent cytochrome c release and apoptosis without causing mitochondrial swelling, suggesting that ANT can modulate apoptotic progression other than via its role in the PT pore [115].

[1.5.3]The relation between BAX and the PT pore

BAX is normally cytosolic [75]. De Giorgi and co-workers have suggested that the signal for BAX translocation to the mitochondrial outer membrane is provided by the PT pore. This group loaded mitochondria in whole cells with tetramethylrhodamine methyl ester (TMRM), and used fluorescence imaging both to measure membrane potential and to induce transient PT pore opening via free radical release from excited TMRM. They observed that this PT pore "flicker" did not affect mitochondrial volume or morphology, but instead appeared to signal the redistribution of BAX and the formation of BAX multimers, thus leading to cytochrome c release [116]. However they were unable to show that this BAX redistribution was not simply a secondary effect resulting from disruption of mitochondrial ATP production following membrane potential dissipation. This would be expected to raise the cellular AMP/ATP ratio and thus activate AMP-activated protein kinase (AMPK) (reviewed in [117]). As shown by Capano and Crompton [118], AMPK activation leads to BAX translocation, via a pathway involving p38 MAP kinase.

In contrast to the work of De Giorgi, Narita and co-workers have shown BAX- or BAK- dependent PT pore activation, dependent on interaction with VDAC, that was inhibited by BCL-X_L or BCL-2 [119]. Also Pastorino and co-workers have demonstrated either transient or sustained PT pore opening induced by different concentrations of BAX (125 – 1000 nM) [120]. Pastorino and co-workers have generated a stably transfected Jurkat T-cell line, in which *bax* expression was inducible by muristerone A [121]. They showed that cell death following induction of *bax* expression was inhibited by a combination of CSA and aristocholic acid (ArA) but not by caspase inhibitors, and concluded that BAX causes cell death via the PT pore.

Wieckowski and co-workers reconstituted an *in vitro* system for BAX-induced membrane permeabilisation of liposomes or outer membrane vesicles, and showed that the presence of the PT pore complex was a prerequisite for cytochrome c release in both these systems [122]. Notably, however,

they were only able to demonstrate release of a small proportion of entrapped cytochrome c under all conditions, and could not show release of another entrapped protein (adenylate kinase), questioning the relevance of their model *in vivo*.

[1.5.4]Induction of the PT pore by BID

Zamzami and co-workers developed a system to study induction of membrane permeabilisation by BID and tBID, both in intact cells and in a cell-free system. They showed that BID-induced permeabilisation of the mitochondrial outer membrane could be inhibited by three inhibitors of the PT pore, namely CSA, N-methyl-4-Val-CSA and bongkrekic acid. Furthermore they showed that tBID was able to permeabilise ANT-containing lipid bilayers, and went on to suggest that tBID exerts its action at least in part by functional interaction with the PT pore via ANT [123].

[1.6]Role of tBID

[1.6.1]Structure

BID was first identified as a death agonist by Wang and co-workers in 1996 [124]. Despite having limited sequence homology with other BCL-2 proteins (other than within the BH3 domain) BID shares the same overall fold [125], containing eight alpha-helices, with two central hydrophobic helices surrounded by six amphipathic ones. As mentioned above, this fold resembles that of pore-forming bacterial toxins.

[1.6.2]Expression and location

BID is one of the most widely expressed BH3-only proteins [126], being strongly expressed throughout development and also in a range of mature tissues. Immunohistochemistry revealed especially strong BID staining in short-lived and/or apoptosis-sensitive tissues such as neurons, germinal centre B cells and peripheral blood granulocytes [127], and BID is also present in brain, spleen and liver [124,128]. BID expression is found to be altered in several types of cancer (e.g. [129]).

Having no membrane targeting domain, BID is a predominantly cytosolic protein [124]. However BID does associate to some extent with intracellular membranes, depending on lipid composition, bilayer curvature and osmotic pressure [126]. Upon activation during apoptosis BID translocates to the mitochondrial outer membrane [82,99,130-132].

[1.6.3]Activation

Like other proapoptotic BCL-2 proteins, BID is normally present in the cytosol in an inactive state. In 1998 Luo and co-workers published a seminal paper revealing BID cleavage by caspase 8, generating the active fragment tBID, to be the critical step in propagation of the apoptotic signal from cell surface death receptors to the mitochondrial outer membrane [93]. The full length protein (197 residues; 20 kD) is cleaved at aspartate 59, after a consensus caspase cleavage site ^{56}LQTD^{59}. Cleavage exposes an N-terminal glycine residue, which is post-translationally N-myristoylated, presumably to enhance membrane targeting [133]. The C- and N- terminal fragments are thought to remain associated following cleavage [125,134]. BID cleavage is regulated by phosphorylation by casein kinases I and II,

with the phosphorylated form being insensitive to cleavage [135]. Cleavage significantly changes the surface charge and hydrophobicity of BID, aiding the change in subcellular localisation [136].

Slee and co-workers have identified an additional pathway of BID activation, wherein BID is cleaved by caspase 3 down-stream of cytochrome c release, in a BCL2-inhibitable manner [137]. This pathway represents a feedback loop for the amplification of mitochondrial cytochrome c release induced by some stimuli; i.e. a small amount of caspase 3 activation can lead to BID activation and therefore to substantial release of cytochrome c.

Finally, Valentijn and co-workers [138] have identified an alternative pathway of BID action, active in anoikis, in which BID cleavage does not occur. In this case full-length BID translocates to mitochondria, and appears able to induce cytochrome c release without association with BAX or BAK.

[1.6.4]Targeting and the mechanism of membrane association

BID is thought to localise to specific regions of the outer mitochondrial membrane. Lutter and co-workers showed by immunogold labelling and electron microscope tomography that tBID localises to contact sites between the inner and outer membrane [139]. Kim and co-workers however showed that a small proportion of tBID can also bind to other sites on the outer membrane [140]. These authors went on to show by mass spectrometry that tBID interacts with cardiolipin in a process requiring alpha helices 4–6, but not the BH3 domain. Additionally, by demonstrating inhibition of apoptosis by 10-N-nonyl acridine orange (a cardiolipin-specific dye that prevents tBID-cardiolipin interaction) they suggested that tBID-cardiolipin interactions are essential for apoptosis. Hu and co-workers recently identified helix 6 as necessary, though not sufficient, for mitochondrial targeting, and subsequently identified a 33-residue stretch spanning helices 6 and 7 as the minimum domain sufficient for binding [141]. Liu and co-workers have confirmed the interaction of tBID with cardiolipin (or monolysocardiolipin), and go on to suggest that this association is the driving force for dissociation of the inhibitory N-terminal fragment from tBID following cleavage [142].

Based on studies of tBID-induced pore formation in liposomes, Yan and co-workers proposed that, on reaching the mitochondrial outer membrane, tBID inserts deep into the hydrophobic core of the membrane [143]. This view has recently been challenged by Gong and co-workers, who performed NMR studies on membrane-associated tBID [144]. These authors showed that association with lipid membranes induces a unique conformation of tBID, in which its helices are parallel with the membrane surface, with no trans-membrane helix insertion. Electron paramagnetic resonance (EPR) spectrometry confirmed that tBID binds to the bilayer without adopting a trans-membrane orientation [145].

[1.6.5]Lipid transfer

BID has homology to plant lipid transfer proteins [146], and lipid transfer activity of BID has been reported [131]. Goonesinghe and co-workers have shown that full-length BID has the ability to insert selected lysolipids into the membrane bilayer [147]. The authors suggest this as the mechanism of action of full-length BID (as opposed to cleaved, activated tBID); insertion of these lipids into the mitochondrial outer membrane would 'prime' the membrane for insertion of other pro-apoptotic proteins (including tBID), and for channel formation.

[1.6.6]Cytochrome c redistribution

Scorrano and co-workers suggested in 2002 that tBID was responsible for inducing a striking remodelling of mitochondrial sub-structure, so that cytochrome c stored in mitochondrial cristae was redistributed to the peripheral inter-membrane space, thus being primed for release across the outer membrane [17]. The authors estimated that approximately 85 % of cytochrome c stores are normally unavailable for rapid release as a consequence of their intra-mitochondrial location. They also propose the tBID-induced redistribution to be independent of BAK but inhibited by CSA, thereby implicating the PT pore in this process.

[1.7]Role of cyclophilins

[1.7.1]Introduction

The cyclophilins are a family of peptidyl- prolyl- cis-trans isomerases (PPIases), present in several cellular compartments. The first member was identified in 1984 as a binding target of the immunosuppressive fungal peptide cyclosporin A (CSA) [148]. Cyclophilins were subsequently discovered to catalyse the cis-trans isomerisation of peptidyl-prolyl bonds and were named PPI-ases [149]. The family comprises more than eight members in humans [150], including cyclophilin A (a cytosolic protein, and the most abundant isoform); cyclophilins B and C (located in the ER); cyclophilin D (mitochondrial); and cyclophilin-40 (a larger cytosolic isoform, of 40 kD, in contrast to cyclophilins A - D which are 18-20 kD).

As proline isomerases, cyclophilins have a role in protein folding, catalysing the conversion of nascent-chain proline amide bonds to their native state. Recently, a number of other functions have been revealed, including regulation of the permeability transition pore; regulation of T-cell function and inflammation; pathogenesis of vascular disease and rheumatoid arthritis; and human immunodeficiency virus infection (reviewed in [151]).

[1.7.2]The role of cyclophilin D in the PT pore

Cyclophilin D is known to be a core component of the PT pore [1.3.2]. Based on the observation that CSA blocks pore activity at concentrations similar to those needed to inhibit PPIase activity, it has been suggested that PPIase activity is a necessary step in pore opening [152,153]. However, the binding of cyclophilin D to ANT is not disrupted by CSA, at least when the two proteins are already associated [29], and diethylpyrocarbonate (DPC; another inhibitor of PPIase activity) does not inhibit pore opening [154]. These results suggest that the activity of cyclophilin D towards the PT pore might be mediated other than by its PPIase activity.

[1.7.3]The role of cyclophilin D in cell death

Lin and Lechleiter showed that cyclophilin D overexpression protects cells from tert-butyl peroxide- (t-BuOOH-) and staurosporine- induced membrane potential collapse, and in fact that the resting membrane potential was higher in these cells [155]. The authors went on to show, by mutagenesis experiments, that the PPIase activity of cyclophilin D was required for these effects, although the active site mutants were still capable of binding to ANT. Similarly, Schubert and Grimm showed that

cyclophilin D was able to specifically repress ANT-1-induced apoptosis, and also that cyclophilin D was upregulated in a number of human tumours, suggesting that inhibition of apoptosis by cyclophilin D is a relevant mechanism *in vivo* [156]. In contrast to the work of Lin and Lechleiter, however, these authors suggest that cyclophilin D's antiapoptotic activity is independent of its catalytic activity. Recently, Li and co-workers showed that cyclophilin D overexpression strongly stimulated PT pore opening; this resulted in inhibition of apoptosis, but enhanced necrosis, indicating that permeability transition is a necrotic, but not an apoptotic mechanism [157].

Nakagawa and co-workers generated cyclophilin D knock-out mice, and investigated the response of cells and mitochondria to various apoptotic and necrotic insults [59]. The authors observed no difference in response to apoptotic stimuli, but found protection from necrotic death induced by reactive oxygen species and calcium overload. Cyclophilin D(-) mitochondria were also unable to undergo permeability transition. Similarly, Baines and co-workers showed that cyclophilin D(-) mitochondria are resistant to swelling and permeability transition *in vitro*, and also that cyclophilin $D^{-/-}$ cells are largely resistant to calcium overload and oxidative-stress-induced necrotic cell death [60]. In agreement with the work of Nakagawa and co-workers they also observed no difference in response to apoptosis induced by staurosporine or TNFα.

Finally, Schinzel and co-workers have also investigated the role of cyclophilin D in apoptotic cell death by generating cyclophilin D knockout mice and inducing apoptosis using a number of different stimuli [158]. These authors observed no difference in mouse embryonic fibroblast (MEF) apoptosis in response to etoposide (a topoisomerase II inhibitor) or staurosporine (a broad-spectrum kinase inhibitor), both of which induce the intrinsic mitochondrial pathway of caspase activation. Similarly, there was no difference in response following treatment with thapsigargin (which inhibits the Ca^{2+} ATP pump), tunicamycin (which inhibits N-linked glycosylation), or brefeldin A (which inhibits ER-Golgi transport), all of which induce apoptosis via an ER stress response resulting from accumulation of mis-folded proteins. Cyclophilin D-deficient MEFs were also equally susceptible to death receptor-induced apoptosis (TNF or TRAIL). However, cyclophilin D-deficient MEFs were found to be significantly less susceptible to apoptosis induced by H_2O_2, specifically implicating cyclophilin D in the apoptotic signalling pathway induced by oxidative stress.

[1.7.4]The role of proline isomerisation in 'switching'

Isomerisation of proline residues has been proposed as a regulatory mechanism in some proteins. Pappenberger and co-workers have shown that prolyl isomerases are able to efficiently catalyse native-state isomerisation reactions, in some cases at least [159]. O'Neal and co-workers suggested in 1996 that an immunophilin such as FK506-binding protein (FKBP) might regulate the activity of the prolactin receptor by proline isomerisation [160]. Johnson and co-workers observe that a proline residue plays a crucial role in a conformational change in diphtheria toxin, leading to membrane insertion [161]. Similarly, Schinzel and co-workers have identified a proline residue in an unstructured loop of BAX to be critical for apoptotic activity [75]. The authors suggest that this residue somehow regulates release of the C-terminal trans-membrane domain from an internal binding pocket, allowing translocation of BAX to the mitochondrial outer membrane and subsequent cytochrome c release.

[1.8]The actions of CSA

[1.8.1]Inhibition of cyclophilins

Cyclosporin A was first isolated as a metabolite of the prokaryote *Tolypocladium inflaturns* [162], initially as an immunosuppressive agent. CSA was subsequently found strongly to inhibit the PPIase activity of cyclophilins; the K_d varies depending on cyclophilin isoform, from around 2 nM for cyclophilin B up to approximately 300 nM for cyclophilin 40 [163,164]. Through its inhibition of mitochondrial cyclophilin D, CSA inhibits opening of the PT pore induced by a number of stimuli ([165]; although pore opening induced by certain stimuli is CSA- and cyclophilin- insensitive [154]). The mechanism of PT pore inhibition is unclear, but may involve CSA-induced dissociation of cyclophilin D from the pore complex [152]. Some workers have shown the cyclophilin D-ANT interaction to be disrupted by CSA [36,166]; however some have found that this interaction is preserved even in the presence of CSA [29]. The difference may be due to the order of binding, with CSA able to prevent association with ANT when pre-incubated with cyclophilin D, but unable to disrupt an existing interaction.

[1.8.2]Effects on other cellular targets

CSA has been shown to have other intracellular effects, in addition to its inhibition of cyclophilins. For example, CSA induces up-regulation of the vasopressin type 1A receptor, apparently via stimulation of superoxide production [167]. CSA inhibits transport activity and surface expression of the Na^+-Ca^{2+} exchanger NCX1, albeit at rather high doses (2 –20 μM) [168]. CSA also modulates activity of the multi-drug transporter P-glycoprotein [168].

CSA has a number of effects on cellular calcium homeostasis. In addition to its effects on the PT pore, CSA is reported to inhibit the calcium uniporter [169] and also to stimulate activity of the sarco-endoplasmic reticulum Ca^{2+}-ATPase (SERCA) [170].

The effects of CSA on respiration are unclear. On the one hand, CSA has been shown to induce a hyper-metabolic state in hepatocytes [171]; the effect is proposed to be due to stimulation of prostaglandin E2 production by Kupffer cells. However, Hokanson and co-workers have demonstrated inhibition of respiration by CSA in skeletal muscle cells [172].

Interestingly, CSA can inhibit sterol processing in mitochondria (e.g. 27-hydroxylation of cholesterol [173,174], and 25-hydroxylation of vitamin D3 [175]). The effect has been found to be mediated via non-competitive inhibition of the mitochondrial 27-hydroxylase (cytochrome $P\text{-}450_{27}$) [174,175], perhaps due to inhibition of substrate binding. On the other hand, CSA activates sterol regulator element binding protein-2 (SREBP-2) via increased messenger RNA (mRNA) levels, leading to an increase in cholesterol biosynthesis and VLDL triglyceride production [176].

CSA is also reported to inhibit membrane fusion events [177], through an effect on the bilayer-to hexagonal phase transition propensity of membrane lipids.

[1.8.3]Gain-of-function effects of CSA

CSA is able to mediate gain-of-function effects via its interaction with cytosolic cyclophilin A [178]. Cyclophilin A is normally unable to interact with the protein phosphatase calcineurin, but, when bound

to CSA, the cyclophilin A-CSA complex can bind and inhibit calcineurin. This is the mechanism by which CSA exerts its medically important immunosuppressive effects; calcineurin inhibition blocks activation of the NFAT, JNK and p38 signalling pathways, inhibiting T-cell activation.

[1.8.4]Effects on cell death

The effects of CSA on cell death, and on apoptosis in particular are widely reported (reviewed in [164]). CSA is able to protect cells against necrotic and apoptotic death induced via PT-dependent mechanisms, but the specific effect of CSA on apoptotic mitochondrial cytochrome c release is unclear. Although BID- or BIK- induced cytochrome c release from isolated mitochondria is CSA-insensitive in some systems [56], other groups have shown inhibition by CSA of BAX- and/or BAK-induced cytochrome c release [119,121,179], and Scorrano and co-workers [17] have shown inhibition of the analogous process induced by tBID.

[1.9]Mitochondrial fission and fusion

[1.9.1]Mechanism and significance

The first 'mito-fusion' to be identified was the fuzzy onions (fzo) gene in *Drosophila*. fzo encodes a large predicted membrane GTPase that was shown to be responsible for mitochondrial fusion during spermatogenesis [180]. Subsequently Hermann and co-workers demonstrated the yeast homologue, Fzo1p, to be a mitochondrial integral membrane protein, making contacts with both membranes, that was responsible for mitochondrial fusion events [181]. Sesaki and co-workers have shown Ugo1p to be another yeast protein, also with homology to fzo, which mediates mitochondrial fusion events [182]. Additionally, Mgm1p, a self-assembling GTPase, present in the inter-membrane space, is proposed to coordinate fusion of the inner and outer membranes, through interactions with both membranes as well as with Fzo1p and Ugo1p [183]. Two proteins, Mfn1 and Mfn2 have been shown to mediate mitochondrial fusion events in mammals [184].

In yeast, Dnm1p and Mgm1p have been identified as fission factors [185], and Smirnova and co-workers have identified the protein Drp1 as a human homologue [186]. These proteins have homology to dynamin, the prototypic membrane fusion protein, known to catalyse GTP-dependent membrane 'budding' and fission events, through a self-assembly mechanism [187-189].

Dynamic fission and fusion appears to be important for mitochondrial function. Thus $Mfn1^{-/-}$ or $Mfn2^{-/-}$ embryonic fibroblasts display fragmented mitochondria that are unable to maintain membrane potential, and these embryos die in mid-gestation [184]. However, by observing the frequency of transcomplementation of two defective mitochondrial genes to be extremely low, Enriquez and co-workers have suggested mitochondrial fusion events to be very rare in most cell types [190].

[1.9.2]Relation to apoptosis

Mitochondrial fragmentation is frequently observed in apoptosis [191,192]. Frank and co-workers have shown that the Drp1 translocates to mitochondria during apoptosis, where it localises to potential sites of organelle division and catalyses this process [191]. These authors also show that inhibition of Drp1 blocks cell death by apoptosis. Breckenridge and co-workers report that caspase 8 activation

leads to cleavage of the integral ER membrane protein BAP31 [193]. One of the cleavage products (p20) induces recruitment of Drp1 to mitochondria, leading to fission of the mitochondrial network, and a strong sensitisation to cytochrome c release. Intriguingly, BAX appears to translocate to sites on mitochondrial that subsequently become scission sites during apoptosis [194]. BAX is associated with Drp1 and Mfn2 at these foci. Karbowski and co-workers have shown that the block of mitochondrial fusion observed during apoptosis occurs within the same timeframe as BAX translocation to mitochondria and membrane permeabilisation, and have suggested the block might be a result of BAX activation [192].

The link between mitochondrial fission and susceptibility to cytochrome c release is unclear. Alterations in membrane lipid composition are likely to be involved in membrane fusion events [195], and these changes may promote binding of proapoptptic proteins, or facilitate pore formation. Alternatively, fission events may be involved in the mobilisation of cytochrome c stores for efflux [196]. In relation to this, an intriguing link has been suggested between alterations in mitochondrial substructure and the fission/fusion machinery: Mgm1p has been implicated as an up-stream regulator of ATP synthase assembly, which in turn is suggested to regulate cristae morphology and cytochrome c sequestration [197].

[1.9.3]The link between cyclophilins and mitochondrial fission/fusion

Galigniana and co-workers have shown cytosolic cyclophilin A to associate with dynein via dynamitin, in a PPIase-domain-dependent manner (although PPIase activity is not required for complex formation) [198]. Tchaicheeyan and co-workers have suggested the intriguing possibility that proline isomerisation might be involved in the mechanism of chemo-mechanical coupling in motor proteins [199], perhaps explaining the function of cyclophilin A association with motor protein complexes. Since mitochondrial fission and fusion events depend on homologous motor proteins, it is possible that cyclophilin D might be involved in these processes.

[1.10]Phosphorylation

[1.10.1]BCL-2 proteins

The activity of BID is known to be regulated by phosphorylation. Dephosphorylation of a number of sites in an unstructured loop between helices 2 and 3 unmasks the caspase 8 clevage site, allowing processing to form the active tBID [135]. Additionally, dephosphorylation is reported to enhance BID binding to PACS-2, resulting in transloaction to mitochondria [200].

BAD is also regulated by phosphorylation; dephosphorylation by calcineurin activates BAD [201,202]. Interestingly, these authors also report that rotenone is able to induce BAD dephosphorylation via the calcineurin pathway.

Finally, recombinant BAX is a substrate for serine/threonine kinases [203]; however the relevance of this process *in vivo* is unknown.

[1.10.2]Mitochondrial proteins

The regulation of various mitochondrial enzymes by phosphorylation is well known - for example, pyruvate dehydrogenase and branched-chain α-oxoacid dehydrogenase [204,205]. Various cAMP-dependent and independent protein kinases have been found in the inner membrane and in the intermembrane space of mitochondria [206-211], and phosphorylation of several membrane-bound proteins (6.5, 18 and 29 kDa), has been shown [209,212,213]. Recently, Azarashvili and co-workers suggested a connection between phosphorylation of subunit c of the F_0F_1 ATPase and the PT pore [214], whereby dephosphorylation was promoted by calcium-induced permeability transition and inhibited by CSA. The authors also raised the possibility that this protein is part of the PT pore. The same group went on to show regulation of phosphorylation of a number of other mitochodrial proteins (3.5, 17 and 23 kD) by calcium levels, possibliy mediated by the PT pore and also by calmodulin [215].

CHAPTER 2 : MATERIALS AND METHODS

[2.1]Chemicals

Unless otherwise stated, all chemicals and reagents were from Sigma-Aldrich United Kingdom, and were reagent-grade.

General DNA Methods

[2.2]Polymerase chain reaction (PCR)

[2.2.1]Primer design

Primers were designed to include the following features: 4 base spacers at the 5' end; restriction sites included as necessary; at least 12 bases complementary to the target sequence; annealing temperature between 60 – 70 °C; annealing temperatures of up-stream and down-stream primers matched to within 5 °C; minimal potential for secondary structure formation; and minimal inter-primer complementarity. Primers were sourced from Sigma-Genosys.

[2.2.2]Enzyme

Pfu DNA polymerase (Stratagene) was used throughout. *Pfu* polymerase has high 5' to 3' DNA polymerase activity as well as a proof-reading 3' to 5' exonuclease activity to improve copying fidelity.

[2.2.3]Reactions

50 µl PCR reactions typically had the following composition : 5 µl of 10X *Pfu* buffer, 1 – 20 ng of DNA template, 35 pmol of upstream primer, 35 pmol of downstream primer, 250 µM each dNTP, 2 mM $MgCl_2$, 2.5 units of *Pfu* polymerase, and dH_2O *q.v.*. *Pfu* buffer contained 200 mM Tris-HCl, pH 8.8, 100 mM $(NH_4)_2SO_4$, 100 mM KCl, 1 % Triton X-100, 1 mg/ml bovine serum albumin (BSA). PCR constituted 35 cycles of denaturing at 96 °C for 45 secs, annealing at 5 °C below the lowest primer melting temperature for 45 secs, and extension at 72 °C for 1 min per kilobase, followed by a final 10 min extension at 72 °C.

[2.3]Agarose gel electrophoresis

Agarose (type V) was dissolved with heating in 40 mM Tris-Cl, 0.12 % (v/v) glacial acetic acid, 1 mM EDTA, pH 8.0 (TAE) to 0.8 – 1.2 %, depending on the size of fragments of interest. The gel was allowed to cool to 50 °C. 2,7,-Diamino-10-ethyl-9-phenyl-phenanthridium bromide (ethidium bromide) was added to 0.5 µg/ml, and the gel was cast in a plastic tray. 6 X loading buffer (0.25 % (w/v) bromophenol blue, 0.25 % (v/v) xylene cyanol FF, 15 % (v/v) Ficol 400) was added to DNA samples, which were then inroduced into the wells. Gels were run at 100 V in TAE in a Horizon 11.14 unit (Gibco) until the dye front reached the end of the gel. Bands were visualised and photographed under UV light using the GeneGenius system (Syngene).

[2.4]DNA purification from agarose gels

DNA was extracted from excised gel slices using the GeneClean II kit (Q-Bio gene) according to the manufacturer's instructions.

[2.5]DNA quantitation

DNA samples were diluted to 1 ml in dH_2O. Absorbance was measured at 260 and 280 nm. The A_{260} value gives DNA concentration by the relationship:

$$[\text{ds DNA}]\ (\text{mg/ml}) = 50 \times A_{260}$$

The value A_{260}/A_{280} gives a measure of DNA purity, with values below 1.8 indicating protein contamination.

[2.6]Plasmid generation

[2.6.1]Double digestion

1 µg of plasmid was added to a 1/3 molar amount of insert, in 100 µl of the appropriate restriction enzyme buffer. Two 10 µl aliquots were removed, and 1 unit of single restriction enzyme added to each tube. 8 units of both enzyme was added to the remainder of the digest mix, and all three tubes were incubated at 37 °C for 2 hr. Enzymes were inactivated by heating to 70 °C for 10 mins, and digestion products were checked by agarose gel electrophoresis [2.3] to confirm complete cleavage by both enzymes. All restriction enzymes and buffers were obtained from New England Biolabs.

[2.6.2]Phenol-chloroform extraction

An equal volume of 1:1 phenol:chloroform was added to the digest mix, vortexed for 1 min and centrifuged in an Eppendorf 3200 bench centrifuge for 2 mins at 13,000 g. The upper layer was removed, and 1/10 volume of 4 M sodium acetate pH 5.2 was added, followed by 3 volumes of 70 % ethanol. The mixture was vortexed for 1 min, left for 1 hr at –20 °C and centrifuged (Eppendorf 3200 bench centrifuge; 13,000 g) for 10 mins at 4 °C. The supernatant was removed, and 3 volumes of 100 % ethanol carefully layered onto the pellet. After 30 mins at –20 °C the mixture was centrifuged for 10 mins at 4 °C, the supernatant removed and the pellet dried for 10 mins at 50 °C.

[2.6.3]Ligation

The DNA pellet was resuspended in 7.5 µl of dH_2O. 1 µl of 10X T4 DNA ligase buffer (New England Biolabs; 330 mM Tris-Acetate, pH 7.8, 660 mM potassium acetate, 100 mM magnesium acetate, 5 mM DL-dithiothreitol (DTT)) was added, along with 0.5 µl 10 mM ATP. 0.5 µl pre-ligate was removed. 1 µl (400 U) T4 DNA ligase (New England Biolabs) was added, and the ligation reaction was allowed to proceed for 15 mins at room temperature. The enzyme was inactivated by heating to 70 °C for 10 mins. 0.5 µl of post-ligate was run alongside the 0.5 µl of pre-ligate on an agarose gel [2.3] to confirm ligation.

[2.7]Generation of bacterial cell lines

[2.7.1]Preparation of competent cells

10 ml of Nutrient Broth (Oxoid; No. 2) was inoculated with a single isolated colony from a freshly made agar plate of the appropriate strain. *E. coli* DH5α was routinely used (genotype F$^-$, ø80d*lacZ*ΔM15, Δ(*lacZYA-argF*)U169, *deoR*, *recA*1, *endA*1, *hsdR*17(rk$^-$, mk$^+$), *phoA*, *supE*44, λ$^-$, *thi*-1, *gyrA*96, *relA*1). The culture was incubated overnight at 37 °C with shaking, and then added to 200 ml of fresh Nutrient Broth. The culture was grown with shaking to an optical density at 600 nm (OD_{600}) of 0.5 – 0.6, and cells were then sedimented by centrifugation for 5 mins at 5000 g. The pellet was gently resuspended in 40 ml of ice-cold 75 mM $CaCl_2$, 15 % (v/v) glycerol, and then re-sedimented for 5 mins at 5000 g in the same rotor. The pellet was gently resuspended in 5 ml of ice-cold 75 mM $CaCl_2$, 15 % (v/v) glycerol, and divided into 250 µl aliquots. Aliquots were rapidly frozen on dry ice and stored at -70 °C.

[2.7.2]Preparation of agar plates

2.5 % granulated agar (Difco laboratories) was added to 500 ml of Nutrient Broth (Oxoid; No. 2), and autoclaved. The mixture was allowed to cool to 50 °C, and antibiotics were added as appropriate (ampicillin to 100 µg/ml, kanamycin to 20 µg/ml or chloramphenicol to 30 µg/ml). 20 ml fractions were poured into sterile 85 mm petri dishes (Sterilin) and allowed to cool.

[2.7.3]Transformation

An aliquot of competent cells [2.7.1] was thawed on ice. 100 ng of plasmid was added, and the cells incubated on ice for 40 mins. The cells were heated to 37 °C for 10 mins, and then added to 5 ml of nutrient broth, pre-warmed to 37 °C. The culture was incubated at 37 °C for 2 hr with shaking, and then centrifuged at 4500 g for 5 mins. The cell pellet was gently resuspended in 150 µl of nutrient broth, and plated on a freshly prepared agar plate [2.7.2]. Plates were incubated overnight at 37 °C.

[2.7.4]Blue-white colour selection

Agar plates were prepared as above [2.7.2], except 40 µg/ml 5-bromo-4-chloro-3-indolyl-β-D-galactoside (X-Gal) and 1 mM isopropyl-β-D-thiogalactopyranoside (IPTG) were added together with the antibiotics. IPTG-induced β-galactosidase production results in a blue colour due to release of the 5-bromo-4-chloro-3-indolyl moiety in cells carrying an intact LacZ gene (non-transformants). Transformant colonies, carrying a disrupted LacZ gene, remain white.

[2.7.5]PCR Screening

Colonies were screened for presence of insert by PCR. A single isolated colony from the overnight plate was inoculated into 200 µl nutrient broth, with the appropriate antibiotic. The culture was incubated at 37 °C for 4 hr, after which 2 µl was used as template for a PCR reaction [2.2], using the appropriate primers. Cultures giving a PCR product (indicating presence of the insert) were streaked onto freshly prepared agar plates, containing the appropriate antibiotic. The template for the negative control was from a culture of non-transformed cells.

[2.8]Gene cloning using the pPCR-Script vector

[2.8.1]Background

The pPCR-Script cloning kit (Stratagene) was used for blunt-end ligation of PCR products into the pPCR-Script vector. The pPCR-Script cloning technique utilises a unique ligation strategy, based on the uncommon restriction site of the enzyme *Srf* I. As shown in Figure 3, the ligation mixture contains *Srf*I in addition to the pPCR-Script vector, insert and T4 DNA ligase. Cleavage of the *Srf* I site generates linear vector, which inter-converts with the closed form through the opposing action of T4 ligase. Insertion of the PCR fragment, however, disrupts the *Srf* I site, trapping the vector in the closed state with insert. Insertion of the fragment also disrupts the LacZ gene carried by the vector, allowing blue-white selection of positive transformants.

[2.8.2]Vector generation

10 µl reactions had the following composition: 10 ng of pPCR-Script Amp SK(+) Vector, 1 µl of PCR-Script 10 X reaction buffer, 0.5 mM ATP, 70 X molar excess PCR product (~15 ng), 5 units of *Srf I* restriction enzyme, 4 units of T4 DNA ligase and water *q.v.*. The reaction mixture was incubated for 1 hr at room temperature, and then heated to 65 °C for 10 mins to inactivate the enzymes.

[2.8.3]Transformation

40 µl of XL10-Gold Kan ultracompetent cells (Stratagene) were thawed on ice. 1.6 µl of β-mercaptoethanol was added, and the cells incubated for 10 mins on ice with gentle mixing. 2 µl of the ligation mix was added, and the cells incubated on ice for 30 mins. The cells were heat-pulsed by heating to 42 °C for exactly 30 sec, and then incubated on ice for a further 2 mins. 450 µl of pre-warmed Nutrient Broth (Oxoid No. 2) was added to the cells, which were then incubated for 1 hr at 37 °C with shaking. 200 µl of the transformation mixture was plated on a freshly prepared X-Gal / IPTG / agar plate [2.7.2], containing ampicillin (100 µg/ml). Plates were incubated overnight at 37 °C and positive transformants (white colonies) picked.

[2.9]Preparation of plasmid DNA from bacteria

Plasmid DNA was extracted from bacterial cultures using the MiniPrep or MaxiPrep kits (Qiagen) according to the manufacturer's instructions.

[2.10]DNA sequencing

DNA sequencing was carried out by UCL scientific support services, using the di-deoxy method of Sanger and co-workers [216] as developed by Ruiz-Martinez and co-workers [217], on a Beckman Coulter CEQ 8000 genetic analysis system.

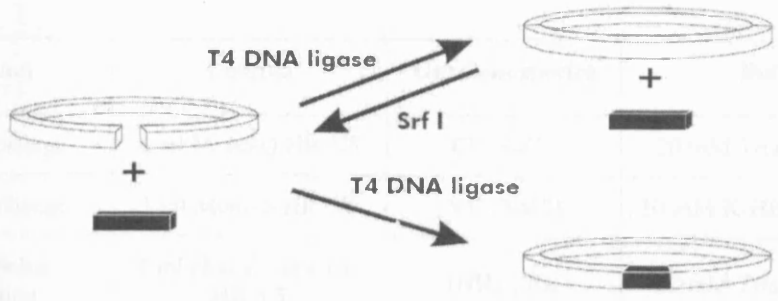

Figure 3 - The pPCR-script cloning strategy (Stratagene).
Inter-conversion of closed and open vector through the opposing actions of T4 ligase and *Srf* I maintains a pool of open vector. Insertion of the PCR fragment disrupts the *Srf* I site and traps the vector in the closed state with insert. Figure taken from Stratagene pPCR-script manual.

[2.11]Preparation of glycerol stocks

10 ml of nutrient broth (Oxoid No. 2) was inoculated with a single isolated colony from a freshly made agar plate [2.7.2]. The culture was incubated overnight at 37 °C with shaking, and cells were then sedimented by centrifugation for 10 mins at 4500 g. The pellet was resuspended in 0.5 ml of sterile 20 % glycerol, frozen rapidly on dry ice and stored at –70 °C.

Protein Methods

[2.12]Fast protein liquid chromatography (FPLC)

FPLC was carried out on a Pharmacia LKB system, using the following columns, at a flow rate of 1 ml/min:

Function	Column	Gradient species	Buffer
Anion exchange	1 ml Mono Q HR 5/5	Cl^- (NaCl)	20 mM Tris-Cl, pH 7.4
Cation exchange	1 ml Mono S HR 5/5	Na^+ (NaCl)	10 mM K-HEPES, pH 7.0
Hydrophobic interaction	1 ml phenyl Superose HR 5/5	$(NH_4)_2SO_4$	20 mM Tris-Cl, pH 7.4
Gel filtration	25 ml Superdex 75 HR 10/30	-	100 mM NaCl, 20 mM Tris pH 7.4

[2.12.1]Calibration of gel filtration column

The column was calibrated using 250 µl of a mixture of blue dextran (3 mg/ml), alcohol dehydrogenase (2 mg/ml), BSA (4 mg/ml), carbonic anhydrase (4 mg/ml), α-chymotrypsin (4 mg/ml), cytochrome c (1.5 mg/ml) and aprotinin (4 mg/ml), as shown in Figure 4 and Figure 5.

[2.13]Sodium dodecyl sulphate polyacrylamide gel electrophoresis (SDS-PAGE)

The method used was a modification of Laemmli [218].

[2.13.1]Reagent preparation

50% Acrylamide Solution (32:1) contained 48 % (w/v) acrylamide, 1.5 % (w/v) methylene-bis-acrylamide. Gel buffer contained 3 M Tris, 0.3 % (w/v) sodium dodecyl sulphate (SDS), pH 8.5. Ammonium persulphate (APS) was 10 % (w/v), and was made immediately before use and stored on ice. Anode buffer was 200 mM Tris, pH 8.9. Cathode buffer was 100 mM Tris, 100 mM Tricine, 0.1 % (w/v) SDS, pH 8.2.

[2.13.2]Gel composition

Stacking and resolving gels were made as follows. Acrylamide percentage was chosen according to the mass of proteins of interest.

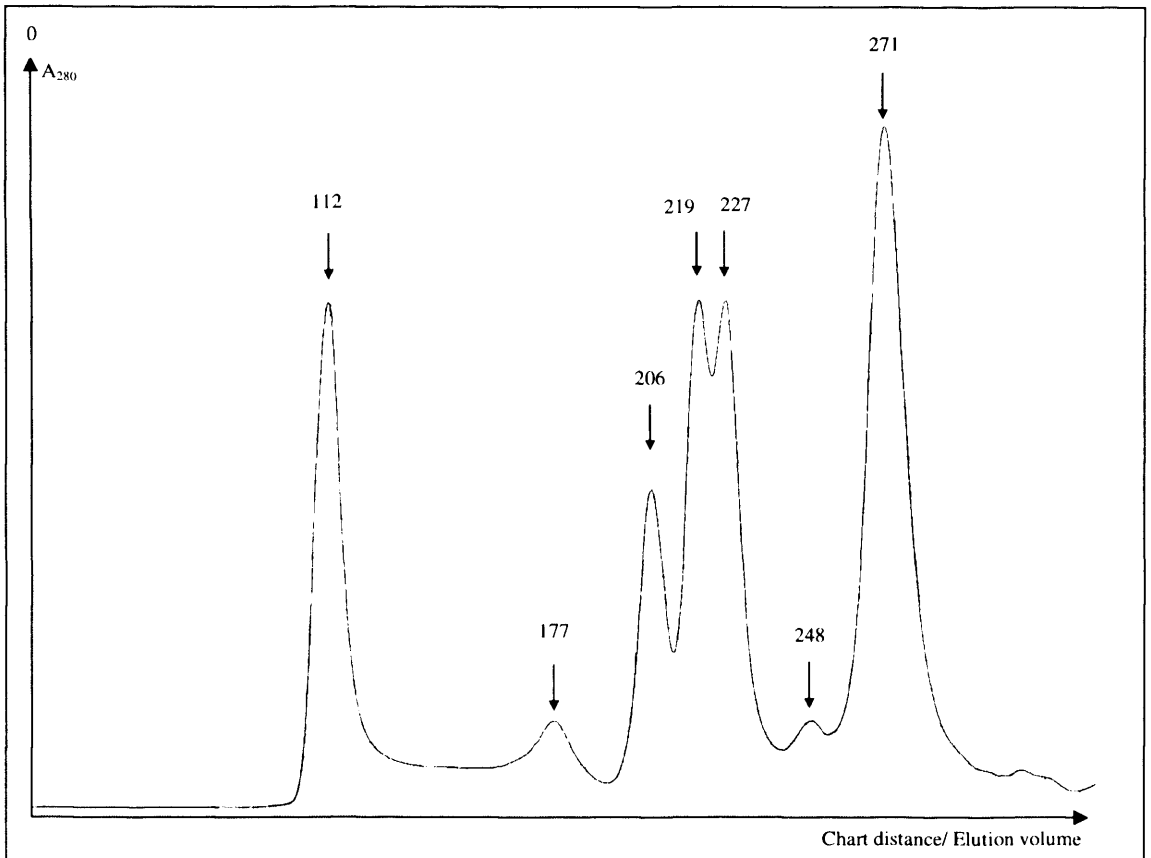

Figure 4 - Gel filtration of protein standards.
A mixture of blue dextran, alcohol dehydrogenase, BSA, carbonic anhydrase, α-chymotrypsin, cytochrome c and aprotinin was applied to a Superdex 75 gel filtration column and eluted with 100 mM NaCl, 20 mM Tris pH 7.4 at 1 ml per min. A trace was recorded using a chart recorder running at 10 mm/min. The distance of peak centres from the point of sample application is indicated in mm.

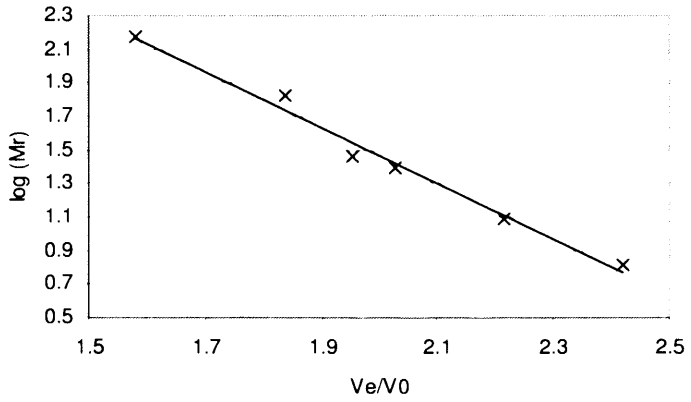

Figure 5 - Calibration graph deriving from gel filtration of protein standards.
The distances indicated on Figure 4 were used to calculate values of V_e/V_0 (distance to peak centre divided by distance to centre of blue dextran peak; assuming blue dextran to be completely excluded from the column). As expected, V_e/V_0 shows a linear relation to log(relative molecular mass) ($\log(M_r)$).

	8%	10%	12%	18%	Stacking (4%)
50% Acrylamide 32:1	4.8	6.0	7.2	10.8	1.0
Gel buffer	10.0	10.0	10.0	10.0	3.1
Glycerol	3.2	3.2	3.2	3.2	0.0
dH_2O	12.0	10.8	9.6	6.0	8.4

Gel solutions were degassed using a vacuum pump whilst warming in a 50 °C water bath for 10 mins. Immediately before casting, N, N, N', N' – tetramethylethylene-diamine (TEMED) and 10 % APS were added to 1.1 µl/ml and 11 µl/ml respectively, to induce polymerisation. Gels were cast using the SE 250-Mighty Small II electrophoresis unit (Hoeffer Scientific Instruments, San Francisco).

[2.13.3]Protein sample preparation

1 volume of 2 X sample loading buffer (10 mM Tris-Cl, 6 % (w/v) SDS, 2 mM EDTA, 20 % (v/v) glycerol, 0.025 % (w/v) bromophenol blue, pH 6.8), and 2 % (v/v) 2-mercapto ethanol was added to the protein samples. Samples were heated at 90 °C for 10 mins.

[2.13.4]Electrophoresis

The gel was electrophoresed at 20 mA until the dye front had moved into the resolving gel, after which the current was raised to 30 – 50 mA until the dye front reached the bottom of the gel. The anode buffer was 200 mM Tris-Cl, pH 8.9 and the cathode buffer was 100 mM Tris-Cl, 100 mM Tricine, 0.1 % (w/v) SDS, pH 8.2.

[2.14]Coomassie staining

[2.14.1]Standard

After electrophoresis [2.13], protein gels were washed three times for 5 mins with 100 ml of dH_2O. The gel was stained with 20 ml of Simply Blue SafeStain (Invitrogen) for 1 hr with gentle shaking, and then washed twice for 30 mins with 100 ml of dH_2O.

[2.14.2]Colloidal

After electrophoresis [2.13] the gel was fixed overnight in 200 ml of 50 % (v/v) ethanol, 2 % (v/v) H_3PO_4. The gel was washed three times for 30 mins with 200 ml of dH_2O and placed in 34 % (v/v) methanol, 17 % (w/v) $(NH_4)_2SO_4$, 3 % (v/v) H_3PO_4. After 1 hr, Coomassie Blue G-250 was added to 0.7 mg/ml and the gel was stained for 3 –4 days.

[2.15]Silver staining

Silver staining of protein gels was carried out using the Silver Stain Plus kit (BioRad) according to the manufacturer's instructions.

[2.16]Western blotting

[2.16.1]Blotting

Filter paper (Wattman 3MM Chr) and nitrocellulose (0.45 µm pore size, Schleicher & Schuell) were cut to size and soaked in transfer buffer (50 mM Tris, 40 mM glycine, 1.5 % (w/v) SDS, 20 % (v/v) methanol, pH 8.5) for 30 mins. After SDS-PAGE [2.13] the gel sandwich was prepared, and proteins were transferred to the nitrocellulose using a constant voltage of 30 V for 1 hr in an XCell II blot module (Invitrogen).

[2.16.2]Probing

Blots were blocked using either powdered milk (Marvel; 10 % in phosphate buffered saline (PBS)), BSA (10 % in PBS) or 1 X Odyssey® blocking buffer (LiCor biosciences) for 1 hr at room temperature with gentle shaking, and then washed for 5 mins in PBS plus 0.1 % Tween-20 (PBS-T). The blot was then incubated for 1 – 24 hr at room temperature with primary antibody, diluted to the appropriate concentration in either powdered milk (Marvel; 4.5 % in PBS-T), BSA (3 % in PBS-T) or Odyssey® blocking buffer (LiCor biosciences; 0.5 X in PBS-T). Blots were washed three times for 5 mins in PBS-T and then incubated for 1 hr at room temperature in the appropriate secondary antibody, in the same solution as for the primary antibody. Blots were washed four times for 5 mins in PBS-T.

The following antibodies and dilutions were used: monoclonal anti-cytochrome c (Calbiochem, AP1030, 1/1500), monoclonal anti-BAK (Upstate, 06-536, 1/2000), monoclonal anti-BAX N20 (Santa Cruz, sc-493, 1/1500), monoclonal anti-VDAC (Calbiochem, 529532, 1/1500), polyclonal anti-AIF (Stratagene, B12000, 1/1500), polyclonal anti-cyclophilin D (AbCam, ab3567, 1/2000), polyclonal anti-cyclophilin A (Upstate, 07-313, 1/1500), polyclonal anti-ANT (produced in-house, 1/1500), fluorescent anti-mouse secondary (800 nm, Rockland, KFB002, 1/5000), fluorescent anti-rabbit secondary (680 nM, Invitrogen, A21076, 1/5000), HRP-conjugated anti-rabbit secondary (Sigma, A0545, 1/5000).

[2.16.3]Detection

For fluorescent secondary antibodies, bands were detected and quantified using the Li-Cor Odyssey system. Alternatively, for HRP-conjugated secondary antibodies, blots were incubated with ECL Detection Reagents (Amersham), and then exposed to Super RX Medical X-Ray film (Fuji). For quantification, the developed film was scanned, and bands analysed using the Scion image program (Scion Corporation).

[2.17]Protein assays

Three protein assays were used, according to the requirement either for speed, accuracy or sensitivity.

[2.17.1] Biuret assay

The Biuret assay was used to quantitate protein samples from 0.5 to 50 mg/ml. The method was that of Kroger and Klingenberg [219]. 167 µl of sample (diluted with water as appropriate) was added to 67 µl of 4% (w/v) sodium cholate, 667 µl of 10% (w/v) NaOH and 100 µl of 1% (w/v) $CuSO_4$. The

reactions were mixed well, left to stand for 10 mins and transferred to 1 ml plastic cuvettes. Absorbance was measured at 540 nm and converted to protein concentration using a BSA standard curve.

[2.17.2]Lowry assay

The Lowry assay was used to quantitate protein samples from 0.01 to 20 mg/ml. The method was that of Harrington [220]. Immediately before use, solution A (0.4 % (w/v) NaOH, 2 % (w/v) Na_2CO_3, 0.16 % (w/v) sodium tartrate, 1 % (w/v) SDS) was mixed with 1/100 volumes of 4 % (w/v) $CuSO_4$. 750 µl of this solution was added to 250 µl of protein sample and left to stand at room temperature for 20 mins. Folin-Ciocalteu's phenol reagent [221] was diluted 1:1 with dH_2O, and 75 µl added to the samples, which were then left to stand for an additional 45 mins, in the dark. Absorbance was measured at 750 nm and converted to protein concentration using a BSA standard curve

[2.17.3]Fluorescence assay

The fluorescence assay was used to rapidly determine the approximate protein concentration of mitochondrial preparations. 3 ml of 395 mM sucrose, 10 mM K-HEPES, 0.5 mM EGTA, pH 7.4 (SH-E) was added to a fluorimeter cuvette. Fluorescence was measured on a Perkin-Elmer LS-5B fluorimeter using excitation at 280 nm and emission at 320 nm. A small volume of the mitochondrial preparation (5 – 10 µl; 20 – 40 µg) was added to the cuvette and mixed thoroughly, and the fluorescence measurement repeated. [Reading – Background] was converted to protein concentration using a standard curve, prepared using parallel assays on a typical mitochondrial preparation by the Biuret method.

[2.18]GST affinity precipitation

[2.18.1]Preparation of Fusion Protein-GSH-Agarose resin

2.5 ml of a small overnight culture of *E. coli* DH5α, harbouring the plasmid of interest, was diluted 10-fold in fresh nutrient broth, containing the appropriate antibiotic. Cells were grown at 37 °C to an OD_{600} of 0.6 – 0.8 (typically around 2 hr). Expression was induced by adding IPTG to 40 µg/ml, and cells were grown overnight at room temperature. Cells were sedimented by centrifugation at 4500 g for 10 mins, and the pellet resuspended in 4 ml of 100 mM NaCl, 20 mM Tris-Cl, 0.5 mM EDTA, pH 7.4 containing 10 mg/ml hen egg white lysozyme. After a 1 hr incubation on ice, cells were sonicated for 4 x 30 secs with a 30 sec cooling period in a Sanyo Soniprep 150 sonicator at 10 µm deflection, using a 6 mm probe. Cells were spun for 15 mins at 13,000 g at 4 °C, and the supernatant collected. Meanwhile, 20 mg reduced glutathione- (GSH-) agarose was swelled overnight in dH_2O, and pipetted into a glass column (Pierce; No. 20055, 8 mm I.D. x 152 mm, 40 µm pore disc). The column was equilibrated with lysis buffer and the supernatant containing recombinant protein was applied to the column in three passes. The column was washed with 7 x 2 ml of PBS-T, followed by 3 x 2 ml of the buffer to be used in the pull-down experiment. The buffer depended on the extract to be used (sub-mitochondrial particles (SMPs), total protein, or soluble protein) – compositions are given below [2.27]. The resin was washed out of the column, centrifuged for 1 min at 100 g, and

resuspended in approximately 500 µl of buffer, to make a 1:1 agarose/buffer mixture. All steps were carried out at 4 °C.

[2.18.2]Pull-down of mitochondrial proteins

1400 µl of mitochondrial extract (SMPs, total protein or soluble protein, as specified in the text) [2.27] was incubated with 60 µl of fusion protein-GSH-agarose resin [2.18.1] in a 1.5 ml Eppendorf tube, for 10 mins at 4 °C on a rotary shaker. Tubes were spun for 5 secs in a bench-top centrifuge and the supernatant removed. 1450 µl of the appropriate buffer was added (again, depending on the extract used; [2.27]), and the tubes incubated for another 5 mins at 4 °C on the rotary shaker. These wash steps were repeated two to four times. Fusion protein and mitochondrial proteins bound to it were eluted by adding 3 x 40 µl of 50 mM GSH in the same buffer. The tubes were centrifuged after each addition, and the supernatants removed and combined. For experiments with inhibitors, the fusion protein-GSH-agarose resin was preincubated with inhibitor for 5 mins at 4 °C before addition of mitochondrial extract.

[2.19]Protein sequencing

[2.19.1]Trypsin digestion

Excised gel bands were washed three times with 200 µl of 50% acetonitrile (ACN) in 5 mM NH_4HCO_3, pH 8.0, and dried in a rotary vacuum evaporator (Savant SpeedVac). 150 µl of 10 mM DTT in 5 mM NH_4HCO_3 pH 8.0 was added to the gel pieces, which were then incubated for 45 mins at 50 °C. The DTT solution was removed, and replaced with 150 µl of 50 mM iodoacetamide in 5 mM NH_4HCO_3, pH 8.0. Gel pieces were incubated for 1 hr at room temperature in the dark, washed twice with 200 µl of 50% ACN in 5 mM NH_4HCO_3, pH 8.0, and dried in the rotary vacuum evaporator. 5 µg/ml trypsin in 15 µl of 5 mM NH_4HCO_3, pH 8.0 was added to the gel pieces, which were then left overnight at 37 °C. The gel pieces were centrifuged and the supernatant removed. 150 µl of 50 % ACN, 5 % trifluoroacetic acid in 5 mM NH_4HCO_3, pH 8.0 was added to the gel pieces, which were agitated gently and then centrifuged. The supernatant was removed, and this last step repeated once more. The combined supernatants were evaporated to dryness in the rotary vacuum evaporator and stored at -20 °C.

[2.19.2]Mass spectrometry

Liquid chromatography tandem mass spectrometry (LC-MS-MS) were carried out at the Proteomics Unit of the Wolfson Institute of Biomedical Research, UCL. Peptide mass matching against the NCBI database was carried out using the Mascot search engine (Matrix Science) [318].

[2.20]^{32}P labelling

B50 cells were grown to 90 % confluence. Cells were washed twice with 20 ml of ice-cold PBS and scraped into 5 ml of 395 mM sucrose, 10 mM K-HEPES, 0.5 mM EGTA, pH 7.4 (SH-E), containing 18 µg/ml phenyl methyl sulphonyl fluoride (PMSF), 7 µg/ml pepstatin A, 4 µg/ml leupeptin, 1.5 µg/ml antipain, 0.25 µg/ml chymostatin as protease inhibitors. Mitochondria were isolated [2.26], and

resuspended in SH-E + 5 µM rotenone at approximately 2 mg/ml. Mitochondria were divided into 250 µg aliquots and centrifuged for 3 mins at 13,000 g to give a mitochondrial pellet. The supernatant was removed and the pellet resuspended in the following buffer: 125 mM KCl, 2 mM EGTA, 5 mM K-succinate, 10 mM K-HEPES, 2 mM $MgCl_2$, 5 mM Na_2HPO_4, 5 µM rotenone, 50 µCi/ml $^{32}P_i$, pH 7.0. In some experiments ADP was added to 0.1 mM. Other additions were made as appropriate. The reaction mixture was incubated at 30 °C for 90 mins to allow labelling of mitochondrial proteins. 20 µl of sample loading buffer was added, and the samples were immediately heated to 90 °C for 10 mins to stop the labelling reaction and denature proteins. 200 µg of mitochondrial protein per lane was run on SDS-PAGE [2.13], and transferred to nitrocellulose by Western blot [2.16.1]. Blots were air-dried and then washed with 50 ml of PBS for 1 hr, three times. Blots were again air-dried, and the membrane was exposed either to Super RX Medical X-Ray film (Fuji) or to a phosphorimager screen for 12 - 96 hr. Film was developed using an Xograph Compact X4 developer, and phosphorimager plates read using a FujiFilm FLA-2000 imager.

[2.21]Immunoprecipitation using protein G-agarose beads

Cell or mitochondrial protein extract [2.27] was incubated with antibody against the target protein (approximately 0.1 µg antibody per mg of protein) for 1 hr at 4 °C using a rotary shaker. 30 µl of protein G-agarose beads were added to the reaction mixture, which was incubated for a further 1.5 hr at 4 °C. Beads were collected by centrifugation (1000 g, 1 min) and the supernatant removed. Beads were washed 3 times with 0.75 ml of buffer, and then resuspended in 30 µl of sample loading buffer.

[2.22]Coupling antibody to CarboLink resin (Pierce)

CarboLink Coupling Gel (Pierce) is an affinity support for immobilizing antibodies via a hydrazine linkage to *cis*-glycol groups in sugars of polysaccharide moieties. Since antibodies only carry these moieties on the F_c portion, they are properly oriented when bound, with their antigen-binding sites unobstructed.

10 µg of antibody was resuspended in 100 µl of 100 mM Na_2HPO_4, pH 7.0. Sodium metaperiodate was added to 15 mM, and the reaction incubated in the dark at room temperature for 30 mins, to oxidise *cis*-glycol groups. The reaction mixture was diluted to 3 ml with 100 mM Na_2HPO_4, pH 7.0, and then concentrated to 50 µl using a centrifugal concentration unit (Centricon). The dilution / concentration procedure was carried out 4 times in total, lowering the sodium metaperiodate concentration to less than 3 nM. The final oxidised antibody solution was diluted to 300 µl, and added to 100 µl CarboLink resin. The mixture was incubated for 5 hr at room temperature using a rotary shaker. Beads were then sedimented by centrifugation (1000g, 1 min), washed twice with 100 mM Na_2HPO_4, pH 7.0 and resuspended in 80 µl of 100 mM Na_2HPO_4, pH 7.0.

[2.23]Pull-down using CarboLink-coupled antibody

Cell or mitochondrial protein extract [2.27] was incubated with CarboLink-coupled antibody against the target protein (approximately 0.1 µg antibody per mg of protein) for 1 hr at 4 °C using a rotary shaker. Beads were collected by centrifugation (1000 g, 1 min) and the supernatant removed. Beads were washed 3 times with 0.75 ml of buffer, and then resuspended in 30 µl of sample loading buffer.

[2.24]Cross-linking

Disuccinimidyl suberate (DSS) was used to cross-link cellular or mitochondrial proteins. DSS was dissolved in dimethylsulphoxide (DMSO) to 50 mM immediately before use. Mitochondria were suspended in 395 mM sucrose, 10 mM K-HEPES, 0.5 mM EGTA, pH 7.4 (SH-E) containing 18 µg/ml PMSF, 7 µg/ml pepstatin A, 4 µg/ml leupeptin, 1.5 µg/ml antipain, 0.25 µg/ml chymostatin as protease inhibitors, at approximately 2 mg of protein/ml, and DSS was added from the DMSO stock, to the desired concentration. The reactions were incubated for 15 – 30 mins at 25 °C, and mixed gently every ten mins. To stop the reaction, 1/10 volume of 1 M Tris-Cl, pH 7.0 was added, and the reaction incubated for an additional 10 mins at 25 °C.

Mitochondrial Methods

[2.25]Isolation of mitochondria from rat liver or heart

Mitochondria were prepared by differential centrifugation, using a modification of the method of Pederson and co-workers [222]. Sprague-Dawley rats (150 – 200 g body weight) were killed by cervical dislocation. The heart or liver was removed and immediately placed into an ice-cold solution of 210 mM mannitol, 70 mM sucrose, 10 mM Tris-Cl, 1 mM EGTA, pH 7.2 (MSTE), with protease inhibitors (18 µg/ml PMSF, 7 µg/ml pepstatin A, 4 µg/ml leupeptin, 1.5 µg/ml antipain, 0.25 µg/ml chymostatin). The tissue was finely chopped using scissors, transferred to a 30 ml centrifuge tube and homogenised for approximately 15 secs using a Polytron homogeniser on setting 5. The probe was pre-cooled to 4 °C. The disrupted tissue was centrifuged for 5 mins at 1200 g (liver) or 800 g (heart) at 2 °C, to pellet unbroken cells and nuclei. The supernatant was further centrifuged for 10 mins at 16,000 g to pellet mitochondria. Mitochondria were washed by gently resuspending in 30 ml of 210 mM mannitol, 70 mM sucrose, 10 mM Tris-Cl, pH 7.2 (MST), and re-sedimented by centrifuging for 10 mins at 16,000 g. The final pellet was re-suspended in MST (1 ml (heart) or 5 ml (liver), giving a concentration of approximately 10 mg mitochondrial protein per ml), kept on ice and used within two hr.

[2.26]Isolation of mitochondria from B50 cells

Typically, B50 cells from 200 cm^2 of culture area [2.38] were washed three times with ice-cold phosphate buffered saline (PBS), gently scraped into 10 ml of 395 mM sucrose, 10 mM K-HEPES, 0.5 mM EGTA, pH 7.4 (SH-E) and centrifuged for 5 mins at 1000 g. The cell pellet was resuspended in 2.5 ml of SH-E, supplemented with protease inhibitors (45 µg PMSF, 18 µg pepstatin A, 10 µg leupeptin, 3.8 µg antipain, 0.63 µg chymostatin). 0.5 ml fractions were passed through a 21-gauge needle five times, using the equipment shown below [Figure 6] to deliver a constant driving pressure. Under standard conditions finally adopted, a pressure of 120 kPa was used, giving a flow rate through the needle of 30.6 m/s. After breaking, the disrupted cells were taken to a volume of 15 ml with SH-E and centrifuged for 5 mins at 1000 g at 2 °C to pellet unbroken cells and nuclei. The supernatant was then centrifuged for 10 mins at 16,000 g at 2 °C. The mitochondrial pellet was resuspended in 200 µl of SH-E. A flowchart of the procedure is shown in Figure 7.

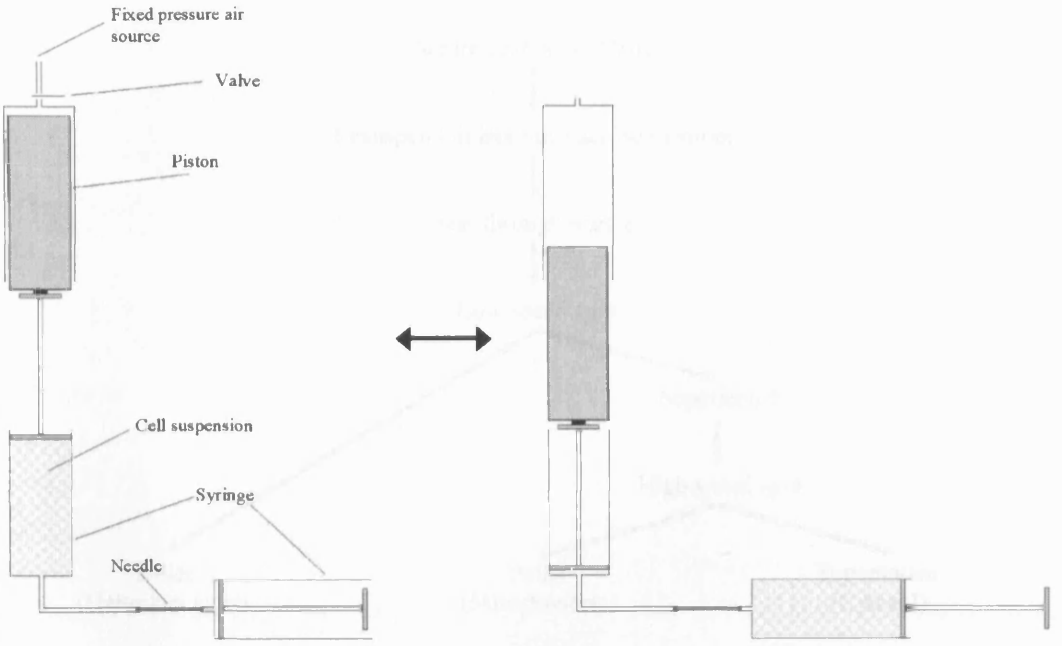

Figure 6 - Apparatus for disrupting B50 cells.
The cell suspension is driven from the upper chamber into the lower by a constant-pressure air source. The suspension is then gently returned to the upper chamber. Sheer forces rupture cells as they pass through the narrow-gauge needle.

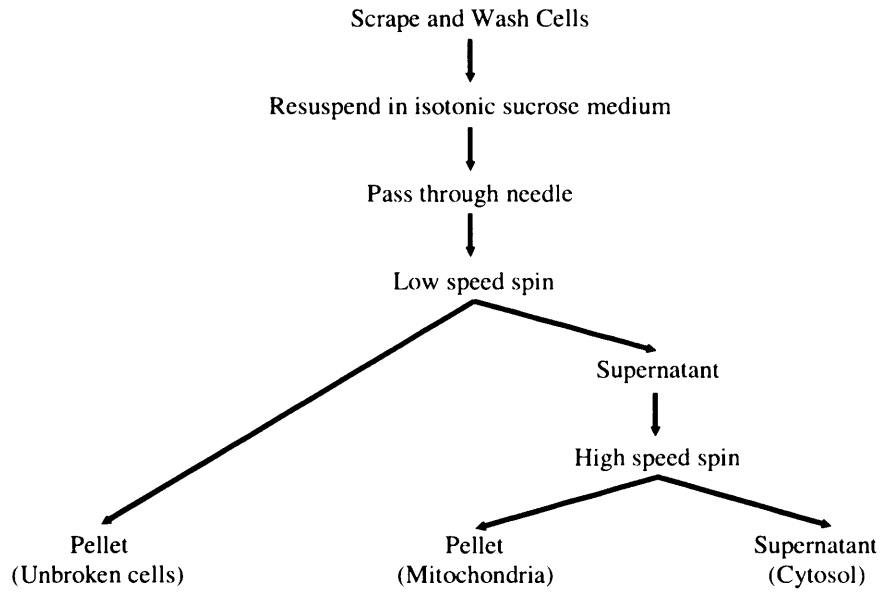

Figure 7 - Strategy for isolating mitochondria from B50 cells.
Cells were suspended in isotonic sucrose medium and disrupted by passage through a 21-gauge needle. Differential centrifugation subsequently separated a mitochondria-enriched fraction from unbroken cells and cytosol. During development of the protocol, KCl was added to the low-speed supernatant to detach electrostatically bound cytochrome c from the surface of mitochondria.

[2.27]Preparation of mitochondrial and cell extracts

[2.27.1]Total protein

Cells [2.38] or mitochondria [2.26] were sedimented for 10 mins at 1000 g or 16,000 g, respectively, and resuspended in 50 mM Tris-Cl, 150 mM NaCl, 1 % (v/v) Nonidet P40, 0.25 % (w/v) deoxycholate, 1 mM EDTA, 0.1 % (w/v) SDS, pH 7.4 (RIPA buffer). For some experiments, RIPA buffer was supplemented with 1 mM NaF, 1 mM sodium orthovanadate, 10 mM β-glycerophosphate, to inhibit protein dephosphorylation by phosphatases. To activate sodium orthovanadate before use, the pH of a 200 mM solution of sodium orthovanadate was adjusted to 10.0 with NaOH or HCl. The solution was boiled until it became colourless, and cooled to room temperature. The pH was readjusted to 10.0, and the procedure repeated until the pH was stable at 10.0 after boiling. This procedure depolymerises the vanadate, converting it into a more potent inhibitor of protein tyrosine phosphatases [223].

[2.27.2]Sub-mitochondrial particles (SMPs)

Mitochondria were sedimented for 10 mins at 16,000 g and resuspended in SH-E at 2 mg protein/ml. Digitonin was dissolved at 60 mg/ml in 50 % ethanol by sonication. Whilst swirling the mitochondrial preparation continuously on ice, digitonin was slowly added drop-wise to a final concentration of 0.12 mg per mg of mitochondrial protein. The preparation was swirled on ice for a further 10 mins, and then diluted with 1 volume of ice-cold SH-E. Mitochondria were then sedimented by centrifuging at 16,000 g for 10 mins, and resuspended in SH-E. This treatment with digitonin removes adherent proteases [224]. The mitochondrial preparation was then sonicated for 10 x 30 secs, with a 30 sec cooling period, in a Sanyo Soniprep 150 sonicator at 10 μm deflection using a 6 mm probe. The preparation was centrifuged at 20,000 g for 15 mins at 4 °C to pellet SMPs. The supernatant was removed and the pellet washed once with SH-E, before re-suspending in RIPA buffer.

[2.27.3]Matrix

Mitochondria were treated as above [2.27.2]. Following the first centrifugation step after sonication, the supernatant (containing matrix proteins) was removed and retained.

[2.28]Calcein release assay

[2.28.1]Introduction

Release of matrix-entrapped calcein is a very sensitive method to monitor even very short periods of transient PT pore opening. Isolated mitochondria were initially loaded with calcein by incubating with calcein-AM [Figure 8]. This molecule is highly lipophilic due to the acetoxymethyl groups, and can rapidly permeate into the matrix through the mitochondrial membranes. The acetoxymethyl group is subsequently cleaved by matrix esterases, trapping the tetra-acid fluorophore in the matrix.

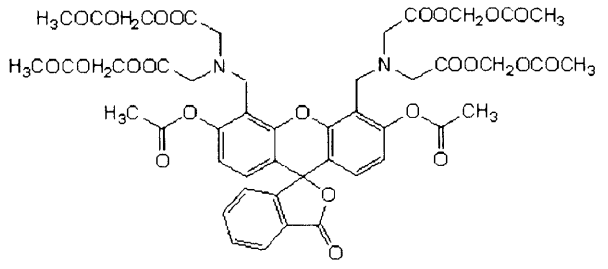

Figure 8 - Calcein acetoxymethyl ester (Calcein-AM).
The molecule is lipophilic, and is accumulated rapidly by mitochondria, where matrix esterases cleave the AM groups, trapping the molecule in the matrix. Calcein fluoresces strongly at 494 nm excitation. The AM derivative is not fluorescent.

Mitochondria were then incubated in respiration buffer, during which time any PT pore opening will rapidly release calcein from the matrix (at 680 Da, calcein is sufficiently small to pass through the PT pore, with a molecular weight cut-off of approximately 1600 Da). Mitochondria are then separated from the assay mixture by centrifugation, and calcein assayed fluorimetrically.

[2.28.2]Method

Mitochondria were isolated from B50 cells as described above [2.26] and resuspended in SH-E at approximately 3 mg protein/ml. Calcein acetoxymethyl ester (Calcein-AM) was added to 10 μM, and cells incubated in the dark at room temperature for 30 mins. After loading, mitochondria were diluted with 10 volumes of SH-E and then sedimented by centrifuging at 13,000 g for 3 mins. Mitochondria were resuspended in 125 mM KCl, 5 mM K-succinate, 10 mM K-HEPES, 2 mM $MgCl_2$, 5 mM Na_2HPO_4, 5 μM rotenone, pH 7.0, with further additions as appropriate. Aliquots were removed at various times, centrifuged for 3 mins at 13,000 g, and the supernatant diluted to 0.5 ml with 10 mM K-HEPES, pH 7.0. Calcein concentration was determined by measuring fluorescence with the wavelength pair 487 nm / 520 nm, on a Perkin-Elmer LS-5B fluorimeter. Total calcein was measured using an aliquot that was not centrifuged. (The hypotonic dilution medium results in osmotic lysis of mitochondria and release of all entrapped calcein into the medium.)

[2.29]Membrane potential measurements

[2.29.1]Principle

The presence of a potential across the mitochondrial inner membrane ($\Delta\Psi$) provides a driving force for the accumulation by mitochondria of positively charged species. At equilibrium the distribution of a freely permeable species C is given by the Nernst equation :

$$\Delta\Psi = 2.3 \cdot \frac{R \cdot T}{z \cdot F} \cdot \log\left(\frac{[C]_i}{[C]_o}\right)$$

where R is the universal gas constant, T is the absolute temperature, F is the Faraday constant, z is the charge of the species C, and $[C]_i$ and $[C]_o$ are the internal and external concentrations of C respectively.

[2.29.2]Choice of cation

Cations must be lipophilic in order to fulfil the criterion of free permeability across the inner membrane. The tetra-phenyl phosphonium (TPP^+; Figure 9) ion's positive charge is delocalised over the phenyl π system and the ion is hence sufficiently lipophilic to cross the membrane.

[2.29.3]Construction of TPP^+ electrode

The construction of the TPP^+ electrode and chamber is shown in Figure 10. The TPP^+ electrode was constructed as described by Kamo and co-workers [225].

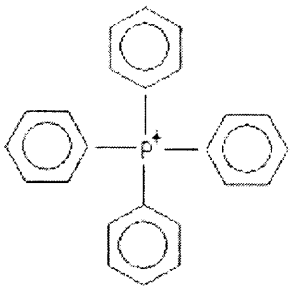

Figure 9 - The tetra-phenyl phosphonium (TPP^+).
The positive charge is delocalised over the phenyl π system and the ion is hence sufficiently lipophilic to cross the membrane. TPP^+ is thus accumulated by mitochondria according to the magnitude of the inner membrane potential.

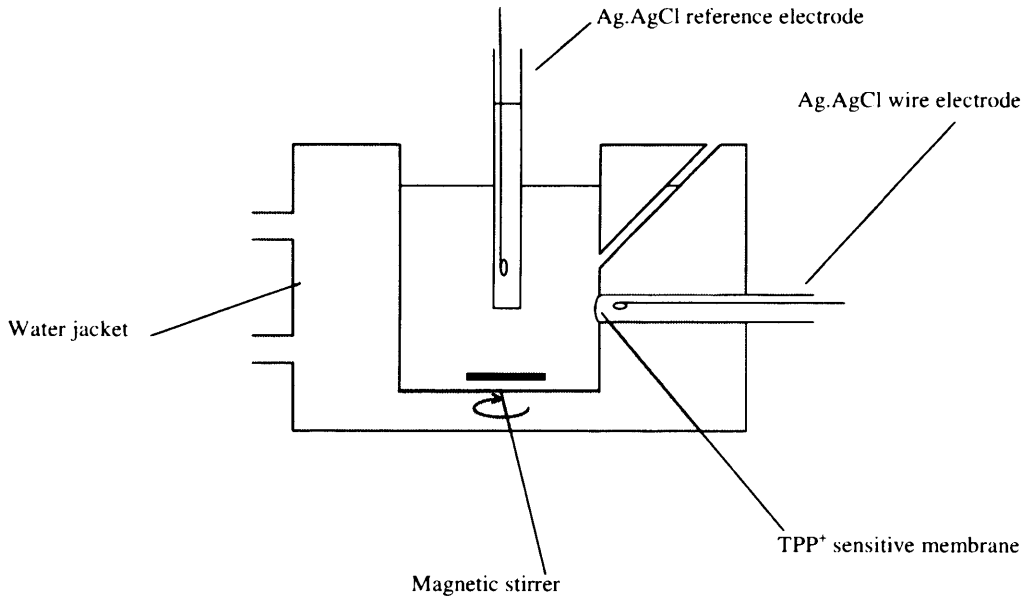

Figure 10 - Set-up of TPP^+ electrode

[2.29.4]Experimental

B50 mitochondria [2.26] were suspended in 600 µl 125 mM KCl, 10 mM K-HEPES, 2 mM $MgCl_2$, 5 µM rotenone, pH 7.0 at approximately 1 mg protein/ml. The instrument was calibrated by adding sequential small amounts of TPP^+, to a final concentration of 1.5 µM. Mitochondrial respiration was started by addition of 5 mM Na-succinate, and followed using an amplifier and chart recorder to measure the potential difference between reference and test electrodes.

[2.30]Mitochondrial swelling assay

B50 mitochondria [2.26] were suspended at 1 mg protein/ml in 0.5 ml of the following buffer at 30 °C, in a spectrophotometer cuvette: 125 mM KCl, 2 mM EGTA, 5 mM K-succinate, 10 mM K-HEPES, 2 mM $MgCl_2$, 5 mM Na_2HPO_4, 5 µM rotenone, pH 7.0. Additions were made as appropriate. To monitor swelling, absorbance was recorded at 540 nm on a Perkin-Elmer 124 spectrophotometer with chart recorder. A decrease in absorbance corresponded to mitochondrial swelling (decrease in light scattering).

Enzyme and cytochrome c release methods

[2.31]Protocol for assaying BID-induced cytochrome c release

[2.31.1]Buffer

Mitochondria were isolated as described above [2.26]. 3.5 µl of mitochondrial suspensions (approximately 20 µg protein) were pipetted into Fppendorf tubes, containing 20 µl of the following buffer: 125 mM KCl, 2 mM EGTA, 5 mM K-succinate, 10 mM K-HEPES, 2 mM $MgCl_2$, 5 mM Na_2HPO_4, 5 µM rotenone, pH 7.0 (respiration buffer), plus BID or tBID as indicated in the figure legends. tBID was generated as described below [2.49] or bought (Sigma; purified caspase 8-cleaved recombinant BID).

[2.31.2]Technique

Reactions were incubated for varying periods at 30 °C, and then stopped by centrifugation at 13,000 g for 3 mins. The supernatant was removed using a fine-tipped pipette, and the pellet resuspended in a volume of reaction buffer equal to the volume of supernatant removed. Cytochrome c in the pellet and/or supernatant fraction was analysed by Western blot [2.16]. A flowchart of the technique is shown in Figure 11.

[2.32]Preincubation with cytochrome c

For cytochrome c preincubations, a mitochondrial pellet containing approximately 0.5 mg of mitochondrial protein [2.26] was resuspended in 250 µl of SH-E containing 1 µM cytochrome c (beef heart). Following 15 mins incubation at 4 °C, mitochondria were pelleted by centrifugation, washed once with SH-E, and then resuspended in SH-E at around 4 mg/ml.

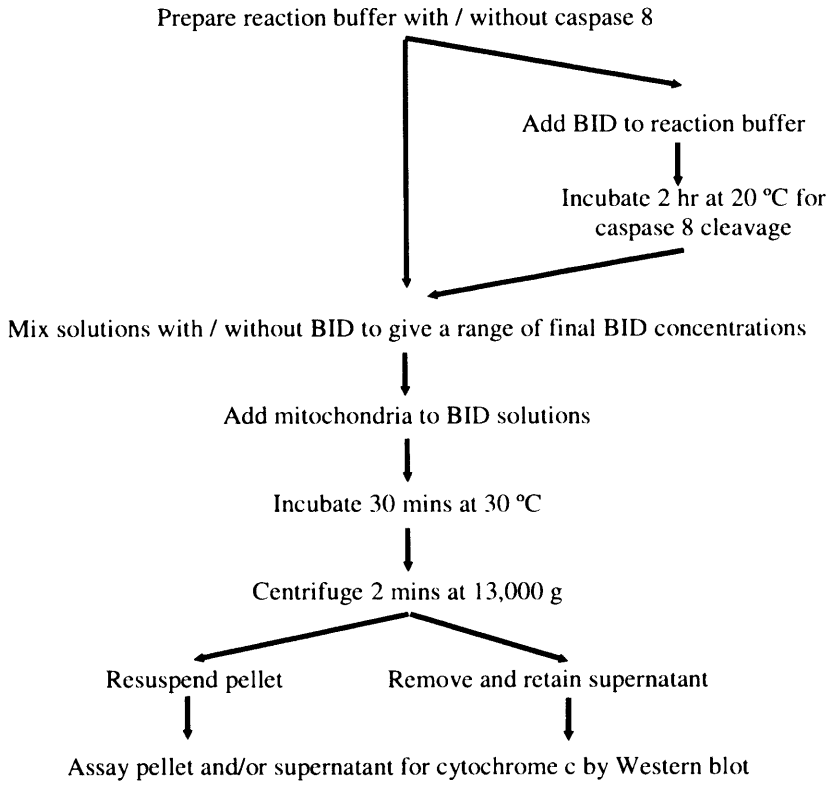

Figure 11 - Procedure for assaying BID-induced cytochrome c release.

[2.33]Peptidyl- prolyl- cis-trans *isomerase (PPIase) assay*

[2.33.1]Rationale

In contrast to all other amino acids, whose peptide bonds exist almost exclusively in the *trans* conformation, an appreciable fraction of proline peptide bonds exist in the *cis* conformation, due to proline's unique imide structure. Depending on the environment, around 15 % of bonds are in the *cis* conformation. Isomerisation occurs slowly in aqueous solvents, but is catalysed by the PPIase family of enzymes. The assay for *cis-trans* isomerase activity makes use of the stereo-specificity of chymotrypsin in cleavage of a test peptide to release a chromophore. Chymotrypsin will only cleave the *trans* conformer; the 85 % of test peptide initially in this conformation is rapidly cleaved, and after this new *trans* conformer is slowly generated from the *cis* state. Thus the rate of chromophore release in this second stage reflects the rate of *cis-trans* isomerisation.

[2.33.2]Protocol

The test peptide, *N*-succinyl-ala-ala-pro-phe-*p*-nitroanilide, was dissolved to 5 mM in an anhydrous solution of 470 mM LiCl in trifluoroethanol [226]. Chymotrypsin was dissolved to 25 mg/ml in 100 mM NaCl, 10 mM K-HEPES, pH 7.2 (NH buffer). 3 ml of NH buffer was added to a glass cuvette and cooled to 12 °C. 20 µl of PPIase enzyme (approximately 5 nM final concentration) was added to the cuvette, followed by 20 µl chymotrypsin and 12 µl of test peptide. The cuvette contents were rapidly mixed, and absorbance was recorded at 395 nm on a Perkin-Elmer 124 spectrophotometer with chart recorder. For assays with PPIase inhibitors, PPIase enzyme and inhibitors were pre-incubated in the cuvette for 5 mins before addition of chymotrypsin and test peptide. This is necessary because the conformation of bound CSA is markedly different to that of CSA free in solution [227], and the transition between the two during binding is slow [228].

[2.33.3]Derivation of rate constants

When the chymotrypsin reaction is not rate-limiting, the isomerisation reaction (production of *trans* isomer) is pseudo-first order with respect to the *cis* isomer. Thus

$$\frac{d[cis]}{dt} = -k \cdot [cis]$$

and so, by integration, at some time t after beginning measurements

$$[cis]_t = [cis]_0 \cdot e^{-k \cdot t}$$

where $[cis]_t$ represents the concentration of *cis* isomer at time t, and $[cis]_0$ is the initial concentration of *cis* isomer. If additionally $[C^*]_t$ and $[C^*]_\infty$ represent the concentration of chromophore at time t and at infinite time, respectively (the chromophore being formed immediately from the *trans* isomer by the chymotrypsin reaction) then

$$[cis]_t = [C^*]_\infty - [C^*]_t$$

and

$$[cis]_0 = [C^*]_\infty - [C^*]_0$$

Thus

$$[C^*]_\infty - [C^*]_t = \left([C^*]_\infty - [C^*]_0\right) \cdot e^{-k \cdot t}$$

and so

$$\ln\left(\frac{[C^*]_\infty - [C^*]_t}{[C^*]_\infty - [C^*]_0}\right) = -k \cdot t$$

Since absorbance A is proportional to [C*] we have

$$\ln\left(\frac{A_\infty - A_t}{A_\infty - A_0}\right) = -k \cdot t$$

and so a graph of $\ln\left(\frac{A_\infty - A_t}{A_\infty - A_0}\right)$ against time will have gradient $-k$. Since the isomerisation reaction proceeds even in the absence of catalysis by cyclophilins, the enzyme rate constant was calculated as

$$k_{enzyme} = k_{apparant} - k_{background}$$

[2.33.4]Derivation of percentage inhibition

For the experiments with cyclophilin inhibitors, percentage inhibition I was calculated as

$$I = 100 \times \frac{k_{enzyme} - k_{enzyme+inhibtor}}{k_{enzyme}}$$

[2.34]Monoamine oxidase (MAO) assay

MAO assays were carried out using the Amplex Red monoamine oxidase assay kit (Molecular Probes). Samples were added to the following mixture: 50 mM Na_2HPO_4, 1 mM benzylamine, 0.2 mM 10-acetyl-3,7-dihydroxyphenoxazine, 1 U/ml Horseradish peroxidase, pH 7.4. MAO activity generates H_2O_2 from the substrate (benzylamine). H_2O_2 reacts with the non-fluorescent 10-acetyl-3,7-dihydroxyphenoxazine to generate 7-hydroxyphenoxazin-3-one (resorufin), which can be detected fluorimetrically using excitation at 563 nm and emission at 587 nm. Continuous measurements were taken over 10 mins at 30 °C, and a reaction rate obtained. A background rate was calculated by pre-incubating samples for 20 mins at 4 °C with 1 µM clorgyline (MAO-A inhibitor) and 1 µM pargyline (MAO-B inhibitor). This rate was subtracted from the rate in the absence of inhibitors to give MAO activity in the sample.

[2.35]Caspase assays

Cells were incubated with or without 400 nM staurosporine to induce apoptosis. At various time-points, a cytosolic extract was made by incubating cells in 20 mM K-HEPES, 2 mM EDTA, 5 % (w/v) CHAPS, 5 mM DTT, pH 7.2, 1 mM PMSF and 10 µg/ml each of pepstatin, leupeptin and aprotinin. Caspase assays on these extracts were carried out in 1 ml of 100 mM K-HEPES, 20 % (v/v) glycerol,

0.5 mM EDTA, 5 mM DTT, pH 7.0. A 7-amino-4-trifluoromethyl coumarin (AFC)-conjugated substrate was added (VEID-AFC for caspase 6 or LEHD-AFC for caspase 8), and fluorescence was followed with excitation at 400 nm and emission at 505 nm in a Perkin-Elmer 124 fluorimeter. The AFC group fluoresces only when cleaved from the peptide moiety by caspase activity. Results were calibrated by measuring the fluorescence of a standard AFC solutions.

[2.36]BAK digestion assay

Mitochondria were incubated in respiration buffer [2.31.1]. At various time-points, a 25 µl volume was removed, added to 5 µl of a pre-cooled trypsin solution and incubated on ice. Under standard conditions, trypsin was present at 0.05 mg/ml, and the digestion carried out for 10 mins. Mitochondria were then isolated by centrifugation. After SDS-PAGE [2.13] and Western blotting [2.16], BAK digestion was assayed by probing with the anti-BAK NT antibody (Upstate).

Cell culture, transfection and imaging methods

[2.37]Preparation of cover-slips

24 mm cover-slips (BDH; thickness no. 1) were autoclaved, and washed in 70 % ethanol. After drying, cover-slips were covered with 250 µl of 15 µg/ml poly-L-ornithine and left for four hr. Cover-slips were washed with sterile dH_2O, covered with 250 µl of 20 µg/ml laminin in PBS and left for 3 hr. Cover-slips were then washed with sterile dH_2O and seeded with cells immediately.

[2.38]B50 cell culture

B50 cells from a rat neuronal cell line (European Collection of Cell Cultures, Salisbury, Wilts, U.K.) were maintained under CO_2/air (1:19) at 37 °C in Dulbecco's minimal essential medium (DMEM) with 10 % (w/v) foetal calf serum (FCS), and 50 µg/ml gentamycin. Cells were typically grown to 90 % confluence in 200 ml plastic flasks (Sterilin; 200 cm^2 culture area per flask). To detach adherent cells, pre-warmed PBS containing 1 mM EDTA was added to the culture medium, and cells incubated for 10 mins at 37 °C.

[2.39]Transient transfection

To transfect cells on cover-slips or 35 mm plates, DNA was diluted to 10 µg/ml in 100 µl OPTI-MEM (Gibco-BRL), and left to stand for 20 mins. Lipofectamine 2000 (Invitrogen) was diluted to 50 µg/ml in 100 µl OPTI-MEM, added to the DNA solution and allowed to stand for 2 hr. Cells were washed twice with PBS, after which the 200 µl of transfection mix was diluted to 1 ml with foetal calf serum (FCS) and added to the culture dish. Cells were incubated for 5 hr in a CO_2 incubator, after which the transfection mixture was removed. 3 ml of fresh FCS was added to the culture dish, and cells were incubated in a CO_2 incubator, typically for 24 – 48 hr.

[2.40]Cell fixing and permeabilisation

Coverslips of transfected cells [2.39] were fixed in freshly prepared 4 % paraformaldehyde, 4 % sucrose in PBS, for 15 mins. Cells were washed twice for 5 mins in PBS, and then permeabilised for 7 mins in 0.25 % Triton-X100. Cells were washed three times for 5 mins in PBS before antibody probing.

[2.41]Cell staining and imaging

Permeabilised cells [2.40] were blocked using 10 % BSA in PBS for 40 mins at room temperature. After washing twice for 5 mins with PBS, cells were incubated with primary antibody (anti-FLAG or anti-ANT) diluted to the appropriate concentration (typically 0.1 – 1 μg/ml, in 3.5 % BSA in PBS), for 3 hr at room temperature. Cells were washed twice for 5 mins with PBS, and incubated for 1 hr with the appropriate secondary antibody (typically 0.1 μg/ml, in 3.5 % BSA in PBS) - either fluorescein-labelled anti-mouse IgG (Invitrogen) for detection of FLAG or Texas red-labelled anti-rabbit IgG (EMD biosciences) for detection of ANT. Cells were washed four times for 5 mins with PBS before imaging. For staining with MitoTracker, cells were incubated for 10 mins with 10 ng/ml MitoTracker red (Molecular probes) prior to fixation. Cells were imaged using an Olympus IX70 fluorescent microscope fitted with a cooled CCD camera (Micromax 1401E; Princeton instruments). Excitation was via band-pass filters for excitation of fluorescein (490 nm), Texas red (570 nm) or MitoTracker red (570 nm). Fluorescent light was collected on a polychroic beam splitter and a two band-pass emission filter in the filter cube (530 nm, 625 nm). The appropriate emission band was then selected by band-pass filters in the emission light path.

[2.42]Generation of cyclophilin D(+) cell line

A cyclophilin D(+) cell line was generated previously in the lab by Li and co-workers [157]; this cell line carries the pcDNA 3.1 plasmid (Invitrogen) [Figure 12] containing the cyclophilin D coding sequence. pcDNA 3.1 is an expression vector carrying the Cytomegalovirus early promoter for strong expression in mammalian systems. Kozak described a consensus sequence for maximum efficiency of translation efficiency [229]. The rat cyclophilin D gene does not conform to this consensus sequence, as shown in Figure 13. Thus the second codon of the gene was altered from CTA to GTA (Leu to Val substitution) in order to incorporate the consensus sequence, to increase translation efficiency. The N-terminal pre-sequence is removed upon import to mitochondria, so the mature protein sequence is unaltered.

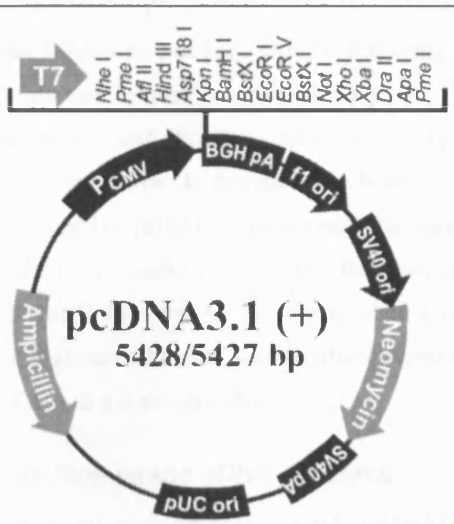

P_{CMV} – Cytomegalovirus early promoter

BGH pA – BGH polyadenylation signal

F1 ori – f1 origin of replication

SV40 ori – SV40 early promoter and origin of replication

Neomycin – Neomycin resistance gene

SV40 pA – SV40 polyadenylation signal

PUC ori – pUC origin of replication

Ampicillin – Ampicillin resistance gene

Figure 12 - The pcDNA 3.1 (+) plasmid.

Kozak Consensus Sequence	:	$\frac{G}{A}$ N N A T G G
Cyclophilin D Translation Start Site	:	G C G A T G C
Modified cyclophilin D Sequence	:	G C G A T G G

Figure 13 - The translation start site of the cyclophilin D gene does not conform to the Kozak consensus sequence.
The required G at position + 4 is in fact a C in the cyclophilin D sequence. This nucleotide was thus replaced by a G during the generation of the cyclophilin D expression plasmid. The resulting Leu -> Val substitution does not affect protein function, since it is part of the N-terminal pre-sequence which is removed following mitochondrial import.

Methods for expression and purification of recombinant proteins

[2.43]Extraction of total RNA from rat liver

Total RNA was extracted from tissue using the High-Pure RNA tissue kit (Roche), according to the manufacturer's instructions. Briefly, a 150 g male Sprague-Dawley rat was killed by cervical dislocation, and the liver removed. Approximately 60 mg of tissue was homogenised in an ethanol/guanidine hydrochloride- based denaturing buffer using a Dounce homogeniser, and centrifuged to pellet cellular debris. The supernatant was applied to a High-Pure filter tube, containing a glass fibre fleece to bind RNA. Residual DNA was removed by the addition of deoxyribonuclease I (DNAse I), followed by 15 mins incubation at room temperature. The column was washed three times in a high-salt ethanolic wash buffer to remove low-Mr contaminants. Total RNA was then eluted by addition of a low-salt buffer.

[2.44]First-strand cDNA synthesis

First-strand complementary DNA (cDNA) was produced using a 1st strand cDNA synthesis kit (Roche). 20 µl reactions contained the following components: 10 mM Tris-Cl, 50 mM KCl, 5 mM $MgCl_2$, 1 mM each of dATP, dCTP, dTTP and dGTP, 1 µM primer, 50 units of ribonuclease (RNase) inhibitor, 20 units of AMV reverse transcriptase, 1 µg RNA template (total RNA; [2.43]), ddH_2O *q.v.*, pH 8.4. The reaction was incubated for 10 mins at 25 °C to anneal the primer, and then for 60 mins at 42 °C to synthesise cDNA. The reverse transcriptase enzyme was denatured by heating to 95 °C for 5 mins, before cooling to 4 °C.

[2.45]Expression of BID

Bacterial cells carrying the *Bid* expression plasmid [2.7] were grown to mid-log phase (OD_{600} = 0.6) at 37 °C and expression induced with 1 mM IPTG. Cells were harvested after 3 hr by centrifugation at 5000 g for 15 mins, and resuspended in 100 mM NaCl, 20 mM Tris-Cl, 1 mM EDTA (lysis buffer) containing protease inhibitors (18 µg/ml PMSF, 7 µg/ml pepstatin A, 4 µg/ml leupeptin, 1.5 µg/ml antipain, 0.25 µg/ml chymostatin). Cells were broken by lysozyme (10 mg/ml for 1 hr at 0 °C) followed by sonication (5 x 30 secs with a 30 sec cooling period in a Sanyo Soniprep 150 sonicator at 10 µm deflection, using a 6 mm probe). The lysate was centrifuged for 15 mins at 13,000 g, and the soluble (supernatant) and insoluble (pellet) fractions retained.

[2.46]Nickel affinity chromatography

10 mM imidazole was added to the protein solution to prevent non-specific binding. The solution was then applied to a nickel-NTA-agarose column at approximately 2 mg fusion protein per ml of resin. The column was washed ten times with 20 mM Tris-Cl, 150 mM NaCl, 35 mM imidazole, pH 7.4, using 10 ml per ml of resin. Protein was eluted using 4 x 0.5 ml of 20 mM Tris-Cl, 150 mM NaCl, 250 mM imidazole, pH 7.4. Typically 85 % of the fusion protein was eluted in the second and third fractions.

[2.47]Removal of poly-histidine tag from recombinant BID

BID (1ml; approximately 1 mg) was diluted 10-fold with 20 mM Tris-Cl, 150 mM NaCl, 2.5 mM $CaCl_2$, pH 8.4 and 0.5 units of thrombin added to cleave the poly-histidine tag. The reaction was incubated for 3 hr at room temperature.

[2.48]Buffer exchange of BID

After ion exchange chromatography, the BID buffer was exchanged to 20 mM K-HEPES, 15 % glycerol, pH 7.4. First, BID was concentrated approximately 10 times using a Centricon centrifugal filter (Amicon). BID was then diluted 10-fold in 20 mM K-HEPES pH 7.4, and again concentrated by centrifugal filtration. This procedure was repeated 3 times in total, and glycerol was then added to 15 %. The preparation was stored in aliquots at –70 °C.

[2.49]Generation of tBID

Recombinant BID was incubated with recombinant caspase 8 (Calbiochem) to produce tBID *in vitro*. 1 – 2.5 units of Caspase 8 was added to 300 µl of respiration buffer [2.31.1] containing 0.5 µg BID. The reaction was incubated at 20 °C for 30 mins – 24 hr. For cytochrome c release experiments, varying quantities of this tBID preparation were mixed with respiration buffer to give 20 µl reaction volumes containing the desired concentration of tBID protein.

[2.50]Expression of recombinant cyclophilin A

[2.50.1]GST-cyclophilin A

A pGEX-cyclophilin A plasmid, encoding human cyclophilin A with an N-terminal GST tag, was available in the lab. An overnight culture of *E. coli* DH5α, harbouring this plasmid, was diluted 10-fold to 500 ml with fresh nutrient broth. After growing to an OD_{600} of 0.6, IPTG was added to 40 µg/ml. Cells were grown for 10 hr at room temperature, and harvested by centrifuging for 15 mins at 4500 g. The pellet was resuspended in 15 ml of 100 mM NaCl, 20 mM Tris-Cl, 0.5 mM EDTA, pH 7.2, containing 18 µg/ml PMSF, 7 µg/ml pepstatin A, 4 µg/ml leupeptin, 1.5 µg/ml antipain, 0.25 µg/ml chymostatin as protease inhibitors, plus 10 mg/ml hen egg white lysozyme, and incubated on ice for 1 hr. Cells were sonicated for 10 x 40 secs with a 30 sec cooling period, in a Sanyo Soniprep 150 sonicator at 10 µm deflection, using a 6 mm probe. Triton X-100 was added to 1 %, and cell debris removed by centrifuging for 15 mins at 13,000 g. The supernatant was passed three times over GSH-agarose beads, in a glass column, which were then washed with 10 x 2 ml of PBS-T. Bound fusion protein was eluted with 7 x 0.5 ml of 150 mM NaCl, 20 mM Tris-Cl, 2.5 mM $CaCl_2$, 50 mM GSH, pH 8.5.

[2.50.2]Cleavage of GST tag

The GST tag was cleaved from the fusion protein (3.5 ml; above) by incubating overnight at 4 °C with 30 units of thrombin. The reaction mixture was diluted to 25 ml with 10 mM K-HEPES, pH 7.0, and dialysed overnight against this buffer. The protein was applied to a Mono-S cation exchange column, and eluted with a gradient of 0 – 250 mM NaCl in 10 mM K-HEPES, pH 7.0. The elution profile is

shown in Figure 14. The un-cleaved GST-cyclophilin A fusion protein co-eluted with cyclophilin A, and so this contaminant was removed by passing over GSH-agarose beads. The final cyclophilin A preparation was concentrated using a Centricon centrifugal filter (Amicon), and stored at 5 mg/ml at -70 °C in 10 mM K-HEPES pH 7.0. Figure 15 shows the protein species present at each stage of the purification.

[2.51]Generating epitope-tagged cyclophiiin D constructs

[2.51.1]Choice of tag

Three alternative tags were used, having the following amino acid sequences: YPYDVPDYA (HA tag); DYKDDDDK (FLAG tag) or DYKDHDGDYKDHDIDYKDDDDK (3xFLAG tag). The triple-flag (3xFLAG) tag was reported to give a ten-fold increase in detection sensitivity over the single FLAG epitope on Western blot [230]. However, it was possible that the high negative charge of this tag (net charge –7) might interfere with protein tertiary structure and/or protein-protein interactions. The single-flag tagged construct was thus also prepared as a precaution.

[2.51.2]Vector

The pcDNA 3.1(+) plasmid [Figure 12] was used to generate the tagged cyclophilin D vectors. The pcDNA vectors are suitable for one-step gene cloning, having an ampicillin resistance gene and pUC replication origin for selection and propagation in *E. coli* as well as sequences for gene expression in mammalian cell culture.

[2.51.3]Template

The rat cyclophilin D gene has previously been cloned in our lab [231], and an expression vector coding for full-length cyclophilin D was available. This was used as a template for preparing the cyclophilin D inserts by PCR.

[2.51.4]Primers

The following primer sequences were used to generate the HA and FLAG tagged constructs. Tags were all C-terminal, since the N-terminal pre-sequence of cyclophilin D is cleaved following import into mitochondria. A Kozak translation initiation sequence was included around the initiator ATG codon [229].

HA

```
Forward - 5' AAAA GGATCC ACC ATGCTAGCTCT
                  BamH1       Coding

Back    - 5' AAAA GAATTC TTA AGCGTAATCCGGAACATCGTATGGGTA GCTCAACTGGC
                  EcoR1 Stop          HA Tag                Coding
```

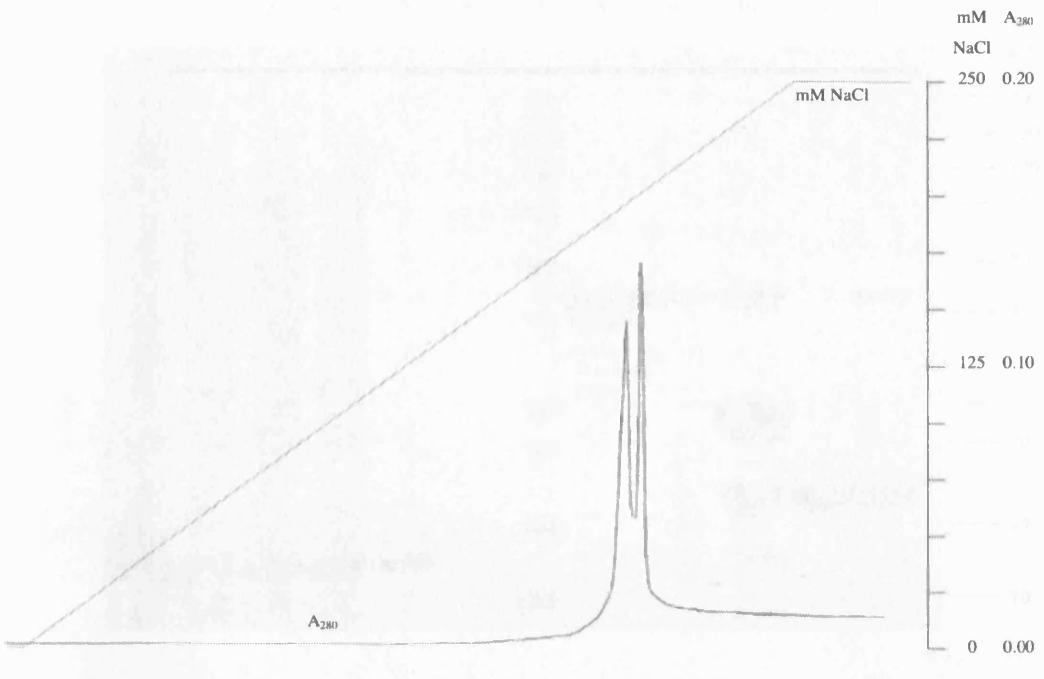

Figure 14 - Cyclophilin A elution profile.
Cleaved GST-cyclophilin A was applied to a mono-S column, and eluted with a linear gradient from 0 to 250 mM NaCl.

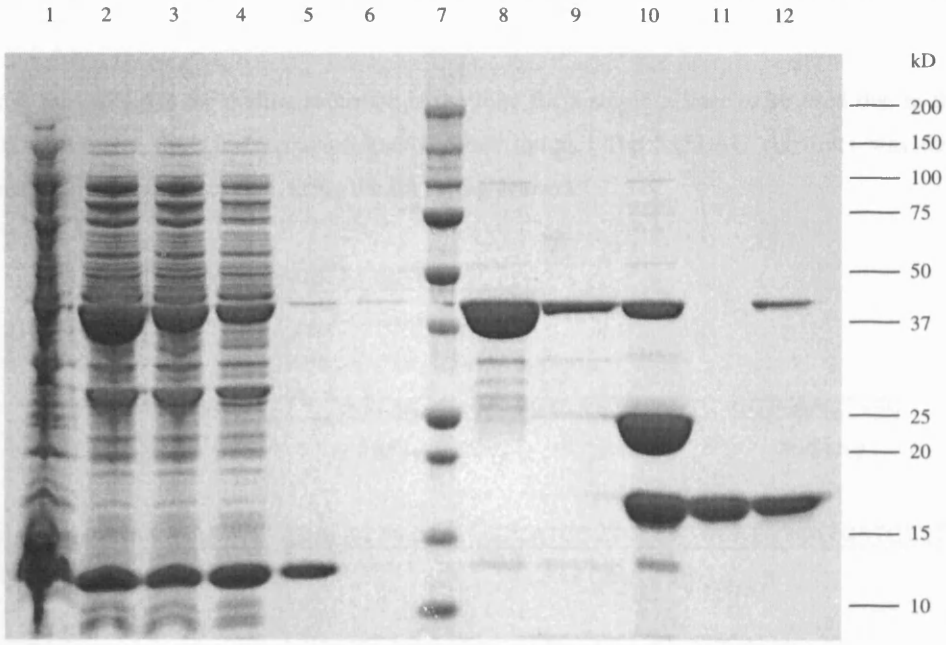

Figure 15 - Purification of cyclophilin A.
Lane 1 – Insoluble fraction from expression cells; Lane 2 – Soluble fraction from expression cells; Lane 3 – GSH-agarose flow-through; Lane 4 – First GSH-agarose wash with PBS-T; Lane 5 – Fifth GSH-agarose wash with PBS-T; Lane 6 – Tenth GSH-agarose wash with PBS-T; Lane 7 – Markers (Odyssey; [12.1.1]); Lane 8 – GST-agarose eluate; Lane 9 – Final 0.5 ml of GST-agarose eluate; Lane 10 – Products of overnight thrombin cleavage reaction; Lane 11 – Final cyclophilin A preparation; Lane 12 – Mono-S elution fraction

FLAG

```
Forward - 5' AAAA GGATCC ACC ATGCTAGCTCT
                  BamH1      Coding

Back    - 5' AAAA GAATTC TTA CTTATCGTCGTCATCCTTGTAATC GCTCAACTGGC
                  EcoR1 Stop       FLAG Tag           Coding
```

3xFLAG

The length of the 3xFLAG tag coding sequence is too long for a single primer to be used due to the potential for secondary structure formation and/or dimerisation. The 3xFLAG construct was thus generated using a two-step procedure, using the following primers:

```
Forward - 5' AAAA GGATCC ACC ATGCTAGCTCT
                  BamH1      Coding

1st back - 5' AAAA TGATCTTTATAATCACCGTCATGGTCTTTGTAGTC GCTCAACTGGC
                                3xFLAG Tag              Coding

2nd back - 5' AAAA GAATTC TTA CTTGTCATCGTCATCCTTGTAATCGATATCATGATCTTT
                  EcoR1 Stop          3xFLAG Tag
```

[2.51.5]Vector production

The cyclophilin D gene was successfully amplified by PCR [2.2], yielding from 2.5 µg (3xFLAG construct) to 17 µg (HA construct) of product of the expected size (655 – 685 base pairs (b.p.)), as shown in Figure 16. The constructs and vector were digested with BamH1 and EcoR1, and ligated with T4 DNA ligase [2.6], as shown in Figure 17.

DH5α competent cells were transformed with the vectors and grown on agar plates with ampicillin selection [2.7]. Several isolated colonies were picked, and plasmid DNA prepared by mini-prep [2.9]. Plasmid DNA was digested with BamH1 and EcoR1 to confirm insert presence, as shown in Figure 18. The cyclophilin D constructs were verified by DNA sequencing [2.10]. All had the expected sequence.

[2.51.6]Expression

B50 cells were transiently transfected with the three expression plasmids [2.39]. Cells were grown for 48 hr.

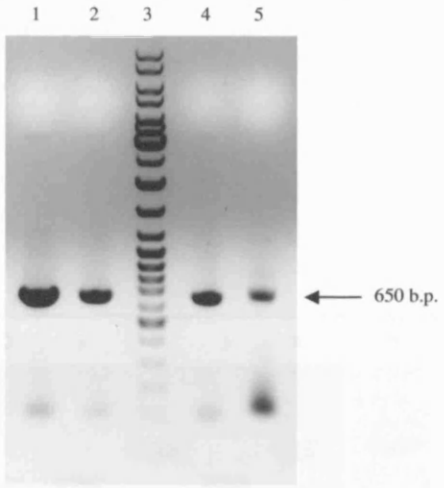

Figure 16 - The cyclophilin D gene was successfully amplified by PCR.
Lane 1 – HA construct. Lane 2 – FLAG construct. Lane 3 – GeneRuler DNA Ladder Mix (Fermentas; [12.1.2]). Lane 4 – 3xFLAG construct – 1st round. Lane 5 – 3xFLAG construct – 2nd round.

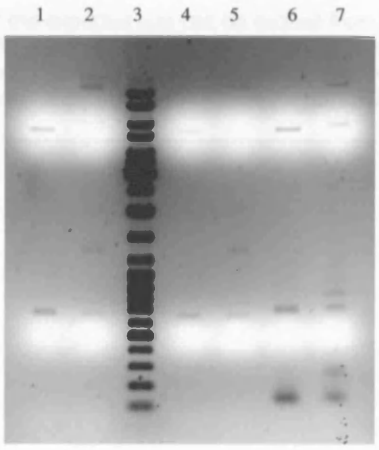

Figure 17 - The cyclophilin D constructs were ligated into pcDNA 3.1 (+).
Lanes 1 and 2 – HA construct pre- and post- ligate (respectively). Lane 3 – GeneRuler DNA Ladder Mix (Fermentas; [12.1.2]). Lanes 4 and 5 - FLAG construct pre- and post-ligate (respectively). Lanes 6 and 7 – 3xFLAG construct pre- and post- ligate (respectively).

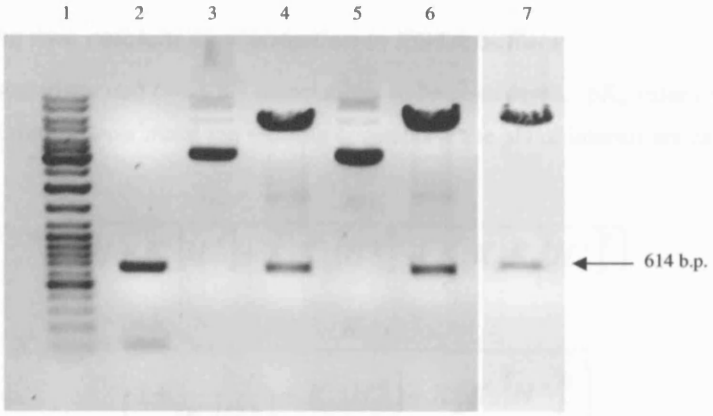

Figure 18 - An insert of the expected size can be excised from the plasmid constructs. Lane 1 – GeneRuler DNA Ladder Mix (Fermentas; [12.1.2]). Lane 2 – HA construct PCR product for size comparison. Lanes 3 and 4 – HA plasmid pre- and post- digest. Lanes 5 and 6 – FLAG plasmid pre- and post- digest. Lane 7 – 3xFLAG construct post- digest.

[2.51.7]Assessment of transfection efficiency

Transfection efficiency was assessed for the 3xFLAG construct. Coverslips were seeded with B50 cells, transfected with 1, 2 or 4 μg of vector, and grown for 48 hr [2.37]. Cells were fixed and permeabilised [2.40] and probed with an anti-FLAG antibody followed by a fluorescein-labelled anti-mouse IgG secondary antibody (Invitrogen) [2.41]. Nuclei were stained using propidium iodide (50 μg/ml in PBS).

Miscellaneous methods

[2.52]Calculating the free calcium concentration in EGTA buffers

There are three H^+ associations and two Ca^{2+} associations to be considered. pK_a values for these are given in Table 1. First the apparent metal ion stability constants at the pH of interest are calculated :

$$K_{4-app} = \frac{K_4}{\left(1 + K_1[H^+] + K_1K_2[H^+]^2 + K_1K_2K_3[H^+]^3\right)}$$

$$K_{5-app} = \frac{K_5}{\left(1 + \frac{1}{K_1[H^+]} + K_2[H^+] + K_2K_3[H^+]^2\right)}$$

Then the apparent combined stability constant for Ca^{2+} binding, k_{comb} is calculated :

$$K_{comb} = K_{4-app} + K_{5-app}$$

Now, if $[Ca]_f$ is the free calcium ion concentration, and $[Ca]_i$ is the initial calcium concentration, and we define:

$$X = \{K_{comb}(E - [Ca]_i)\} + 1$$

Then:

$$[Ca]_f = \frac{-X + \sqrt{X^2 + 4 \cdot K_{comb} \cdot [Ca]_i}}{2 \cdot K_{comb}}$$

Since the association constant (K_a) for other divalent cations is orders of magnitude lower than that for calcium (e.g. pK_a for the first metal ion association -10.97 for calcium compared with -5.19 for magnesium), the effect of these other ions can be ignored for practical purposes if their concentration is comparable to that of calcium.

Association constant	Association equation	pK_a
K_1	Ca.EGTA / EGTA + Ca	-10.97
K_2	Ca.H.EGTA / H.EGTA + Ca	-5.30
K_3	H.EGTA / EGTA + H	-9.47
K_4	H_2.EGTA / H.EGTA + H	-8.85
K_5	H_3.EGTA / H_2.EGTA + H	-2.66

Table 1 - EGTA pK_a values for H^+ and Ca^{2+}.
Data taken from [232].

CHAPTER 3 : CLONING AND EXPRESSION OF BID

[3.1]Introduction

[3.1.1]Choice of BID

BID is one of the less well characterised BCL-2 proteins. Multiple mechanisms have been suggested to explain its mechanism of action in initiating mitochondrial outer membrane permeabilisation. These mechanisms are based on a number of reported properties of clear relevance to apoptotic signalling in mitochondria, including cleavage by caspases [93,135]; catalysis of oligomerisation of multi-domain pro-apoptotics in mitochondria [8,102,233,234]; pore-forming ability [80,143]; and lipid transfer activity [131,146].

Several groups have purified native or recombinant BID for use in *in vitro* studies. BID was originally purified as a cytochrome c releasing factor by Luo and co-workers [93]. These authors used a series of gel filtration and ion exchange chromatography steps to purify approximately 10 μg of BID from 3 g of HeLa cell extract. The same authors subsequently expressed recombinant human BID as a 6xHis-tagged fusion protein in *E. coli*.

[3.1.2]Choice of specie

BID amino acid sequence is not well conserved across species. Figure 19 shows a multiple alignment of the human, rat and mouse sequences. The mouse and human sequences show only 65 % identity, as compared to an average value of around 85 % for orthologous genes across these two species [235]. There is only 60 % identity between all three sequences.

Thus the choice of specie from which to clone *Bid* was important. Previously available in the lab were a selection of B50 cell lines (a rat neuroblastoma cell line) of various different genotypes. Additionally, rats provide a plentiful source of mitochondrial protein for *in vitro* studies. Thus it was decided to work entirely with rat systems, and therefore to clone the rat *Bid* gene.

[3.2]Generation of expression plasmid

[3.2.1]Production of first-strand cDNA from rat liver

Total RNA was extracted from rat liver using a commercial kit [2.43]. The extract was analysed by agarose gel electrophoresis [2.3] [Figure 20]. As expected, the 28S and 18S ribosomal RNA bands were clearly visible, with the 28S band approximately twice the intensity of the 18S band. However there was some smearing, potentially indicating RNA degradation. The absorbance ratio A_{260} / A_{280} of the extract was measured. RNA absorbs at 260 nm, so that A_{260} is proportional to [RNA], and protein absorbs at 280 nm, so that A_{280} is proportional to [protein]. Protein contamination of RNA samples thus lowers the ratio A_{260} / A_{280}; a value above 1.8 indicates the RNA is free from protein contamination. The value for this RNA preparation was 2.01, indicating no protein contamination.

```
Rat             MDSEVSNGSGLGAEHITNLLVFGFLR-NNDRDFHQELEVLGQELPVQV-YLEGDREDELQ 58
Mouse           MDSEVSNGSGLGAEHITDLLVFGFLQ-SSG-CTRQELEVLGRELPVQA-YWEADLEDELQ 57
Human           MDCEVNNGSSLRDECITNLLVFGFLQSCSDNSFRRELDALGHELPVLAPQWEG--YDELQ 58
                **.**.***.*  * **:*******:  ..   ::**:.**:**** .   *.   ****

Rat             TDGSRASRSFYHGRIEPDSESQDEVIHNIARHLAQAGDELDHSIQPTLVRQLAAQFMNGS 118
Mouse           TDGSQASRSFNQGRIEPDSESQEEIIHNIARHLAQIGDEMDHNIQPTLVRQLAAQFMNGS 117
Human           TDGNRSSHSR-LGRIEADSESQEDIIRNIARHLAQVGDSMDRSIPPGLVNGLALQLRNTS 117
                ***.::*:*   ****.*****:::*:******** **.:*:.* * **. ** *: * *

Rat             LSEEDKRNCLAKALDEVKTSFPRDMENDKAMLIMTMLLAKKVASHAPSLLRDVFRTTVNF 178
Mouse           LSEEDKRNCLAKALDEVKTAFPRDMENDKAMLIMTMLLAKKVASHAPSLLRDVFHTTVNF 177
Human           RSEEDRNRDLATALEQLLQAYPRDMEKEKTMLVLALLLAKKVASHTPSLLRDVFHTTVNF 177
                 ****:.. **.**:::  ::*****::*:**::::*********:********:*****

Rat             INQNLFSYVRDLVRNEMD 196
Mouse           INQNLFSYVRNLVRNEMD 195
Human           INQNLRTYVRSLARNGMD 195
                ***** :***.*.** **
```

Figure 19 - Multiple sequence alignment of rat, mouse and human BID proteins by the ClustalW tool.
Alignment of the three sequences with ClustalW [236] shows that the proteins have only 60% sequence identity. * = Identical residue, : = Conserved residue, . = Semi-conserved residue.

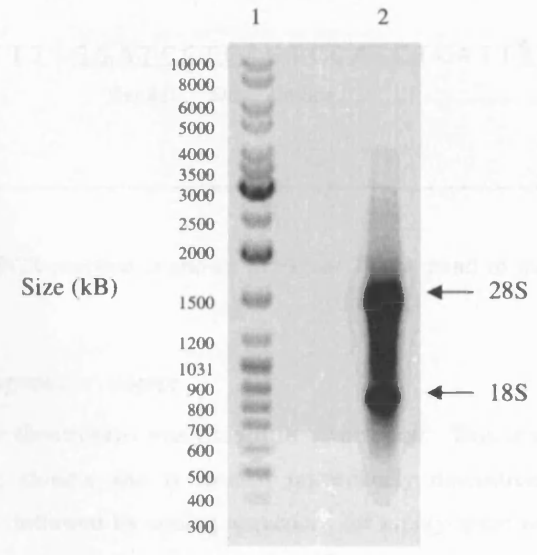

Figure 20 - Extraction of rat liver total RNA.
Total RNA was isolated from 60 mg of rat liver [2.43]. 2 % of the extracted RNA (5 µl) was run on a 0.8 % agarose gel containing ethidium bromide (1 µg/ml) and visualised under UV illumination [2.3]. Lane 1 – GeneRuler DNA Ladder Mix (Fermentas; [12.1.2]), 1.5 µg total DNA. Lane 2 – Extracted RNA

First-strand cDNA was produced from the total RNA using AMV reverse transcriptase and a commercial kit [2.44]. The following primer was used, which is complementary to the 3' end of the BID gene :

5' - T T T T T G G A T C C T C A G T C C A T C T C A T T T C T A A C C A - 3'
BamH1 Stop Coding.....

The product of 1st strand synthesis is shown in Figure 21. A band of the expected size (612 b.p. plus 5' untranslated region = approximately 640 b.p.) was generated.

[3.2.2]Generation of BID fragment for ligation into expression vector

The *Bid* cDNA was used as a template for PCR [2.2], using the following primers. The primers were complementary to the 5' and 3' ends of the BID gene, with the addition of NdeI and BamH1 cleavage sites.

5' Primer

5' - T T T T T C A T A T G G A C T C T G A G G T C A G C A A C G G - 3'
Nde1 Coding.....
Start

3' Primer

5' - T T T T T G G A T C C T C A G T C C A T C T C A T T T C T A A C C A - 3'
BamH1 Stop Coding.....

The product of the PCR reaction is shown in Figure 22. A band of the expected size (612 b.p.) was generated.

[3.2.3]Choice of expression vector

The pET-15b vector (Invitrogen) was chosen for expression. This is an *E. coli* expression vector in which the multiple cloning site is located immediately downstream of transcription/translation initiation sequences, followed by coding sequences for a poly-histidine tag and a thrombin cleavage site. This allows production of an N-terminal 6xHis-tagged fusion protein which can be purified by nickel affinity chromatography. Since the 6xHis tag can interfere with protein function, it is desirable to remove it after purification; this can be achieved by cleavage of the fusion protein with thrombin.

[3.2.4]Ligation into pET-15b

Insertion of the BID fragment into the pET-15b vector was attempted by standard restriction enzyme digestion and ligation [2.6].

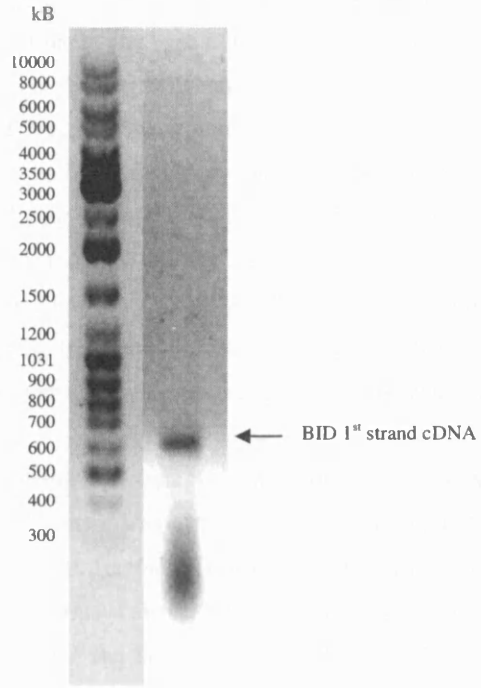

Figure 21 - Production of *Bid* first-strand cDNA.
cDNA was generated from total RNA by RT-PCR, using AMV reverse transcriptase and a commercial kit [2.44]. 5 % of the reaction product (5 µl) was run on a 0.8 % agarose gel containing ethidium bromide (1 µg/ml) and visualised under UV illumination [2.3]. Lane 1 – DNA Ladder Mix (Fermentas; [12.1.2]), 1.5 µg total DNA. Lane 2 – cDNA synthesis reaction.

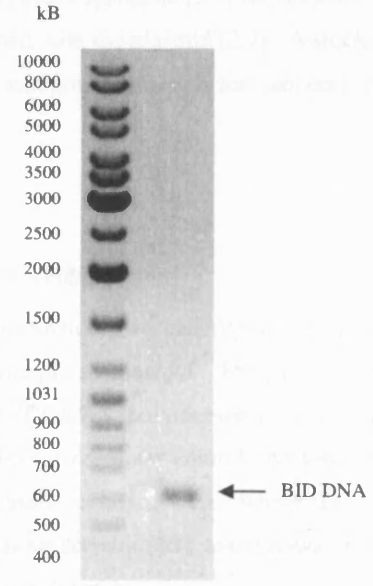

Figure 22 - Generation of BID cDNA by PCR.
Bid DNA was amplified from the first-strand cDNA by PCR [2.2]. 5 % of the reaction product (5 µl) was run on a 0.8 % agarose gel containing ethidium bromide (1 µg/ml) and visualised under UV illumination [2.3]. Lane 1 – Ladder Mix (Fermentas; [12.1.2]), 1.5 µg total DNA. Lane 2 – PCR reaction

However, despite repeated attempts, this was unsuccessful, and no positive transformants were generated. This was possibly due to inefficient cleavage of the PCR product by the restriction enzymes due to the cleavage sites being too close to the fragment end.

To overcome this problem, the PCR fragment was blunt-end ligated into the pPCR-Script vector (Stratagene). This vector utilises a unique ligation strategy, based on the uncommon restriction site of Srf1. As described above [2.8], the ligation mixture contained *Srf* I in addition to the pPCR-Script vector, insert and T4 DNA ligase. Cleavage of the *Srf* I site generates linear vector, which inter-converts with the closed form through the opposing action of T4 ligase. Insertion of the PCR fragment, however, disrupts the *Srf* I site, trapping the vector in the closed state with insert. Insertion of the fragment also disrupts the LacZ gene carried by the vector, allowing blue-white selection of positive transformants [2.7.4].

Positive transformants were generated using this strategy. Plasmid DNA was isolated from one of the clones by mini-prep [2.9]. The BID fragment was excised by digestion with BamH1 and NdeI, as shown in Figure 23. The expected 612 b.p. fragment (*Bid* DNA) was excised when both restriction enzymes were used to digest the vector. This was the *Bid*-coding fragment which contained the two sticky-ended restriction sites generated by the two restriction enzymes, Nde1 and BamH1. An additional band of 650 b.p. was generated by digestion with BamH1 alone, due to the presence of a BamH1 site in the pPCR-Script vector sequence upstream of the Nde1 cleavage site. In the double digest, the predicted extra 38 b.p. Nde1-BamH1 fragment was not recovered.

The excised *Bid* DNA was purified from an agarose gel fragment [2.3] using a commercial kit [2.4]. The pET-15b vector was digested with BamH1 and NdeI to generate sites for insertion of the BID DNA [2.6.1], and the purified BID fragment was ligated into the vector with T4 DNA ligase [2.6.3]. Ligation was confirmed by agarose gel electrophoresis [2.3], as shown in Figure 24.

DH5α competent cells were transformed with the plasmid [2.7]. A stock of the expression plasmid was made from an overnight culture by miniprep [2.9], and the sequence of the *Bid* gene confirmed by DNA sequencing [2.10].

[3.3]Expression

[3.3.1]Development of expression conditions

The expression plasmid was used to transfect two cell types [2.7.3]: firstly *E. coli* DE3 cells, and secondly *E. coli* DE3 cells carrying the pLysS plasmid. The pLysS plasmid directs production of T7 lysozyme, a natural inhibitor of the T7 RNA polymerase used in the pET-15 expression system. DE3 pLysS cells thus have more stringent promoter control and lower background expression levels. This can help in establishing stable transfectants in cases where the recombinant protein is toxic to *E. coli* (given that BID has pore-forming activity [80], toxicity was a potential problem). Figure 25 shows the result of transfecting the two cell types.

Bid was poorly expressed in the DE3 pLysS strain, but was well expressed in DE3 cells following induction, and was the major protein in the soluble fraction. Expression was repeated with growth at 30 °C, in order to increase the proportion of protein present in the soluble compared to the insoluble fraction. However, the effect was marginal [not shown].

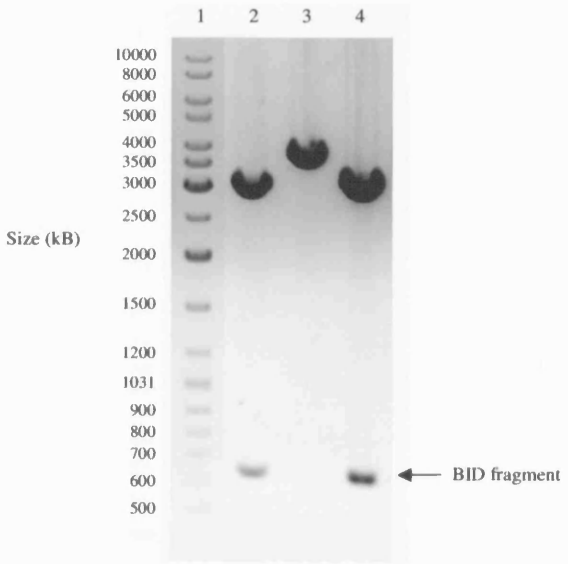

Figure 23 - Excising BID DNA from the pPCR-Script vector.
500 ng of plasmid DNA was digested with BamH1 (lane 2), NdeI (lane 3) or both BamH1 and NdeI (lane 4). Products were run on a 0.8 % agarose gel containing ethidium bromide (1 µg/ml) and visualised under UV illumination [2.3]. The band at 650 b.p. in lane 2 results from a BamH1 cleavage site in the vector DNA sequence. Lane 1 – DNA Ladder Mix (Fermentas; [12.1.2]), 1.5 µg total DNA.

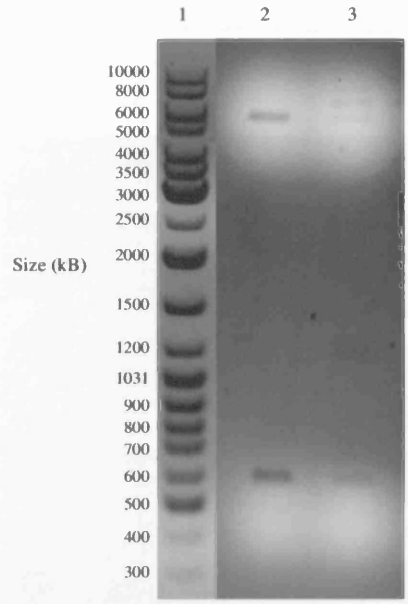

Figure 24 - Ligation of BID DNA into pET-15b.
Vector DNA was digested with BamH1 and NdeI and the BID fragment ligated into the cloning site using T4 DNA ligase [2.6]. 80 ng of the pre-ligate (lane 2) and post-ligate (lane 3) was run on a 0.8 % agarose gel containing ethidium bromide (1 µg/ml) and visualised under UV illumination. Lane 1 – DNA Ladder Mix (Fermentas; [12.1.2]), 1.5 µg total DNA.

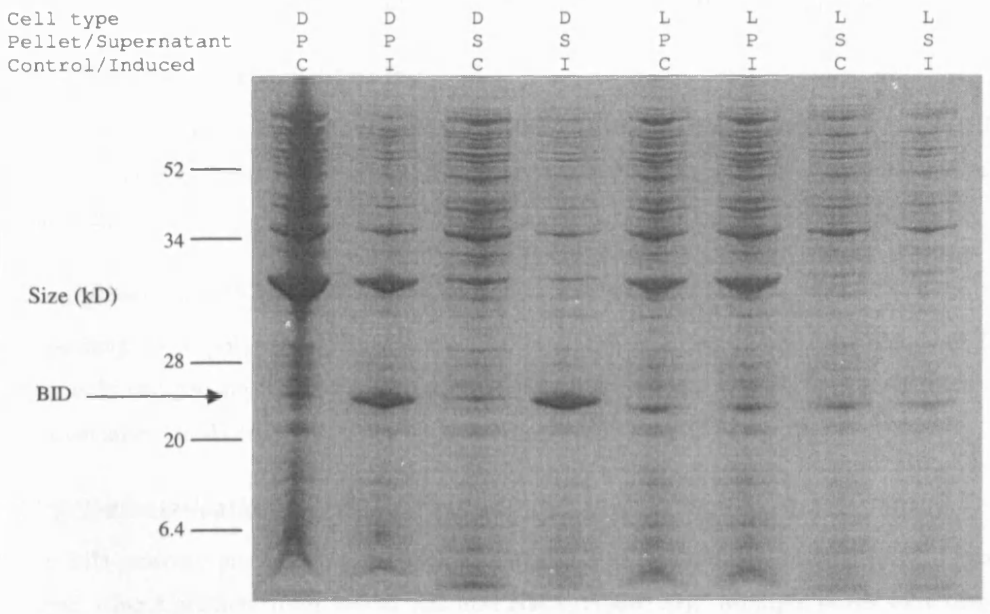

Figure 25 - Expression of recombinant BID.
BID was expressed in *E. coli* DE3 cells (D) or *E. coli* DE3 pLysS cells (L) [2.45].
Approximately 5 µg of the insoluble (pellet; P) and soluble (supernatant; S) fractions from control (non-induced; C) and induced (I) cells were run on 10 % SDS-PAGE [2.13].
Bands were visualised by Coomassie staining [2.14.1].

An expression time-course was carried out, as shown in Figure 26. Maximal expression of BID relative to other cellular proteins occurred after 4 hr induction, and this time was thus used for large-scale expression.

[3.4]Purification

[3.4.1]Nickel affinity chromatography

BID was expressed as above [3.3] on a large scale, and the soluble fraction used to purify the N-terminally 6xHis-tagged fusion protein by nickel affinity chromatography [2.46]. The flow-through, wash and elution fractions were retained and analysed by SDS-PAGE [2.13] [Figure 27].

[3.4.2]Removal of poly-histidine tag

The 6xHis tag was removed from recombinant BID by digestion with thrombin [2.47]. BID pre- and post- digestion is shown in Figure 28. It is clear that BID was essentially completely cleaved from the 6xHis tag.

[3.4.3]Aberrant mobility on SDS-PAGE

Depending on the polyacrylamide gel type, BID runs with an apparent molecular weight of 24 – 30 kD. This is in comparison with its predicted molecular mass of 22.2 kD. This is most likely due to the unusual amino acid composition of BID, and especially of rat BID [Table 2].

[3.5]Characterisation of recombinant BID by ion exchange chromatography

The BID cleavage products were applied to a Mono-Q anion exchange column [2.12]. Proteins were eluted using a gradient from 150 to 500 mM NaCl [Figure 29]. Multiple peaks were detected. The fractions indicated [Figure 29; 1 – 13] were then further analysed by SDS-PAGE [2.13] [Figure 30]. Fractions 1 – 3 contained multiple species, but fractions 4 – 13 all appeared to contain BID as the major protein specie. The difference in behaviour on FPLC presumably related to a difference in conformational state or oligomeric form. This may be due to intermolecular disulphide formation; to intermolecular hydrophobic interactions; or to interaction of BID with cardiolipin or other membrane lipids from *E. coli* (BID binds to cardiolipin and mono-lyso-cardiolipin [237]).

[3.6]Characterisation of recombinant BID by gel filtration

To investigate the oligomeric form of the various fractions above, samples were passed through a gel filtration column [2.12], and the apparent molecular mass of protein species recorded. The column was calibrated using a mixture of blue dextran and standard proteins; the calibration curve is shown in Figure 5 (page 44). A selection of the BID fractions shown in Figure 29 was then applied to the same column, and eluted under the same conditions. By comparison with the standards, the apparent molecular mass of the BID species present was calculated, as shown in Table 3. A range of oligomers was detected, but no BID monomer was evident.

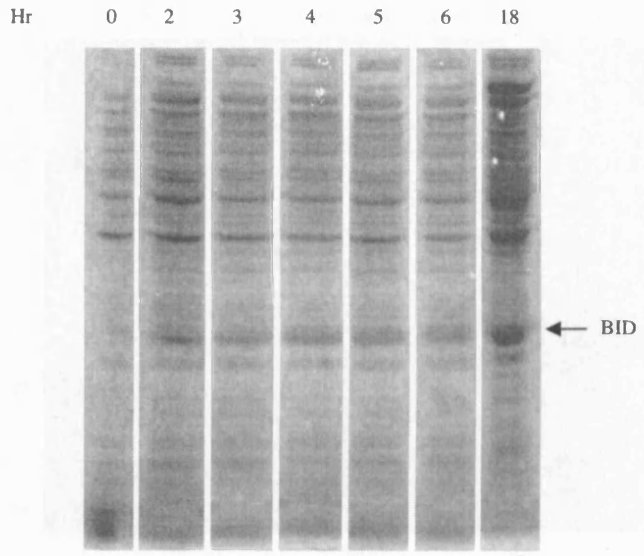

Figure 26 - Time-course of Bid expression.
BID was expressed in *E. coli* DE3 cells [2.45]. Culture samples were taken at the indicated times and the soluble cell fraction run on 10 % SDS-PAGE [2.13]. Bands were visualised by Coomassie staining [2.14.1].

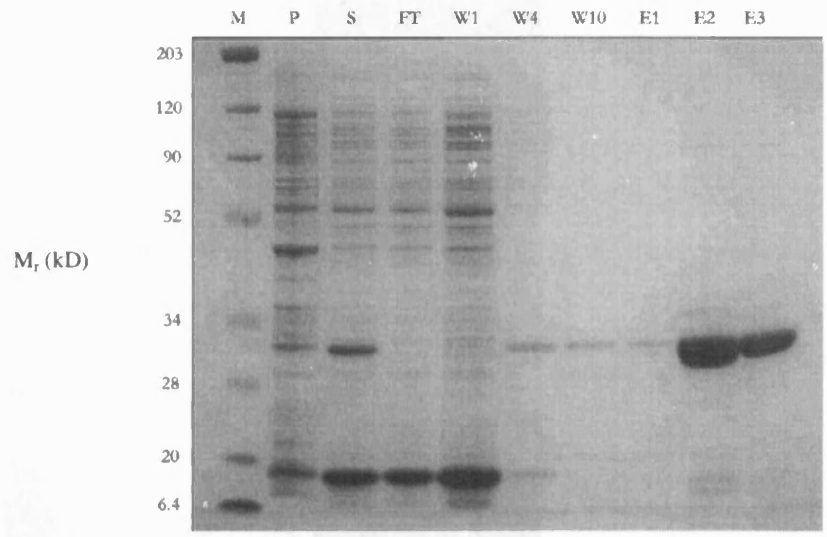

Figure 27 - Purification of BID by nickel affinity chromatography.
A large-scale culture of BID expression strain [2.45] was separated into insoluble (pellet; P) and soluble (supernatant; S) fractions. The supernatant was applied to a 0.5 ml nickel-NTA-agarose column [2.46]. The flow-through (FT) was retained. The column was washed 10 times with 35 mM imidazole (W1, W4, W10) and BID was then eluted with 4 x 0.5 ml of 250 mM imidazole (E1, E2, E3). 10 µl of each fraction was run on 10 % SDS-PAGE [2.13], and bands visualised by Coomassie staining [2.14.1]. M – Size markers [12.1.1].

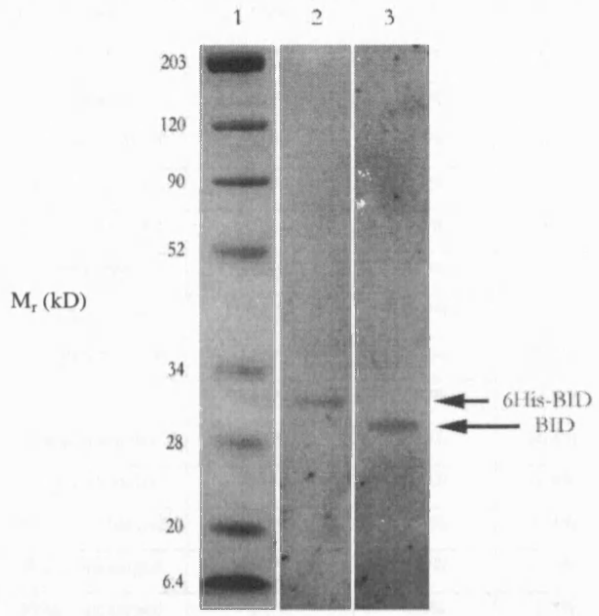

Figure 28 - Removal of the polyhistidine tag from recombinant BID by digestion with thrombin.
Approximately 1 mg of 6xHis-BID was digested with thrombin [2.47]. 2 µg of the cleavage reaction was run on 10 % SDS-PAGE [2.13], and bands visualised by Coomassie staining [2.14.1]. Lane 1- Size markers [12.1.1]. Lane 2 - Uncleaved His6-BID. Lane 3 - Cleaved BID.

Amino Acid	Character	Frequency in Vertebrates	Frequency in Rat BID	Difference	Frequency in Human BID	Difference
Alanine	Small nonpolar	7.4%	6.6%	-0.8%	6.7%	-0.7%
Arginine	Charged positive	4.2%	7.1%	+2.9%	9.2%	5.0%
Asparagine	Polar, uncharged	4.4%	6.1%	+1.7%	6.7%	2.3%
Aspartic Acid	Charged negative	5.9%	8.7%	+2.8%	7.7%	1.8%
Cysteine	Polar, uncharged	3.3%	0.5%	-2.8%	1.5%	-1.8%
Glutamate	Charged negative	5.8%	8.7%	+2.9%	7.2%	1.4%
Glutamine	Polar, uncharged	3.7%	5.1%	+1.4%	4.6%	0.9%
Glycine	Small nonpolar	7.4%	5.1%	-2.3%	5.1%	-2.3%
Histidine	Polar, uncharged	2.9%	3.6%	+0.7%	2.6%	-0.3%
Isoleucine	Large nonpolar	3.8%	3.6%	-0.2%	3.6%	-0.2%
Leucine	Large nonpolar	7.6%	11.7%	+4.1%	14.4%	6.8%
Lysine	Charged positive	7.2%	3.1%	-4.1%	2.1%	-5.1%
Methionine	Large nonpolar	1.8%	3.6%	+1.8%	2.6%	0.8%
Phenylalanine	Large nonpolar	4.0%	4.6%	+0.6%	2.6%	-1.4%
Proline	Small nonpolar	5.0%	2.6%	-2.4%	3.1%	-1.9%
Serine	Polar, uncharged	8.1%	7.7%	-0.4%	8.7%	0.6%
Threonine	Polar, uncharged	6.2%	3.6%	-2.6%	4.6%	-1.6%
Tryptophan	Polar, uncharged	1.3%	0.0%	-1.3%	0.5%	-0.8%
Tyrosine	Polar, uncharged	3.3%	1.5%	-1.8%	1.5%	-1.8%
Valine	Large nonpolar	6.8%	6.6%	-0.2%	5.1%	-1.7%

TOTALS:						
	+ve	11.4%	10.2%	-1.2%	11.3%	-0.1%
	-ve	11.7%	17.4%	5.7%	14.9%	3.2%
	Polar uncharged	33.2%	28.1%	-5.1%	30.7%	-2.5%
	Small nonpolar	19.8%	14.3%	-5.5%	14.9%	-4.9%
	Large nonpolar	24.0%	30.1%	6.1%	28.3%	4.3%
	% -ve minus % +ve	**0.3%**	**7.2%**		**3.6%**	

Table 2 - Sequence comparison of rat and human BID, compared to vertebrate averages. Both human and rat BID have an excess of negative residues (glutamate and aspartate), and are thus predicted to carry a net negative charge.

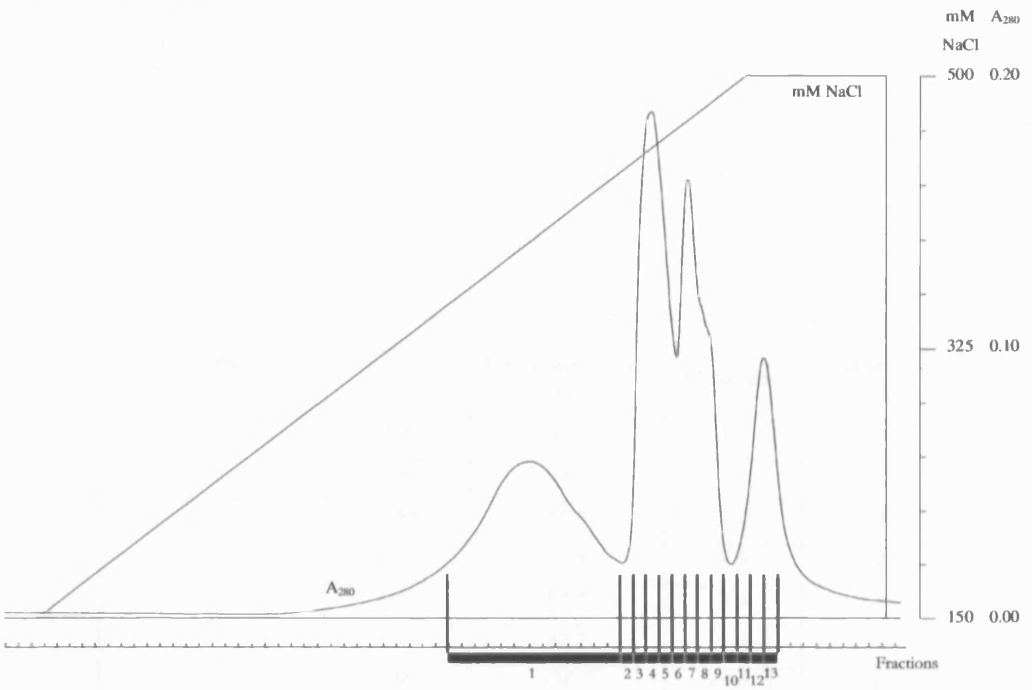

Figure 29 - Anion exchange chromatography of thrombin-digest of recombinant BID.
BID thrombin cleavage products were fractionated by FPLC on an anion exchange column [2.12] using a linear gradient from 150 to 500 mM NaCl. The absorption of the eluate at 280 nm was monitored. 0.5 ml fractions were collected.

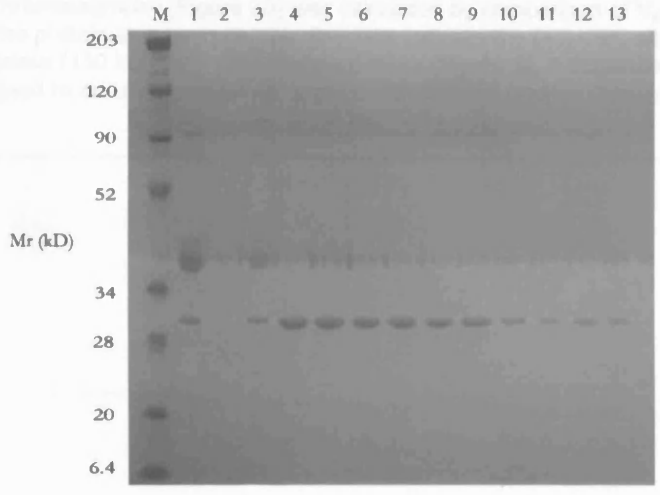

Figure 30 - SDS-PAGE analysis of FPLC peaks.
20 µl of fractions 1 – 13 shown in Figure 29 were run on 10 % SDS-PAGE [2.13], and bands visualised by Coomassie staining [2.14.1]. Lane 1 - Size markers [12.1.1].

Fraction (From Figure 29)	V_e/V_0	**Calculated mass (kD)**	**Oligomer**	**Oligomer** (1 S.F)
1	1.99	38.4	1.7	2
	3.00	0.63	-	-
4	1.80	85.4	3.9	4
	1.97	41.8	1.9	2
6	1.80	82.7	3.8	4
	1.97	42.7	1.9	2
7	1.69	130.7	(5.9)	(6)
	1.80	85.4	3.9	4
8	1.68	136.4	(6.2)	(6)
	1.79	89.1	4.0	4
13	1.07	1635.6	-	-

Table 3 - Gel filtration of BID protein.
The apparent molecular mass of the species present in fractions recovered from anion exchange chromatography [Figure 30] was calculated by comparison of V_e/V_0 values with those for the protein standards [2.12]. Brackets indicate the fact that, although alcohol dehydrogenase (150 kD) lay on the standard curve [Figure 5], a Superdex 75 column is not designed to accurately separate species with masses greater than approximately 80 kD.

[3.7]Generating monomeric BID

The entire purification was repeated in the presence of 1 mM DTT to reduce inter-molecular disulphides. The Mono-Q elution profile obtained is shown in Figure 31. Gel filtration analysis [2.12] showed the first major peak to be monomeric BID, and the second dimeric BID, presumably formed by hydrophobic interactions between molecules. The gel filtration profile and apparent molecular weights are shown in Figure 32. Peak 1 shown in Figure 31 was collected and stored in aliquots at -70 °C. However, on storage some breakdown of BID was noted (SDS-PAGE; not shown), possibly due to residual contaminating thrombin. Therefore an additional step was introduced, whereby the first peak shown in Figure 31 was further purified by hydrophobic interaction chromatography [2.12]. In this step, the protein was applied to a phenyl Superose column, and BID was eluted with a gradient from 1.7 to 0 M $(NH_4)_2SO_4$. The elution profile is shown in Figure 33; the indicated fraction was collected. SDS-PAGE [2.13] confirmed that the protein fraction indicated in Figure 33 was essentially pure BID [Figure 34]. BID was aliquoted and stored at 0.5 mg/ml at -70 °C, after conversion of the buffer to 20 mM K-HEPES, 15 % glycerol, pH 7.4 [2.48]. The final yield of the BID preparation was approximately 0.5 mg protein per litre of culture medium.

[3.8]Generation of tBID

The active form of BID *in vivo* (truncated BID; tBID) is generated by cleavage of BID at aspartate 59 by caspase 8 to yield an active 15 kD C-terminal fragment and a 7 kD N-terminal fragment. The two fragments are thought to remain associated following cleavage [238]. Recombinant BID was incubated with recombinant caspase 8 (Calbiochem) to produce tBID *in vitro* [2.49]. The reaction was carried out for varying periods, and analysed by SDS-PAGE [2.13] [Figure 35]. As expected, BID was cleaved into p15 and p7 fragments *in vitro* by caspase 8.

[3.9]Discussion

[3.9.1]Purification achieved

The final BID preparation produced was extremely pure, as evidenced by the single species visible on hydrophobic interaction chromatography [Figure 33], SDS-PAGE [Figure 34] and gel filtration [Figure 36].

[3.9.2]Stability of purified recombinant BID

To verify that the final BID preparation was stable over long-term storage, a sample of BID was thawed and analysed by gel filtration immediately after freezing. After two months storage, a further sample was analysed in the same way; the resulting profile was identical [Figure 36].

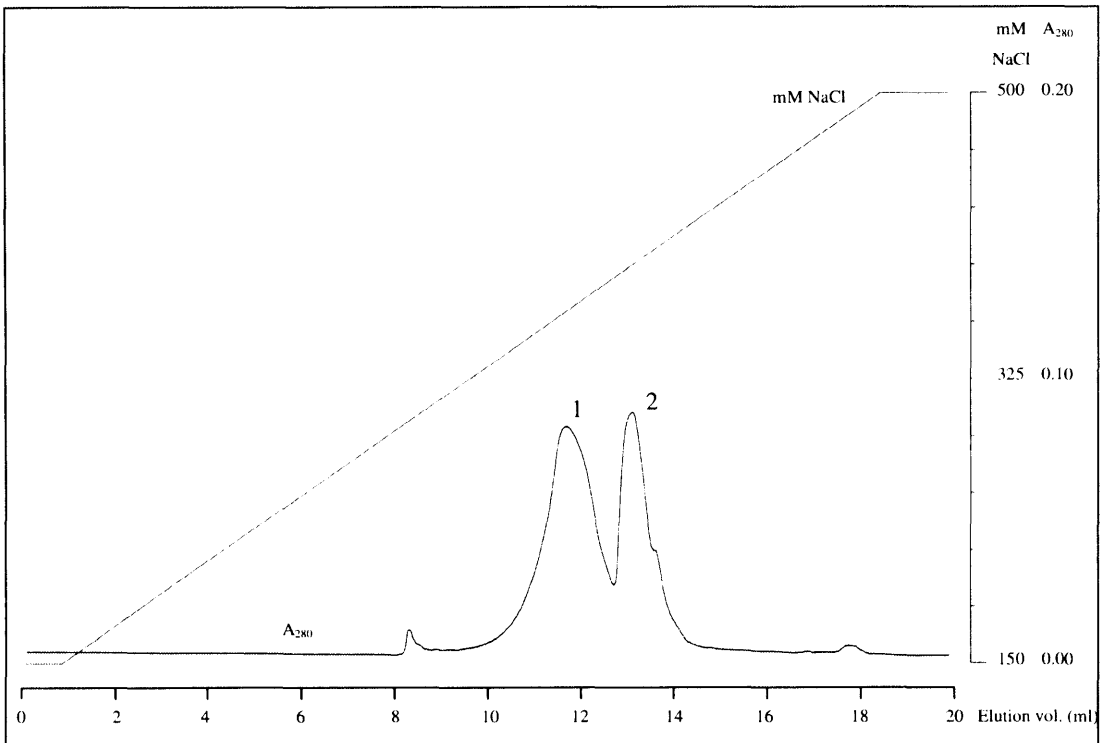

Figure 31 - Anion exchange chromatography of thrombin-digest of recombinant BID purified in the presence of 1 mM DTT.
DTT was present at every stage up to thrombin cleavage. BID thrombin cleavage products were fractionated by FPLC on an anion exchange column [2.12] using a linear gradient from 150 to 500 mM NaCl. The absorption of the eluate at 280 nm was monitored.

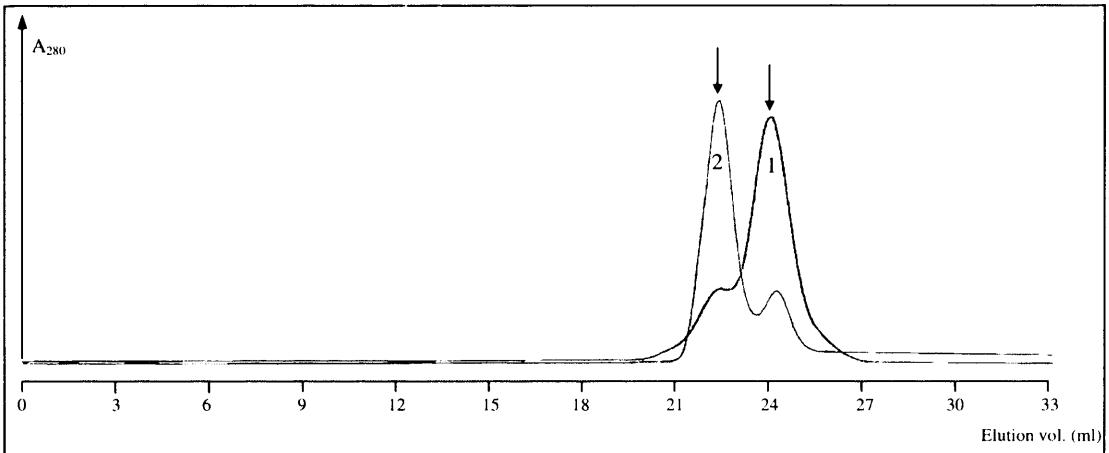

Peak	V_e/V_0	Apparent mass (kD)	Oligomer
2	1.95	45.0	2
1	2.11	23.3	1

Figure 32 - Gel filtration of BID, purified in the presence of 1 mM DTT.
The peaks labelled 1 and 2 in
Figure 31 were analysed by gel filtration [2.12]. By comparison of V_e/V_0 values with protein standards [Figure 5], peak 1 was revealed to be monomeric BID, and peak 2 to be dimeric BID.

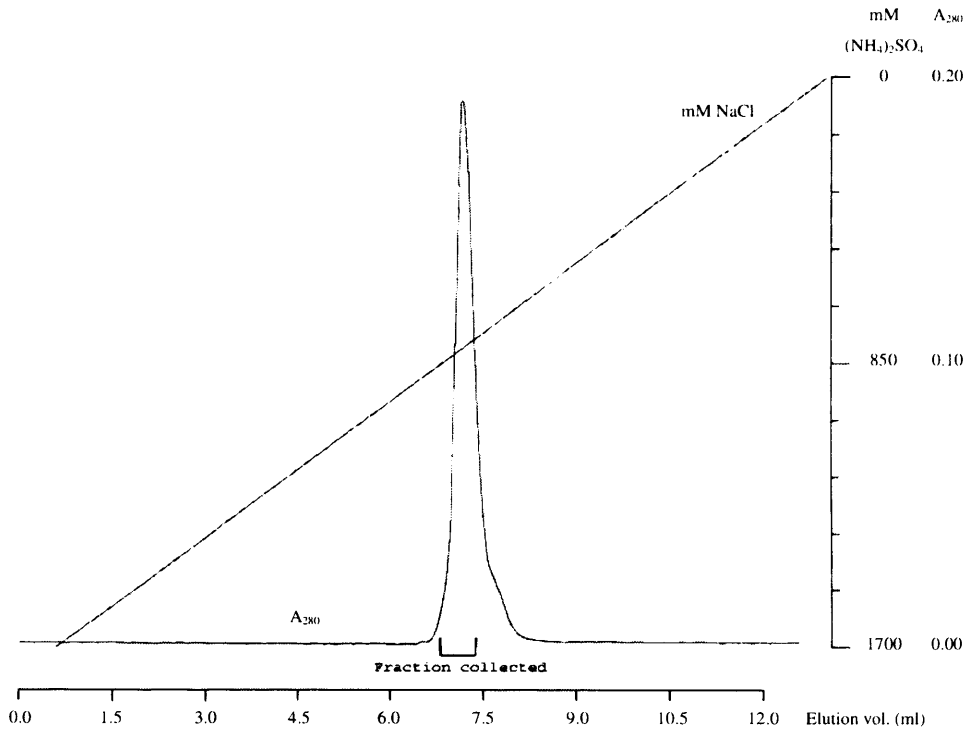

Figure 33 – Hydrophobic column chromatography elution profile of BID.
BID protein was applied to a hydrophobic interaction column [2.12], and eluted with a gradient from 1.7 to 0 M $(NH_4)_2SO_4$ [2.12]. The indicated fraction (pure BID protein; 0.5 ml) was aliquoted and stored at –70 °C.

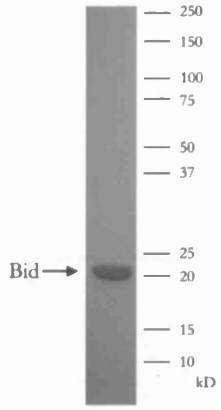

Figure 34 - SDS-PAGE analysis of the BID fraction eluted from the phenyl Superose column.
5 µl of the indicated fraction [Figure 33] was run on 10 % SDS-PAGE [2.13] and bands visualised by Coomassie staining [2.14.1]. BID is > 95% pure, as indicated by the absence of any other visible bands on the gel.

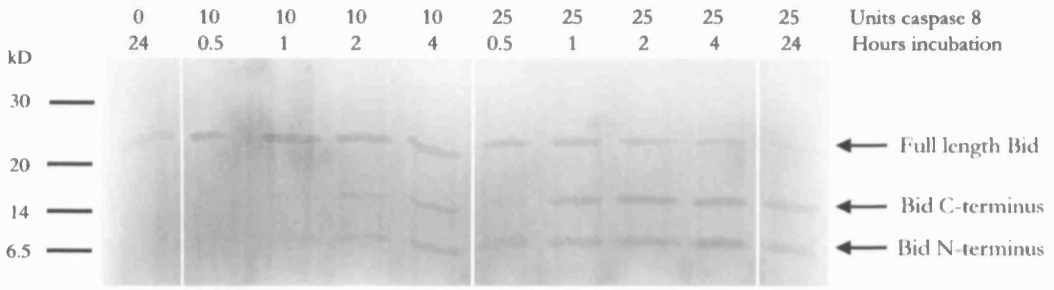

Figure 35 - Cleavage of recombinant p22 BID by caspase 8 *in vitro.*
BID was incubated with caspase 8 at 20 ºC for 0.5 – 24 hr [2.49]. 10 µl of the products was run on 18 % SDS-PAGE [2.13], and bands visualised by Coomassie staining [2.14.1].

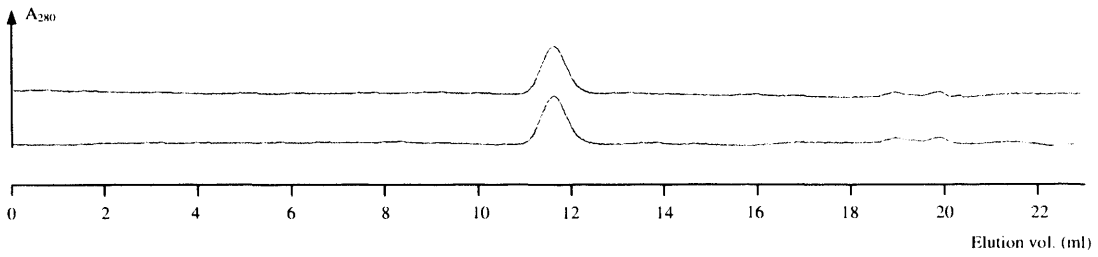

Figure 36 - Gel filtration of stored BID protein.
BID was analysed by gel filtration [2.12] either immediately after storing (top trace) or after 2 months storage at -70 °C (bottom trace). The two traces were identical. By comparison of V_e/V_0 values with protein standards [Figure 5], BID was revealed to be monomeric.

[3.9.3]Formation of BID multimers

The formation of BID multimers observed during purification is interesting. Whilst the intramolecular disulphides presumably responsible for formation of the high-level oligomers certainly would not occur in the reducing intracellular environment of the cell, BID dimers at least nevertheless remain after purification in the presence of DTT to reduce disulphides. Homo-oligomerisation of tBID has been suggested to be a mechanism of activation *in vivo* [103], and the speculation that the homo-dimers observed here might represent an activated form of BID warrants further investigation.

[3.9.4]Aberrant mobility on SDS-PAGE

Depending on the gel type, BID runs as a protein of between 23 – 30 kD. This is in contrast to its predicted molecular weight of 22 kD. As shown in Table 2 (above), vertebrate proteins contain on average approximately equal amounts of positive (lysine, arginine) and negative (aspartate, glutamate) amino acids. In contrast, human BID has a 3.6 % excess of negative over positive residues, and the figure for rat BID is 7.2 %. Unusual amino acid compositions such as these are known to influence mobility markedly on SDS-PAGE, probably due to inhibition of SDS binding [239]. Thus the apparent M_r of BID on SDS-PAGE is an overestimation of the true value.

CHAPTER 4 : BID-INDUCED CYTOCHROME C RELEASE FROM ISOLATED MITOCHONDRIA – DEVELOPMENT OF A REPRODUCIBLE PROTOCOL

[4.1]Introduction

One of the key roles of mitochondria in apoptosis is the release of cytochrome c from the inter-membrane space into the cytosol in response to pro-apoptotic stimuli delivered by members of the BCL-2 protein family [240]. In order to study this process in an *in vitro* system, several groups have developed systems to recreate this effect using isolated mitochondria and a range of BCL-2 proteins. The majority of these workers have used animal tissues, for example rat heart [241,242], rat liver [24,56,91,108,110,119,243-246], rat brain [242,247] or mouse liver [57,83,93,102,140,146,233]. Alternatively, mitochondria have been isolated from a variety of cell lines – HL60 cells [54,248], Rat-1 cells [249], HeLa cells [99,104,142,243,250-254], 293T cells [114,250], PC12 cells [254], HEK, LoVo, LS180 and DU145 cells [99], GT17 cells [247] and KB cells [100]. Finally, some groups have worked with *Xenopus* egg mitochondria [107,245] or yeast mitochondria [9,233,255]. Amongst the above workers, 21 groups have induced cytochrome c release using BID or tBID proteins [54,56,57,93,99,100,102,104,107,110,140,142,146,233,238,242-245,252,253]. Cytochrome c release was assayed primarily by Western blot, although some groups have used an ELISA system [91,247]. Additionally, Appaix and co-workers [241] describe a method to quantify cytochrome c levels spectrophotometrically, utilising the Soret (gamma) peak of cytochrome c at 414 nm. However, the sensitivity of this technique lies only in the low micromolar range, and thus requires at least milligram levels of mitochondrial protein. Finally, Petrosillo and co-workers [256] have recently developed a very sensitive technique for assaying cytochrome c, based on reverse-phase HPLC.

[4.2]Development of mitochondrial isolation procedure for cell lines

[4.2.1]Introduction

Standard techniques for isolating mitochondria from animal tissue are well established [257]. However for cell lines there are a number of alternative possibilities, each with their own advantages and disadvantages. For the purposes of isolating mitochondria in order to study apoptotic cytochrome c release, several groups have made use of mechanical homogenisers; either Dounce homogenisers, which crush cells between the cylinder wall and plunger, or rotating Potter homogenisers, in which cells are broken as a result of shear forces between the cylinder and a motorised plunger [54,99,114,247,248,250,251]. Alternatively, the Polytron homogeniser, in which rotating blades disrupt cells, has been used by some [100]. Finally, cells have also been broken by passage through a small-gauge needle; in this case shear forces between the moving cells and the walls of the needle are responsible for disrupting cells [104,142,252,253].

The major consideration for the studies undertaken here was that mitochondrial preparations made on different days should be as similar as possible, so that results could be compared across multiple experiments. Consequently the procedure needed to rely as little as possible on human error. An additional consideration was that the procedure should be as gentle as possible, in order to maximise

the proportion of unbroken mitochondria (since permeabilisation of the outer membrane was the process to be studied).

[4.2.2]Equipment and strategy

In this study, reproducible cell disruption, yielding largely intact mitochondria, was obtained by forcing the cell suspensions through a 21-gauge needle under constant pressure [2.26]. Mitochondria were isolated from the cell homogenate by differential centrifugation; a flow diagram of the complete procedure is shown in Figure 7 (page 52). Initially, different conditions were investigated, whereby the driving pressure and the number of passes through the needle were varied, in order to maximise mitochondrial yield and integrity.

[4.2.3]Measurement of mitochondrial yield and integrity

The mitochondrial fraction, as well as unbroken cells, were assayed for monoamine oxidase (MAO) activity [2.34] and for total protein [2.17.2]. MAO is a protein of the mitochondrial outer membrane, and so gives a measure of the quantity of mitochondria (both broken and intact) present in the fraction. In addition, the mitochondrial pellet fraction was assayed for cytochrome c by Western blot [2.16]. As a soluble protein of the inter-membrane space, cytochrome c would be released from any broken mitochondria; thus the ratio of cytochrome c : MAO gives a measure of the relative intactness of the mitochondrial preparation.

[4.2.4]Effect of driving pressure

The shear stress acting on cells as they pass through the needle is proportional to the velocity of the fluid through the needle (assuming laminar flow). The fluid velocity is in turn proportional to the driving pressure; thus increasing driving pressure will increase the force breaking cells. Cells were passed through the needle using driving pressures of 120, 200 or 265 kPa, and the time taken for the cell suspension to pass through the needle recorded using electronic sensors. The flow rate (Q) and fluid velocity (v) were then calculated based on the volume of fluid and the internal diameter (I.D.) of the needle (0.51 mm for a 21-Gauge needle), according to Equation 1 [Table 4].

Equation 1

$$Q = \frac{volume}{time} \qquad v = \frac{Q}{\pi \cdot r^2} = \frac{4 \cdot Q}{\pi \cdot I.D.^2}$$

Table 5 shows the relative yield and intactness of mitochondria isolated at these three pressures. Increasing pressure resulted in only a marginal increase in yield, but produced a marked fall in cytochrome c recovery (mitochondrial intactness). A driving pressure of 120 kPa was therefore adopted.

[4.2.5]Effect of passage number

In an attempt to improve yield, cells were passed through the needle 5, 10 or 20 times at a pressure of 120 kPa, and whole-cell and mitochondrial fractions assayed as above [Table 6].

Driving pressure (kPa)	Time taken (ms)	Flow rate (µl/ms)	Fluid velocity (m/s)
120	80.7	6.20	30.6
200	54.7	9.15	45.1
265	46.3	10.79	53.2

Table 4 - Flow rates and fluid velocity at the three driving pressures used.
The time taken for the cell suspension to be forced through the needle [2.26] was measured using electronic sensors. Flow rate and fluid velocity were then calculated based on the volume of fluid and the internal diameter of the needle (0.51 mm for a 21-Gauge needle).

Pressure (kPa)	**Fraction**	**Protein (mg)**	**MAO Activity (A.U.)**	**Cytochrome c (A.U.)**	**Yield (% total MAO recovered in mitochondrial fraction)**	**Relative intactness (120 kPa = 1)**
120	Cells	0.78	2.75		49.5	1.00
	Mitochondria	0.13	2.69	1780		
200	Cells	0.65	2.36		49.8	0.89
	Mitochondria	0.11	2.34	1379		
265	Cells	0.26	1.18		61.7	0.45
	Mitochondria	0.11	1.90	571		

Table 5 - Effect of driving pressure on the yield and intactness of mitochondria isolated from B50 cells.
Mitochondria were isolated using the procedure described [2.26], using three different driving pressures. Unbroken cells and the mitochondrial fraction were assayed for MAO (as a measure of amount of both broken and unbroken mitochondria) and cytochrome c (as a measure of amount of unbroken mitochondria only). Percentage yield was calculated as the percentage of total MAO activity present in the mitochondrial pellet. Relative intactness was calculated as the ratio of the amounts of cytochrome c and MAO activity in the mitochondrial pellet, relative to the value for 120 kPa driving pressure. MAO activity was assayed fluorimetrically by following the release of a fluorophore from a synthetic MAO substrate [2.34]. Cytochrome c was assayed by Western blot [2.16].
A.U. = Arbitrary units

Passages	Fraction	Protein (mg)	MAO Activity (A.U.)	Cytochrome c (A.U.)	Yield (% total MAO recovered in mitochondrial fraction)	Relative intactness (120 kPa = 1)
5	A	3.54	16.90		30.0	1.00
	B	0.31	7.24	3041		
10	A	2.61	11.89		52.7	0.52
	B	0.40	13.22	2864		
20	A	1.48	7.12		69.6	0.49
	B	0.53	16.32	3332		

Table 6 - Effect of passage number on the yield and intactness of mitochondria isolated from B50 cells.
Mitochondria were isolated using the procedure described [2.26], using a variable number of passages through the needle. Unbroken cells and the mitochondrial fraction were assayed for MAO (as a measure of amount of both broken and unbroken mitochondria) and cytochrome c (as a measure of amount of unbroken mitochondria only). Percentage yield was calculated as the percentage of total MAO activity present in the mitochondrial pellet. Relative intactness was calculated as the ratio of the amounts of cytochrome c and MAO activity in the mitochondrial pellet, relative to the value for 120 kPa driving pressure. MAO activity was assayed fluorimetrically by following the release of a fluorophore from a synthetic MAO substrate [2.34]. Cytochrome c was assayed by Western blot [2.16]. A.U. = Arbitrary units

Increasing passage number had a large effect on yield, increasing from 30 % (5 passes) to 70 % (20 passes). However, the more important parameter is intactness – mitochondria with broken outer membranes (whilst potentially acceptable for some studies) would be of no use in investigating cytochrome c release from the inter-membrane space. At both 10 and 20 passes, the intactness was less than 50 % of the value at 5 passes. Thus the standard conditions chosen were a driving pressure of 120 kPa and 5 passes through the needle.

There was lower yield compared with the pressure experiments above [4.2.4]. This was likely to be due to the increased mitochondrial concentration used in these experiments.

[4.2.6]Intactness

The values given above for intactness of the mitochondrial preparation are expressed on a relative scale since the total amount of cytochrome c in the unbroken cells was unknown. To estimate the actual intactness (i.e. percentage of unbroken mitochondria), both MAO and cytochrome c were measured in a sample of unbroken B50 cells, and in a preparation of mitochondria made from these cells under standard conditions [Table 7]. Cytochrome c was enriched 3.5 times in the mitochondrial preparation, whereas MAO was enriched 4.8 times. Thus the intactness was $3.5 \div 4.8 = 73$ %.

[4.2.7]Reproducibility

To assess the reproducibility of the technique, mitochondria were isolated from B50 cell cultures on six different days. Protein and cytochrome c levels were assayed, and are shown in Figure 37.

Cytochrome c levels were comparable in all six preparations, indicating that the procedure developed for isolation of mitochondria from B50 cells is reproducible.

[4.3]Cytochrome c release assay

[4.3.1]Buffers

Several different buffers are reported in the literature. Among these, isosmolarity is maintained by sucrose, mannitol, KCl or some combination of these. Most workers have used energised mitochondria, with either succinate (complex II substrate) or malate/glutamate (complex I substrate) as fuel. $MgCl_2$, KH_2PO_4, PMSF, $Mg(C_2H_3O_2)_2$, EDTA, EGTA and NaCl are included in some buffers [57,93,102,258].

Based on a consideration of the work of the above authors, and others, and also on the basis of maintaining the composition as close as possible to the *in vivo* intracellular state, A KCl-based buffer was chosen [2.31.1], containing succinate, rotenone, $MgCl_2$ and inorganic phosphate. KCl was used to maintain isosmolarity, since potassium is the main intracellular cation *in vivo*. Succinate was used to energise mitochondria, with rotenone included as a complex I inhibitor. Without complex I inhibition, a sufficient NAD^+ pool is maintained to convert malate (generated from succinate oxiadation, via fumarate) to oxaloacetate, which inhibits succinate dehydrogenase. Under these conditions only a very low electron transport flux is possible, and mitochondria are essentially de-energised. Magnesium ions and inorganic phosphate are reported to be necessary for BID-induced cytochrome c release [57].

	[Protein] (mg/ml)	Cytochrome c (A.U./µg protein)	Cytochrome c Enrichment	MAO (A.U./µg protein)	MAO Enrichment	Intactness (%)
Whole cells	4.80	0.205	**3.52**	0.031	**4.81**	**73**
Mitochondria	4.85	0.721		0.148		

Table 7 - Cytochrome c and MAO levels in unbroken cells and a mitochondrial preparation made from these cells.
Enrichment was calculated by dividing the MAO or cytochrome c value for the mitochondrial preparation [2.26] by the value for whole cells. Intactness was calculated by dividing the cytochrome c enrichment by the MAO enrichment. MAO activity was assayed fluorimetrically by following the release of a fluorophore from a synthetic MAO substrate [2.34]. Cytochrome c was assayed by Western blot [2.16]. A.U. = Arbitrary units

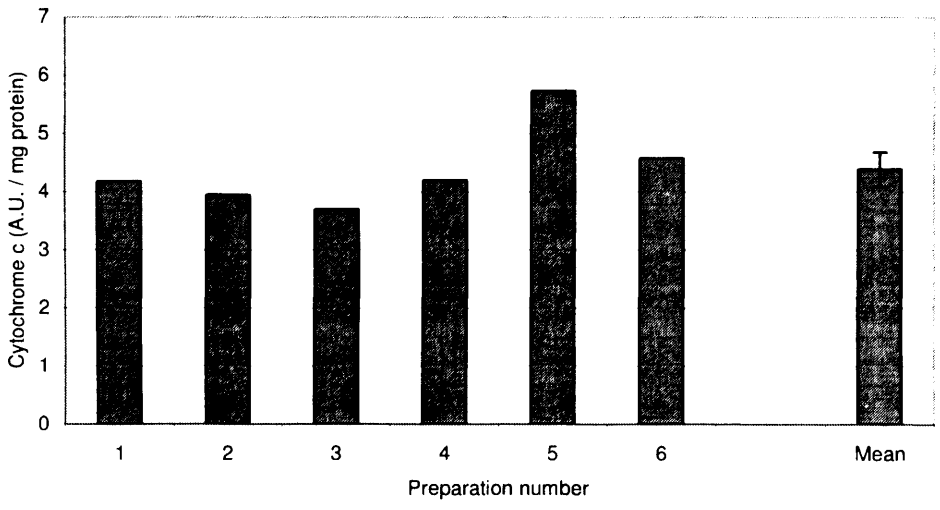

Figure 37 - Comparison of cytochrome c levels in six different mitochondrial preparations, made on different days.
Mitochondria were isolated from B50 cells by the procedure developed above [2.26], and cytochrome c was assayed by Western blot [2.16]. Values are displayed per mg of mitochondrial protein, as a measure of intactness. Mean value error bars are +/- SEM. A.U. = Arbitrary units

Finally, EGTA was included to chelate trace amounts of calcium present following mitochondrial isolation, which might otherwise induce PT pore opening. For experiments using buffered calcium, an EGTA-Ca^{2+} buffer pair was constructed using known EGTA pK_d values [2.52]. Total EGTA concentration was maintained at 2 mM.

[4.3.2] Experimental

The procedure for assaying BID-induced cytochrome c release is described above [2.31] (page 57). The presence of caspase 8 does not induce cytochrome c release independently of BID [93,242]. Thus to generate tBID for use in experiments, full-length BID was incubated with caspase 8 [2.49] before adding the reaction mixture (containing cleaved BID and caspase 8) to mitochondria. Alternatively, in some experiments, a pure tBID preparation (purified caspase 8-cleaved recombinant BID; Sigma) was used.

[4.3.3]Analysis

Cytochrome c release from mitochondria was measured by Western blotting [2.16]. Quantification of the release required densitometric analysis of these blots, and it was therefore important to ensure that the signal obtained was linear over the required range. Various quantities of a mitochondrial preparation [2.26] were analysed by Western blot, and values for amount of cytochrome c were extracted by densitometry, as in cytochrome c release assays. Values are shown in Figure 38. The signal is linear with increasing [mitochondria].

[4.4]Effect of BID on mitochondria from different tissues

Initial experiments compared the capacity of BID (full-length, uncleaved; CHAPTER 3) to induce the release of cytochrome c from isolated B50 cell mitochondria [2.26] with the effect on those isolated from rat heart and rat liver [2.25]. As shown in Figure 39, mitochondria isolated from rat heart or liver did not give a good response to BID. A considerable amount of cytochrome c was released over the course of the assay, even with no BID added. There was a slow increase in cytochrome c release over a large range of [BID], and a substantial amount of cytochrome c remained un-released at the highest [BID] tested (the response plateaus). Mitochondria taken from the B50 cell line gave by far the best response to BID, with a low background release in absence of tBID, only a small amount of un-released cytochrome c at maximum [BID], and a sharp response to increasing [BID]. This could be due to the more gentle procedure for isolating mitochondria (no homogenisation of tissue required) leading to less disruption of mitochondrial structure, and also to the homogeneous nature of mitochondria isolated from cell culture compared to those from animal tissue. Thus in all further experiments mitochondria for use in cytochrome c release studies were isolated from B50 cell cultures.

[4.4.1]Comparison of cytochrome c release elicited by BID and tBID

tBID is reported to be considerably more potent in releasing cytochrome c from mitochondria than BID. For example, Kim and co-workers report a 10 – 20 fold activation using isolated mitochondria [57], whereas Madesh and co-workers report tBID to be 100-fold more effective in a system using permeabilised HepG2 cells [258].

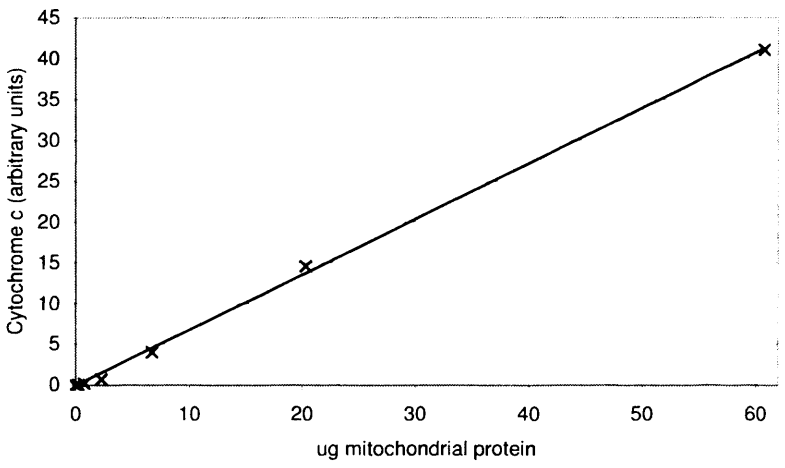

Figure 38 - Linearity of the assay for cytochrome c in samples taken from cytochrome c release assays.
Various quantities of a mitochondrial preparation [2.26] were analysed by the same procedure used to quantify cytochrome c release (SDS-PAGE [2.13] followed by Western blot [2.16], with signals quantified by fluorimetry using the Odyssey system (Li-Cor)). The signal is linear with increasing [cytochrome c].

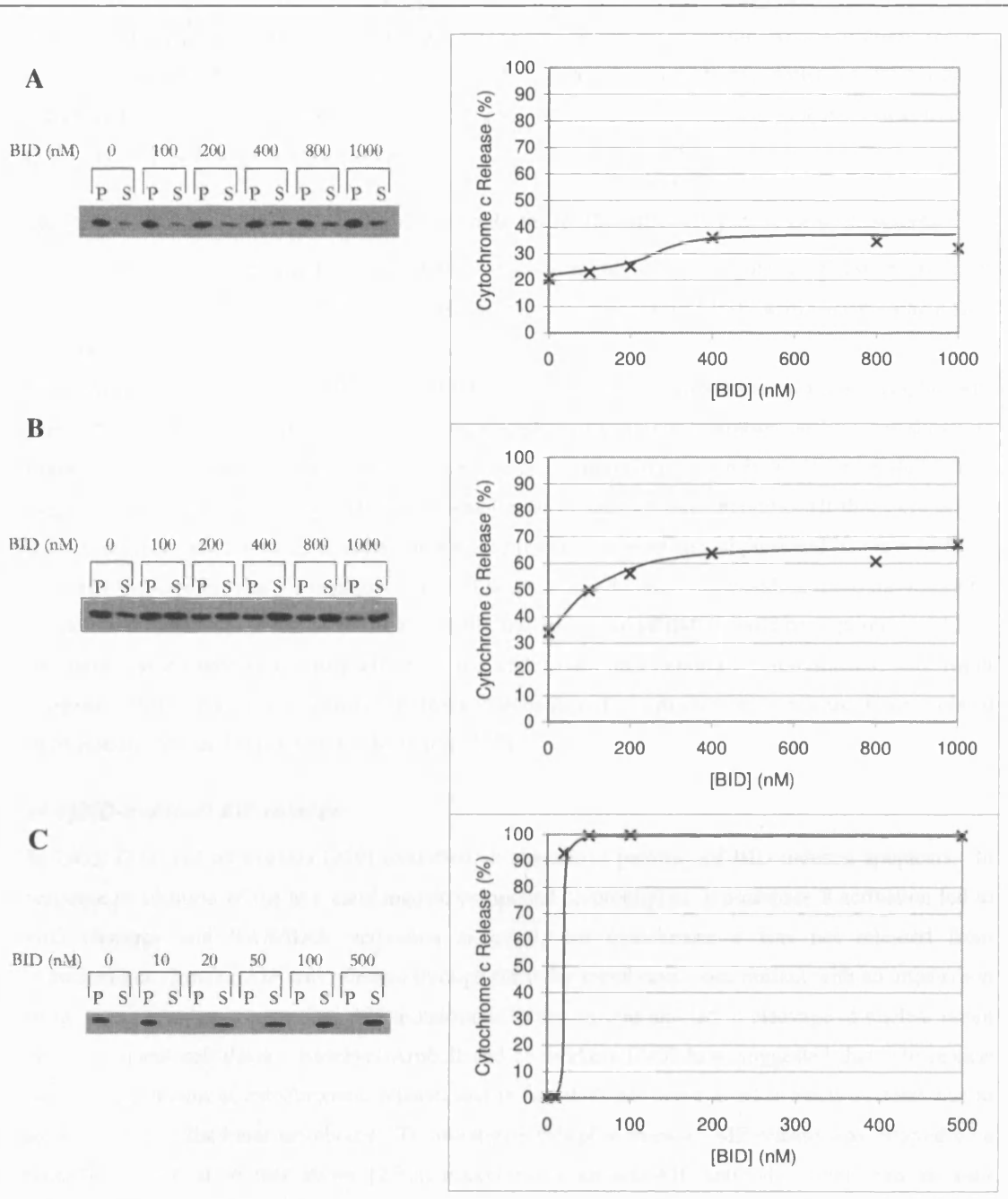

Figure 39 - BID-induced cytochrome c release, using mitochondria isolated from different tissues.

Mitochondria were isolated from rat liver (A), rat heart (B) or B50 cells (C), as described above [2.25],[2.26]. Cytochrome c release was induced by incubation with various quantities of BID (full-length) [3.7] for 30 mins, and mitochondria were then sedimented [2.31]. The cytochrome c present in the mitochondria pellet (P) or supernatant (S) was assayed by Western blot [2.16]. Percentage cytochrome c release was calculated by dividing the cytochrome c reading in the supernatant fraction by the total cytochrome c content (pellet plus supernatant), and plotted against BID concentration. Results are representative of three independent experiments.

To investigate the activation by cleavage with the BID and tBID preparations generated here [CHAPTER 3], cytochrome c release assays [2.31] were carried out using the two preparations [Figure 40]. The EC_{50} for BID-induced cytochrome c release was around 140 nM, whilst for tBID-induced cytochrome c release the figure was around 10 nM. The activation of BID by cleavage was thus 14 times; this is in line with literature values.

[4.5]Effect of concentration of mitochondria on tBID-induced cytochrome c release

The importance of controlling the amount of mitochondria in cytochrome c release assays was investigated by performing tBID-induced cytochrome c release assays [2.31] with varying amounts of mitochondrial protein.

EC_{50} values were derived from the plots of [tBID] vs. percentage cytochrome c release [Figure 41]. These were then used to plot the effect of mitochondrial protein concentration on EC_{50}, as shown in Figure 42. EC_{50} was proportional to concentration of mitochondria over the range tested. This suggests that essentially all the added tBID was bound to sites on mitochondria. (If this were not so then increasing the amount of mitochondria would result in a less-than-proportional increase in EC_{50}. Consider the case in which a negligible amount of tBID was bound – then adding more mitochondria would not change the free concentration of tBID, and no additional tBID would be required to achieve the same cytochrome c-releasing effect in the additional mitochondria.) Additionally, this result suggested that there is no positive feedback mechanism for cytochrome c release from isolated mitochondria, as has been suggested by others [137].

[4.6]BID-induced AIF release

In 2003, Diaz and co-workers [259] identified an alternative pathway of BID-induced apoptosis. In response to addition of the anti-carcinogenic compound chlorophyllin, pro-caspase 8 activation led to BID cleavage and BAX/BAK activation as usual, but cytochrome c was not released from mitochondria. Instead AIF was released through the outer membrane, concomitant with an attenuation of the inner membrane potential. AIF translocated to the nucleus and led to cleavage of nuclear lamin and subsequent cell death. However Arnoult and co-workers [243] have suggested that AIF release occurs downstream of cytochrome c release, and in fact does not occur at all in many systems due to association with the inner membrane. To investigate this phenomenon, AIF release was assayed by a procedure identical to that above [2.31], except using an anti-AIF antibody rather than an anti-cytochrome c antibody for Western blots [2.16]. Representative graphs comparing AIF and cytochrome c release induced by BID and tBID are shown in Figure 43. There was no significant release of AIF paralleling the release of cytochrome c.

[4.7]Effect of energy state on BID-induced cytochrome c release

Shimizu and co-workers [56] have shown previously that BID- or BIK- induced cytochrome c release was respiration-independent. To confirm this finding, cytochrome c release was induced by tBID in the presence and absence of succinate as respiratory substrate. (B50 cell mitochondria do not develop a membrane potential in the absence of succinate; endogenous substrate is consumed rapidly [157].) The response to tBID in both cases is shown in Figure 44.

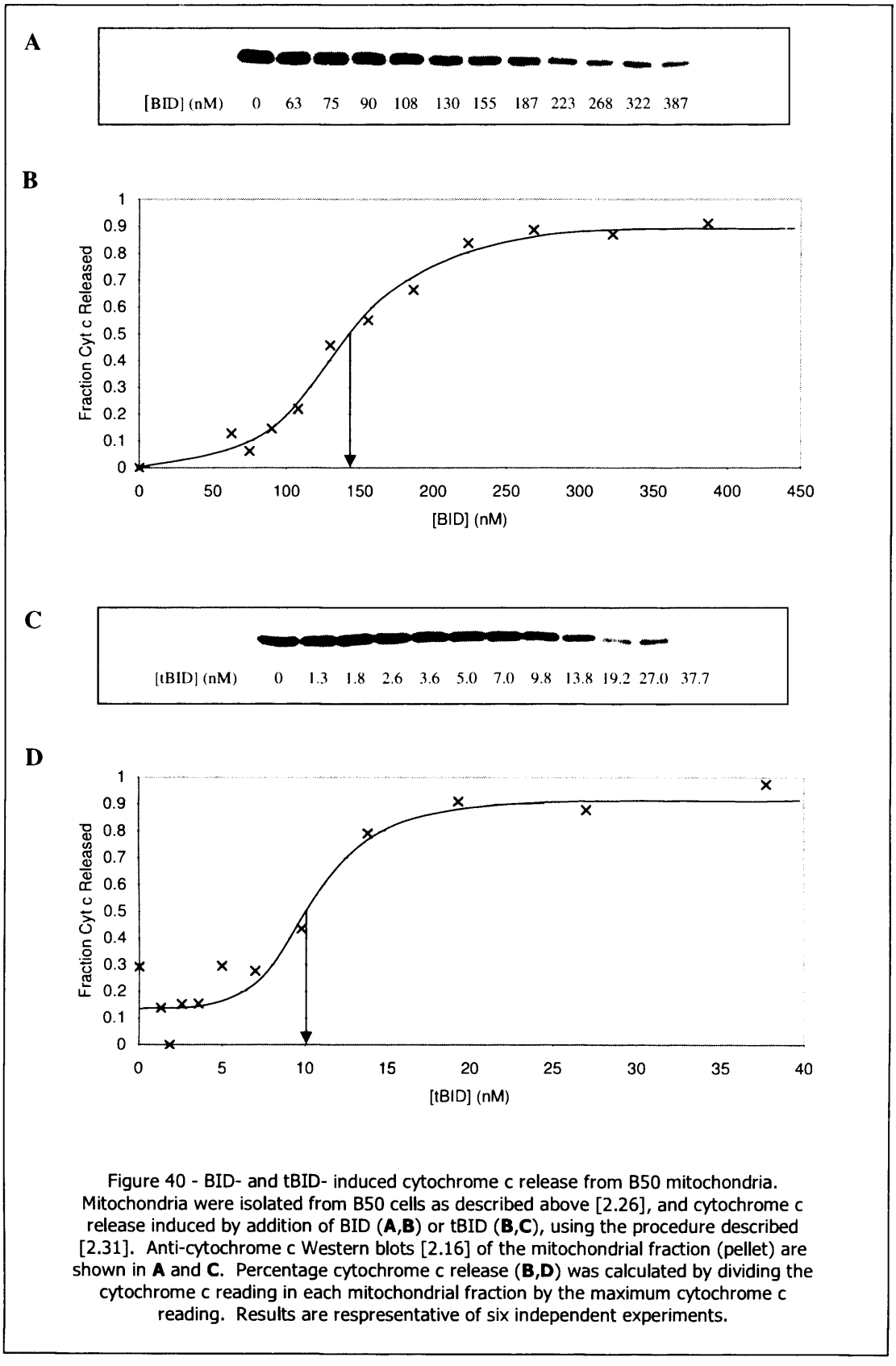

Figure 40 - BID- and tBID- induced cytochrome c release from B50 mitochondria. Mitochondria were isolated from B50 cells as described above [2.26], and cytochrome c release induced by addition of BID (**A**,**B**) or tBID (**B**,**C**), using the procedure described [2.31]. Anti-cytochrome c Western blots [2.16] of the mitochondrial fraction (pellet) are shown in **A** and **C**. Percentage cytochrome c release (**B**,**D**) was calculated by dividing the cytochrome c reading in each mitochondrial fraction by the maximum cytochrome c reading. Results are respresentative of six independent experiments.

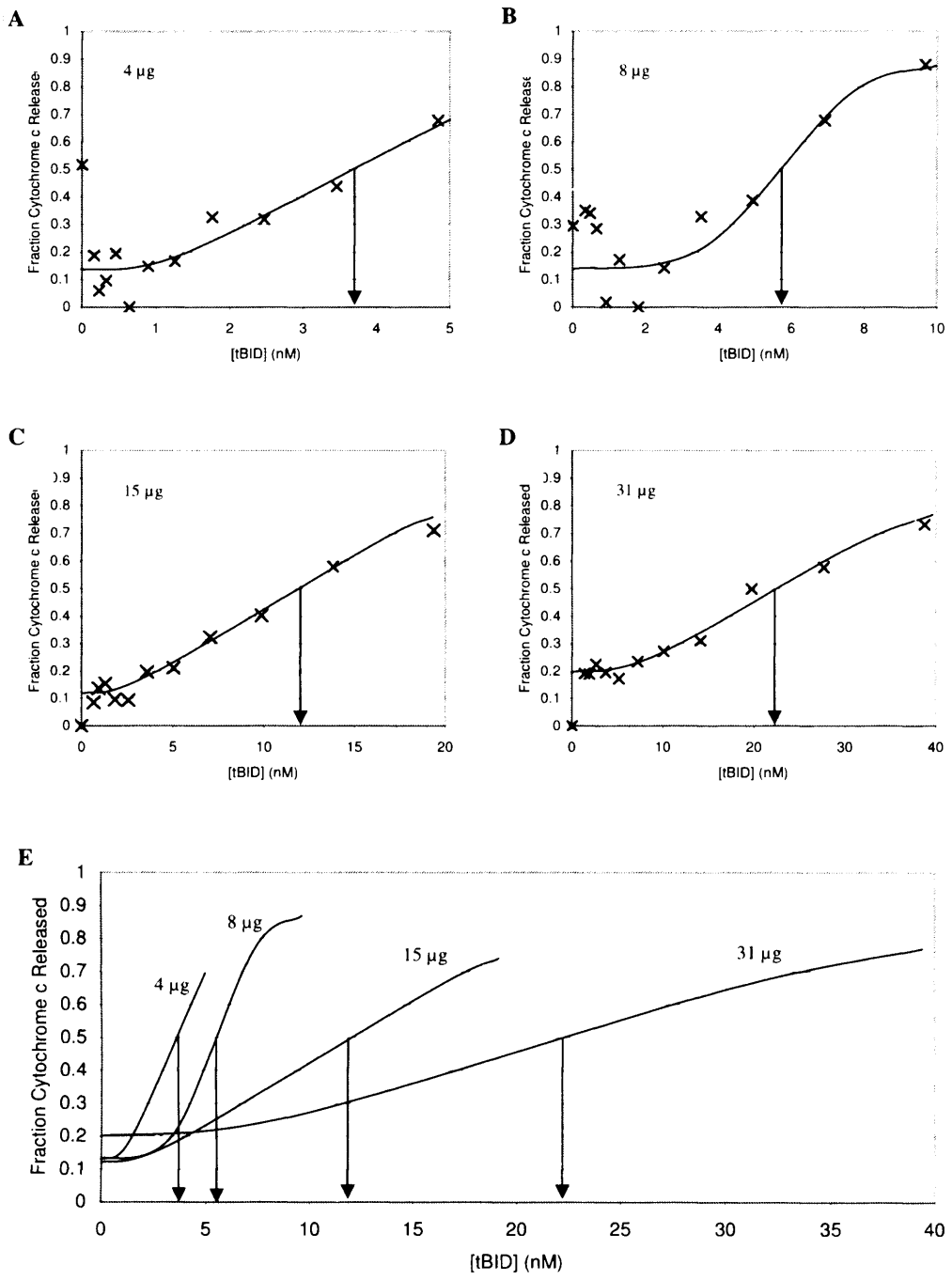

Figure 41 - tBID-induced cytochrome c release from preparations containing different amounts of mitochondrial protein.
Cytochrome c release assays were carried out as above [2.31]. (**A-D**) Four different quantities of mitochondria, containing 4, 8, 15 and 31 µg mitochondrial protein, as indicated, were added to solutions containing various concentrations of tBID [3.8]. Reactions were incubated for 30 mins at 30 °C, and centrifuged to pellet mitochondria. Cytochrome c in the mitochondrial pellet was assayed by Western blot [2.16]. (**E**) Overlay of the cytochrome c release curves taken from **A** – **D**. Results are representative of two independent experiments.

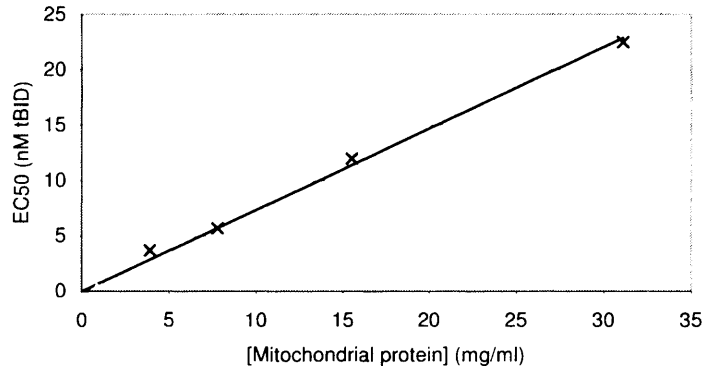

Figure 42 - Effect of [mitochondria] on BID-induced cytochrome c release. EC_{50} values are derived from tBID-induced cytochrome c release assays [2.31] with varying concentrations of mitochondrial protein [Figure 41]. Values are plotted against mitochondrial protein concentration. tBID EC_{50} is linear with increasing [mitochondrial protein], indicating that essentially all tBID is bound to sites on mitochondria.

A

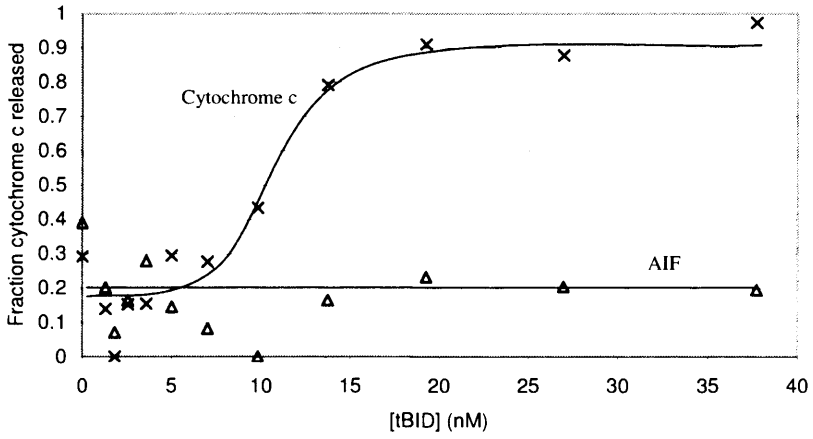

B

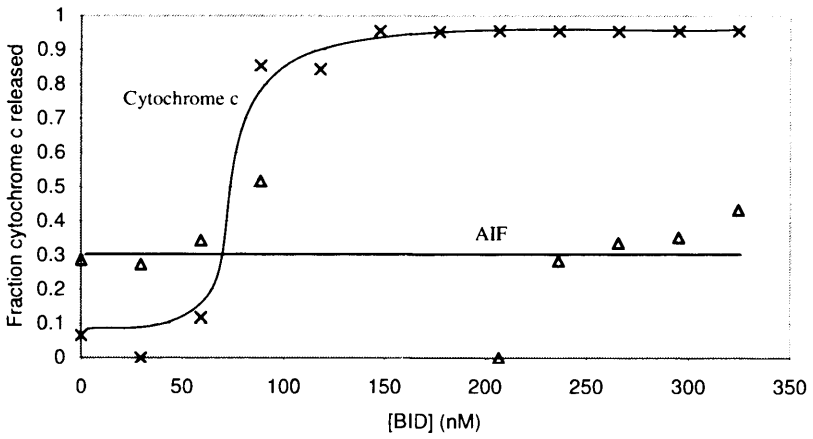

Figure 43 - Comparison of cytochrome c and AIF release induced by full-length BID and by tBID.

A release assay was carried out as above [2.31]. Mitochondria were added to solutions containing various concentrations of tBID (**A**) or BID (**B**) [CHAPTER 3]. Reactions were incubated for 30 mins at 30 °C, and centrifuged to pellet mitochondria [2.31]. The mitochondrial pellet was assayed for cytochrome c (x) or AIF (Δ) by Western blot [2.16], showing that tBID and BID are unable to induce AIF release under conditions in which cytochrome c is released. Results are representative of two independent experiments.

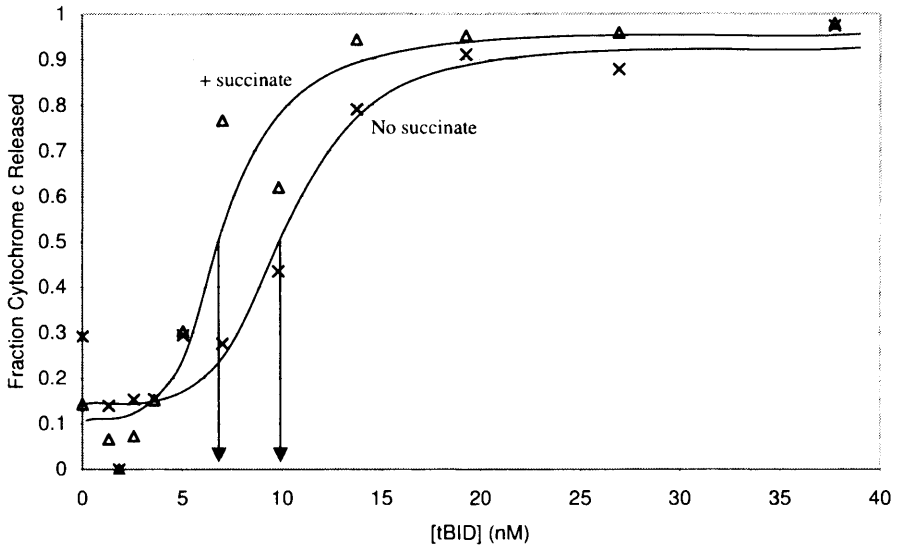

Figure 44 - The release of cytochrome c from isolated mitochondria in response to tBID occurs at different [tBID] in respiring and non-respiring mitochondria.
A release assay was carried out as above [2.31]. Mitochondria were added to solutions containing various concentrations of tBID [3.8]; solutions either contained 5 mM succinate (as above; respiring mitochondria; Δ) or no succinate (non-respiring mitochondria; x). Reactions were incubated for 30 mins at 30 °C, and centrifuged to pellet mitochondria [2.31]. The mitochondrial pellet was assayed for cytochrome c by Western blot [2.16]. Results are representative of three independent experiments.

Non-respiring mitochondria were less sensitive to tBID-induced cytochrome c release than respiring mitochondria. However the effect was small (EC_{50} was increased from 7 nM to around 10 nM) in broad agreement with published data [56].

[4.8]Effect of exogenous cytochrome c on BID-induced cytochrome c release

Cytochrome c can induce perturbations in lipid bilayers [260]. The release of a small amount of cytochrome c from mitochondria during apoptosis may thus influence the release of the remaining cytochrome c pool, by affecting bilayer properties. To investigate this possibility in the *in vitro* system developed here, tBID was used to induce cytochrome c release either from normal B50 mitochondria, or from mitochondria that had been pre-incubated with exogenous cytochrome c [2.32]. As shown in Figure 45, preincubation with exogenous cytochrome c had no effect either on mitochondrial cytochrome c content or on tBID-induced cytochrome c release, thus ruling out any feedback regulation of cytochrome c release by this mechanism.

[4.9]Equivalence of commercial and in-house generated tBID

The tBID used to obtain the data presented above was generated by incubating recombinant BID with purified recombinant caspase 8, and then adding this mixture (containing caspase 8-cleaved BID (tBID) and active caspase 8) directly to mitochondria [2.49]. This technique has a number of potential problems. Firstly, BID is not completely cleaved by caspase 8 during the incubation times used [3.8] so that the tBID concentration will be slightly less than anticipated. Secondly, BID cleavage will continue during incubation of the preparation with mitochondria, changing the tBID concentration over the course of the incubation and thus affecting the kinetics of tBID-induced cytochrome c release. And finally, although the presence of caspase 8 has previously been shown not to affect cytochrome c release [93,242] it remains possible that its presence might have some effect in the system used here. Thus it was considered preferable to use a commercial preparation of purified tBID [2.31.1] in all further experiments. To demonstrate equivalence of the two preparations, mitochondria were incubated either with the commercial tBID or with tBID prepared by caspase 8 cleavage of full-length BID (as above) and the cytochrome c release response compared. As shown in Figure 46, although the EC_{50} is slightly lower in the case of the commercial preparation (perhaps because of incomplete caspase 8 cleavage of full-length BID) there is very little difference in response between the two preparations. Thus the commercial preparation was used in all further experiments.

[4.10]Discussion

[4.10.1]Mitochondrial isolation

A procedure was developed to isolate mitochondria from a B50 cell line. Mitochondria were substantially intact, and retained cytochrome c during isolation. Importantly, the procedure was reproducible, yielding preparations with similar contents of cytochrome c on several different occasions.

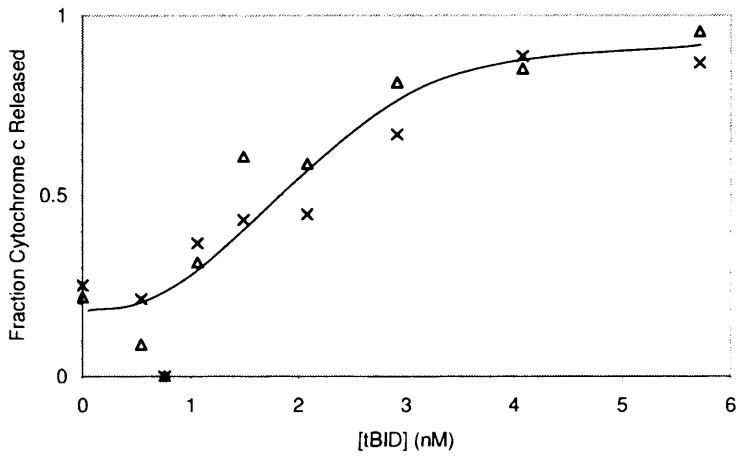

Figure 45 - Neither mitochondrial cytochrome c content nor tBID action is affected by preincubation with exogenous cytochrome c.
tBID was used to induce cytochrome c release either from normal B50 mitochondria (x) [2.26] or from mitochondria that had been pre-incubated with exogenous cytochrome c (Δ) [2.32]. Reactions were incubated for 30 mins at 30 °C, and centrifuged to pellet mitochondria [2.31]. The mitochondrial pellet was assayed for cytochrome c by Western blot [2.16]. Pre-incubation with cytochrome c had no effect on mitochondrial cytochrome c content or on tBID-induced cytochrome c release. Results are representative of three independent experiments.

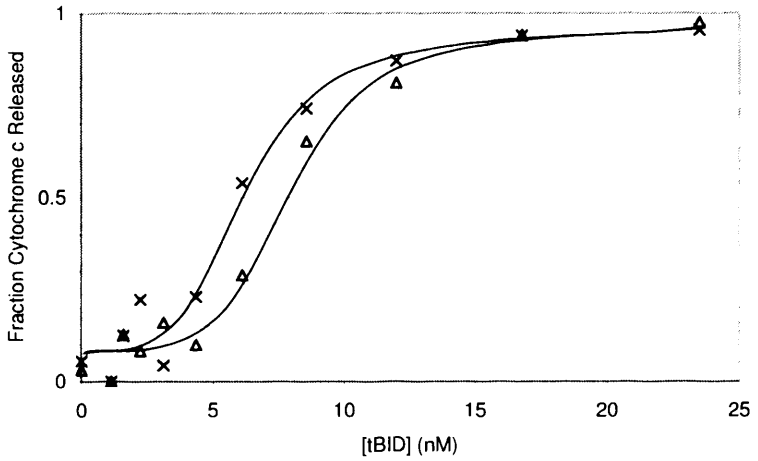

Figure 46 – A commercial tBID preparation has a cytochrome c releasing activity equivalent to that of the tBID preparation used above.
Cytochrome c release was induced from B50 mitochondria using either a commerical tBID preparation [2.31.1] (x) or tBID generated by caspase 8 cleavage of full-length recombinant BID [2.49] (Δ). Reactions were incubated for 30 mins at 30 °C, and centrifuged to pellet mitochondria [2.31]. The mitochondrial pellet was assayed for cytochrome c by Western blot [2.16]. The cytochrome c release response to the two tBID preparations was essentially identical.

[4.10.2]Cytochrome c release assay

Cytochrome c release was induced from mitochondria from various sources using BID and tBID proteins. Mitochondria isolated from B50 cells gave a better response to BID than those isolated from rat heart or rat liver. Cytochrome c release was assayed by Western blot; values thus derived were shown to accurately reflect mitochondrial cytochrome c levels, with the signal linear over the required range. As reported previously, tBID was approximately 14 times more potent than full-length BID in inducing cytochrome c release. The amount of mitochondria used in assays was revealed to be important; increasing the level of mitochondrial protein present let to a proportional increase in the EC_{50} for tBID-induced cytochrome c release. Additionally, this result showed that the majority of tBID protein is bound to sites on mitochondria, rather than free in solution. Energising mitochondria had a slightly stimulatory effect on tBID action, but the effect was small. Finally, AIF was shown to be retained by mitochondria over the course of tBID- and BID- induced cytochrome c release, and exogenous cytochrome c was demonstrated to have no effect on mitochondrial cytochrome c content or tBID-induced cytochrome c release.

[4.10.3]Equivalence of tBID preparations

A commercial preparation of tBID was shown to have the same cytochrome c-releasing activity as the tBID preparation used above (caspase 8-cleaved full-length recombinant BID). Since the commercial preparation had no contaminating caspase 8, it was decided to use this tBID stock in all further experiments.

CHAPTER 5 : ON THE INVOLVEMENT OF THE PERMEABILITY TRANSITION PORE IN BID ACTION

[5.1]Introduction

There is considerable controversy over the involvement of the permeability transition pore (PT pore) in cytochrome c release from mitochondria during apoptosis. On the one hand, PT pore effectors such as CSA, Ca^{2+} and bongkrekic acid have been shown to modulate the mitochondrial apoptotic response, in some systems at least [123,261,262]. Additionally, BCL-2 family members are known to associate with PT pore components [108,110], and alterations in levels of these components (ANT and VDAC) influence apoptosis [112,114]. On the other hand, it is certainly the case in some systems that cytochrome c release precedes the swelling and membrane depolarisation that would be predicted to accompany PT pore opening [53-57]. It is also unlikely that sustained PT pore opening occurs early in the apoptotic process, since mitochondrial function (or ATP production at least) is necessary for completion of the active process of cell demise [263].

[5.2]Effect of calcium on tBID action

Ca^{2+} strongly activates PT pore opening (reviewed in [50]). Thus, if PT pore opening is mechanistically involved in BID action, exposure to Ca^{2+} should sensitise mitochondria to BID-induced cytochrome c release. Mitochondria were incubated with tBID or BID, using the *in vitro* system developed above [CHAPTER 4], in the presence or absence of 0.8 μM buffered extra-mitochondrial free Ca^{2+} [2.52]. Under these conditions a steady state of Ca^{2+} influx (through the Ca^{2+} uniporter) and efflux (through the Na^{2+}-Ca^{2+} carrier) is established. At 0.8 μM external concentration, the internal Ca^{2+} concentration is approximately 2 μM (at least in heart mitochondria [264]). Figure 47 shows that there was no stimulatory effect of Ca^{2+} under these conditions; rather, there was a small inhibition. This result was in line with those of Shimizu and co-workers [56], who showed that BID- or BIK-induced cytochrome c release was Ca^{2+} -independent, and suggested PT pore opening did not occur during BID-induced cytochrome c release in this system.

[5.3]Calcein release during tBID-induced cytochrome c release

[5.3.1]Introduction

Notwithstanding the results presented in Figure 47, it was possible that PT pore opening may still be involved at some stage in BID action. Any stimulatory effect of Ca^{2+} might be small, and undetectable by the above assay at the Ca^{2+} concentrations used. Alternatively tBID might stimulate pore opening in a Ca^{2+}-independent manner. Accordingly, PT pore opening was assayed by the release of matrix-entrapped calcein [2.28]. This provides a very sensitive means of detecting even very transient periods of pore opening, which will result in release of the fluorophore into the medium [17,57,265].

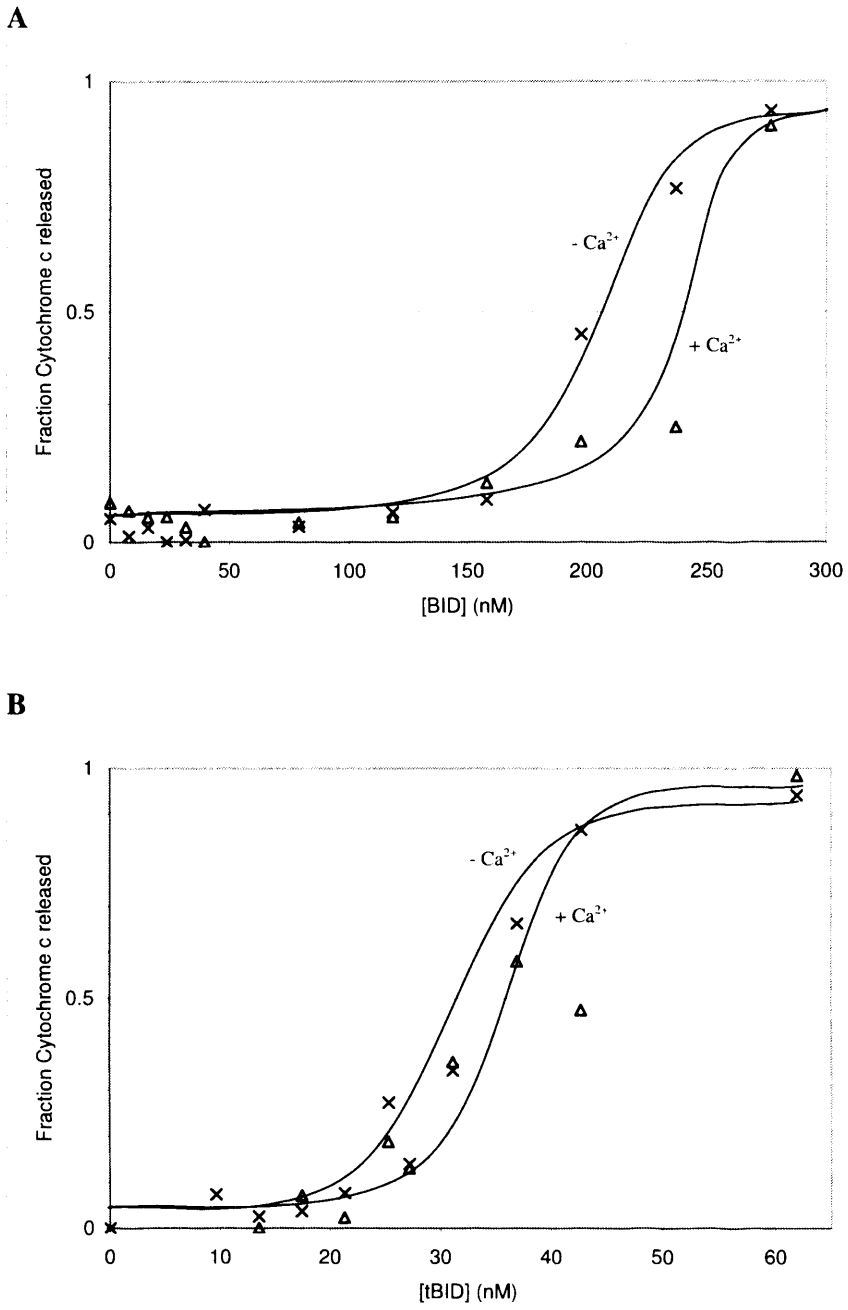

Figure 47 - Ca^{2+} does not stimulate BID or tBID -induced cytochrome c release from isolated mitochondria.
Mitochondria were incubated with varying concentrations of BID (**A**) or tBID (**B**), either in Ca^{2+}-free buffer (containing 2 mM EGTA; x) or in buffer supplemented with 0.8 μM Ca^{2+} (buffered with EGTA; Δ). After 30 mins incubation at 30 °C, mitochondria were separated by centrifugation [2.31] and assayed for cytochrome c by Western blot [2.16]. Results are representative of five independent experiments.

[5.3.2]The effects of Ca^{2+} and tBID on calcein release

Mitochondria were loaded with calcein [2.28], and then incubated under the same conditions as in BID-induced cytochrome c release experiments [2.31]. In some experiments, 400 μM Ca^{2+}, 1.2 μM CSA or 150 nM tBID was added. Calcein release (expressed as % of total entrapped fluorophore) is shown in Figure 48. With no additions [Figure 48; control] there was a slow loss of calcein from mitochondria (approximately 1% of the total entrapped per min), probably due to a gradual loss of integrity of the mitochondrial inner membrane over time. As expected, Ca^{2+} induced rapid loss of calcein, due to induction of PT pore opening. This effect was inhibited by CSA (a PT pore blocker). However, permeability transition still occurred after around 8 mins under these conditions; this was expected to be the case, as CSA inhibition is overcome in a time-dependent manner at high [Ca^{2+}] [266]. Notably, 150 nM tBID did not induce any calcein loss above the control level (in agreement with the results of Kim and co-workers [57]).

[5.3.3]Verifying cytochrome c release

To verify tBID-induced cytochrome c release under these conditions, mitochondrial samples were also assayed for mitochondrial cytochrome c content by Western blot [2.16] [Figure 49). Cytochrome c release still occurred in response to tBID under these conditions. The absence of any parallel release of calcein confirmed that PT pore opening was not involved in tBID action. Interestingly, there was no release of cytochrome c from the mitochondria incubated with Ca^{2+}, suggesting that PT pore opening does not lead to mitochondrial swelling sufficient to rupture the outer membrane under these conditions, or that cytochrome c is firmly attached to the inner membrane.

[5.4]The effect of cyclophilin D on apoptosis and mitochondrial cytochrome c release

[5.4.1]Introduction

Even if pore opening *per se* is not involved in BID-induced cytochrome c release, the PT pore, or PT pore components, might still be involved in BID action. For example, the PT pore has been suggested to be a binding site for BCL-2 family proteins [108,110], and may additionally facilitate release of a sub-population of cytochrome c during apoptosis [61]. To probe further the involvement of the PT pore in the system developed here, the effect of modulation of cyclophilin D levels was investigated. Cyclophilin D is the matrix component of the PT pore [Figure 50], and is a PPIase [1.7]. However its role in the pore is not clear. It has been suggested either to facilitate the conversion of the pore to the open state, or to stabilise this state [31]. Clarke and co-workers have suggested that cyclophilin D's PPIase activity is required for pore opening (although not for binding to ANT) [36].

[5.4.2]Cyclophilin D overexpression

A B50 cell line overexpressing cyclophilin D (designated cyclophilin D(+) cells) had been previously produced in our lab [2.42]. To check the expression level of cyclophilin D, mitochondria were prepared from normal and over-expressing B50 cells [2.26], and cyclophilin D levels analysed by Western blot [2.16]. Figure 51 shows that cyclophilin D is overexpressed approximately 10 times in this cell line.

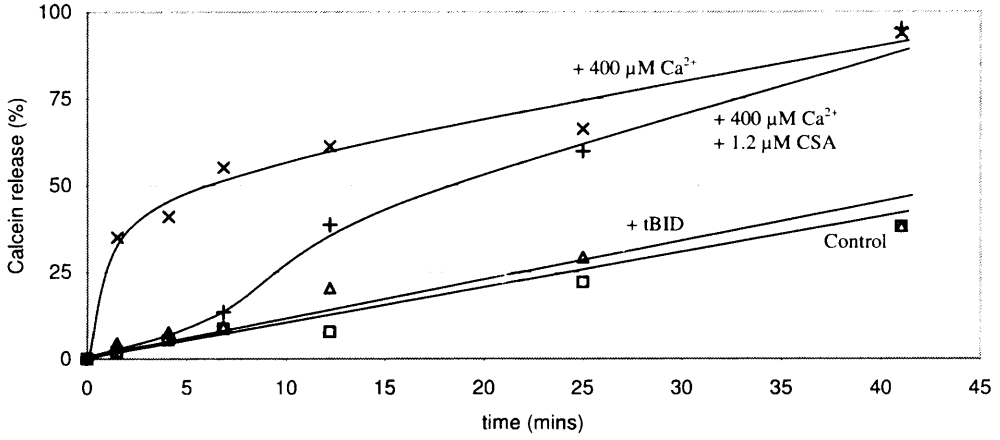

Figure 48 - Release of matrix-entrapped calcein from mitochondria is induced by Ca^{2+} but not by tBID.
Mitochondria were loaded with calcein by incubating with calcein-AM [2.28]. Mitochondria were then incubated in respiration medium, containing either no additions ( ), 400 μM Ca^{2+} (x), 400 μM Ca^{2+} + 1.2 μM CSA (+) or tBID (Δ) as indicated. After incubation for varying times, mitochondria were separated from the assay mixture by centrifugation, and calcein in the mitochondrial pellet and supernatant was determined fluorimetrically [2.28.2]. Values are presented as calcein released as a percentage of the total entrapped calcein at zero time. Results are representative of three independent experiments.

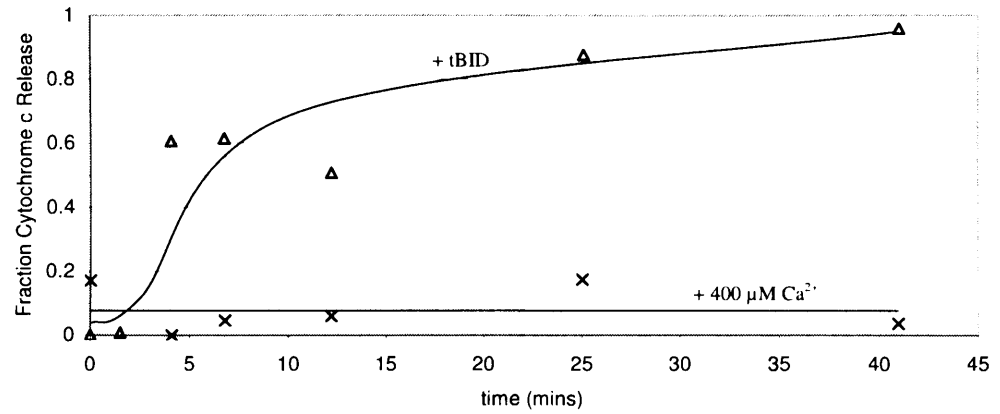

Figure 49 - tBID, but not Ca^{2+}, induces cytochrome c release from calcein-loaded mitochondria.
Sedimented mitochondria taken from the calcein-release experiments [Figure 48] were resuspended in sample loading buffer and run on a 10 % SDS-PAGE gel [2.13]. Cytochrome c was assayed by Western blot [2.16], in the samples incubated with 400 μM Ca^{2+} (x) and in those incubated with tBID (Δ). Results are representative of three independent experiments.

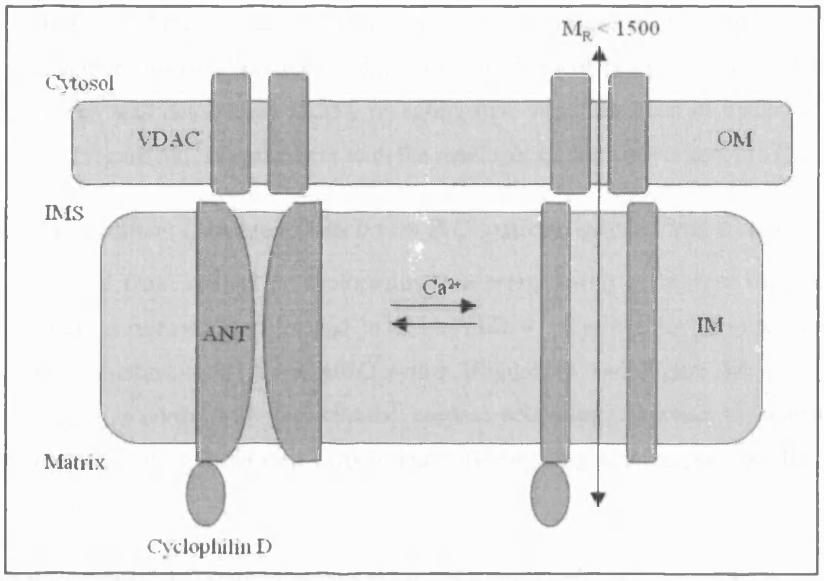

Figure 50 - Proposed structure of the PT pore.
Cyclophilin D is the matrix component of the pore, and has been suggested either to facilitate the conversion of the pore to the open state, or to stabilise this state.

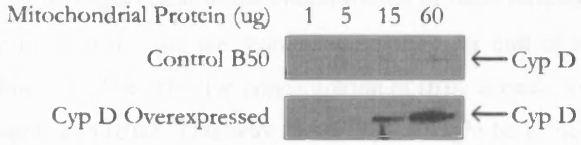

Figure 51 - Cyclophilin D overexpression in B50 cells carrying the pcDNA 3.1–cyclophilin D plasmid.
Mitochondria were prepared from control B50 cells and from cells carrying the cyclophilin D plasmid, as described above [2.26]. Mitochondrial protein concentration was determined [2.17], and either 1, 5, 15 or 60 µg protein loaded on a 10 % SDS-PAGE gel [2.13]. After running, cyclophilin D was assayed by Western blot [2.16]. Cyclophilin D is overexpressed approximately 10 times in the cyclophilin D(+) cells.

[5.4.3]Effect of cyclophilin D overexpression on apoptosis in whole cells

The effect of cyclophilin D overexpression on whole-cell apoptosis was investigated by incubating control B50 and cyclophilin D(+) cells with staurosporine. Staurosporine is a broad-spectrum protein kinase inhibitor, known to strongly induce apoptosis in a number of cell types [267]. The time-course of caspase activation was determined [2.35], revealing that overexpression of cyclophilin D inhibits caspase activation [Figure 52], in agreement with the results of Li and co-workers [157].

[5.4.4]Effect of cyclophilin D overexpression on BID-induced cytochrome c release

Mitochondria isolated from control or cyclophilin D-overexpressing cells were used to assay BID-induced cytochrome c release, as described in CHAPTER 4. Cyclophilin D(+) mitochondria were significantly more resistant to BID and tBID action [Figure 53 and Figure 54; p = 0.002 (BID); 0.030 (tBID)]. This accords with the blunted caspase-activation response to staurosporine, and suggests that inhibition of BID-induced cytochrome c release might be responsible for this effect in cyclophilin D(+) cells.

[5.4.5]Effect of cyclophilin D overexpression on mitochondrial protein levels

In the course of the above experiments, it was observed that levels of some key mitochondrial proteins differ between mitochondria isolated from normal B50 cells and from the cyclophilin D-overexpressing clone. Figure 55 compares levels of ANT, MAO and cytochrome c in these two cell types. Levels of both ANT and MAO (relative to mitochondrial protein content) were increased to about 150 % of control levels in the cyclophilin D(+) mitochondria (p=0.05 (MAO), p=0.02 (ANT)), whilst cytochrome c levels were equal in the two cell types. Interestingly, this ratio is similar to the ratio of the EC_{50} for tBID-induced cytochrome c release in the control and cyclophilin D(+) mitochondria [Figure 53] – approximately 50 % more tBID is required to release cytochrome c from the clone mitochondria. Since EC_{50} is proportional to the concentration of tBID binding sites [Figure 42] (page 107), this result may indicate that there are more binding sites per unit of mitochondrial protein in cyclophilin D(+) mitochondria. The effective concentration of tBID at each binding site would thus be lower, inhibiting the response to tBID. One way in which this might be achieved is by an decrease in mitochondrial size as a result of cyclophilin D overexpression – the mitochondrial surface area:volume ratio would then be increased, and so the area of membrane surface presented by a given quantity of mitochondrial protein would rise. The surface concentration of a given quantity of tBID (i.e. $nmol/\mu m^2$) would then be lower in cyclophilin D(+) mitochondria, potentially decreasing tBID efficacy.

[5.5]Discussion

[5.5.1]PT pore opening during BID-induced cytochrome c release

Based on the lack of any stimulatory effect of Ca^{2+} on BID and tBID action, and on the lack of release of entrapped calcein during BID-induced cytochrome c release, it is clear that PT pore opening is not necessary for cytochrome c release.

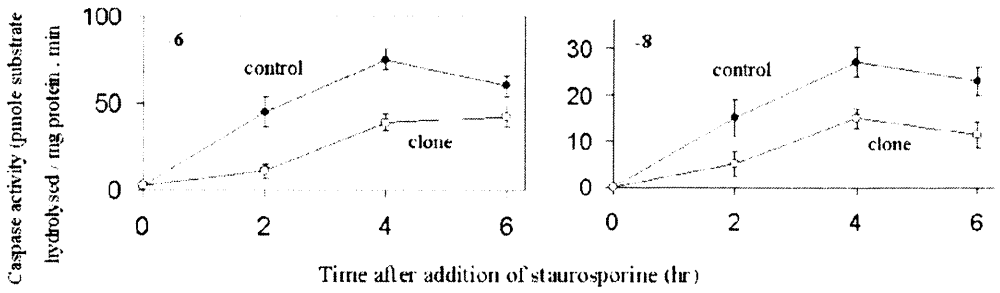

Figure 52 - Caspase activation is inhibited in cells overexpressing cyclophilin D compared to control B50 cells.
Normal B50 cells (control) and cyclophilin D(+) cells (clone) were incubated with staurosporine [2.35]. Cells were extracted at the times indicated after the addition of staurosporine, and the cytosolic fractions was assayed for caspase 6 (left) or caspase 8 (right). The results are expressed as the means +/− S.E.M. for 5 separate experiments.

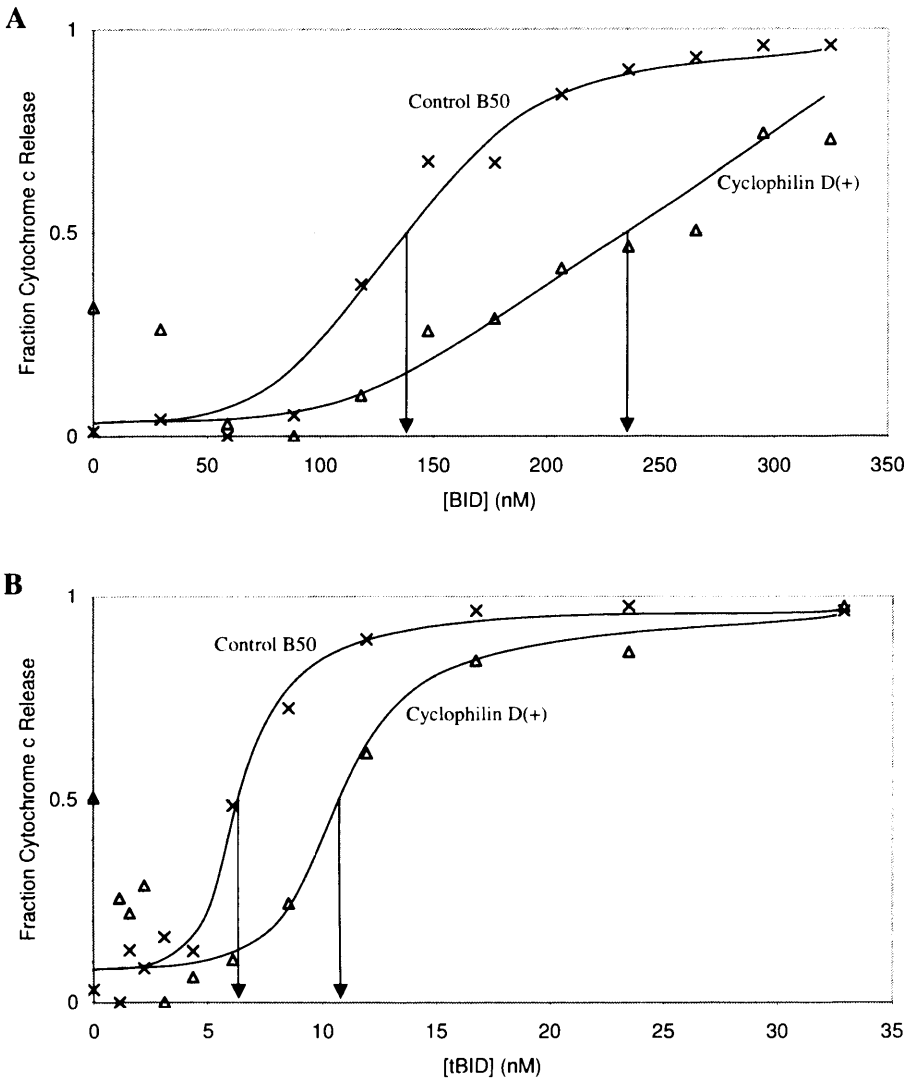

Figure 53 - Cyclophilin D overexpression inhibits BID- and tBID- induced cytochrome c release.

Mitochondria were isolated either from normal B50 cells or from a B50 cell line overexpressing cyclophilin D by approximately 10 times (cyclophilin D(+)), as indicated. Mitochondria were incubated with varying concentrations of BID (**A**) or tBID (**B**) [2.31]. After 30 mins incubation at 30 °C, mitochondria were separated from the assay mixture by centrifugation and assayed for cytochrome c by Western blot [2.16]. Results are representative of six (**A**) or four (**B**) independent experiments.

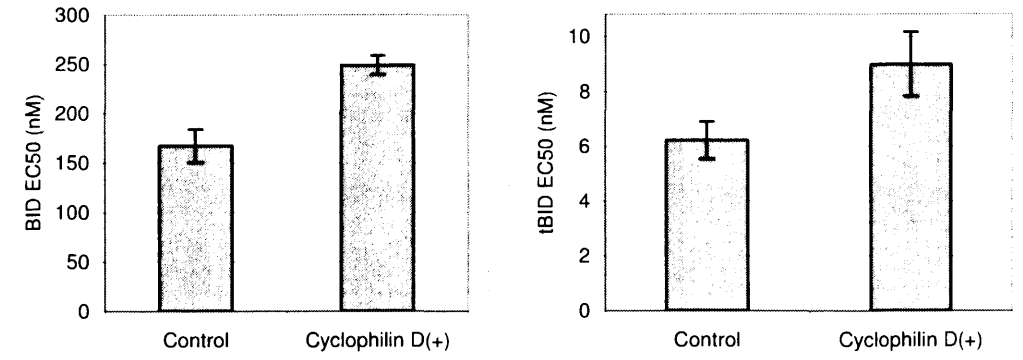

Figure 54 - Cyclophilin D overexpression raises the EC_{50} for cytochrome c release. Cytochrome c release was induced either by BID (**A**) or by tBID (**B**), in several independent experiments. Data are means +/- SEM for the following (number of independent experiments): Control cells + BID (6); cyclophilin D(+) cells + BID (6); Control cells + tBID (4); cyclophilin D(+) cells + tBID (4). The effects of cyclophilin D overexpression were statistically significant relative to control cells ($p<0.005$ for BID, panel A; $p<0.05$ for tBID, panel B).

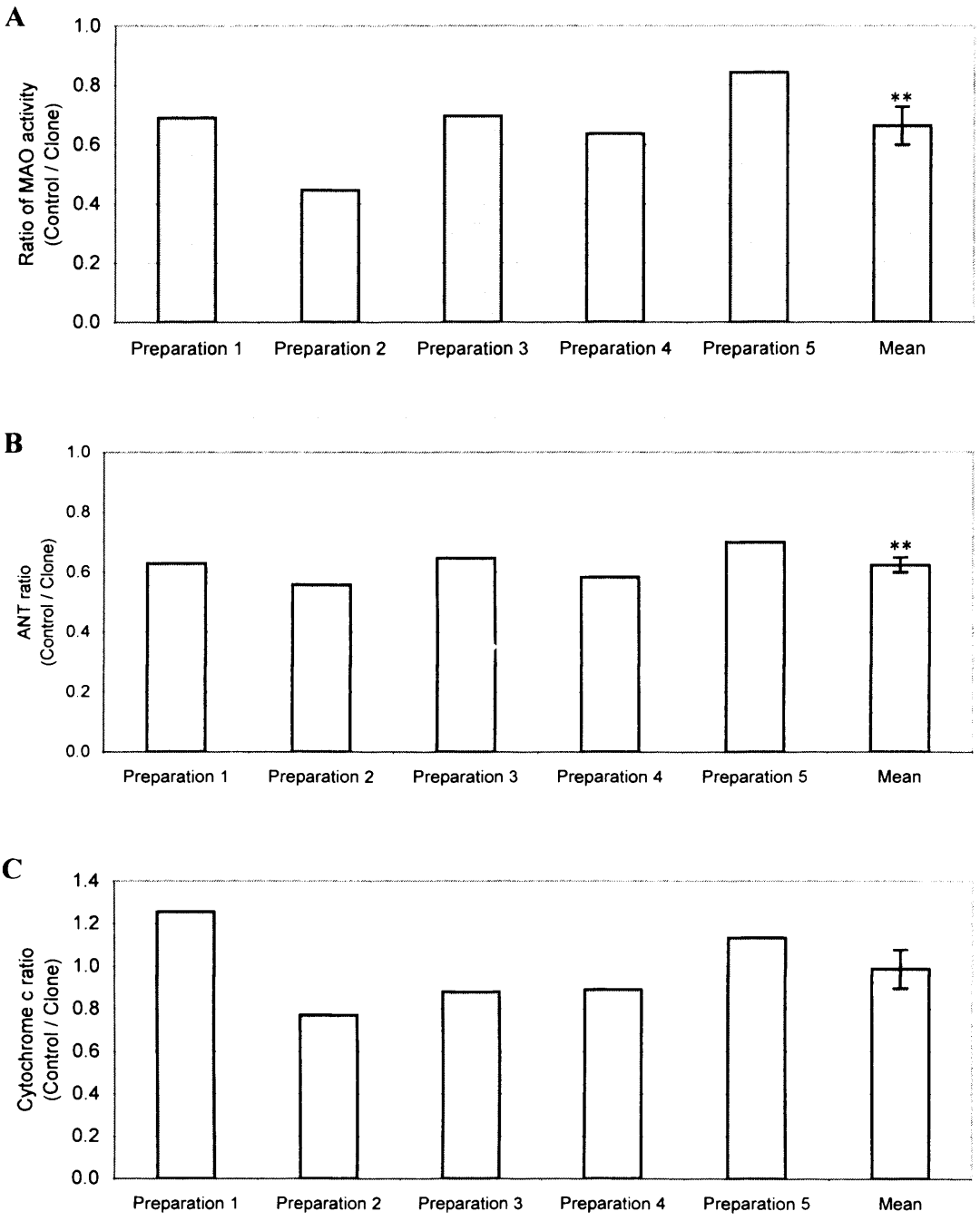

Figure 45 - Comparison of MAO, ANT and cytochrome c levels in mitochondria isolated from control and cyclophilin D(+) cells.

Mitochondria were isolated from B50 cell cultures on five separate dates. Protein levels were calculated per mg total mitochondrial protein, and values are presented as the ratio of protein levels in the control mitochondria compared to the cyclophilin D(+) mitochondria (clone mitochondria). Mean values are presented ± standard error. (**A**) Mitochondria were assayed for MAO activity by a fluorimetric assay [2.34]. MAO activity per unit of mitochondrial protein in control cells was on average 66 % of that in the clone cells ($p=0.05$) (**B**) Mitochondria were assayed for ANT by Western blot [2.16]. Quantity of ANT per unit of mitochondrial protein in control cells was on average 62 % of that in the clone cells ($p=0.02$). (**C**) Mitochondria were assayed for cytochrome c by Western blot [2.16]. There was no statistically significant difference in cytochrome c content between the two cell types.

This is in disagreement with the work of Scorrano and co-workers, who suggested that transient pore opening was responsible for mobilising cytochrome c stores during apoptosis [17]. The results also directly contradict one popular model, which has suggested outer membrane rupture following PT pore opening and mitochondrial swelling to be responsible for cytochrome c release [268]. They do this on two counts: firstly the calcein release experiments [5.3.2] show that PT pore opening does not occur during tBID-induced cytochrome c release; and secondly the fact that cytochrome c is not released from mitochondria following Ca^{2+}-induced pore opening [5.3.3] suggests that even sustained pore opening would be unable to release cytochrome c during apoptosis.

[4.7.1]Involvement of cyclophilin D

Cyclophilin D overexpression inhibits caspase activation in response to staurosporine, and thus clearly influences some stage of the apoptotic process. Additionally, the ability of cyclophilin D(+) mitochondria to release cytochrome c in response to BID and tBID is attenuated, suggesting BID-induced cytochrome c release may be the stage at which cyclophilin D exerts its protective effect. Interestingly, cyclophilin D overexpression results in an increase in the relative abundance of some mitochondrial proteins (MAO and ANT), but not others (cytochrome c). This may reflect an increased availability of tBID binding sites in these mitochondria, which might be involved in the mechanism of cyclophilin D's effect on apoptosis.

CHAPTER 6 : KINETICS OF BID-INDUCED CYTOCHROME C RELEASE

[6.1]Introduction

The majority of previous work on BID action has assessed cytochrome c release in a qualitative or semi-quantitative manner, following the appearance or disappearance of bands on Western blots of cytosolic or mitochondrial fractions, respectively. However, Goldstein and co-workers have carried out a kinetic analysis of cytochrome c release in whole cells following induction of apoptosis by staurosporine, actinomycin D, TNF and ultraviolet C [269]. These authors followed release of cytochrome c from individual mitochondria in HeLa cells stably expressing a cytochrome c-GFP fusion protein. Although cytochrome c release from the whole mitochondrial population occurred over several tens of mins, they observed cytochrome c release from any individual mitochondrion to be a rapid event, complete in around one min. Release was also temperature insensitive between 24 and 37 °C, indicating that release is a passive process. Aside from this work, little has been done to analyse the kinetics of cytochrome c release from mitochondria. This chapter describes an attempt to fit a kinetic model, derived from first principles, to experimental data on cytochrome c release from isolated mitochondria.

BID is believed to release cytochrome c from mitochondria by inducing the oligomerisation of membrane-associated BAK or BAX molecules into efflux pores [1.4.7]. Although both BAK and BAX are superficially associated with the outer mitochondrial membrane, it is only BAK that is constitutively integrated into the membrane [74]. The trans-membrane domain of BAX is folded back into a pocket formed by the BH1, 2 and 3 domains and is unavailable for membrane insertion before it is released during protein activation in apoptosis [75]. Thus mitochondria isolated from non-apoptotic cells tend to contain far greater amounts of BAK compared to BAX [Figure 71, below], and BID-induced release of cytochrome c from these mitochondria occurs predominantly via BAK channels.

[6.2]Time-course of tBID-induced cytochrome c release

[6.2.1]Introduction

Cytochrome c release was induced by the addition of tBID to a mitochondrial preparation, and the degree of release was assayed at several time-points [Figure 56]. Interestingly, although the duration to onset of release varied according to tBID concentration, the shape of the curve during release did not vary greatly. Specifically, the maximum rate of cytochrome c release (the maximum gradient of the release curve) appeared to be largely independent of tBID concentration. This is in keeping with a model whereby cytochrome c is released from mitochondria through a channel whose opening is induced by tBID. tBID determines the rate of opening of this release channel, but not its properties, once opened. The maximum efflux rate is an intrinsic property of the channel, and will be determined by the channel permeability and by the number of channels per mitochondrion. To develop a complete kinetic model, therefore, expressions for cytochrome c release from maximally permeabilised mitochondria and for tBID-induced appearance of open channels were first obtained separately [6.2.2], [6.2.3] and then combined [6.2.4].

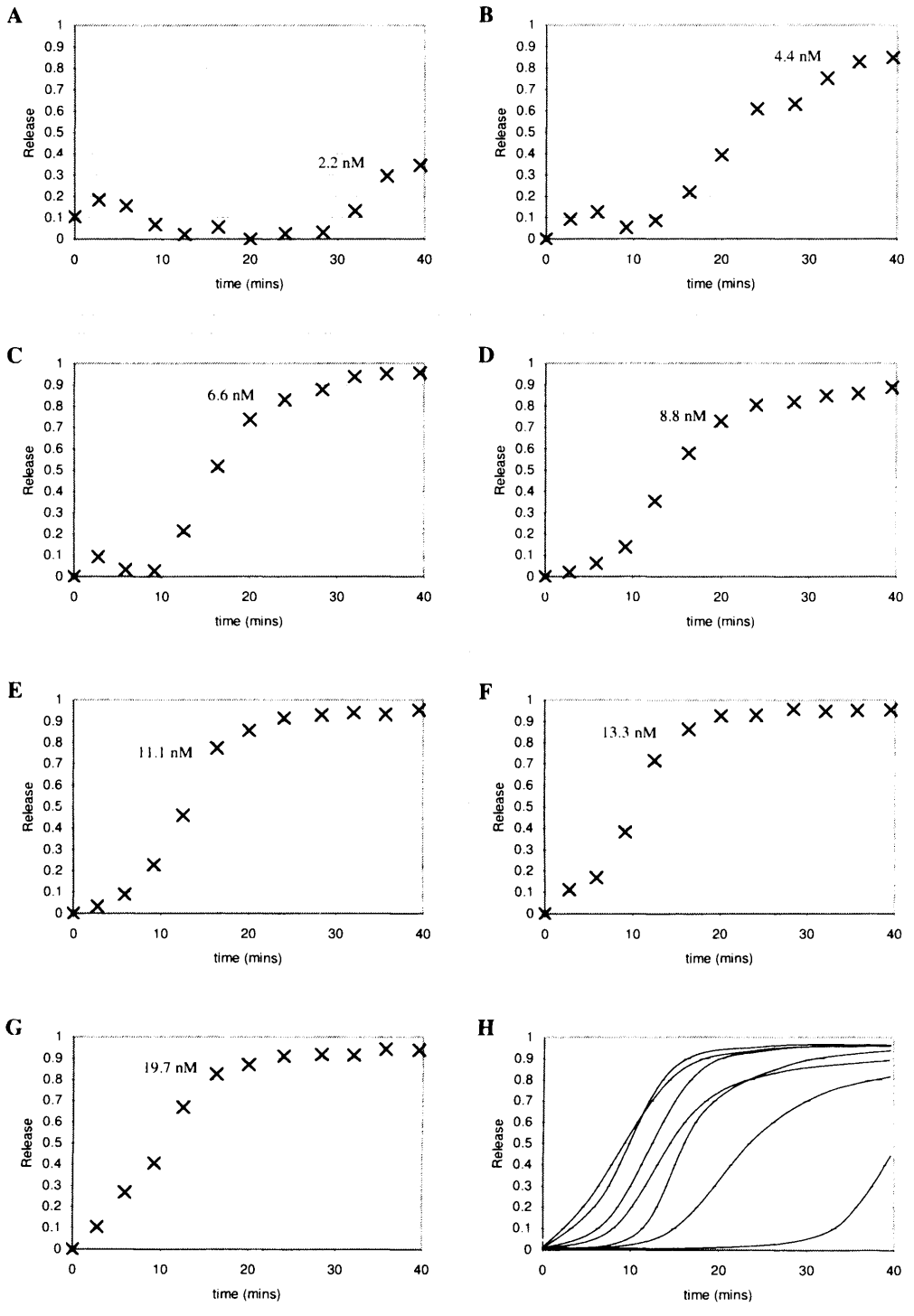

Figure 56 - Time-course of tBID-induced cytochrome c release at seven different tBID concentrations.
(**A-G**) Mitochondria were isolated from B50 cells [2.26] and cytochrome c release induced by addition of tBID, to the concentrations indicated. After various times, an aliquot was removed and centrifuged to pellet mitochondria [2.31]. Cytochrome c present in the mitochondrial fraction was assayed by Western blot [2.16] and is expressed relative to the cytochrome c content of mitochondria at the zero time-point. (**H**) Overlay of the cytochrome c release curves for all seven tBID concentrations.

[6.2.2]Maximal release rate

When channel opening is complete, the rate of cytochrome c efflux will be given by:

Equation 2

$$-\frac{d[Cytc]}{dt} = a \cdot [Cytc]_t$$

where $[Cytc]$ is the fractional amount of cytochrome c remaining inside mitochondria, and a is a constant reflecting the maximal number of channels and their intrinsic permeability.

The value of a defines the progress of cytochrome c release when all channels are open; i.e. the shape of the upper portion of the release curves in Figure 56. Integrating Equation 2 gives:

Equation 3

$$[Cytc]_t = b \cdot e^{-a \cdot t}$$

where$[Cytc]_t$ is the fractional internal concentration of cytochrome c at some time t, and b is a constant. Since $[Cytc]_t = 1$ at $t = 0$, $b = 1$ and therefore:

Equation 4

$$[Cytc]_t = e^{-a \cdot t}$$

The value of the constant a was determined using the release curves shown in Figure 56. The point of inflection was determined for each tBID concentration, and the release of the *remaining* cytochrome c was modelled from this point up to the point at which 95% was released. If all release channels were indeed open at the inflection point and above for each curve and, in addition, if cytochrome c effluxed from a single (or functionally single) pool of cytochrome c in the intermembrane space, then release would be first-order, with the value of a independent of [tBID] – i.e. :

Equation 5

$$[Cytc]_t^* = e^{-a \cdot t^*}$$

where t^* and $[Cytc]^*$ are defined to be 0 and 1 respectively at the point of inflection. Thus a plot of $\ln([Cytc]_t^*)$ against t^* should be linear with a slope of $-a$. These plots are shown in Figure 57 for the six highest tBID concentrations. The curves are indeed linear, with slopes largely independent of [tBID], showing release channels to be substantially open in this region of the release curves. Measurement of BAK conformational change [7.4] subsequently confirmed this observation. The value of a approaches 0.19 min^{-1}.

[6.2.3]Appearance of open channels

The time-course of tBID-induced release of a functionally single pool of cytochrome c, if all channels were open from time zero, would be as shown in Figure 58. However, clearly it is not the case that cytochrome c release channels are maximally open immediately following induction of release by tBID. Channels appear in the outer membrane slowly over time, in a manner dependent somehow on tBID concentration. Ruffolo and co-workers [100] and others have provided evidence that the cytochrome c channels form from BAK molecules in the outer membrane in an auto-catalytic fashion [6.4.2].

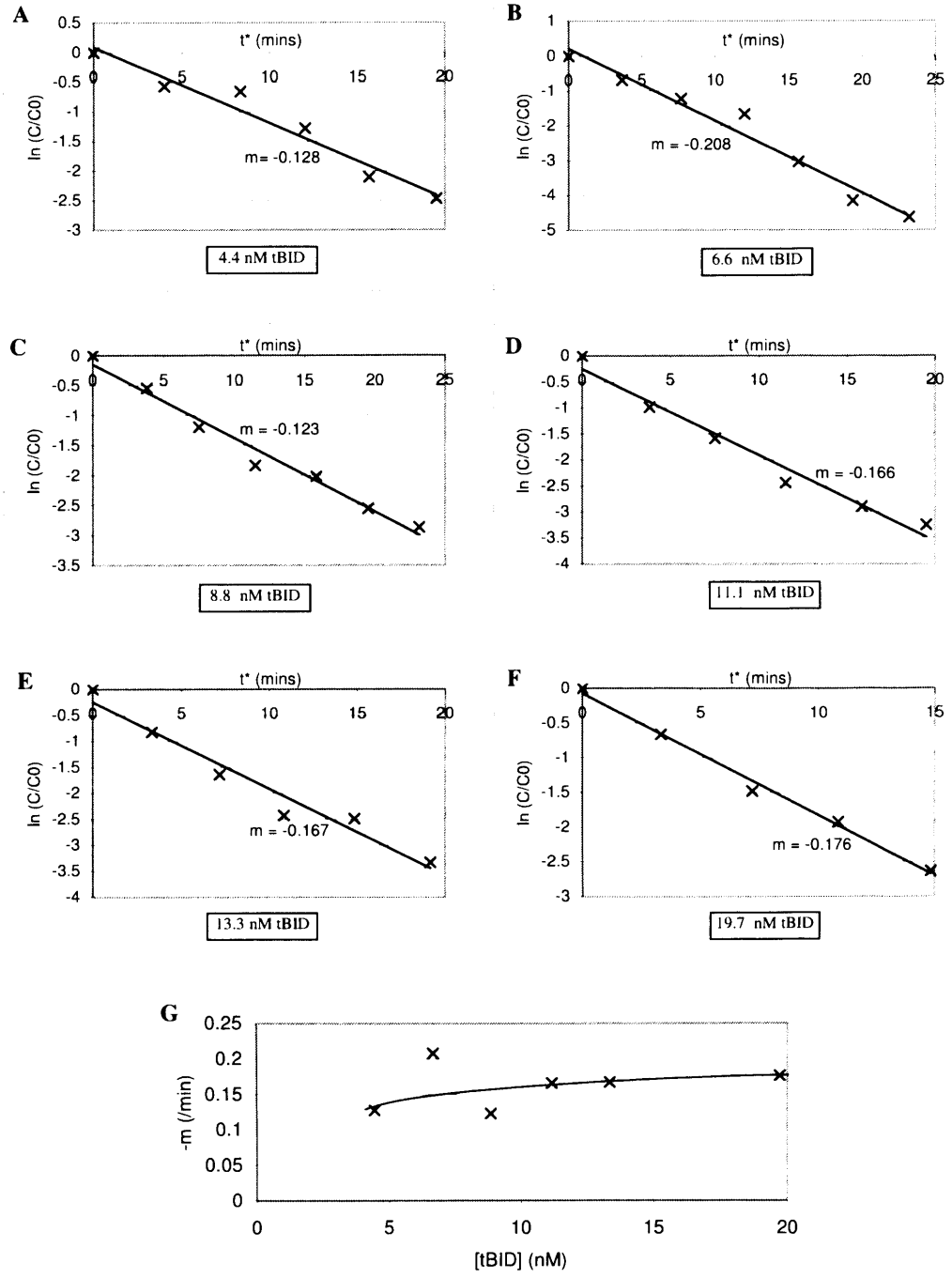

Figure 57 - Determination of the value of the constant *a*.
(**A-F**) Release of cytochrome c was analysed after the point of inflection of the curves shown in Figure 56. If release channels are essentially completely open after this point, release of the remaining cytochrome c should be a first-order process, with rate constant *a*. Thus plots of t* (time elapsed after the point of inflection) against $\ln(C/C_0)$ (where C takes values between 1 and 0, and represents the cytochrome c remaining after the point of inflection; i.e. $C_0=1$) should have gradient $m = -a$. (**G**) The relationship between [tBID] and the first-order rate constants (negative gradient of the plots in **A-F**) shows that the value of the constant *a* is approximately 0.19 min^{-1}.

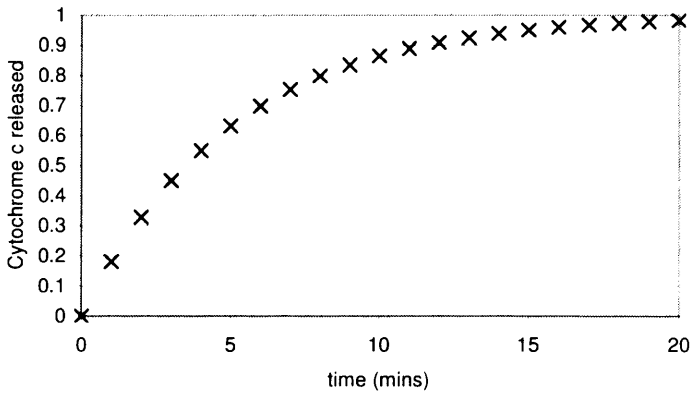

Figure 58 - Theoretical release of cytochrome c from mitochondria with fully open channels.
Cytochrome c is assumed to diffuse passively through channels, and the fractional amount remaining is therefore described by Equation 4. The value of the constant *a* was determined to be 0.19 min^{-1} [6.2.2].

According to this, an activated BH3-only protein such as tBID induces formation of an 'open' conformer of BAK, and these open conformers then catalyse the conversion of further 'closed' conformers into the 'open' form. 'Open' molecules can then self-assemble into active efflux channels. The process is shown in Figure 59, where c and f are constants defining the rates of tBID-induced and BAK*-induced conformational changes, respectively.

This model predicts that open channels will form in the membrane in an exponential fashion, with open channels appearing slowly at first, and then more and more quickly as the amount of 'open' conformer increases, up to a maximum defined by the initial total amount of BAK.

Mathematically, the composite rate constant for channel formation is:

Equation 6

$$c + f \cdot [Open]_t$$

where $[Open]$ is the fractional amount of open channels, taking values from 0 to 1. The constant c defines the initial rate of formation of open conformers (dependent on tBID concentration), and f defines the rate of auto-catalysis (an inherent property of BAK molecules) [Figure 59]. Open conformer formation is also a first-order process, with the rate of formation proportional to the amount of substrate (i.e. closed conformer) remaining. Thus Equation 7 gives the rate of open conformer formation.

Equation 7

$$\frac{d[Open]}{dt} = (c + f \cdot [Open]_t) \cdot [Closed]_t$$

It follows by integration [12.3.1], that:

Equation 8

$$[Open]_t = 1 - \frac{c + f}{c \cdot e^{(c+f)t} + f}$$

The appearance of open channels with time thus has the form shown in Figure 60, at the predicted value of $f = 0.33$ min^{-1} [6.3.1] and an arbitrary value of $c = 0.02$ min^{-1} (c is dependent on [tBID]; Figure 63 below).

[6.2.4]Rate of cytochrome c efflux

Assuming the rate of efflux is proportional to the concentration of open channels, combining Equation 2 and Equation 8 gives:

Equation 9

$$-\frac{d[Cytc]}{dt} = \left(1 - \frac{c + f}{c \cdot e^{(c+f)t} + f}\right) \cdot a \cdot [Cytc]_t$$

Thus, by integration [12.3.2], it follows that:

Equation 10

$$[Cytc]_t = \frac{\exp\left[a.\left(-t + (c+f)\left[\frac{t}{f} - \frac{1}{f \cdot (c+f)} \cdot \ln\left(c \cdot e^{(c+f)t} + f\right)\right]\right)\right]}{\exp\left[\frac{-a \cdot \ln(c+f)}{f}\right]}$$

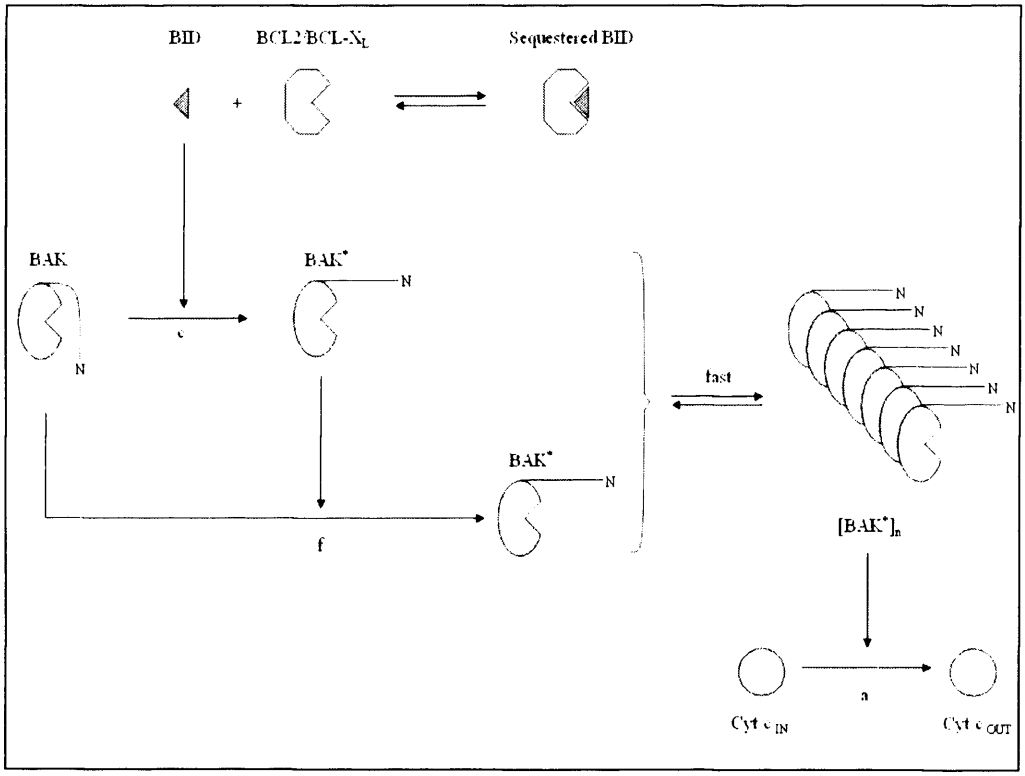

Figure 59 - Model for release of mitochondrial cytochrome c though BAK channels. Free tBID induces an open conformer of BAK, which can then induce the conversion of other BAK molecules to the open form. Open molecules self-assemble into an active efflux pore $[BAK]_n$, through which cytochrome c molecules cross the outer membrane. Adapted from [100].

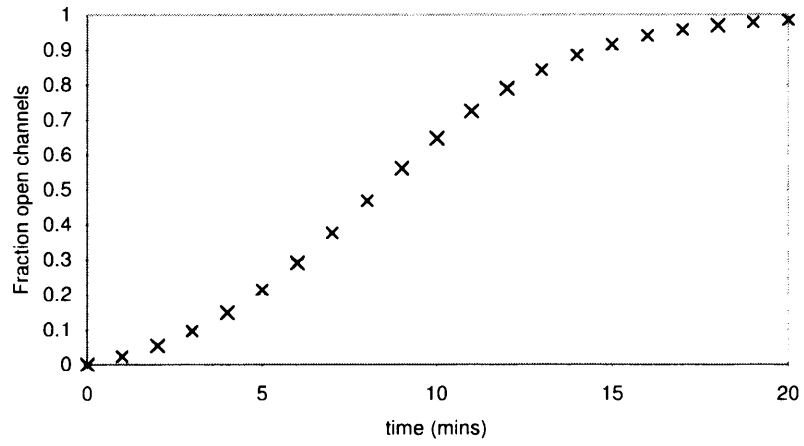

Figure 60 - Appearance of open BAK channels with time.
BAK channel formation was modelled according to the scheme shown in Figure 59, with $c = 0.02$ min^{-1} and $f = 0.33$ min^{-1}. Appearance of channels is initially exponential with time, but is limited by the availability of substrate (closed BAK conformer) at later time-points. The maximum channel activity is defined by the total initial amount of BAK.

This gives the predicted mitochondrial cytochrome c content at any time in terms of the constants a, f and c.

[6.2.5]Effect of changes in a, f and c

The constants included in the complete model are defined in Table 8. a and f should be dependent only on characteristics of the mitochondrial preparation used, and so should not vary when fitting the model to experimental data from any one preparation. The value of c should depend on the tBID concentration.

[6.3]Fitting the model to experimental data

[6.3.1]Deriving the value of the constants c and f

The relationship between the value c and the tBID concentration was investigated by fitting curves generated by the model above to the experimental data shown in Figure 56. The value of a was fixed at 0.19 min^{-1}, for the reason discussed above [6.2.2]. The values of f and c were initially chosen arbitrarily. Additionally, a scaling factor was introduced to take account of the fact that the range of release values is frequently less than 1 – i.e. the response to tBID plateaus at 90 – 98 % release, and there is some release even at zero time. Thus a predicted release value x was adjusted to give a new value y that was used for comparison with the experimental value, where:

Equation 11

$$y = r_{min} + x \cdot (r_{max} - r_{min})$$

r_{max} is the apparent maximum release value, when the tBID response has plateaued, and r_{min} is the apparent minimum release value.

An error function was then defined for each tBID concentration as the sum of the squares of the differences between experimental and predicted values for cytochrome c release. The value of c was then adjusted for each of the seven tBID concentrations tested, to minimise the value of this error function, thus generating an optimal fit of the model to the experimental data, for the initial arbitrary value of f. A second error function was then defined as the sum of the error function over all seven tBID concentrations. The value of the constant f was then altered, and the fitting process repeated to give a new value of this second error function. Figure 61 shows the effect on the second error function of changing the value of f, and reveals the optimal value of f to be approximately 0.33 min^{-1}. (The change of units from $min^{-1}.M^{-1}$ to min^{-1} reflects the use in the model of fractional BAK concentrations (i.e. the total concentration of BAK is defined to be 1, and the concentration of 'closed' and 'open' conformer ranges from 0 to 1).) Figure 62 shows the fit between experimental and predicted values for this value of f. The derived values for c at the seven tBID concentrations are shown in Figure 63.

[6.3.2]*Significance of the relationship between [tBID] and* c

It seems reasonable to suppose that tBID should affect the value of c in a linear manner – double the amount of tBID should give twice the rate of 'seeding' of open BAK conformers. Figure 63 does indeed appear to show a linear relationship, apart from an initial lag.

Constant	Units	Definition	Determined by
a	min^{-1}	Rate constant for cytochrome c efflux, with maximal channel activity (fully open channels)	Characteristics of open channel
c	min^{-1}	Rate constant for 'seeding' of open BAK conformers – i.e. for tBID-induced conversion of BAK from closed to open conformer	Characteristics of tBID action
f	$M^{-1}.min^{-1}$	Rate constant for auto-catalysis of open BAK conformer formation – i.e. for BAK-induced conversion of new BAK molecules from closed to open state	Characteristics of channel subunits

Table 8 - Constants included in the model for tBID-induced cytochrome c release developed above.

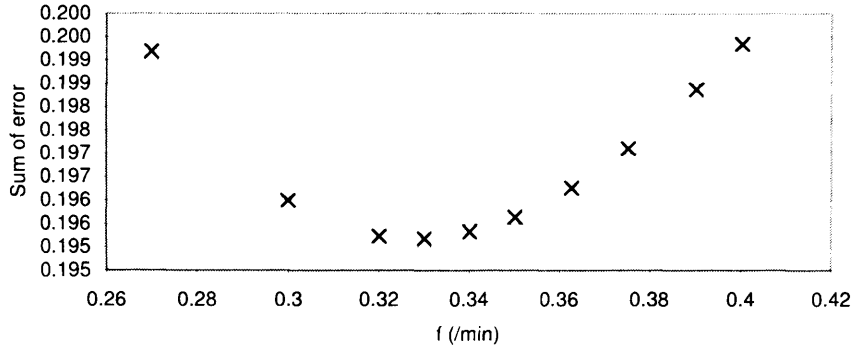

Figure 61 - Determination of the value of the constant *f*.
The value of *f* was adjusted iteratively to minimise the value of the error function defined as the sum of the square of the difference between predicted and experimental values over all 84 experimental points (12 time-points at 7 different tBID concentrations). The change of units from $min^{-1}.M^{-1}$ to min^{-1} reflects the use in the fitting model of fractional BAK concentrations (ranging from 0 to 1), with the sum of concentrations of 'closed' and 'open' conformer always equal to 1.

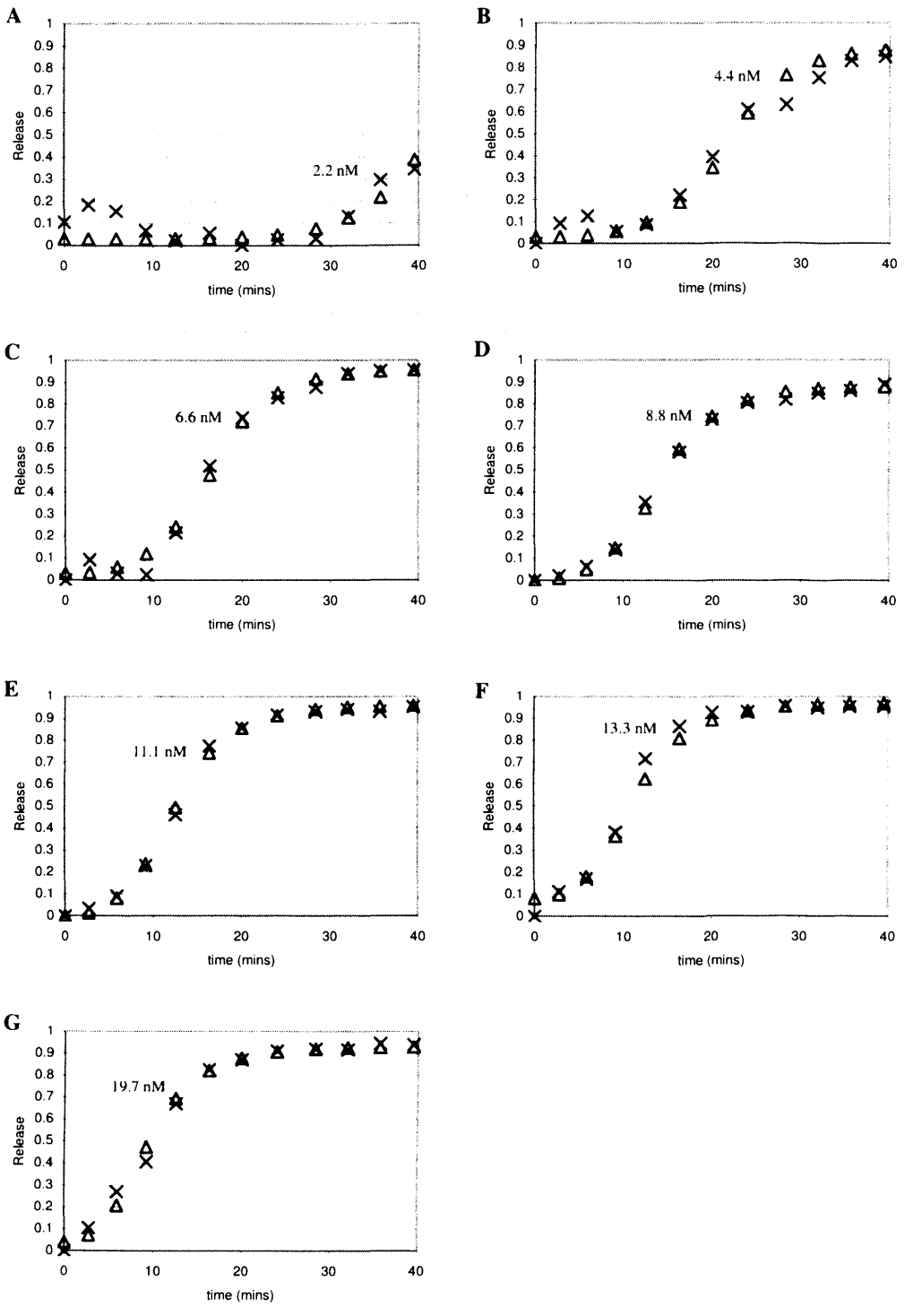

Figure 62 - Comparison of experimental data on tBID-induced cytochrome c release and predicted release data from the model developed above.
The values of *a* and *f* were fixed at 0.19 min^{-1} and 0.33 $M^{-1}.min^{-1}$ respectively, and the value of *c* was altered to fit the predicted values (Δ) to the experimental points (x), by a least-squares method. (**A**) 2.2 nM tBID (**B**) 4.4 nM tBID (**C**) 6.6 nM tBID (**D**) 8.8 nM tBID (**E**) 11.1 nM tBID (**F**) 13.3 nM tBID (**G**) 19.7 nM tBID.

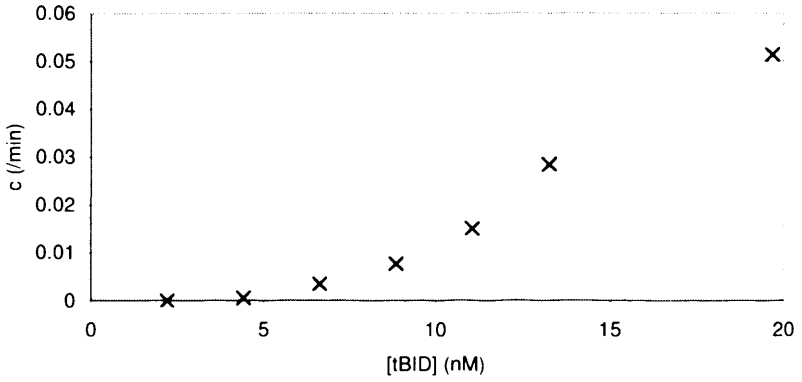

Figure 63 - Values of c for the seven different tBID concentrations, derived by fitting the model to the experimental data points of Figure 56.

The lag may represent sequestering of tBID by antiapoptotic BCL2 family proteins such as BCL-2 and BCL-X_L; these proteins contain a deep groove formed by the BH1 and BH2 domains, into which the BH3 domain of a binding partner can insert [270]. This interaction would sequester tBID, preventing it from binding to BAK effectors and stimulating their conversion to 'open' conformers able to oligomerise into active efflux pores [101]. According to this, the response to low concentrations (< 5 nM) of tBID would be very small, since there would be no free tBID to catalyse BAK oligomerisation. Above 5 nM tBID or so, the response to tBID becomes linear; in this region all anti-apoptotics would be saturated. Alternatively, the sigmoidal relation seen in Figure 63 may reflect cooperative behaviour of tBID. In this connection, tBID oligomers have been observed in mitochondria, and have been causally associated with apoptotic progression [103]. BID oligomers were also observed during purification of the recombinant protein [3.6].

[6.4]Discussion

[6.4.1]Summary of the model

A model is described above which predicts the efflux of cytochrome c from mitochondria with time, following treatment with tBID. tBID molecules initially catalyse the conversion of BAK molecules to an open state; they do this at a rate proportional to the concentration of free tBID, and to a constant c. 'Open' BAK conformers are able to self-catalyse the conversion of more BAK molecules from a closed to an open state; they do this at a rate proportional to the existing concentration of 'open' conformers, and to a constant f. Open BAK conformers rapidly self-assemble into channels for cytochrome c efflux, and cytochrome c diffuses passively through these channels. The rate of efflux is proportional to a constant a. The blunted response to small amounts of tBID may be explained by the presence of anti-apoptotic BCL2-family proteins in the outer membrane. These proteins would initially sequester a small amount of tBID, so that a strong response is seen only when they become saturated, leaving tBID free in the membrane. The complete model is represented in Figure 59 (page 131).

[6.4.2]Correspondence with experimental data

The model has a good correspondence with the experimental data presented here [Figure 62], and allows calculation of kinetic parameters for tBID action. The model is also entirely consistent with the work of Ruffolo and co-workers [100]. These authors used cross-linkers or trypsin digestion to identify the activated conformer of BAK; conversion to this form exposes a novel trypsin site and also removes the potential for inter-molecular cross linking of two cysteine residues to form a structure with increased mobility on SDS-PAGE. They showed that a BID BH3 peptide was able to induce conversion of BAK to the open form, and that these open BAK molecules could then oligomerise, concomitant with release of cytochrome c from mitochondria. Additionally, by incubating mitochondria with a synthetic 'open' BAK conformer lacking the inhibitory N-terminus, they showed that existing open conformer was able to catalyse conversion of new BAK molecules to the open form (self-catalysis).

Clearly, however, the model developed here is in some ways speculative, given that there remains considerable disagreement over the precise mechanisms of tBID action and of cytochrome c efflux.

For example Goldstein and co-workers [269] suggest that the shape of cytochrome c efflux curves with time might be a result of heterogeneity amongst the mitochondrial population, with any one mitochondrion releasing cytochrome c very rapidly, but the population as a whole releasing cytochrome c slowly over time. This is in contrast with the model described above, which assumes a homogeneous mitochondrial population, with all mitochondria releasing cytochrome c over a similar time-course.

[6.4.3]Fitting the model to experimental data

The value of a model for tBID action is in determining the reasons for changes in response to tBID under different experimental conditions. If the EC_{50} or shape of release curve for tBID action is changed as a result of the addition of some inhibitor, or the use of a different mitochondrial preparation, the model should help to determine the reason for this change - i.e. which of the constants *a, f* or *c* have changed - since changing each constant gives a characteristic change in the predicted tBID response. Clearly though it is ultimately impossible to make firm predictions concerning mechanistic changes on the basis of information derived from a theoretical model; the effect of one change may be masked by that of another, and de-convoluting the effects of several concurrent changes is unlikely to be possible given only a limited amount of experimental data. Nevertheless, the model described above may certainly suggest or rule out some possibilities in attempting to explain the effect of some variation in experimental conditions, and in particular, it can be used to provide information on otherwise experimentally inaccessible parameters (e.g. *a*). Below [7.3.2] the model is used to analyse how CSA affects cytochrome c release.

CHAPTER 7 : THE EFFECT OF CYCLOSPORIN A ON CYTOCHROME C RELEASE

[7.1]Introduction

Cyclosporin A (CSA) [Figure 64] was first isolated as a metabolite of the prokaryote *Tolypocladium inflaturns* [162]. CSA binds tightly to cyclophilins and inhibits their PPIase activity; the K_d varies depending on cyclophilin isoform, from 2-5 nM for cyclophilins A, B and D, to 300 nM for cyclophilin 40 [163,164]. CSA also strongly inhibits PT pore opening, presumably by inhibiting cyclophilin D [165]. CSA affects other mitochondrial systems, independent of cyclophilins; for example CSA inhibits the calcium uniporter, albeit only at relatively high concentrations (1 – 10 μM) [169]. CSA also inhibits activity of the cytosolic phosphatase calcineurin, via an unusual mechanism involving cyclophilin A. Cyclophilin A is normally unable to interact with calcineurin, but upon CSA binding the binary complex is able to bind and inhibit the phosphatase; thus as well as inhibiting cyclophilin A's isomerase activity, CSA concurrently gives a gain-of-function effect [271].

There are numerous reports of effects of CSA on cell death, and on apoptosis in particular (reviewed in [164]). Several groups have looked specifically at the effect of CSA on cytochrome c release from isolated mitochondria, with conflicting results. Shimizu and co-workers demonstrated that BID- or BIK- induced cytochrome c release from isolated mitochondria was CSA-insensitive in their system [56]. However a number of workers have shown inhibition by CSA of BAX- and/or BAK-induced cytochrome c release [119,121,179], and Scorrano and co-workers [17] report inhibition of the analogous process induced by tBID. The latter authors attributed this effect to inhibition by CSA of a process of mitochondrial remodelling facilitating diffusion of cytochrome c from intracristal spaces to outer membrane BAX/BAK pores.

The objectives of the work presented here were firstly to determine the effect of CSA on tBID-induced release of cytochrome c from isolated B50 cell mitochondria and, secondly, to analyse the nature of any inhibition using the kinetic model developed in CHAPTER 6.

[7.2]Effect of CSA on mitochondrial respiration

It has been reported that CSA affects mitochondrial respiration. Hokanson and co-workers observed an 18% decrease in succinate/rotenone-stimulated mitochondrial oxygen consumption in the presence of CSA [172]. In contrast, Zhong and co-workers reported that CSA stimulates a hypermetabolic state in liver cells, inducing a 60 % *increase* in mitochondrial oxygen consumption [171]. Since mitochondrial cytochrome c release is affected by mitochondrial inner membrane potential $\Delta\Psi_m$ [4.7], determined in part by the rate of respiration, it was important first to check the effect of CSA on $\Delta\Psi_m$ under conditions used to measure BID-induced cytochrome c release.

Mitochondria from normal B50 cells and from cyclophilin D-over-expressing B50 cells were resuspended in respiration buffer containing tetraphenylphosphonium ion (TPP^+) [2.29.4]. TPP^+ is accumulated by respiring mitochondria according to the magnitude of $\Delta\Psi_m$; at equilibrium the Nernst equation describes the distribution:

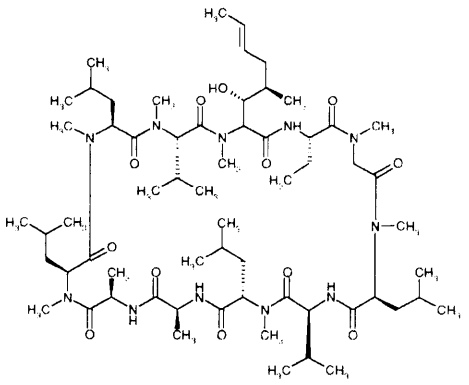

Figure 64 - The structure of Cyclosporin A (CSA).
CSA is [R-[R*,R*-(E)]]-cyclic(L-alanyl-D- alanyl-N-methyl-L-leucyl-N-methyl-L-leucyl-N-methyl-L-valyl-3-hydroxy-N, 4-dimethyl-L-2-amino-6-octenoyl-L-α-amino-butyryl- N-methylglycyl-N- methyl-L-leucyl-L-valyl-N-methyl-L-leucyl). This 11-residue polypeptide was originally isolated from *Tolypocladium inflaturns.* It binds to and inhibits cyclophilins with a K_d of 2 – 300 nM.

$$\Delta\Psi = 2.3 \cdot \frac{R \cdot T}{F} \cdot \log\left(\frac{[TPP^+]_{in}}{[TPP^+]_{out}}\right)$$

Mitochondria were pre-incubated in respiration buffer [2.31.1] in the absence of the respiratory substrate succinate. Subsequent addition of succinate to generate $\Delta\Psi_m$ induced rapid TPP^+ uptake [Figure 65], decreasing the extramitochondrial TPP^+ from 1.43 μM to approximately 1.25 μM. This was followed by a slow progressive loss of TPP^+ over time. Negligible change was induced by addition of CSA. Similar data were obtained with mitochondria isolated from the cyclophilin D overexpressing cells. Thus, under the experimental conditions used to measure BID-induced cytochrome c release, changes in $\Delta\Psi_m$ induced by CSA or by cyclophilin D overexpression were very small.

[7.3]The effect of CSA on tBID- induced cytochrome c release

[7.3.1]Cytochrome c release

Cytochrome c release from isolated mitochondria was induced by tBID using the system developed in CHAPTER 4. Experiments in the presence and absence of CSA were conducted in parallel. tBID-induced cytochrome c release was clearly inhibited by CSA [Figure 66] - over 12 such experiments, the degree of inhibition was variable from preparation to preparation, but overall 1.2 μM CSA increased tBID EC_{50} by 105 % (standard error 35 %; p = 0.011) [Figure 67]. In contrast, CSA had no effect on BID-induced cytochrome c release [Figure 67]. Inhibition by CSA was surprising – given that cyclophilin D overexpression inhibits BID-induced cytochrome c release [5.4.4], CSA would be expected to reverse this effect by inhibiting cyclophilin D action.

[7.3.2]Defining the effect of CSA on tBID-induced cytochrome c release

The model developed in Chapter 6 accurately predicts the kinetics of tBID-induced cytochrome c release. For a defined mitochondrial preparation, the model may be used to predict the time-course of cytochrome c release at a given tBID concentration. Moreover, since the model allows predictions to be made about the effect of changing one or more of the kinetic parameters, it may be used to analyse which of these constants are affected by CSA.

Cytochrome c release was induced from a mitochondrial preparation by tBID, in the presence or absence of CSA. Inhibition of tBID-induced cytochrome c release by CSA was confirmed by assaying for cytochrome c [Figure 68]. The kinetic model was used to derive values for the relevant parameters [Figure 68(**A**)], which were a = 0.26 min^{-1}, f = 0.43 min^{-1} and c=0.000988 min^{-1}. The only parameter requiring adjustment to fit the predicted points to the experimental points in the presence of CSA [Figure 68(**B**)] was the rate of seeding of 'open' BAK conformer by tBID: c was reduced to 0.000161 min^{-1}. Adjustment of either f or a was not able to fit the predicted cytochrome c release to the experimental data [Figure 68(**C,D**)]. In both cases, if the value of the parameter was adjusted so as to fit the predicted cytochrome c release to the experimental data at early time-points, the model predicted release values at later time-points that were too low; and vice versa.

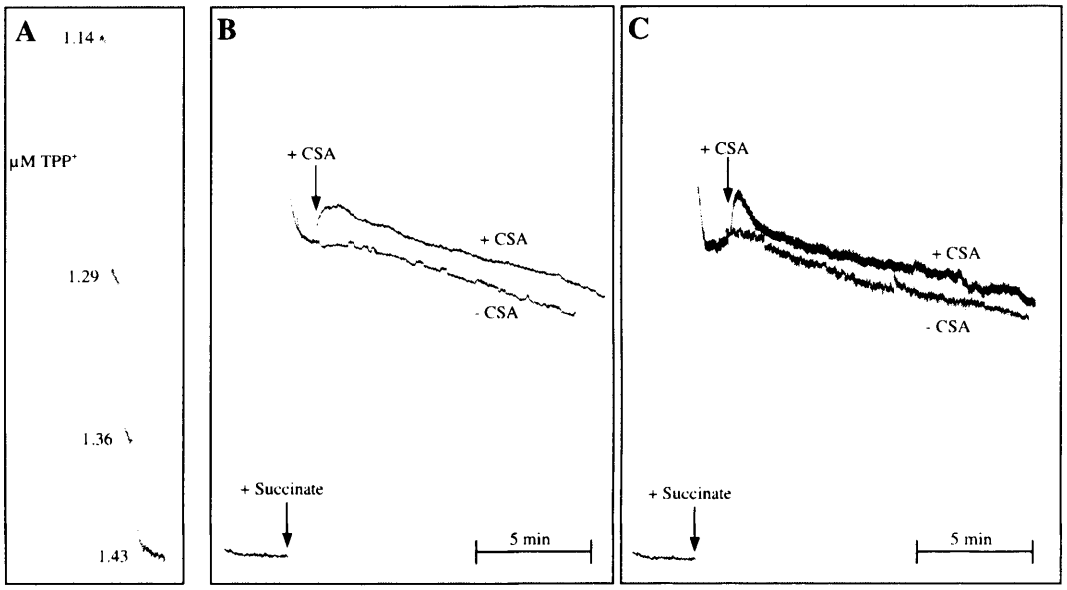

Figure 65 - Neither CSA nor cyclophilin D overexpression affects mitochondrial inner membrane potential.
A TPP^+-sensitive electrode was used to measure membrane potential [2.29].
(**A**) Calibration with TPP^+: B50 mitochondria [2.26] were resuspended in respiration buffer [2.31.1]. Aliquots of TPP-Cl were added sequentially to 1.43 µM.
(**B,C**) Mitochondrial respiration was started by addition of succinate (arrow). TPP^+ accumulation was followed for approximately 15 mins both in control B50 mitochondria (**B**) and cyclophilin D(+) mitochondria (**C**). 1.2 µM CSA was added after 3 mins where indicated. Results are representative of three independent experiments.

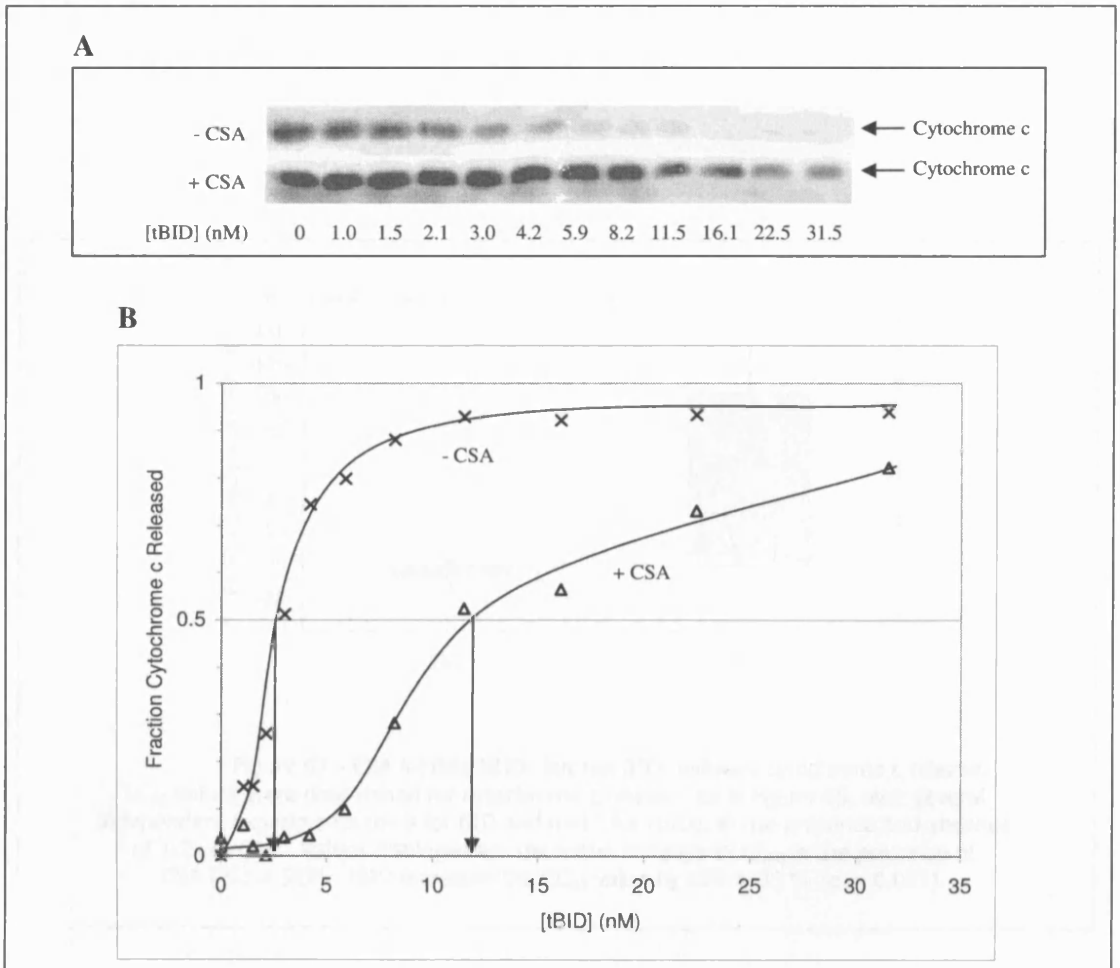

Figure 66 - CSA inhibits tBID-induced cytochrome c release from isolated mitochondria. Cytochrome c release [2.31] was induced in the presence (Δ) or absence (x) of 1.2 μM CSA, as indicated. Mitochondria were incubated with varying concentrations of tBID. (**A**) After 30 mins incubation at 30 ºC, mitochondria were separated from the assay mixture by centrifugation. After Western blotting, the membrane was probed with an anti-cytochrome c antibody [2.16]. (**B**) Fraction cytochrome c remaining in each mitochondrial pellet was calculated by dividing the cytochrome c signal from the pellet by the maximum cytochrome c reading. Results are representative of twelve independent experiments.

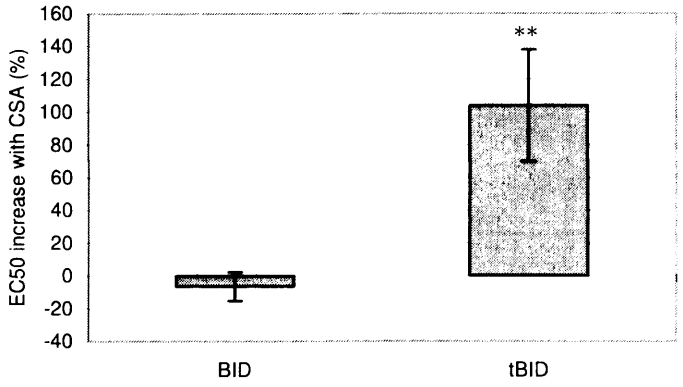

Figure 67 - CSA inhibits tBID- but not BID- induced cytochrome c release. EC_{50} values were determined for cytochrome c release, as in Figure 66, over several independent experiments (n=6 for BID and n=12 for tBID), in the presence and absence of 1.2 μM CSA. Values displayed are the mean increase in EC_{50} in the presence of CSA (%) ± SEM. tBID increases the EC_{50} value by 105 ± 35 % ($p = 0.011$).

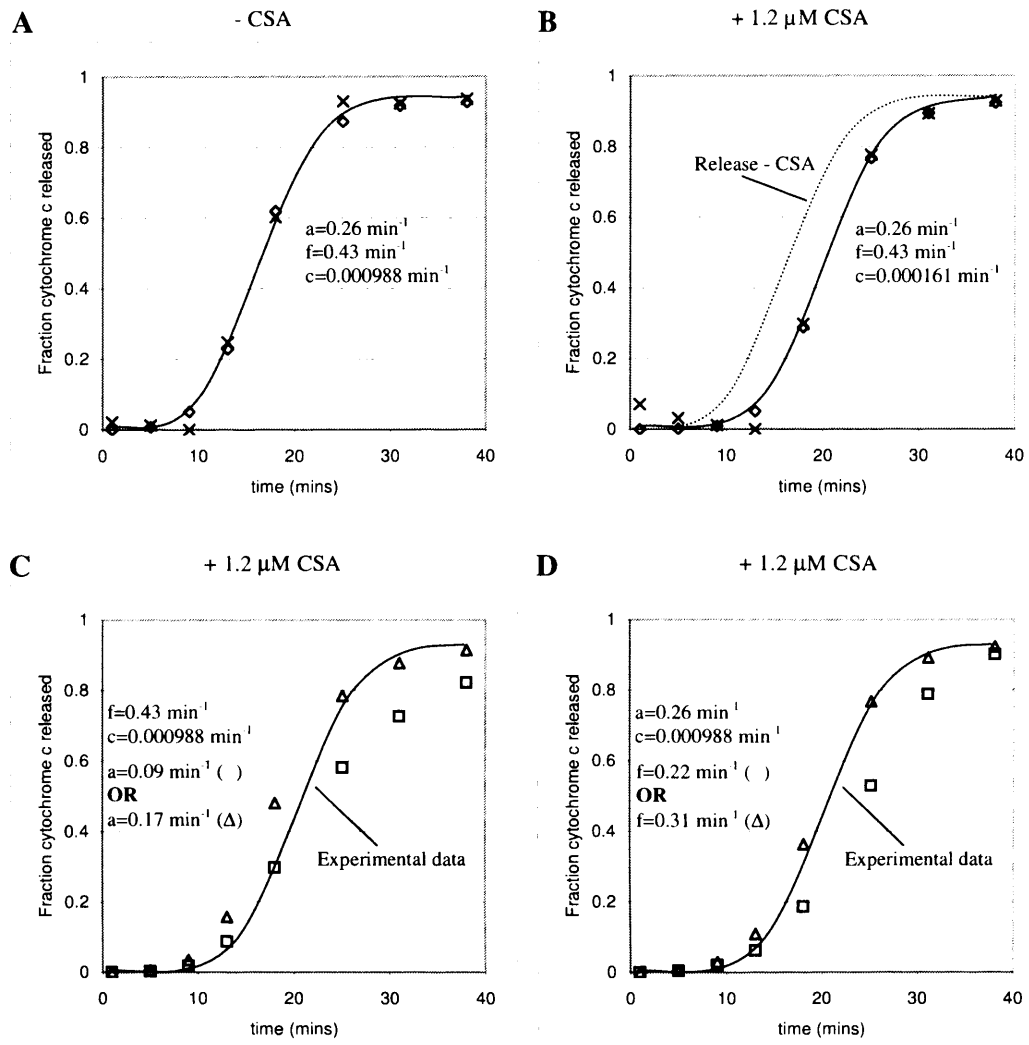

Figure 68 - CSA inhibition of tBID-induced cytochrome c release; analyses according to the kinetic model.

Mitochondria were incubated with 1 nM tBID, with (**B**,**C**,**D**) or without (**A**) 1.2 μM CSA, and an aliquot removed at the indicated times [2.31]. Mitochondria were separated by centrifugation and assayed for cytochrome c content by Western blot [2.16] (**A** and **B**; x). The kinetic model developed in CHAPTER 6 was used to predict cytochrome c release at each time-point (**A** and **B**; ◇), using Equation 10 (page 130). The model shows that the effect of CSA can be explained by an alteration in the constant *c*: RMS deviation of predicated from experimental points = 0.025 (- CSA), 0.028 (+ CSA). Conversely, the effect of CSA is less explicable by a change in the constant *a* (**C**) or *f* (**D**). It was attempted to fit the predicted release (**C** and **D**; Δ and) to the experimental data obtained in the presence of CSA (**C** and **D**; line). (**C**) Changing the value of *a* did not accurately reflect the effect of CSA. The RMS deviation for an optimum fit was 0.060. (**D**) Changing the value of *f* allowed a closer fit to the experimental data (RMS deviation 0.040), but the fit was less close than that obtained by changing *c* (RMS deviation 0.028).

The root-mean-square (RMS) deviation of predicted values from the experimental data points was 0.028 when the predicted values were adjusted by altering c; 0.060 when a was altered, and 0.040 when f was altered. This compares with an RMS deviation of 0.025 for the fitting of the model to the experimental data in the absence of CSA. It appears, therefore, that CSA inhibits tBID-induced cytochrome c release by inhibiting tBID-induced conformational change of BAK. This possibility was investigated further in [7.4] below.

[7.4]Assay for BAK conformational change

[7.4.1]Introduction

Ruffolo and co-workers [100] describe a technique for assaying the conformational change in BAK that occurs prior to oligomerisation and cytochrome c release. The assay relies on the closed conformer having no exposed trypsin cleavage sites. Upon conformational change a site is exposed, so that 'open' BAK is digested into fragments which are unreactive against a certain BAK antibody. As discussed above, the kinetic model predicts that CSA alters the value of c, the rate constant for tBID-induced conformational change of BAK. This prediction was therefore checked using this trypsin cleavage technique to detect BAK conformational change induced by tBID in the presence and absence of CSA.

[7.4.2]Development of assay

The BAK digestion assay [2.36] was used in this study to reveal the time-course of BAK conformational change during tBID-induced cytochrome c release assays [2.31]. Figure 69 shows the development of the assay, in which a range of trypsin concentrations and two digestion times were compared for their ability efficiently to digest BAK only after treatment with tBID to induce the open conformer. With 20 mins incubation, some BAK was digested even without tBID treatment. No such digestion was apparent after 10 mins of trypsin digestion. Therefore a 10 min digestion period with 0.05 mg/ml trypsin was adopted as standard.

Since the purpose of the assay was to correlate BAK conformational change with cytochrome c release, it was important to verify that no further cytochrome c release or conformational change occurred during the period of BAK digestion. As shown in Figure 70, 10 mins pre-incubation on ice prior to trypsin treatment had no effect on either BAK conformational change or cytochrome c release, confirming that both reactions are effectively stopped during the period of BAK digestion by trypsin.

In intact cells, BAX translocates to mitochondria during apoptosis, and is also able to oligomerise into cytochrome c efflux pores [88]; the kinetics of BAX oligomerisation would not necessarily follow those of BAK. Thus it was important to confirm that there was no BAX associated with the mitochondria used here, and therefore that the efflux pore was composed of BAK molecules. A shown in Figure 71, although BAX is present in whole cells, there is indeed none detectably associated with the mitochondrial fraction.

Figure 72 shows the correspondence between BAK conformational change and cytochrome c release. As predicted by the kinetic model [CHAPTER 6], BAK conformational change precedes cytochrome c release; at 50 % cytochrome c release over 85 % of BAK has been converted to the 'open' conformer.

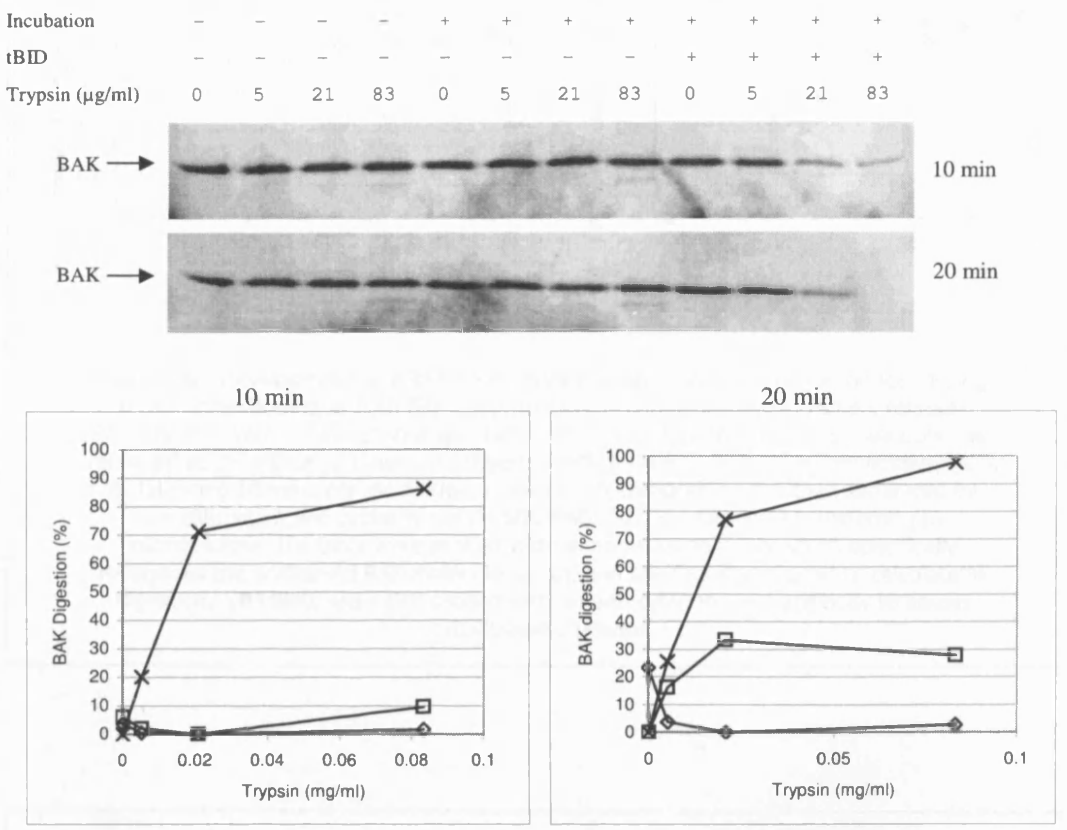

Figure 69 - Development of a BAK conformation assay : trypsin concentration and incubation time.

Mitochondria were incubated in respiration buffer [2.31.1] with or without 2 nM tBID. An aliquot was removed at zero time (◇) and after 30 mins incubation with tBID (x) or without tBID (□). The aliquots were then treated with the indicated concentration of trypsin at 0 °C, either for 10 mins or for 20 mins. Mitochondria were separated by centrifugation and proteins run on SDS-PAGE [2.13]. After transferring to nitrocellulose, the blots were probed with an anti-BAK antibody [2.16] which specifically recognises the uncleaved BAK molecule (top). The BAK signal was used to calculate % digestion (bottom). The data show that with 10 mins incubation, trypsin digests BAK only following incubation with tBID.

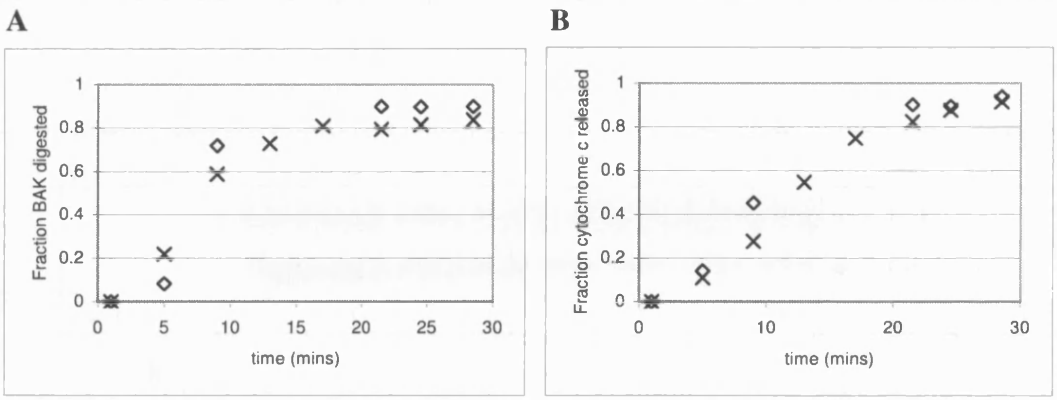

Figure 70 - Development of a BAK conformation assay : does incubation on ice (during trypsin digestion) stop both BAK conformational change and cytochrome c release? Mitochondria were incubated in respiration buffer [2.31.1] with 2 nM tBID. Aliquots were removed at the indicated times, and digested with trypsin [2.36] either immediately (◇), or following 10 mins pre-incubation on ice (x). Mitochondria were then separated by centrifugation and proteins run on SDS-PAGE [2.13]. (**A**) After transferring to nitrocellulose, the blots were probed with an anti-BAK antibody which specifically recognises the uncleaved BAK molecule [2.16], and the BAK signal used to calculate % digestion. (**B**) Blots were also probed with an anti-cytochrome c antibody to assess cytochrome c release.

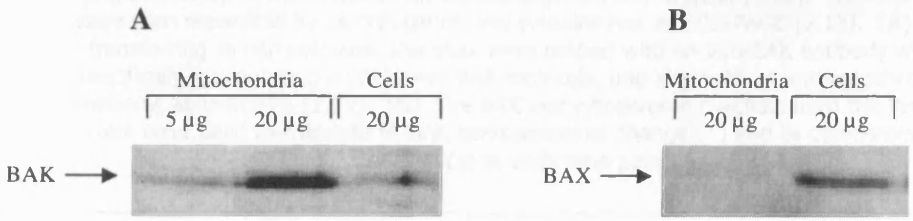

Figure 71 - BAK, but not BAX, associates with the mitochondrial fraction. Mitochondria were isolated from B50 cells [2.26] and the indicated quantity (µg protein) run on SDS-PAGE [2.13] together with whole B50 cells, as indicated. Proteins were transferred to nitrocellulose by Western blotting [2.16]. (**A**) The blot was probed with an anti-BAK antibody (Upstate), showing that the BAK protein is enriched in the mitochondrial fraction (compare lanes 2 and 3). (**B**) A separate blot was probed with an anti-BAX antibody, showing that, although BAK is present in whole cells (lane 2) it is not associated with the mitochondrial fraction (lane 1).

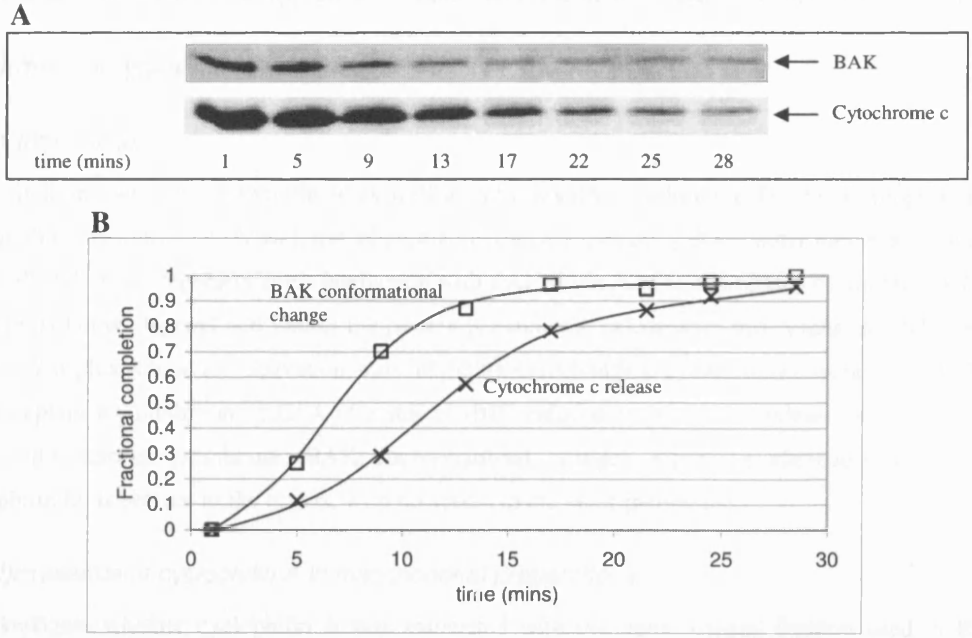

Figure 72 - Development of a BAK conformation assay : correspondence between BAK conformational change and cytochrome c release.
Mitochondria were incubated in respiration buffer [2.31.1] with 1.5 nM tBID. Aliquots were removed at the indicated times, and digested with trypsin [2.36]. Mitochondria were then separated by centrifugation and proteins run on SDS-PAGE [2.13]. (**A**) After transferring to nitrocellulose, the blots were probed with an anti-BAK antibody which specifically recognises the uncleaved BAK molecule, and also with an anti-cytochrome c antibody, as indicated [2.16]. (**B**) The BAK and cytochrome c signals from the Western blot were used to calculate % BAK conformational change ( ) and % cytochrome c release (x) at each time-point.

[7.4.3]The effects of CSA on BAK conformational change

To confirm that CSA does inhibit this step of tBID-induced cytochrome c release, the above technique [7.4.2] was used to assay for BAK conformational change [Figure 73]. As expected, the presence of CSA inhibited the appearance of the open BAK conformer [Figure 73; compare (**A**) with (**B**)]. Strikingly, with the values of the kinetic parameters calculated from the cytochrome c release data, the model accurately predicted the appearance of open conformer in the presence and absence of CSA.

[7.5]Effect of cyclophilin A

[7.5.1]Introduction

CSA binds to cytosolic cyclophilin A as well as mitochondrial cyclophilin D. Some proportion of cyclophilin A might co-purify with mitochondria through association with the outer membrane, and the effect of CSA might represent some interaction with cyclophilin A. For example, a cyclophilin A-CSA complex is known to bind and inhibit the protein phosphatase calcineurin; this results in inhibition of BAD dephosphorylation and activation, thus inhibiting mitochondrial cytochrome c release [272]. This might explain the inhibition by CSA of a step in tBID-induced cytochrome c release occurring at the outer mitochondrial membrane (BAK conformational change), since the alternative target (i.e. cyclophilin D) is present in the matrix, with no access to the outer membrane.

[7.5.2]Presence of cyclophilin A in mitochondrial preparations

To investigate whether cyclophilin A was associated with the mitochondrial fraction used in BID-induced cytochrome c release experiments, mitochondrial preparations were analysed for cyclophilin A by Western blot [2.16]. As shown in Figure 74, cyclophilin A was detectable in all preparations, at approximately 1.0 μg/mg mitochondrial protein. In fact, this is considerably more than the estimated content of cyclophilin D in B50 cell mitochondria (60 ng/mg mitochondrial protein; [157]).

[7.5.3]Effect of exogenous cyclophilin A on tBID-induced cytochrome c release

In an attempt to probe the involvement of cyclophilin A, tBID-induced cytochrome c release experiments were carried out in the presence or absence of recombinant cyclophilin A. As shown in Figure 75, 5 μg/mg mitochondrial protein or 50 μg/mg mitochondrial protein cyclophilin A had no effect on tBID-induced cytochrome c release. However, higher cyclophilin A concentrations inhibited cytochrome c release: as shown in Figure 76, cyclophilin A at 1000 μg/mg mitochondrial protein raised the EC_{50} from 3 to 5.5 nM (1.8-fold inhibition). In the same experiment, 1.2 μM CSA had an almost identical inhibitory effect. Furthermore, the effects of cyclophilin A and CSA were not additive [Figure 76 (**C**)]. This may suggest that it is a cyclophilin A-CSA complex which is exerting an effect on tBID-induced cytochrome c release. CSA would inhibit release by binding to endogenous cyclophilin A, and the binary complex would interact with some down-stream target. Low concentrations of exogenous cyclophilin A would therefore have no effect, since cyclophilin A would presumably only interact with the target with low affinity in the absence of CSA. However at high concentrations added cyclophilin A may be able to bind sufficiently well to give inhibition.

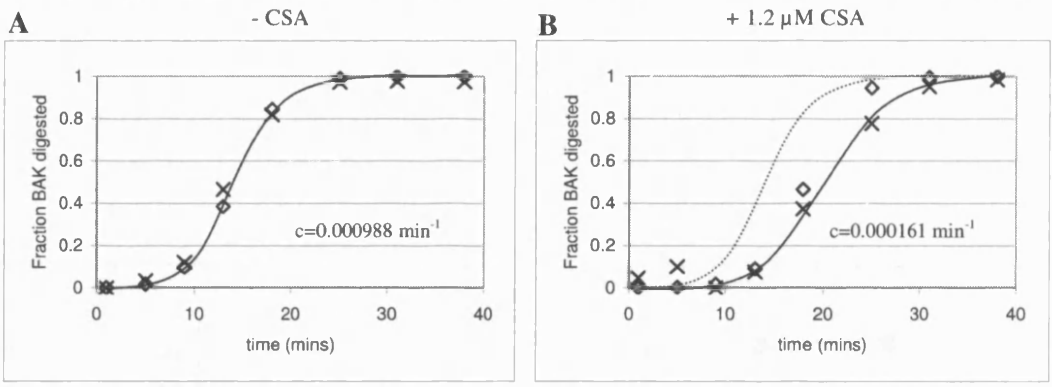

Figure 73 - CSA inhibits tBID-induced conformational change of BAK.
Mitochondria were incubated in respiration buffer [2.31.1] with 1 nM tBID, with (**A**) or without (**B**) 1.2 μM CSA. An aliquot was removed at the indicated times, and digested with trypsin [2.36]. Mitochondria were separated by centrifugation; proteins were run on SDS-PAGE [2.13] and transferred to nitrocellulose [2.16.1]. The blot was probed with an anti-BAK antibody [2.16] to assay for uncleaved ('closed') BAK (x). The kinetic model was used to predict the amount of 'open' BAK conformer at each time-point (◇), using Equation 8. The dashed line in (**B**) is the BAK digestion curve taken from (**A**). The digestion data confirms that the effect of CSA is to inhibit the tBID-induced conformational change in BAK. Results are representative of three independent experiments.

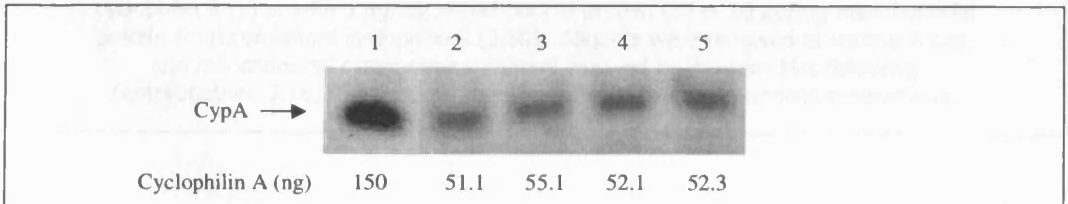

Figure 74 - Cyclophilin A is present in mitochondrial preparations.
A selection of mitochondrial preparations [2.26] (each containing 50 μg of protein) was run on SDS-PAGE [2.13] (lanes 2 – 4), along with 150 ng of pure recombinant cyclophilin A (lane 1; [2.50]). Proteins were transferred to nitrocellulose and the blot probed with an anti-cyclophilin A antibody [2.16]. Cyclophilin A levels were calculated by comparison with the reference band, revealing an average value of 1.0 μg/mg mitochondrial protein.

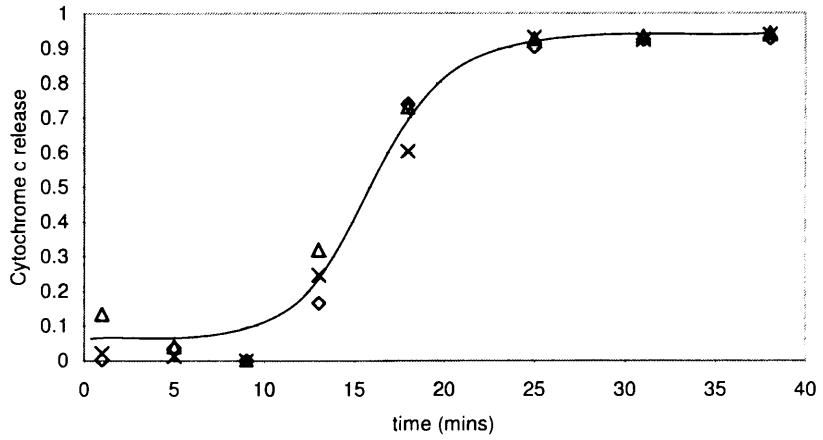

Figure 75 - Physiological cyclophilin A levels have no effect on tBID-induced cytochrome c release.

Mitochondria were incubated with 1.7 nM tBID [2.31], either with no exogenous cyclophilin A (x) or with 5 μg/mg mitochondrial protein (Δ) or 50 μg/mg mitochondrial protein (◊) recombinant cyclophilin A [2.50]. Aliquots were removed at various times, and mitochondrial cytochrome c content assayed by Western blot following centrifugation [2.16]. Results are representative of four independent experiments.

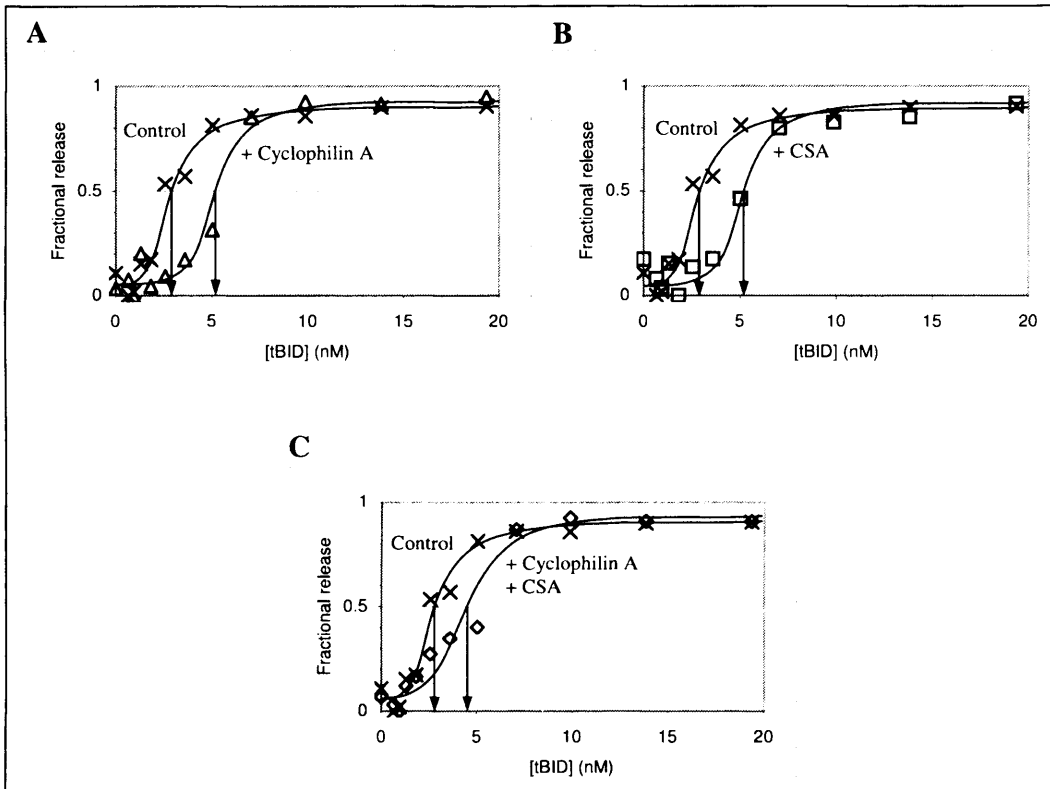

Figure 76 - CSA and a high concentration of cyclophilin A inhibit tBID-induced cytochrome c release to a similar extent, and in a non-additive fashion.
Recombinant cyclophilin A was prepared as above [2.50]. Mitochondria were incubated with varying concentrations of tBID [2.31] either with no additions [(**A-C**);(x)] or in the presence of either cyclophilin A [1000 µg/mg mitochondrial protein; (**A**)(Δ)] or CSA [1.2 µM; (**B**)( )] or both [(**C**)(◇)]. After 30 mins incubation at 30 °C, mitochondria were separated from the assay mixture by centrifugation and assayed for cytochrome c by Western blot [2.16]. The degree of inhibition caused by the additions in each experiment was essentially identical. Results are representative of two independent experiments.

[7.5.4]Effect of cyclophilin A on BID-induced cytochrome c release

As shown in Figure 77, there was no effect of cyclophilin A (1000 μg/mg) on BID-induced cytochrome c release. This correlates with the lack of any CSA effect on the action of full-length BID [Figure 67].

[7.6]Discussion

[7.6.1]Effect of CSA

CSA inhibited tBID-induced cytochrome c release, despite having no effect on mitochondrial respiration. It was surprising that CSA should inhibit the tBID effect, given that overexpression of cyclophilin D (CSA's presumed target) also inhibited tBID-induced cytochrome c release.

[7.6.2]Inhibition of BAK conformational change

The model developed in Chapter 5 allowed prediction of the specific step in tBID-induced cytochrome c release that was inhibited by CSA, based on fitting of predicted values to experimental data points for cytochrome c release. On this basis, CSA appeared to inhibit the conversion of BAK molecules from the closed to the open conformation. Specifically, CSA inhibited 'seeding' of open conformers by tBID (CSA reduced the value of the constant *c)* [Figure 59] (page 131). An assay for BAK conformational change confirmed that this process was inhibited by CSA.

This result was unexpected; if cyclophilin D was the target of CSA, then CSA would have been expected to inhibit cytochrome c release through some effect on a matrix system, whereas BAK conformational change presumably occurs via a process acting at the outer membrane. The result is also in contrast with the findings of Scoranno and co-workers [17], who suggested that CSA inhibits tBID-induced cytochrome c release by blocking a process of mitochondrial remodelling. This process would occur downstream of BAK oligomerisation, and would presumably be reflected by a change in the constant *a* (the rate constant for cytochrome c egress through open BAK pores).

The fact that the action of full-length BID was not inhibited by CSA is in keeping with this result. By the logic of Scorrano and co-workers, CSA should inhibit BID and tBID action to a similar extent (since CSA affects a down-stream step). However if CSA specifically inhibits tBID-induced conformational change of BAK, then it is conceivable that it does not have any effect of the action of full-length BID (which must presumably catalyse the change in BAK via a slightly different mechanism, or induce cytochrome c release via a different route).

[7.6.3]Effect of cyclophilin A

It was possible that CSA might be exerting its inhibitory effect on BAK oligomerisation through interaction with cyclophilin A molecules associated with the mitochondrial outer membrane. Addition of recombinant cyclophilin A did indeed appear to stimulate tBID-induced cytochrome c release, albeit only at very high concentrations. Interestingly, the inhibition was almost identical in extent to that observed in the presence of CSA, suggesting that cyclophilin A may be exerting its inhibitory effect through interaction with a down-stream target, its interaction with which being strengthened in the presence of CSA.

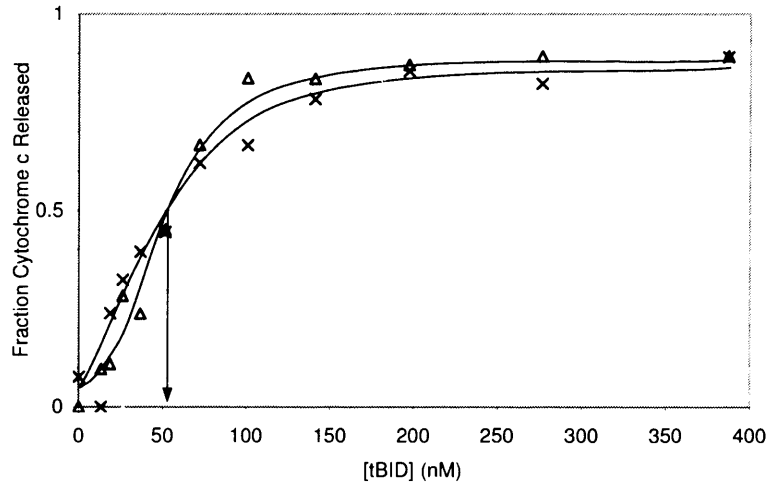

Figure 77 - Cyclophilin A does not stimulate BID-induced cytochrome c release. Mitochondria were incubated with varying concentrations of full-length BID [2.31] in the presence (Δ) or absence (x) of cyclophilin A [2.50] at 1000 μg/mg mitochondrial protein. After 30 mins incubation at 30 °C, mitochondria were separated from the assay mixture by centrifugation and assayed for cytochrome c by Western blot [2.16]. Results are representative of two independent experiments.

[7.6.4]Purity of the mitochondrial preparation

Alternatively, since cyclophilin A is thought to be a predominantly cytosolic protein [150], it is possible that the large amounts detected here might simply represent an artifact of the mitochondrial isolation technique used, arguing against an involvement of cyclophilin A in tBID-induced cytochrome c release *in vivo*. In this regard, cyclophilin A, being a positively charged protein at cellular pH [150] is predicted to associate with intracellular membranes via electrostatic interactions with membrane phospholipids. Mitochondria are isolated in a low ionic strength medium [2.26] and so peripherally associated cyclophilin A would be found in the mitochondrial fraction. Furthermore, any non-mitochondrial contaminants (for example endoplasmic reticulum or Golgi membranes) might also introduce large amounts of cyclophilin A to the mitochondrial fraction. When incubated in the high ionic strength medium used for cytochrome c release experiments [2.31.1] any electrostatically associated cyclophilin A would be dissociated from membranes and exist free in aqueous solution.

1 μg of cyclophilin A per mg mitochondrial protein would certainly represent a significant component if concentrated specifically at mitochondrial membranes (i.e. if associated with mitochondria via protein-protein interactions or present as an integral membrane component), and would be a likely candidate for a CSA effector. However when free in solution this amount corresponds to just 90 nM cyclophilin A, and might be unlikely to exert an effect on mitochondrial membrane systems. This latter situation would be the case if cyclophilin A was simply pulled down into the mitochondrial fraction by electrostatic association with non-mitochondrial contaminants, and the purity of the mitochondrial preparation is therefore an important consideration, which deserves further investigation.

CHAPTER 8 : THE EFFECTS OF DB25

[8.1]Introduction

Several CSA derivatives with varying affinities for cyclophilins have been synthesised. Table 9 shows some of these compounds, along with their IC_{50} for cyclophilin D inhibition.

One feature of CSA action is that, as well as inhibiting the PPIase activity of cyclophilins by binding to the enzymes' active site, CSA binding can allow cyclophilins to interact with novel downstream targets by creating a new binding surface on the Cyp-CSA complex. As mentioned above, one such downstream target is the cytosolic protein phosphatase calcineurin. Cyclophilin A is normally unable to interact with calcineurin, but a cyclophilin A-CSA complex binds calcineurin tightly and inhibits its phosphatase activity [164]. Amongst the compounds shown in Table 9, the compound DB25 (D-MeAla-3-EtVal-4-CSA; Figure 78) is particularly interesting, since it inhibits cyclophilins with an IC_{50} close to that of CSA, but does not permit interaction with downstream targets such as calcineurin (Grégoire Vuagniaux, personal communication). DB25 thus enables the distinction to be made between CSA effects occurring through an 'enzyme inhibition' mechanism and those occurring through a 'gain-of-function' mechanism.

[8.2]The effects of CSA and DB25

[8.2.1]Effects on tBID-induced cytochrome c release and BAK conformational change

The effects of CSA and DB25 on tBID-induced cytochrome c release are compared in Figure 79. Whilst CSA completely inhibited cytochrome c release over the tBID concentrations tested, DB25 instead had a slight stimulatory effect.

CSA was shown to inhibit an early stage of tBID-induced cytochrome c release - tBID-induced BAK conformational change [7.4.3]. It remained possible that DB25 might have a similar effect, this being masked by a secondary stimulatory effect on a later stage of cytochrome c release. To exclude this possibility, mitochondria incubated with tBID in the presence and absence of DB25 were assayed for BAK conformational change [2.36]. A shown in Figure 80, the stimulatory effect of DB25 on tBID-induced cytochrome c release was paralleled by a stimulation of BAK conformational change, thus showing the effect of DB25 to be entirely opposite to that of CSA.

Since the effects of CSA and DB25 might simply reflect some effect of these compounds in the absence of tBID, it was important to verify that they had no effect *per se* on mitochondrial cytochrome c release. As shown in Figure 81 neither compound induces cytochrome c release over a 1 hr incubation in respiration buffer.

[8.2.2]Does DB25 inhibit mitochondrial PPIase activity?

To verify that DB25, like CSA, does indeed inhibit mitochondrial PPIase activity, PPIase assays [2.33] were carried out on an osmotically lysed B50 mitochondrial extract [2.26] in the presence of either CSA or DB25.

Name	Substituted residue	Substituent residue	IC_{50} for cyclophilin D inhibition (nM)
D-MeSer-3-CSA	Sarcosine	N-methyl-D-serine	2.4
MeVal-4-CSA	N-methylleucine	N-methylvaline	4.7
CSA	-	-	6.0
Nva-2-CSA	L-α-aminobutyric acid	Norvaline	6.4
Val-2-MeBmt(6,7-DH)-1-CSA	4[R]-4-((E)-2-butenyl)-4,N-diethyl-L-threonine (MeBmt)	(4R)-4-butyl-4/N-dimethyl-L-threonine	7.0
D-Lys(dansyl)-8-CSA	D-alanine	N-ε-dansyl-D-lysine	32.6
D-MeVal-11-CSA (CSH)	N-methyl-L-valine	N-methyl-D-valine	No inhibition
D-MeAla-3-EtVal-4-CSA (DB25)	Sarcosine and N-methylleucine	N-methyl-D-alanine and N-ethylvaline	Not reported

Table 9 - There exist several Cyclosporin derivatives with differing patterns of interaction with cyclophilins.
Adapted from [273].

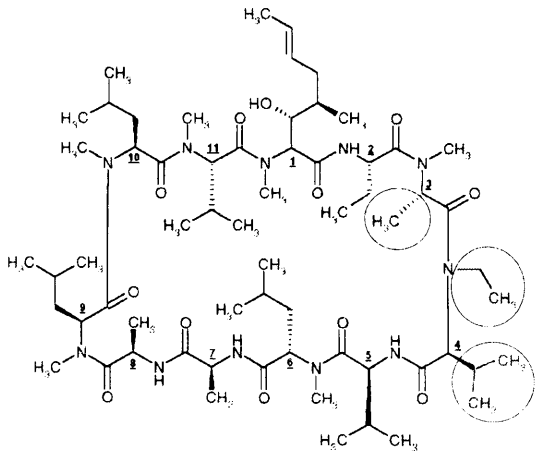

Figure 78 - DB25 (D-MeAla-3-EtVal-4-cyclosporin A).
DB25 inhibits cyclophilins with an IC_{50} close to that of CSA, but does not permit interaction with downstream targets such as calcineurin. Structural differences with CSA [Figure 64, page 140] are ringed.

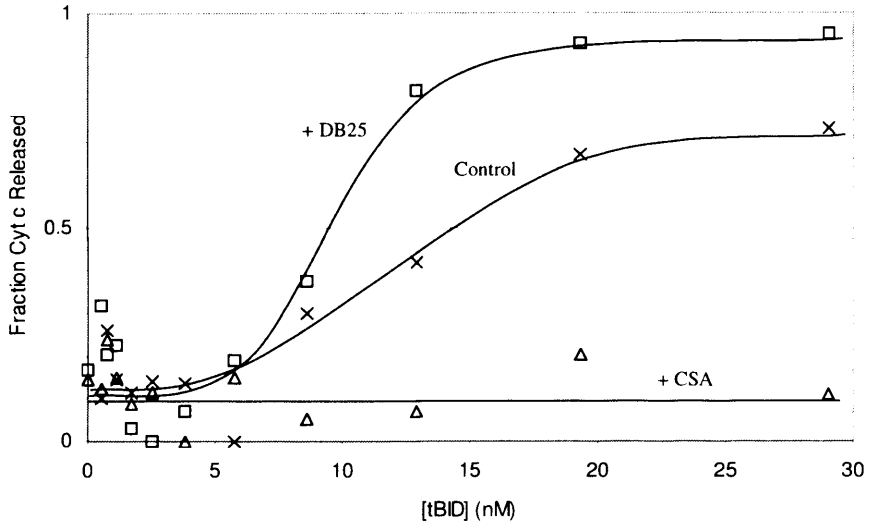

Figure 79 - The effect of DB25 on tBID-induced cytochrome c release is markedly different to that of CSA.

Mitochondria were incubated with varying concentrations of tBID in the presence or absence of 1.2 μM CSA or DB25 [2.31]. After 30 mins incubation at 30 °C, mitochondria were separated from the assay mixture by centrifugation and assayed for cytochrome c by Western blot [2.16]. Whilst CSA (Δ) completely inhibits cytochrome c release over the tBID concentrations tested, DB25 ( ) instead has a slight stimulatory effect compared to the control conditions (x). Results are representative of two independent experiments.

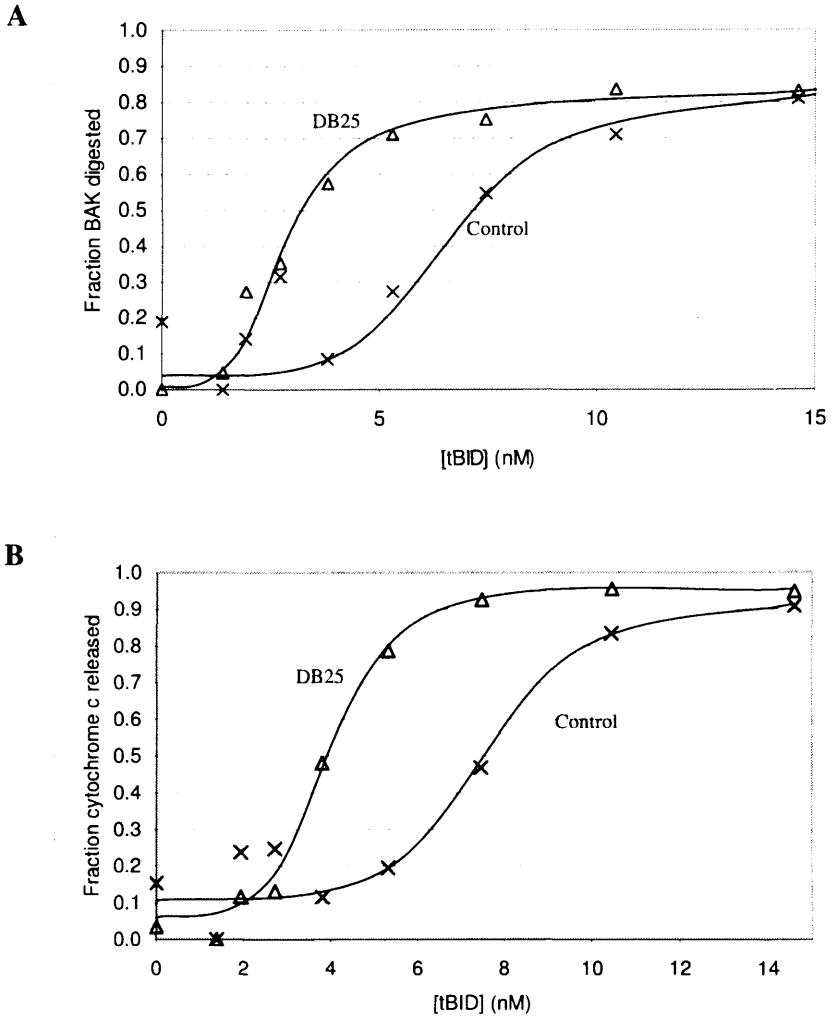

Figure 80 - The stimulation of tBID-induced cytochrome c release by DB25 is paralleled by a stimulation of BAK conformational change.
B50 mitochondria were incubated in respiration buffer [2.31.1] with varying concentrations of tBID, in the presence or absence of 1.2 μM DB25, as indicated. (**A**) After 10 mins incubation, trypsin was added, and mitochondria were incubated on ice for 10 mins to digest BAK molecules that had undergone conformational change [2.36]. Mitochondria were sedimented, and assayed for undigested BAK by Western blot [2.16]. (**B**) The mitochondrial pellet was also assayed for cytochrome c by Western blot, to assess the extent of cytochrome c release induced by tBID. Results are representative of two independent experiments.

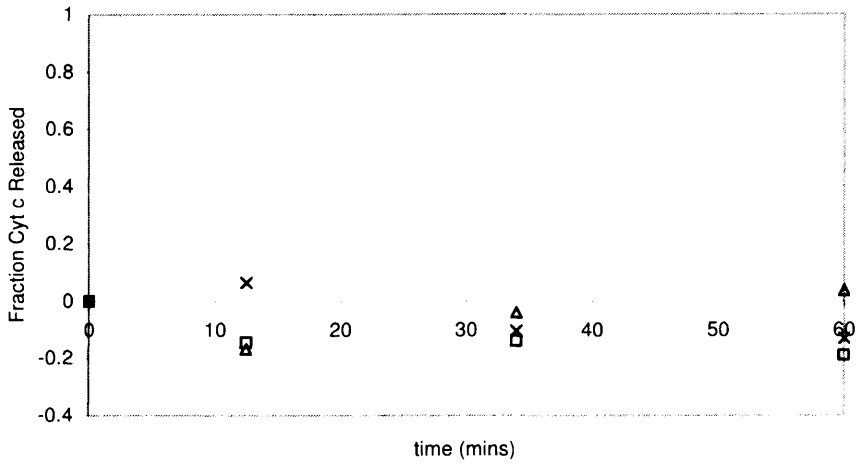

Figure 81 - Neither CSA nor DB25 cause cytochrome c release from isolated mitochondria during a 1-hr incubation.
Mitochondria were incubated at 30 ºC in respiration buffer [2.31.1] either with no additions (x) or in the presence of 1.2 µM CSA ( ) or DB25 (Δ). An aliquot was removed at various time points. Mitochondria were separated from the assay mixture by centrifugation and assayed for cytochrome c by Western blot [2.16].

Assuming the two inhibitors bind reversibly to cyclophilins with simple equilibrium kinetics, it is possible to calculate the K_d for this interaction from the extent of inhibition at various concentrations of inhibitor.

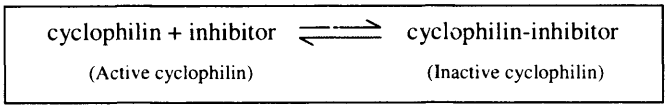

Equation 12

$$K_d = \frac{[E]\cdot[I]}{[EI]} \quad \text{and} \quad P = \frac{[EI]}{[E]_0}$$

where K_d is the dissociation complex for the cyclophilin-inhibitor complex, P is proportion inhibition, [I] is the concentration of free inhibitor, [E] is the concentration of free cyclophilin, [EI] is the concentration of cyclophilin-inhibitor complex and $[E]_0$ is the total concentration of cyclophilin (i.e. bound plus un-bound). The following relationship then follows [12.4]:

Equation 13

$$P = \frac{[I]_0 + [E]_0 + K_d - \sqrt{(-[I]_0 - [E]_0 - K_d)^2 - 4\cdot[E]_0\cdot[I]_0}}{2\cdot[E]_0}$$

This gives predicted values for the proportion inhibition at a given total added inhibitor concentration, and so K_d can be calculated by a least-squares fitting algorithm – i.e. optimising the value of K_d to minimise the value of $\Sigma(P_{predicted} - P_{measured})^2$ over all tested inhibitor concentrations. The treatment depends on having a value for $[E]_0$; this can be calculated by the method of Henderson [274], who derived the following relationship:

Equation 14

$$\frac{[I]_0}{P} = \frac{1}{(1-P)}\cdot K_d \cdot \left(1 + \frac{[S]}{K_m}\right) + [E]_0$$

where [S] is substrate concentration and K_m is the Michaelis constant for the enzyme. Thus a graph of $\frac{[I]_0}{P}$ plotted as a function of $\frac{1}{(1-P)}$ will have y-intercept $[E]_0$. Significant deviation from linearity is observed for points for which $P > 0.9$, and so this data is excluded from the analysis.

The relationship of inhibition of mitochondrial PPIase activity to inhibitor concentration, as well as the Henderson plot to calculate $[E]_0$, is shown in Figure 82. From these data, K_d values were calculated using the above technique to give a value of 2.5 nM for CSA and 0.23 nM for DB25. These values confirm that DB25 is able to inhibit mitochondrial PPIase activity. In fact, DB25 is a more effective inhibitor than CSA, the EC_{50} for inhibition being approximately 11 times lower. This increased affinity for cyclophilins is presumably as a result of the modification at the 3 position of the ring, which is predicted to increase apparent binding affinity by favouring the ring conformation recognised by the cyclophilin CSA binding site [275].

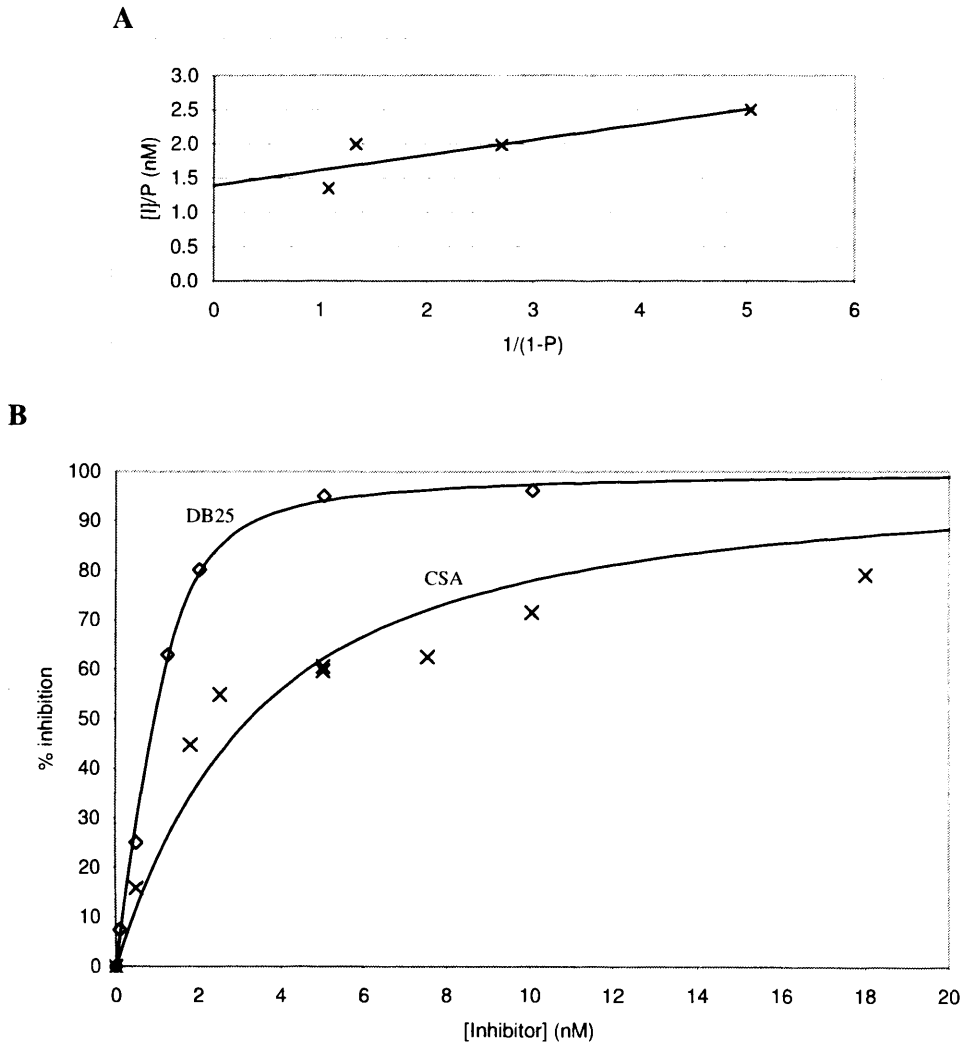

Figure 82 - DB25 inhibits mitochondrial PPIase activity with a lower K_d than CSA. PPIase assays [2.33] were carried out on a preparation of osmotically lysed B50 mitochondria [2.26], in the presence of CSA or DB25 as indicated. (**A**) The y-intercept of a Henderson plot ($[I]_0/P$ vs. $1/(1-P)$) using the DB25 data revealed $[E]_0$ to be 1.4 nM. (**B**) A plot of % inhibition (P) against $[I]_0$ indicated that DB25 (◊) inhibited PPIase activity with an 11-fold higher affinity that CSA (x). Lines indicate predicted % inhibition using Equation 31 and the calculated values of K_d.

[8.2.3]Does DB25 inhibit mitochondrial permeability transition?

CSA inhibits mitochondrial permeability transition by binding to cyclophilin D [165]. To confirm that DB25 had a similar effect on the PT pore via cyclophilin D, pore activity in response to addition of calcium to a B50 mitochondrial preparation [2.26] was assayed by following mitochondrial swelling [2.30]. Whilst addition of Ca^{2+} resulted in rapid swelling of the mitochondrial preparation due to PT pore opening [Figure 83(**A**)] both CSA and DB25 inhibited swelling following Ca^{2+} addition [Figure 83(**B**,**C**)]. Thus DB25, like CSA, inhibits PT pore opening, presumably through interaction with mitochondrial cyclophilin D.

[8.2.4]To what extent do CSA and DB25 adsorb to plastic tubes and pipette tips?

CSA and its derivatives are hydrophobic, and are only sparingly soluble in aqueous media – the solubility of CSA is 27.67 μg/mL (23 μM) at 25°C [276]. Accordingly these compounds in aqueous solution will adsorb to plastic surfaces (tubes, pipette tips etc.). Thus it was important to quantify the extent to which the different compounds remain in aqueous solution following dilution, since surface adsorption would change the effective concentration of inhibitor. In other words, the different effects of DB25 might be due to a different effective concentration of this inhibitor in the reaction buffer compared to that of CSA, due to an altered aqueous solubility.

PPIase assays [2.33] were carried out on recombinant cyclophilin A, prepared as described above [2.50], in the presence of CSA or DB25 added either neat from ethanolic solution, or from a 1.2 μM aqueous solution. Both compounds are highly soluble in ethanol, and so the amount added directly from ethanolic solution will be as calculated. However, when a 1.2 μM aqueous solution is prepared, some proportion of CSA and DB25 will adsorb to the plastic surfaces of the tubes and pipette tips. Thus the effective concentration of inhibitor will be less than 1.2 μM, and the amount of inhibitor added to the assay mixture will be less than that calculated. From the apparent concentration of inhibitor in the diluted aqueous solutions (by comparison of the K_d value with that derived following addition of ethanolic inhibitor), it was possible to estimate the proportion of CSA or DB25 that remained free in aqueous solution at this concentration. Figure 84 shows the inhibition of recombinant cyclophilin A by CSA and DB25 solutions prepared in this way, together with the Henderson plot used to derive the value for $[E]_0$; Table 10 shows the derived K_d values.

The affinity of DB25 for cyclophilin A was approximately 14 times greater than that of CSA, in broad agreement with the results using mitochondrial PPIase activity [8.2.2]. Assuming that K_d is proportional to the concentration of free (non-adsorbed) inhibitor, it was possible to calculate the amount of inhibitor adsorbed in each case - in the case of CSA 79 % was adsorbed, whilst for DB25 the value was 89 %. Thus the free concentration of CSA is approximately twice that of DB25, although this would presumably be countered by the 14-fold higher affinity of DB25 for cyclophilin A. The inhibitory effect of DB25 is therefore predicted to be *greater* than that of CSA, and a lowered activity in aqueous solution is not the explanation for the lack of any inhibitory effect of DB25 on tBID-induced cytochrome c release.

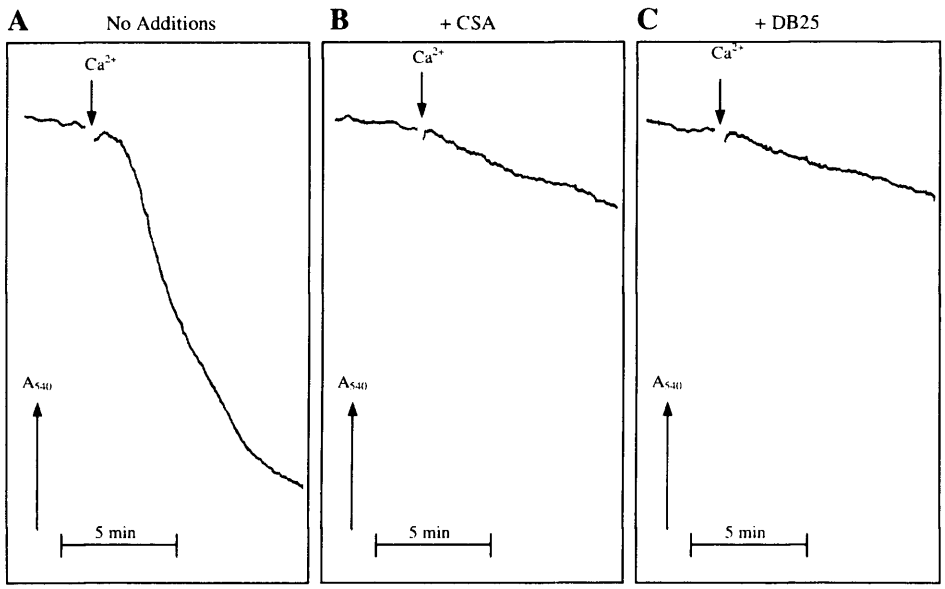

Figure 83 - Both DB25 and CSA inhibit mitochondrial permeability transition induced by Ca^{2+}.

Mitochondria were incubated in respiration buffer [2.31.1], either with no additions (**A**) or with 1 μM CSA (**B**) or DB25 (**C**). Absorbance of the mitochondrial suspension was recorded at 540 nm to monitor swelling [2.30]. At the indicated points, $CaCl_2$ was added to 100 μM to induce opening of the PT pore. (**A**) Control mitochondria swell rapidly due to permeability transition following $CaCl_2$ addition. (**B**,**C**) Pre-incubation with either CSA (**B**) or DB25 (**C**) protects mitochondria from Ca^{2+}-induced permeability transition. Results are respresentative of three independent experiments.

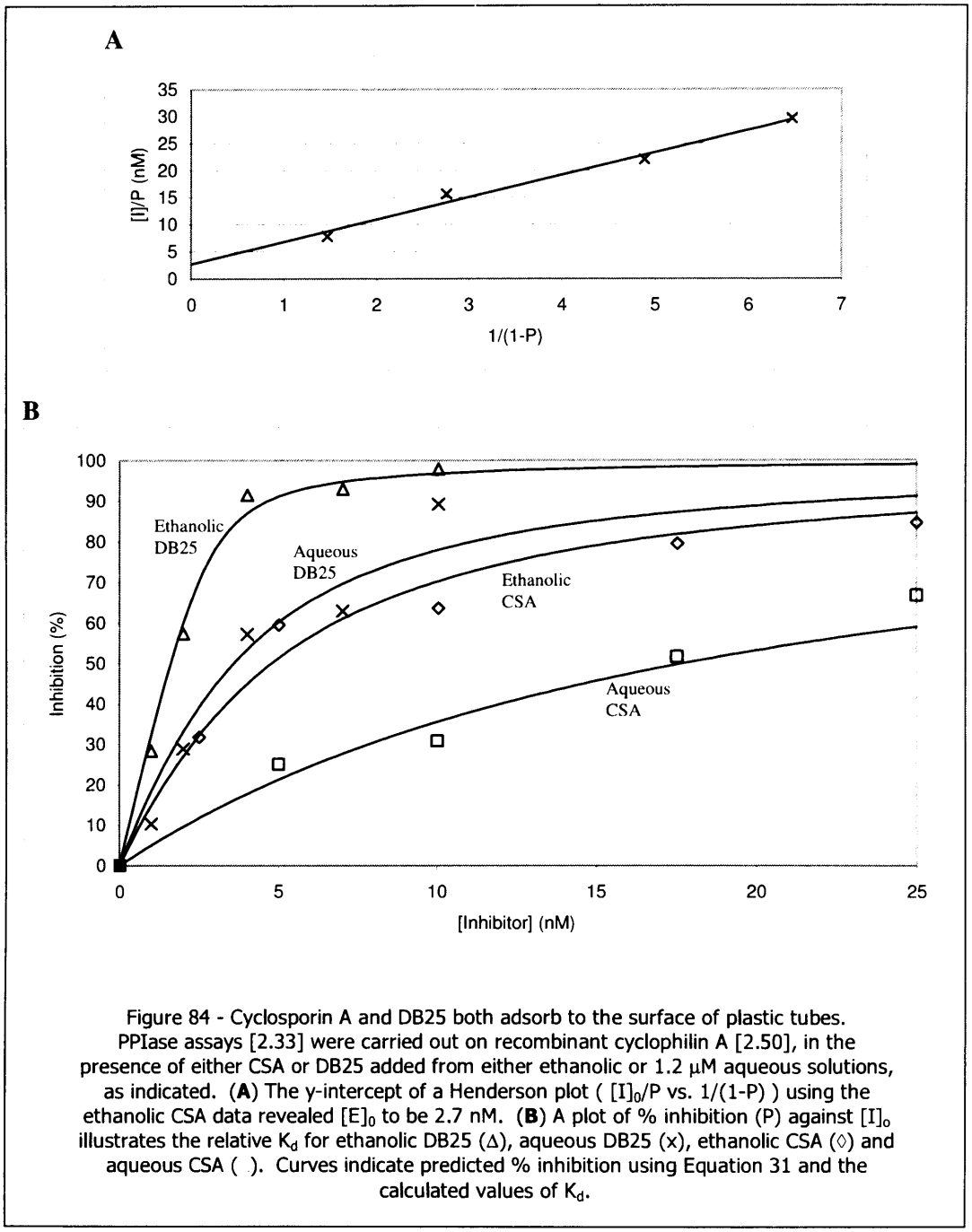

Figure 84 - Cyclosporin A and DB25 both adsorb to the surface of plastic tubes. PPIase assays [2.33] were carried out on recombinant cyclophilin A [2.50], in the presence of either CSA or DB25 added from either ethanolic or 1.2 μM aqueous solutions, as indicated. (**A**) The y-intercept of a Henderson plot ($[I]_0/P$ vs. $1/(1-P)$) using the ethanolic CSA data revealed $[E]_0$ to be 2.7 nM. (**B**) A plot of % inhibition (P) against $[I]_o$ illustrates the relative K_d for ethanolic DB25 (Δ), aqueous DB25 (x), ethanolic CSA (◊) and aqueous CSA ( ). Curves indicate predicted % inhibition using Equation 31 and the calculated values of K_d.

	Ethanolic CSA	Aqueous CSA	Ethanolic DB25	Aqueous DB25
Kd (nM)	**3.4**	**16.3**	**0.24**	**2.2**

Table 10 – Apparent K_d values for CSA and DB25 inhibition of recombinant cyclophilin A. K_d was calculated as described [8.2.2], from the data presented in Figure 84.

[8.3]Discussion

CSA has an interesting effect on tBID-induced cytochrome c release (inhibition of BAK conformational change), which has not been reported previously [CHAPTER 7]. CSA is known to affect multiple cellular pathways, and to exert its effects by different mechanisms. Specifically, CSA can, on the one hand, inhibit the catalytic (PPIase) activity of the cyclophilins - a 'loss-of-function' mechanism, leading to, for example, blocking of PT pore opening. On the other hand, CSA can also operate by a 'gain-of-function' mechanism, as is the case in calcineurin inhibition, whereby cyclophilin A acquires the ability to interact with a downstream target following CSA binding.

The availability of certain CSA derivatives allows these mechanisms to be distinguished experimentally. The compound DB25 (D-MeAla-3-EtVal-4-CSA) remains a potent inhibitor of PPIase activity, but does not support interaction of bound cyclophilins with downstream targets. Despite a 2-fold lower inhibitor concentration in aqueous solution, the 14-fold higher affinity of DB25 for cyclophilins indicated that the inhibitory effect of DB25 on mitochondrial cyclophilins should be not less than that of CSA when added in equal amounts. Despite this fact, DB25 had a markedly different effect to CSA on tBID-induced cytochrome c release; rather than inhibiting tBID action, DB25 stimulated cytochrome c release [Figure 79]. Based on BAK digestion assays [Figure 80], this action appeared to be at the level of BAK conformational change, as is the case for CSA. This result strongly suggested that CSA exerts its inhibitory effect via a 'gain-of-function' mechanism, rather than by cyclophilin inhibition.

CHAPTER 9 : CYCLOPHILIN D INTERACTION PARTNERS

[9.1]Introduction

From the results presented in Chapter 6, it seems that cyclophilin D is somehow involved in the mitochondrial apoptotic pathway. Cyclophilin D overexpression inhibits BID-induced cytochrome c release, suggesting it has an inhibitory role [5.4.4]. The work of Lin, Lechleiter, Osada, Tsujimoto, Grimm and others [59,156,277] has also implicated cyclophilin D in apoptotic cell death, but has been unable to assign a clear role to this protein. Thus to probe cyclophilin D's involvement in apoptosis further, the identification of cyclophilin D interaction partners was attempted using pull-down assays. In all, three different types of pull-down were attempted (sections [9.2], [9.4], [9.5].)

[9.2]Pull-downs from cyclophilin D(+) cells

The cyclophilin D(+) cell line available in the lab [2.42] overexpresses mitochondrial cyclophilin D approximately 10 times [5.4.2]. Thus it was attempted to pull down interacting proteins from these cells using an anti-cyclophilin D antibody, reactive against the epitope SQNPLVYLDVGAD (corresponding to amino acids 42-54 of rat cyclophilin D). Anti-cyclophilin D antibody was conjugated to agarose beads [2.22]. Comparison of the antibody bands from samples taken from the supernatant before and after the conjugation reaction [Figure 85; lanes 1 and 2 respectively] indicated that approximately 50 % of the input antibody was coupled to the beads after incubation. However, as shown in Figure 86, the resin was unable to pull down any detectable quantity of cyclophilin D from the overexpressing cells [2.23]. Thus, although pull-down bands were detected (e.g. at 85 kD; lane 3), these could not have been pulled down by cyclophilin D, and were considered spurious.

[9.3]Production of epitope-tagged cyclophilin D in B50 cells

Mammalian expression vectors can give transient protein expression levels greater than the 10 times achieved with the cyclophilin D(+) cells used above [9.2] [278]. Additionally, antibodies directed against epitope tags are typically able to pull down tagged proteins with greater affinity than antibodies against the target protein [279]. Vectors were generated to code for the cyclophilin D protein carrying three alternative tags: HA, FLAG and triple-FLAG [2.51].

[9.3.1]Expression

B50 cells were transiently transfected with the three expression plasmids [2.39], and HA, FLAG and 3xFLAG protein levels in control and transfected cells were compared by Western blot [2.16] [Figure 87]. The blots were also probed with an anti-ANT antibody (raised against the peptide YDEIKKYV, corresponding to the C-terminus of rat ANT-1; this laboratory) as a loading control [not shown].

All three fusion proteins were successfully expressed in the transfected cells. In the case of the HA and 3xFLAG constructs there was little difference between 0.25 $\mu g/cm^2$ and 0.5 $\mu g/cm^2$ of vector. However the FLAG construct was less well expressed at 2 $\mu g/cm^2$ vector.

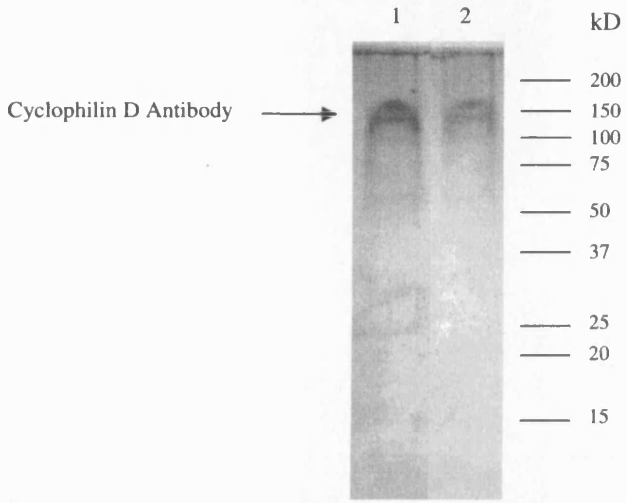

Figure 85 - Cyclophilin D antibody was efficiently conjugated to Carbolink™ beads. Cyclophilin D antibody was incubated with Carbolink coupling beads [2.22]. Supernatant from the coupling reaction was run on SDS-PAGE before (Lane 1) or after (Lane 2) incubation, and bands visualised by Coomassie staining. Comparison of the band intensity in lanes one and two indicated that approximately 50 % of the antibody was coupled to the beads during incubation.

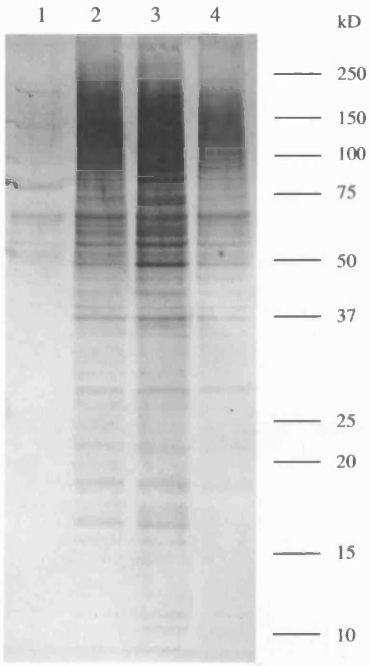

Figure 86 - Mitochondrial cyclophilin D was not efficiently pulled down by the anti-cyclophilin D resin.
The resin prepared above [Figure 85] was incubated with a mitochondrial extract [2.27.1] from normal B50 cells (lane 2), or from B50 cells overexpressing mitochondrial cyclophilin D (lanes 3 and 4), either in the absence (lane 3) or presence (lane 4) of 5 μM CSA. After washing, bound proteins were released using sample loading buffer and run on SDS-PAGE [2.13]. Bands were visualised by silver staining [2.15]. There is no band corresponding to cyclophilin D (18 kD), which should be much greater in lane 3 than in lane 2. Lane 1 – Anti-cyclophilin D resin alone.

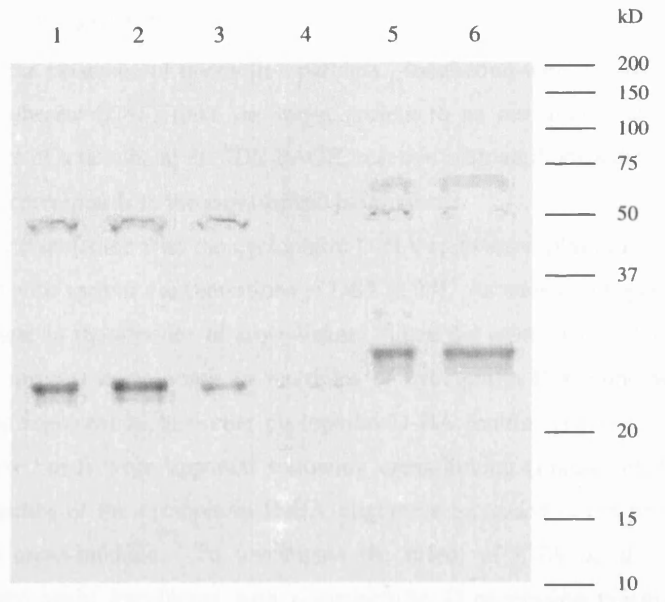

Figure 87 - Expression of epitope-tagged cyclophilin D proteins in B50 cells. Cells were transiently transfected [2.39] with an expression plasmid encoding cyclophilin D-HA – Lane 1 (0.25 μg/cm^2 culture area) and Lane 2 (0.5 μg/cm^2); cyclophilin D-FLAG – Lane 3 (0.25 μg/cm^2) and Lane 4 (0.5 μg/cm^2); or cyclophilin D-3xFLAG – Lane 5 (0.25 μg/cm^2) and Lane 6 (0.5 μg/cm^2) and grown for 48 hr. Total cellular protein was run on SDS PAGE [2.13] and transferred to nitrocellulose. The blot was probed with anti-HA and anti-FLAG antibodies [2.16]. Protein loading was equal between lanes, as judged by probing for ANT as a mitochondrial marker [not shown].

[9.3.2]Mitochondrial localisation

To verify that the fusion protein was correctly localised to mitochondria, coverslips were transfected with the 3xFLAG construct [2.39], grown for 48 hr, and then fixed [2.40] and probed with an anti-FLAG antibody [2.41]. Cells were co-stained either with MitoTracker red (before fixation [2.41]) or with an anti-ANT antibody (raised against the peptide YDEIKKYV, corresponding to the C-terminus of rat ANT-1; this laboratory; after fixation) to reveal the location of mitochondria, as shown in Figure 88. The 3xFLAG fusion protein was correctly localised to mitochondria.

[9.3.3]Cross-linking of fusion protein

Cross-linking can reveal the existence of interaction partners. Incubation with a cross-linking reagent such as disuccinimidyl suberate (DSS) links the target protein to an interaction partner; linkage is detected by the appearance of a new band on SDS-PAGE, reactive with antibodies directed against the target protein. This band corresponds to the cross-linked heterodimer.

B50 cells were transiently transfected with the cyclophilin D-HA expression plasmid [2.39], grown for 48 hr, and then incubated with various concentrations of DSS [2.24]. As shown in Figure 89 (lane 1), a variety of bands are present in the absence of cross-linker. Since the calculated molecular weight of these bands [Figure 89; arrows] corresponds to multiples of cyclophilin D's monomeric molecular weight, they are likely to represent higher-order cyclophilin D-HA multimers (from dimers up to at least decamers). No new bands were apparent following cross-linking [Figure 89, lanes 2 – 11]. However, the band intensities of the cyclophilin D-HA oligomers increased in the presence of DSS, indicating that they are cross-linkable. To investigate the effect of CSA on the cyclophilin D multimers, B50 cells were again transfected with a cyclophilin D expression plasmid (coding for cyclophilin D-3xFLAG), grown for 48 hr, and then incubated with various concentrations of DSS in the presence or absence of 1.2 μM CSA [2.24]. As shown in Figure 90, CSA did not affect multimer formation.

Although no interaction partners were revealed by this technique, the absence of any clear bands indicative of interaction between cyclophilin D and a second protein may be due to these bands being obscured by the cyclophilin D multimers, or to a lack of antibody reactivity of the cross-linked heterodimer.

[9.4]FLAG pull-down from transiently transfected B50 cells

Anti-FLAG antibody was conjugated to agarose beads [2.22]; approximately 50 % of the input antibody was coupled to the beads after incubation [not shown]. A mitochondrial extract [2.27.1] was prepared from cells transiently transfected [2.39] with the cyclophilin D-3xFLAG plasmid. The extract was incubated with the anti-FLAG-conjugated agarose beads, to pull down the tagged cyclophilin D protein, along with any interaction partners [2.23]. A small amount of cyclophilin D-3xFLAG was pulled down by the resin [not shown]; however no proteins specifically pulled down with the fusion protein could be detected. This could be due to the small amount of cyclophilin D-3xFLAG pulled down. In the future, generation of a stable cyclophilin D-3xFLAG-expressing cell line would allow for production of much larger quantities of fusion protein.

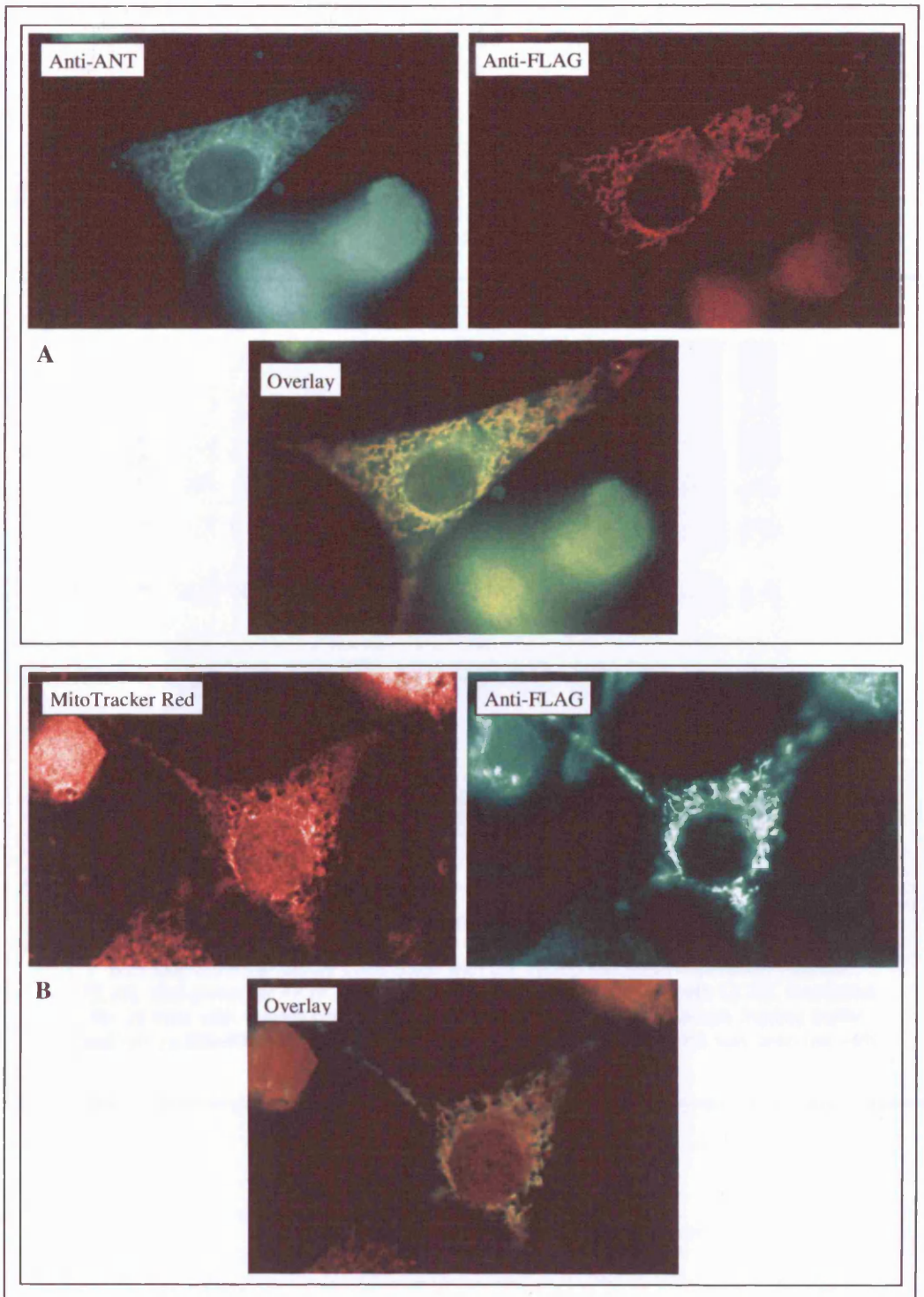

Figure 88 - The 3xFLAG-tagged fusion protein was correctly localised to mitochondria following transient transfection of B50 cells.
Cells were transiently transfected with the cyclophilin D-3xFLAG construct [2.39] and grown for 48 hr. (**A**) Cells were fixed and stained with anti-FLAG and anti-ANT antibodies, as described [2.40]; [2.41]. (**B**) Cells were treated with mitotracker red and then fixed and stained with an anti-FLAG antibody.

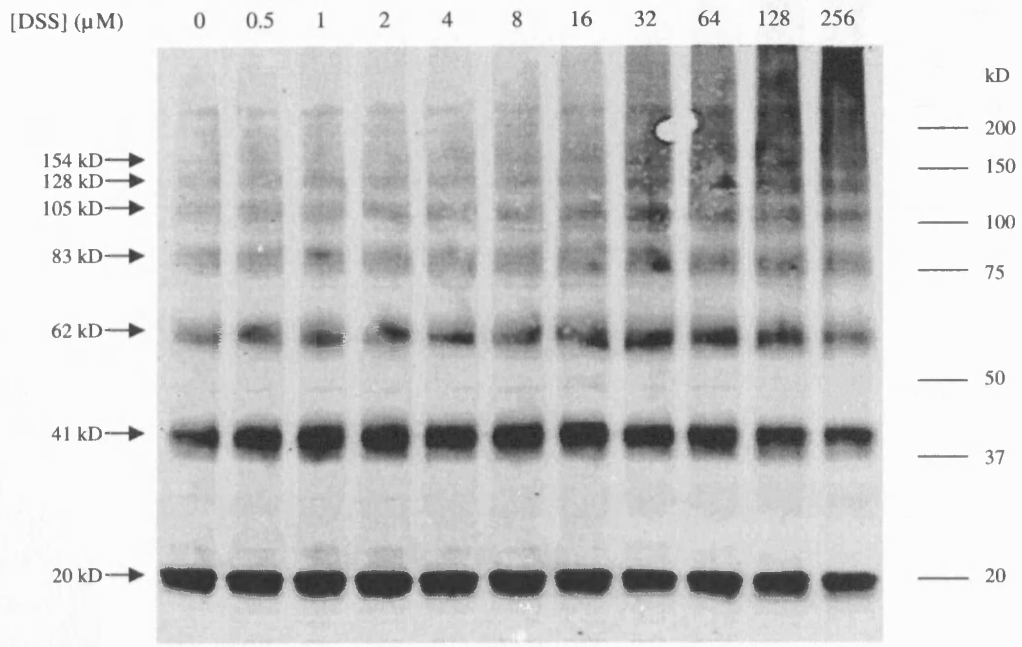

Figure 89 - The cyclophilin D-HA protein oligomerises to form cross-linkable multimers that are stable during SDS-PAGE.
B50 cells were transiently transfected with the cyclophilin D-HA expression plasmid [2.39], and grown for 48 hr. Mitochondria were isolated from the cells [2.26], incubated for 20 mins with various concentrations of DSS [2.24], heated in sample loading buffer and run on SDS-PAGE [2.13]. After Western blotting, cyclophilin D-HA was detected with an anti-HA antibody [2.16].

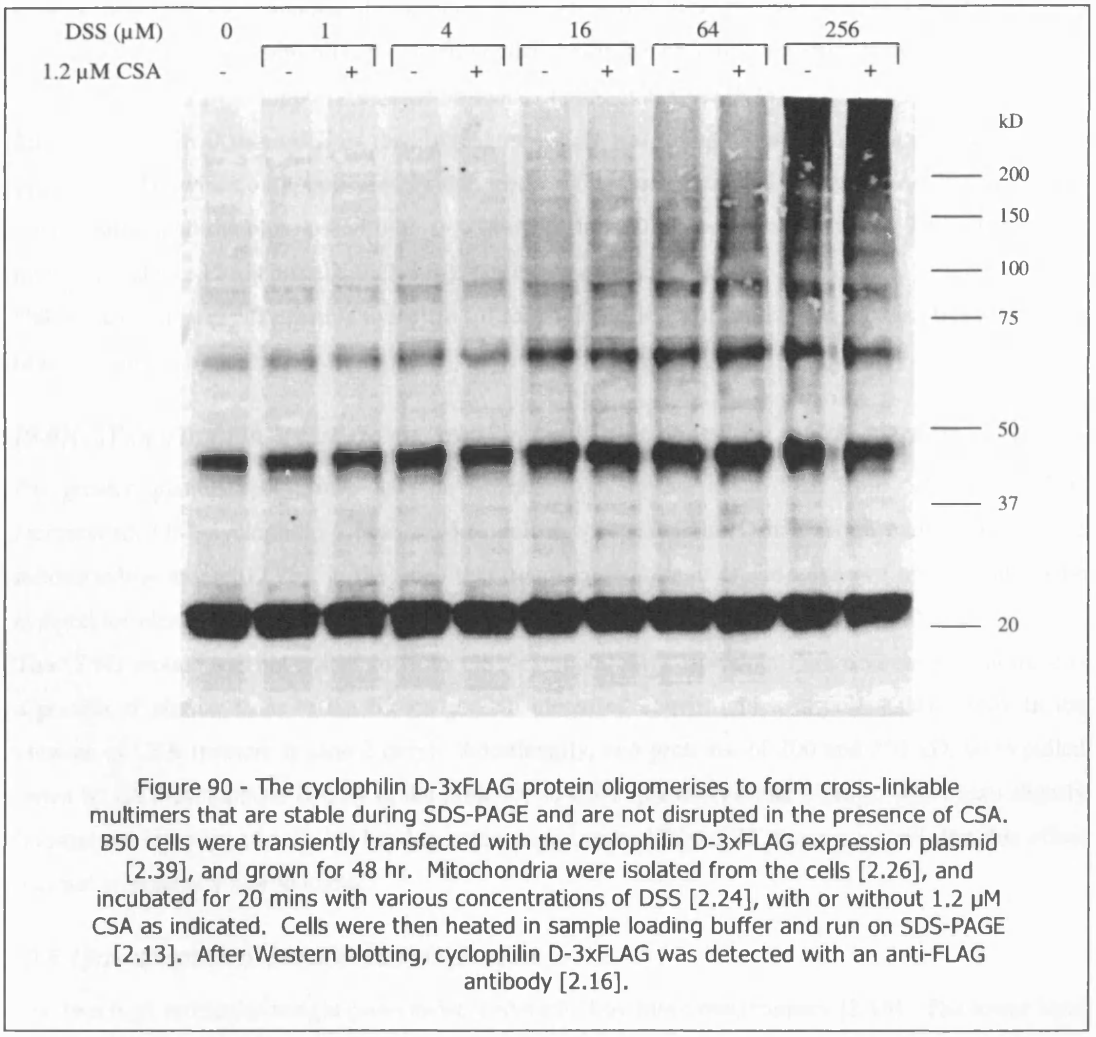

Figure 90 - The cyclophilin D-3xFLAG protein oligomerises to form cross-linkable multimers that are stable during SDS-PAGE and are not disrupted in the presence of CSA. B50 cells were transiently transfected with the cyclophilin D-3xFLAG expression plasmid [2.39], and grown for 48 hr. Mitochondria were isolated from the cells [2.26], and incubated for 20 mins with various concentrations of DSS [2.24], with or without 1.2 μM CSA as indicated. Cells were then heated in sample loading buffer and run on SDS-PAGE [2.13]. After Western blotting, cyclophilin D-3xFLAG was detected with an anti-FLAG antibody [2.16].

[9.5]GST-cyclophilin D pull-down from B50 cells

Rather than using endogenously expressed cyclophilin D to pull down interaction partners, it is also possible to use bacterially expressed recombinant cyclophilin D to bind proteins. This technique has the advantage that it is not limited by amount of cyclophilin D protein, since large amounts can be expressed in *E. coli*. A GST-cyclophilin D fusion protein was expressed, and extracted from the bacterial cell extract using GSH-agarose beads [2.18.1]. These beads were then incubated with extract from a B50 cell mitochondrial preparation [2.18.2], and bound proteins analysed by SDS-PAGE [Figure 91]. GST-cyclophilin D specifically pulled down two proteins of approximately 18 and 65 kD; these interactions were suppressed in the presence of either CSA or DB25.

Since cyclophilin D oligomerises readily [Figure 89], it was thought that the 18 kD protein might be cyclophilin D (which is approximately this size). Therefore extracted proteins were transferred to nitrocellulose and the blot probed with an anti-cyclophilin D antibody [not shown]. The antibody did not react with the 18 kD protein, indicating that it was not cyclophilin D.

Unfortunately it was not possible to isolate sufficient quantities of the unknown proteins from B50 cells to identify them by mass spectrometry.

[9.6]GST-cyclophilin D pull-down from rat heart mitochondrial matrix extracts

Far greater quantities of protein can be isolated from animal tissue than from cell lines. Thus recombinant GST-cyclophilin D was used to pull down cyclophilin D interaction partners from a rat mitochondrial extract [2.25], in the hope that a sufficient amount of the unknown proteins might be isolated for identification [Figure 92]. Initially a soluble (matrix) fraction was used [2.27.3].

The 18 kD protein was not pulled down by GST-cyclophilin D. However, Figure 92 shows that there is a protein of similar mass to the 65 kD protein identified above, which is pulled down only in the absence of CSA (present in lane 2 only). Additionally, two proteins, of 200 and 250 kD, were pulled down by GST-cyclophilin D only in the presence of CSA (present in lane 3 only). CSA also slightly boosted the intensity of a 30 kD band in some experiments [Figure 92, bottom arrow], but this effect was not consistently reproducible.

[9.6.1]Identification of the 200-250 kD proteins

The two high molecular weight proteins were identified by mass spectrometry [2.19]. The lower band corresponded to myosin heavy chain, and the upper to alpha spectrin [12.2]. These proteins are not mitochondrial, and thus represent cytosolic contamination of the mitochondrial protein preparation. They were most likely present as insoluble aggregates which were centrifuged down along with the agarose beads. The beads seemed to pack down less well after centrifugation in the presence of CSA, and so some of these proteins were removed along with the supernatant following elution of target proteins with free GSH. These proteins thus appeared to have been pulled down specifically by GST-cyclophilin D in the presence of CSA. Re-centrifuging the eluted fraction and carefully removing only the top part of the supernatant eliminated these bands [not shown].

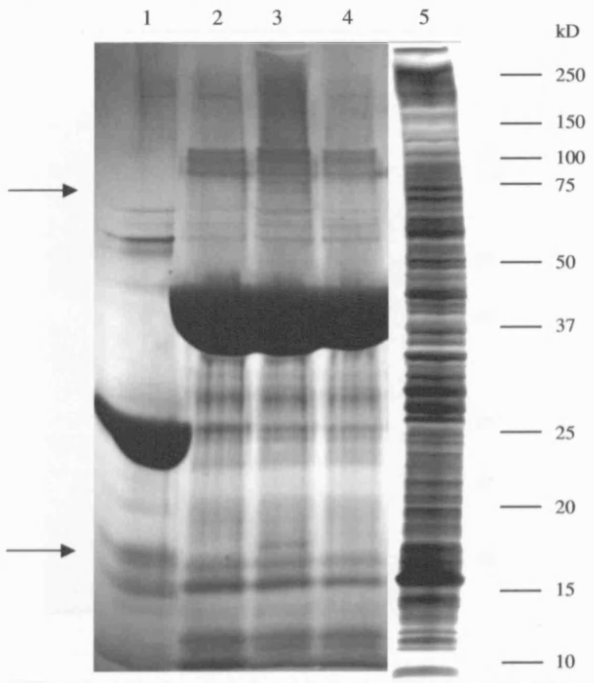

Figure 91 - GST-cyclophilin D specifically pulled down two proteins from a B50 cell mitochondrial extract.
Recombinant GST or GST-cyclophilin D [2.18.1] was incubated with a B50 cell mitochondrial extract ([2.27.1]; lane 5), and bound proteins pulled down with GSH-Agarose [2.18.2]. Lane 1 – GST + extract. Lane 2 – GST-cyclophilin D only. Lane 3 – GST-cyclophilin D + extract. Lane 4 – GST-cyclophilin D + extract + 15 μM CSA. Arrows indicate the interaction partners, visible in lane 3 alone.

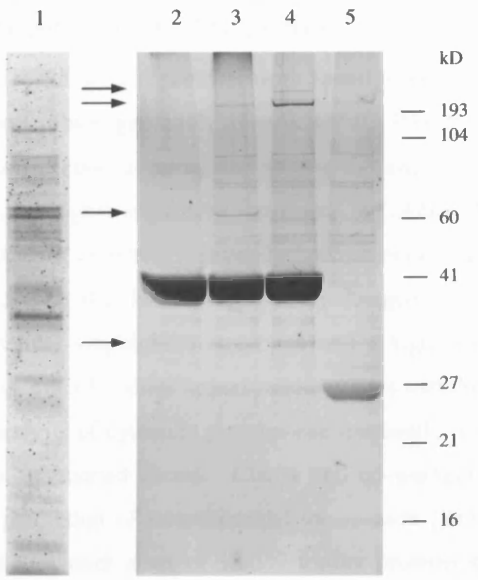

Figure 92 - GST-cyclophilin D pulled down three proteins from a rat heart mitochondrial extract.

Recombinant GST-cyclophilin D [2.18.1] was incubated with a rat heart [2.25] mitochondrial matrix extract ([2.27.3]; lane 1), and bound proteins pulled down with GSH-Agarose [2.18.2]. Lane 2 – GST-cyclophilin D only. Lane 3 – GST-cyclophilin D + extract. Lane 4 – GST-cyclophilin D + extract + 15 μM CSA. Lane 5 – GST + extract. Arrows indicate the ~60 kD protein (lane 3 only) and the two >200 kD proteins (lane 4 only) pulled down specifically by GST-cyclophilin D.

[9.6.2]Identification of the 54kD protein

The ~60 kD protein was revealed by mass spectrometry to be an uncharacterised 524 residue protein of molecular weight 54 kD, coded for by the rat gene RGD1305387 [12.2.5]. A homology search using BLAST [280] revealed that the protein contains a predicted short-chain dehydrogenase domain and a sterol binding domain, as well as four low-complexity regions, as shown in Figure 93. Searching the BLOCKS database [281] showed that the large low-complexity region between residues 298 – 404 has homology to involucrin.

[9.6.3]Mitochondrial targeting of the 54 kD protein

Since the two high-molecular weight proteins were found to be cytosolic [9.6.1], it was important to verify that the 54 kD protein was genuinely mitochondrial. Precursor forms of mitochondrial nuclear-encoded proteins contain specific targeting and sorting signals, which may be present either internally or as cleavable N-terminal signal sequences (reviewed in [282]). The N-terminal sequences are the most well characterised; their common features include an enrichment of arginine, leucine, serine and alanine residues, the presence of at least two positively charged residues, an absence of acidic residues, the ability to form α-helical amphiphilic structures and a high isoelectric point [283]. Despite the presence of these signals, mitochondrial import sequences are extremely diverse, and can be difficult to detect. Additionally, analysis of cytosolic proteins can frequently reveal the presence of some or all of the targeting hallmarks mentioned above. Claros and co-workers have developed the MitoProt II program to aid in the prediction of mitochondrial localisation [283]. The algorithm is based on an evaluation of 47 parameters over a set of 13,039 trainer proteins of known location, and is able to predict mitochondrial import with a success rate of 93.1%. In the case of the 54 kD protein, MitoProt predicts a probability of import to mitochondria of 0.9748, with the cleavage site after lysine 29. Thus the 54 kD protein is very likely to be genuinely mitochondrial.

[9.6.4]Role of the 54 kD protein

The SCP2 domain is named after sterol carrier protein 2 (SCP2), in which it was first identified. Based on overexpression studies, SCP2 has been proposed to be involved in intracellular cholesterol transport in steroidogenic tissues [284]. However, there is scant *in vitro* evidence to suggest a physical interaction of SCP2 with cholesterol sufficiently stable to permit carrying of the lipid through the aqueous phase [285]. On the other hand, the SCP2 lipid binding site can accommodate a phospholipid molecule upon interaction with membranes [286,287], and SCP2 has been shown to bind fatty acids and long-chain fatty-acyl-CoAs [288]. Because of its low affinity, the binding site is occupied by lipid only in the presence of membrane [289].

The short-chain dehydrogenase family contains a wide variety of dehydrogenases, most of which are known to be NAD- or NADP-dependent oxidoreductases. Although little sequence similarity has been found in the coenzyme binding domain, there is a large degree of structural similarity, and it has therefore been suggested that the family has arisen through gene fusion of a common ancestral coenzyme binding sequence with various substrate-specific domains [290]; in this case the SCP2 domain.

MLPNTGKLAG CTVFITGASR GIGKAIALKA AKDGANIVIA AKTTQRHPKL LGTIYTAAEE
IEAAGGKALP CVVDVRDEQQ INSAVEKAVE RFGGIDILVN NASAISLTNT LETPTKRVDL
MMSVNTRGTY LTSKACIPFL KKSKVAHILN LSPPLNLNPM WFKQHCAYTI AKYGMSMCVL
GMAEEFRGEI AVNALWPRTA IHTAAMDMLG GAGVESQCRK VDIIADAAYS IFKRPKSFTG
NFIIDENILK EEGIKDFDIY AITPGHPLLP DFFLDEHPDA VMEEKESYDP VPEVKEEKLQ
LQEQPQLQEQ PQLQEKPQLQ EQPQLQEKPQ LQEQPQLQEQ PQLQEQPQQQ PQLQEQPQLQ
EKPQLQEQPQ QQEKPQPQQQ PQQQPQQRPQ QRPQPQPQPQ PLLQSVLPPK PHFGAVEETF
RIVKDSLSDE VVRATQAVYQ FELSGEDGGT WFLDLKSKGG KVGHGEPSDR ADVVMSMATE
DFVKMFSGKL KPTMAFISGK LKIKGNIALA IKLEKLMTHM NSRL

Figure 93 - Amino acid sequence of the 54 kD cyclophilin D interaction partner, coded for by the uncharacterised rat gene RGD1305387.
The protein contains a predicted short-chain dehydrogenase domain (adh_short) and a sterol binding domain (SCP2), as well as four low-complexity regions (light grey).

The family contains members from a wide range of species, and is responsible for dehydrogenation of a diverse range of substrates, including 20-β-hydroxysteroid, 3-β-hydroxysteroid, 15-hydroxyprostaglandin, D-β-hydroxybutyrate, estradiol, corticosteroid, ethanol, sorbitol-6-phosphate, biphenyl-*cis*-diol and others [290].

As well as the two conserved domains described above, the 54 kD protein contains a 107 residue region of low complexity, from amino acids 298 – 404. This region contains predominantly glutamine and proline residues, and it is presumably these prolines that mediate the interaction with cyclophilin D. Ward and co-workers [291] have developed the DISOPRED algorithm to predict ordered (structured) and disordered (unstructured) regions based on amino acid sequence data. The algorithm derives from a machine learning process, with a support vector machine trained on a set of 750 non-redundant sequences with corresponding high resolution X-ray structures. Regions were classified as disordered when residues appearing in the sequence records had no associated coordinates in the electron density map. DISOPRED2 predicts the majority of this region to be unstructured [Figure 94].

The disordered central regional has homology to Involucrin, one of a number of proteins responsible for forming the highly insoluble cornified cell envelope in terminally differentiated keratinocytes. The glutamine residues are substrates for trans-glutaminases, which cross-link the γ-carboxyamide group of these residues to primary amines on target proteins (commonly the ε-amino group of lysine), thus forming insoluble macromolecular assemblies [292,293]. Although this phenomenon would seems to be unlikely in a mitochondrial setting, the possibility that this central domain may be responsible for intermolecular cross-linking reactions having some physiological function is intriguing (see below) [11.7.3].

Glutamine-rich tracts also occur in a number of other proteins, and are thought in some cases to occur by expansion of CAG repeats by replication slippage [294]. CAG forms a metastable conformation, and the complementary CTG oligomers form a stable anti-parallel duplex [295]; if these structures form in the nascent DNA lagging strand following primer slippage, template codons can be replicated multiple times [Figure 95]. Subsequent mutation of the CAG codon generates related codons, for example CCG (proline), GAG (glutamate) and CTG (leucine) and AAG (lysine), as observed here.

From the above analysis, the primary structure of the 54 kD protein seems to suggest that its function is to catalytically dehydrogenate some lipid specie or species at the inner mitochondrial membrane. Although the central low-complexity region may simply be a non-functional result of erroneous replication, it is tempting to speculate that the presence of a proline-rich motif serves to tether the protein to mitochondrial contact sites via interaction with cyclophilin D. Since contact sites are thought to be the route of lipid import to the inner membrane [296-298], this would bring the catalytic activity close to the lipids for which it is required. This mechanism would assume either that cyclophilin D interacts with ANT at contact sites via a non-active site region, or that it dimerises via a non-active site region, allowing one active site to bind to ANT and another, on a second molecule, to the 54 kD protein. Since CSA occludes the active (PPIase) site of cyclophilins, the lack of CSA-inhibition of cyclophilin D multimerisation [Figure 90] suggests that cyclophilin D does indeed dimerise via a non-active site region.

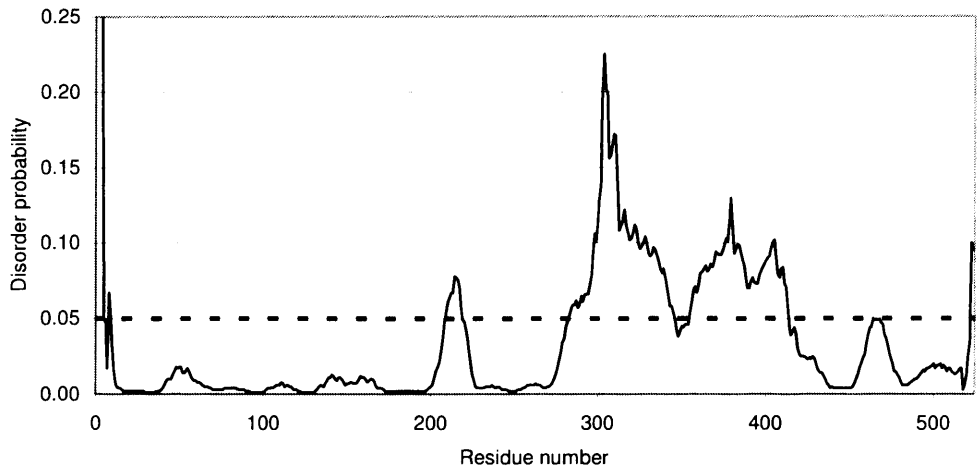

Figure 94 - Disorder prediction based on the primary structure of the 54 kD protein, as calculated by the DISOPRED algorithm [291].
The protein contains a large predicted disordered region, corresponding to the low complexity region between residues 298 and 404. The false-positive cut-off of 0.05 is indicated by the dashed line.

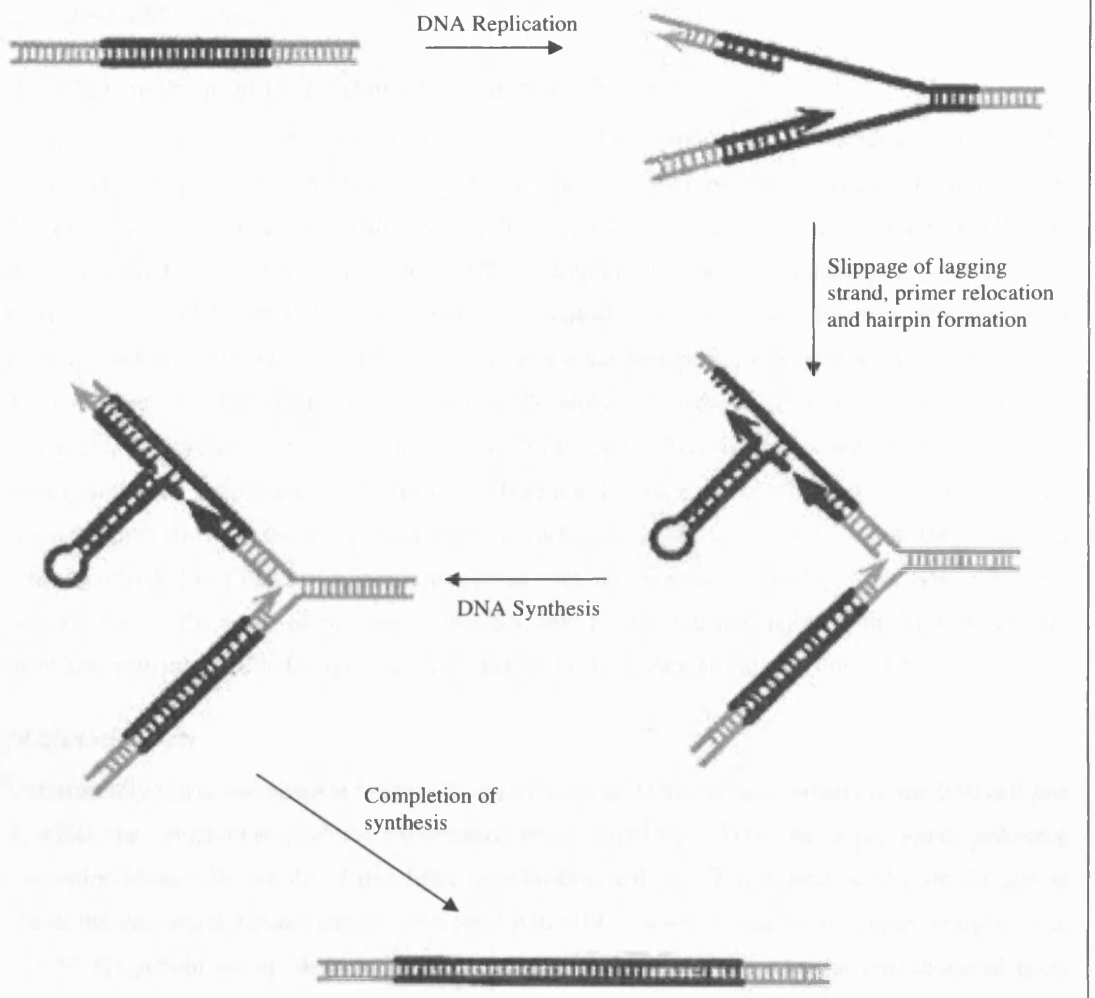

Figure 95 - Strand slippage during DNA replication can lead to extension of codon repeats with the potential to form stable hairpins.
The nascent lagging strand can dissociate from the template, and re-anneal at a site 3' to the dissociation site, within a repeated region. Hairpin formation encourages this event. Downstream codons are thus copied for a second time, resulting in codon duplication.

[9.6.5]54 kD CSA-sensitive band

To further investigate the 54 kD CSA-sensitive band, the experiment above [Figure 92] was repeated in the presence of varying concentrations of CSA and DB25. As shown in Figure 96, the interaction was disrupted by low concentrations of both CSA and DB25 – the EC_{50} was around 500 nM for DB25 and around 800 nM for CSA.

[9.7]GST-cyclophilin D pull-down from rat heart SMPs

To investigate the interaction of cyclophilin D with mitochondrial inner membrane proteins, the experiment above [9.6] was repeated using sub-mitochondrial particles prepared from rat heart mitochondria [2.27]. GST-cyclophilin D specifically pulled down a protein of around 30 kD [Figure 97]. This band was reactive against anti-ANT and anti-VDAC antibodies [not shown], and therefore represented the ANT-VDAC complex present in the mitochondrial membrane fraction. The interaction between cyclophilin D and ANT in the inner membrane has been demonstrated previously (e.g. [29]).

To investigate the effect of the two cyclophilin D inhibitors on the interaction, the experiment was repeated in the presence of 1.2 μM CSA or 1.2 μM DB25. Both inhibitors reduced the amount of VDAC and ANT pulled down by 60 to 75 % [Figure 98]. Some workers have previously obtained a similar result, whereby the cyclophilin D-ANT interaction is disrupted by CSA [36,166]; however some have found that this interaction is preserved even in the presence of CSA [29]. The difference may be due to the order of binding, with CSA able to prevent association with ANT when pre-incubated with cyclophilin D (as in this case), but unable to disrupt an existing interaction.

[9.8]Discussion

Unfortunately it was not possible to identify any cyclophilin D interaction partners in the B50 cell line in which the cytochrome c release experiments were carried out. However, a previously unknown interaction partner was identified in a heart mitochondrial extract. This protein is of a similar size to one of the interaction partners pulled down from B50 cells. Based on conserved domain identification, this 54 kD protein seems likely to have a role in lipid dehydrogenation at the mitochondrial inner membrane. A proline-rich motif may serve to anchor the protein to mitochondrial contact sites via its interaction with cyclophilin D.

Additionally, the ability of ANT to interact with cyclophilin D was confirmed. In rat heart mitochondria, at least, the 54 kD protein and ANT/VDAC were the only proteins detected in pull-down experiments and may therefore comprise the principle binding partners of mitochondrial cyclophilin D.

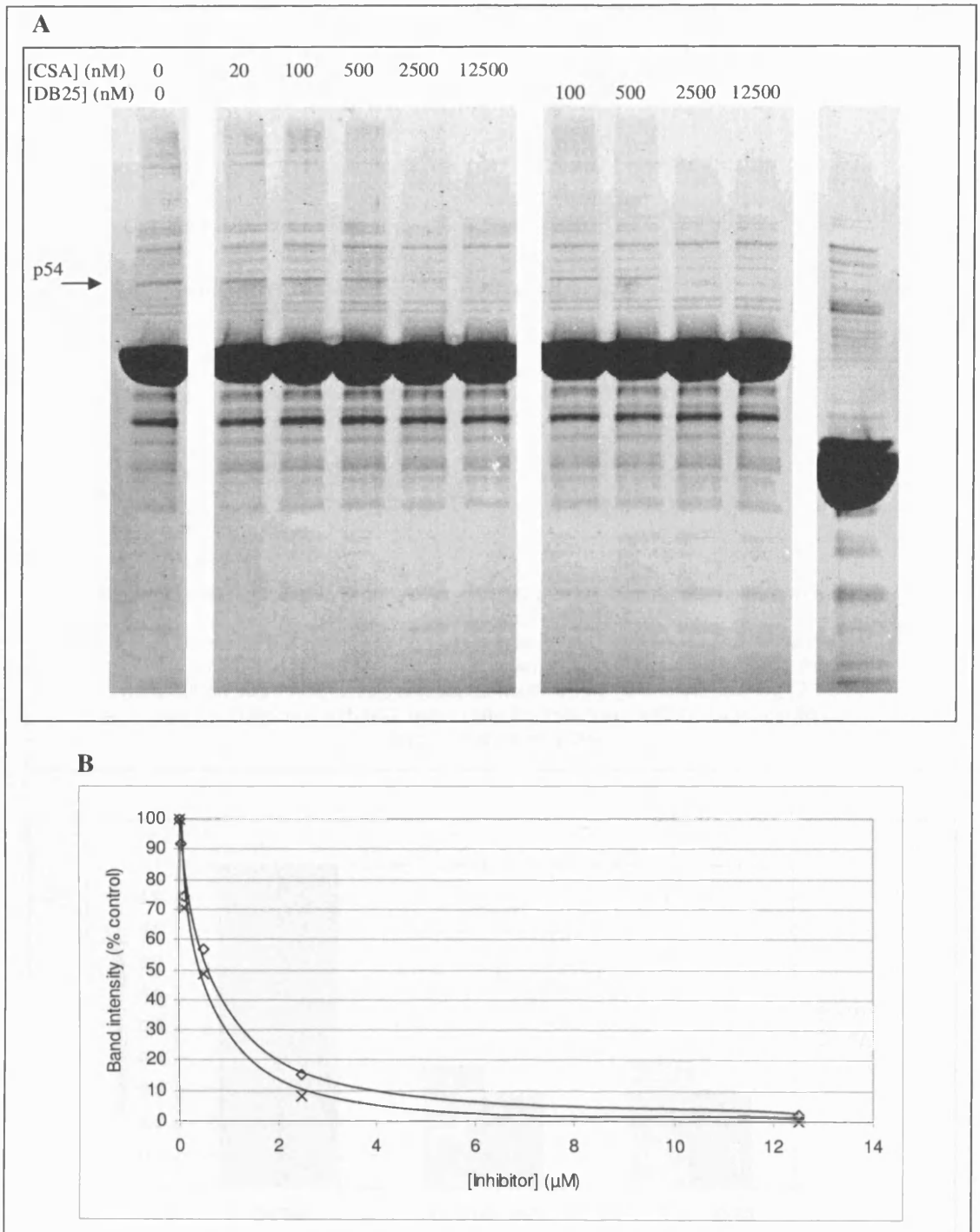

Figure 96 - CSA/DB25-sensitive removal of the 54 kD cyclophilin D interaction partner. Recombinant GST-cyclophilin D [2.18.1] was incubated with a rat heart mitochondrial extract [2.27.1] in the presence of varying concentrations of CSA or DB25, and bound proteins pulled down with GSH-Agarose [2.18.2]. (**A**) SDS-PAGE [2.13] and Coomassie staining [2.14.1] of pulled down proteins. (**B**) The 54 kD band was quantified by densitometry; the graph shows the decrease in signal strength (disruption of cyclophilin D interaction) with increasing CSA (◊) or DB25 (x) concentration.

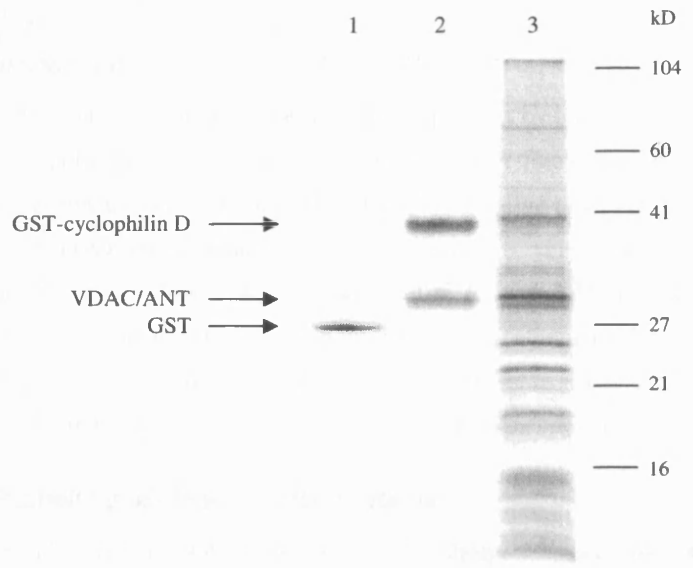

Figure 97 - GST-cyclophilin D pulls down a 30 kD protein from a mitochondrial membrane extract.
Recombinant GST-cyclophilin D [2.18.1] was incubated with a rat heart mitochondrial SMPs [2.27.2], and bound proteins pulled down with GSH-Agarose [2.18.2]. Proteins were run on SDS-PAGE [2.13], and bands visualised by Coomassie staining [2.14.1]. Lane 1 – Pull-down with GST only. Lane 2 – Pull-down with GST-cyclophilin D. Lane 3 – Rat heart SMPs.

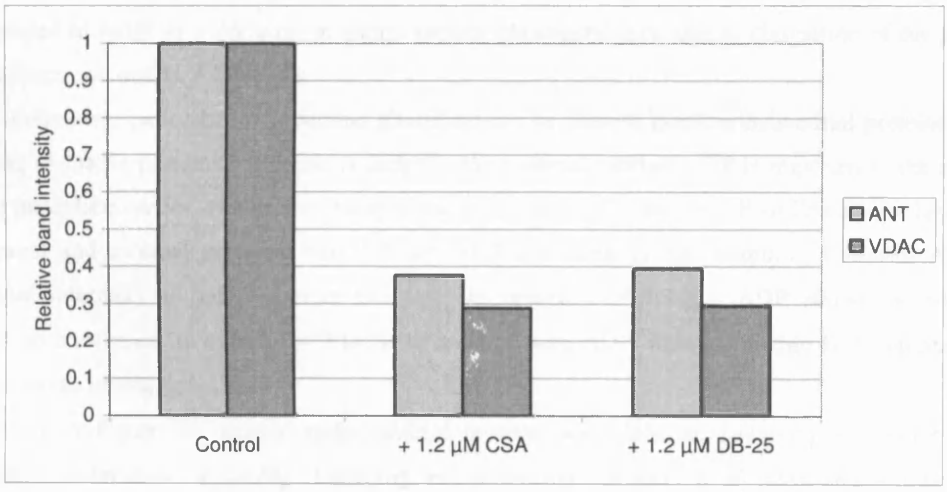

Figure 98 - The interaction of GST-cyclophilin D with the VDAC-ANT complex is disrupted by CSA and DB25.
ANT and VDAC were pulled down from rat heart mitochondrial SMPs by GST-cyclophilin D as in Figure 97, in the presence or absence of 1.2 µM CSA or DB25. ANT and VDAC were detected and quantified by Western blot [2.16], and signals used to calculate the degree of disruption of the interaction by CSA and DB25.

CHAPTER 10 : PHOSPHORYLATION CHANGES IN ISOLATED MITOCHONDRIA

[10.1]Introduction

CSA affects the phosphorylation state of cytosolic proteins by interacting with the cytosolic cyclophilin isoform cyclophilin A. The resultant cyclophilin A-CSA complex specifically inhibits the calmodulin-dependent phosphatase calcineurin [271]. It seemed possible that CSA might influence mitochondrial protein phosphorylation via an analogous mechanism, involving either adherent cyclophilin A [Figure 74] or cyclophilin D. Moreover, this might relate to why BID-induced cytochrome c release was inhibited by CSA, implicating a cyclophilin, but was not stimulated by cyclophilin D overexpression [Figure 54] or by addition of cyclophilin A [Figure 75]. Thus it was decided to investigate the effects of CSA, DB25 and tBID on phosphorylation of mitochondrial proteins.

[10.2]^{32}P labelling of mitochondrial proteins

Protein phosphorylation involves the transfer of a phosphate group from ATP to serine, threonine or tyrosine residues on the target protein. Thus incubation of mitochondria with [γ-^{32}P]ATP will result in labelling of mitochondrial phospho-proteins. Although this method has been used by several groups to investigate mitochondrial proteins phosphorylation levels (e.g. [215]), it has the disadvantage that exogenous ATP will only label proteins to which it has access – i.e. initially only those of the outer membrane and inter-membrane space. Observed changes in phosphorylation levels may thus reflect changes in the accessibility of mitochondrial compartments as well as changes in kinase and phosphatase activity. For example opening of the PT pore would allow [γ-^{32}P]ATP to enter the matrix, leading to labelling of previously inaccessible matrix proteins, despite the fact that pore opening would be expected to result in a *decrease* in matrix protein phosphorylation due to dissipation of the proton motive force and matrix ATP levels.

As an alternative, radiolabelled inorganic phosphate can be used to label mitochondrial proteins. For labelling of matrix proteins, ^{32}P alone is added to the external medium. ^{32}P is imported to the matrix via the phosphate carrier, and is then incorporated into matrix ATP by the F_0F_1-ATPase. For labelling of internal and external proteins, both ^{32}P and ADP are added to the medium. Labelled ATP is generated internally as before, but in this case the presence of external ADP allows the adenine nucleotide translocase to export [γ-^{32}P]ATP in antiport with ADP, thus generating both internal and external pools of labelled ATP.

As shown in Figure 99, several mitochondrial proteins were labelled following incubation with respiration buffer plus $^{32}P_i$ [2.20]. Labelling was essentially complete at 90 mins, and so this time-point was used for further experiments. No difference in labelling was observed in experiments with and without external ADP [not shown], suggesting that the proteins labelled were largely intramitochondrial.

[10.3]The effect of CSA, DB25, tBID and cyclophilin D on phosphorylation levels

Mitochondria were incubated in respiration buffer plus $^{32}P_i$ [2.20] as in Figure 99, with or without tBID, CSA and DB25.

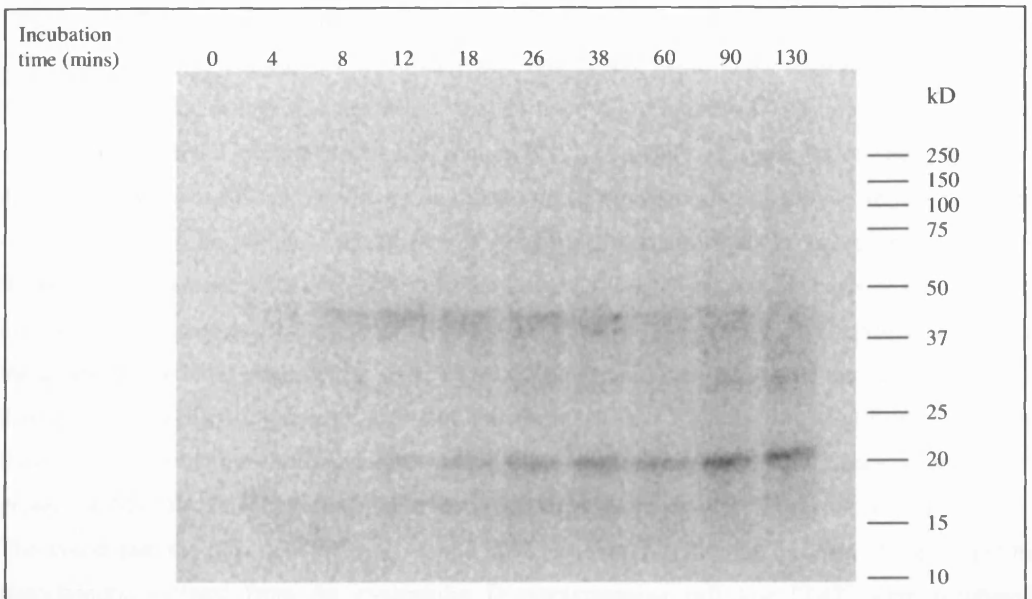

Figure 99 - Several mitochondrial proteins are labelled following incubation with $^{32}P_i$. Mitochondria were incubated in respiration buffer with 50 µCi/ml $^{32}P_i$ [2.20] for the indicated times, and then heated with sample loading buffer. Proteins were run on SDS-PAGE [2.13] and transferred to nitrocellulose [2.16.1]. The blot was exposed to a phosphorimager screen for 48 hr.

As shown in Figure 100, none of these additions affected the phosphorylation state of the labelled proteins. Again, no difference in labelling was observed between experiments with and without external ADP [not shown].

To investigate the effect of cyclophilin D on phosphorylation levels, labelling experiments [2.20] were carried out using mitochondria isolated from the cyclophilin D-overexpressing cell line [2.42]. As shown in Figure 101(**A**), a 17 kD protein was specifically labelled in cyclophilin D-overexpressing mitochondria; the band was not visible in mitochondria isolated from the control B50 cell line. Since cyclophilin D is approximately this size, the blot was probed with an anti-cyclophilin D antibody [2.16]. However the 17 kD band did not react, suggesting that it was not cyclophilin D [Figure 101(**B**,**C**)]. A band corresponding to cyclophilin D is visible in the Western blot above the 17 kD band. To investigate the possibility that this 17 kD band might represent a phosphorylated cyclophilin D protein that was unreactive against the anti-cyclophilin D antibody, the cyclophilin D sequence was entered into the NetPhosII program [299], to predict phosphorylation sites. NetPhosII is a neural network-based method for predicting potential phosphorylation sites at serine, threonine or tyrosine residues in protein sequences. It predicts non-kinase-specific phosphorylation sites in independent sequences with a sensitivity in the range 69 % to 96 %, on the basis of the existence of known phosphorylation sites in a large set of trainer proteins. The cyclophilin D epitope recognised by the antibody (ab3567; AbCam) is SQNPLVYLDVGAD (residues 42 – 54); the program predicts a significant probability of phosphorylation of both Serine 40 and Tyrosine 48. Modification of either of these residues could conceivably inhibit antibody binding, and might also influence migration of the protein on SDS-PAGE (e.g. [300]). Thus the 17 kD band might possibly represent cyclophilin D.

The investigate the effects of tBID, CSA and DB25 on the phosphorylation level of the 17 kD band, mitochondria isolated from the cyclophilin D-overexpressing cell line [2.42] were incubated in respiration buffer plus $^{32}P_i$, with or without these compounds [2.20]. There was no obvious effect of any compound, apart from a slight decrease in intensity of all the bands following incubation with tBID [not shown]. This general decrease in labelling may be due to inhibition of respiration following cytochrome c release in these experiments.

[10.4]Discussion

Mitochondria contain a wide range of protein kinases [206-211] and several mitochondrial enzymes are known to be regulated by phosphorylation; for example pyruvate dehydrogenase and branched-chain α-oxoacid dehydrogenase [204,205]. Phosphorylation of a number of other soluble and membrane proteins has also been shown [209,212,213]. Given that CSA is known to regulate cytosolic protein phosphorylation levels [271] it was possible that it might have a similar function in mitochondria. If tBID were exerting its effects through some phosphorylation-dependent pathway, the effects of CSA might thus be mediated by changes in protein phosphorylation levels.

Incubation of isolated mitochondria with $^{32}P_i$ labelled a variety of mitochondrial proteins. Initial experiments indicated that neither tBID, CSA nor DB25 were able to influence this labelling pattern. However, when the labelling of mitochondria isolated from a cyclophilin D-overexpressing cell line was compared with that of control B50 mitochondria, a novel 17 kD band was apparent.

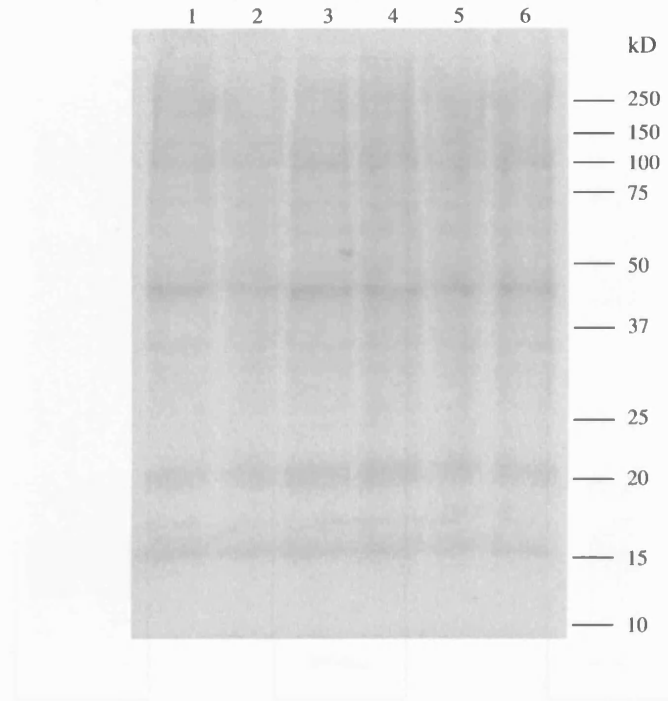

Figure 100 - tBID, CSA and DB25 do not affect the phosphorylation level of mitochondrial proteins.

Mitochondria were incubated in respiration buffer with 50 µCi/ml $^{32}P_i$ [2.20] with (lanes 1 - 3) or without (lanes 4 – 6) 0.65 µM tBID. Cyclophilin D inhibitors were included in some experiments: 1.2 µM CSA (lanes 2 and 5) or 1.2 µM DB25 (lanes 3 and 6). After incubation for 90 mins, proteins were run on SDS-PAGE [2.13] and transferred to nitrocellulose [2.16.1]. The blot was exposed to a phosphorimager screen for 48 hr.

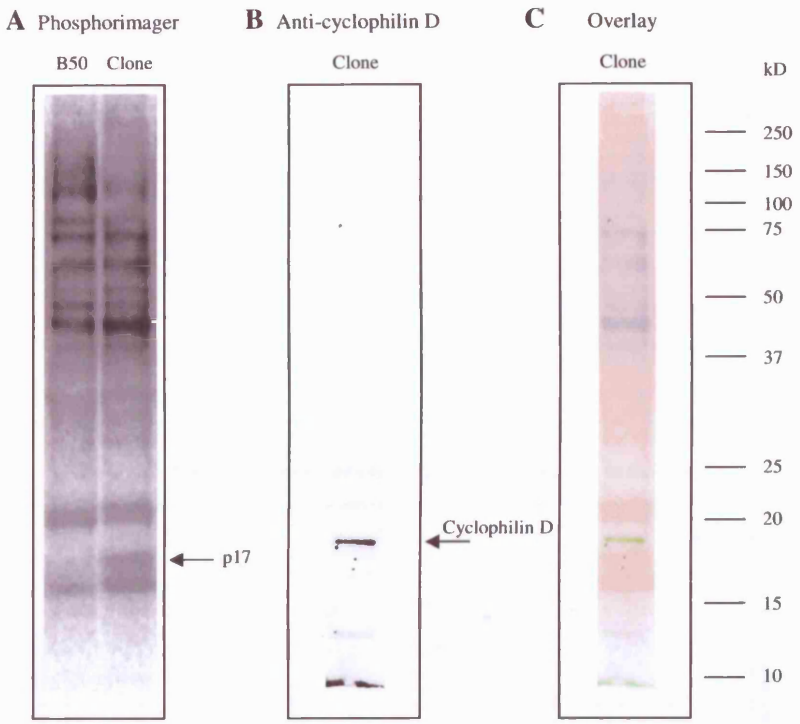

Figure 101 - A 17 kD protein that is not cyclophilin D is phosphorylated in cyclophilin D overexpressing cells.
(**A**) Mitochondria isolated from normal (left) or cyclophilin D-overexpressing cells (right) were incubated in respiration buffer with 50 µCi/ml $^{32}P_i$ [2.20]. After incubation for 90 mins, proteins were run on SDS-PAGE [2.13] and transferred to nitrocellulose [2.16.1]. The blot was exposed to a phosphorimager screen for 48 hr. (**B**) Subsequently, the blot was probed with an anti-cyclophilin D antibody [2.16.2] to reveal the location of cyclophilin D. (**C**) Overlay of the images from the lane loaded with proteins from the cyclophilin D-overexpressed mitochondria – phosphorimager (red) and anti-cyclophilin D (green). Cyclophilin D labelled by the antibody runs as a higher molecular weight specie than the 17 kD phosphorylated protein.

Serine predictions

Name	Position	Context	Score	Pred
		v		
Sequence	15	LGLLSGPRS	0.041	.
Sequence	19	SGPRSAPLL	0.014	.
Sequence	25	PLLLSTTRT	0.725	*S*
Sequence	31	TRTCSDGGA	0.986	*S*
Sequence	40	RGANSSSQN	0.858	*S*
Sequence	41	GANSSSQNP	0.141	.
Sequence	42	ANSSSQNPL	0.055	.
Sequence	92	GYKGSTFHR	0.003	.
Sequence	118	TGGKSIYGS	0.977	*S*
Sequence	122	SIYGSRFPD	0.383	.
Sequence	140	PGVLSMANA	0.114	.
Sequence	151	NTNGSQFFI	0.061	.
Sequence	185	KKIESFGSK	0.098	.
Sequence	188	ESFGSKSGK	0.470	.
Sequence	190	FGSKSGKTS	0.989	*S*
Sequence	194	SGKTSKKIV	0.930	*S*
Sequence	206	CGQLS----	0.027	.
		^		

Threonine predictions

Name	Position	Context	Score	Pred
		v		
Sequence	26	LLLSTTRTC	0.056	.
Sequence	27	LLSTTRTCS	0.015	.
Sequence	29	STTRTCSDG	0.206	.
Sequence	73	VVPKTAENF	0.084	.
Sequence	82	RALCTGEKG	0.091	.
Sequence	93	YKGSTFHRV	0.212	.
Sequence	109	AGDFTNHNG	0.015	.
Sequence	114	NHNGTGGKS	0.057	.
Sequence	130	DENFTLKHV	0.551	*T*
Sequence	148	AGPNTNGSQ	0.028	.
Sequence	157	FFICTIKTD	0.457	.
Sequence	160	CTIKTDWLD	0.047	.
Sequence	193	KSGKTSKKI	0.662	*T*
Sequence	200	KIVITDCGQ	0.036	.
		^		

Tyrosine predictions

Name	Position	Context	Score	Pred
		v		
Sequence	48	NPLVYLDVG	0.773	*Y*
Sequence	89	KGFGYKGST	0.294	.
Sequence	120	GKSIYGSRF	0.142	.
		^		

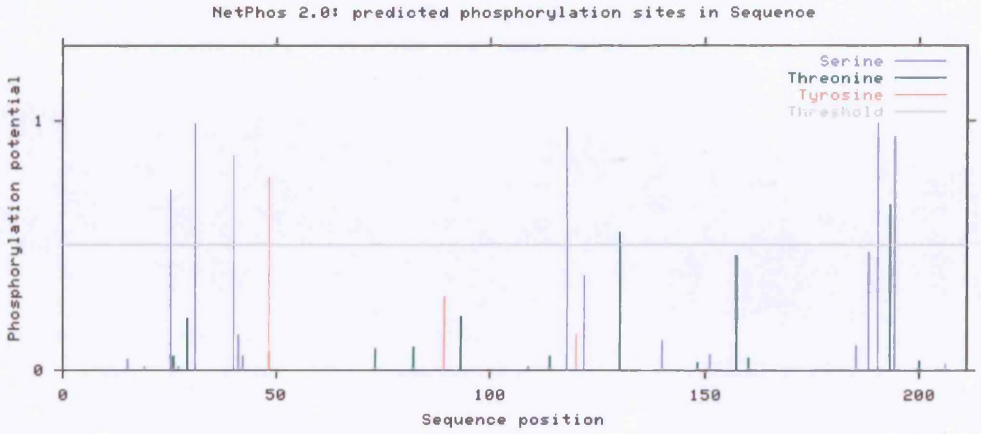

Figure 102 - Prediction of Cyclophilin D phosphorylation sites by the NetPhosII program. The rat Cyclophilin D sequence was entered into the NetPhosII program [299]. The program predicts non-kinase-specific phosphorylation sites via a neural network algorithm; phosphorylation potentials above 0.5 are considered significant. The program revealed both Serine 40 and Tyrosine 48 to have a strong probability of phosphorylation, which might inhibit antibody binding to the epitope ^{42}SQNPLVYLDVGAD^{54}.

This band was shown not to be cyclophilin D; however beyond this its identity remains unknown. Although CSA was unable to affect the labelling of this protein, a variation in its phosphorylation state might nonetheless be related to the inhibition of cytochrome c release from these mitochondria. This possibility clearly deserves further investigation.

CHAPTER 11 : DISCUSSION

[11.1]Overview of the project

Following cloning of the rat *bid* gene and expression of the BID protein [CHAPTER 3], a system was developed to assess quantitatively the extent of mitochondrial cytochrome c release induced by the addition of recombinant BID or tBID to isolated B50 cell mitochondria [CHAPTER 4]. In contrast to the qualitative measurements of cytochrome c release made in several other studies, this technique was able to reveal subtle changes in release progression under different experimental conditions, thus providing a powerful tool to probe the root mechanisms of release across the mitochondrial outer membrane.

The absence of any effect of calcium ions on BID-induced cytochrome c release, together with the inhibitory effect of cyclophilin D overexpression [CHAPTER 5], indicated that the mitochondrial permeability transition is not involved in BID action, as was suspected from previously published data. This was confirmed by calcein release experiments, which ruled out even transitory periods of pore opening during BID-induced cytochrome c release. However the inhibitory effect of cyclophilin D was intriguing, and even more so was the failure of CSA to remove this inhibition, CSA instead also being inhibitory [CHAPTER 7].

A kinetic model of tBID-induced cytochrome c release was developed from first principles, which accurately predicted the time-course of release at various tBID concentrations [CHAPTER 6]. The model is based on tBID-induced cytochrome c release occurring via a tBID-induced conformational change in BAK molecules resident at the outer mitochondrial membrane, thus seeding a pool of 'open' BAK conformers. These 'open' molecules then auto-catalyse conversion of other BAK molecules into the 'open' state, from which they oligomerise into a pore for cytochrome c efflux. Efflux occurs by passive diffusion. For a given cytochrome c release time-course, the model provided values of three key kinetic parameters, which together completely defined release progression: the rate of tBID-induced conformational change of BAK (c), the rate of BAK-induced conformational change of BAK (f) and the rate of cytochrome efflux through BAK channels (a). Cytochrome c release values predicted by the model showed an excellent correlation with experimental data. The model predicted that the locus of CSA inhibition was the BID-induced conformational change of BAK at the outer membrane, and this prediction was confirmed by a direct assay of BAK conformation during BID-induced cytochrome c release [CHAPTER 7].

Since the effect of CSA appeared to be at the outer membrane, rather than in the mitochondrial matrix, alternative (non-cyclophilin D) targets were considered. Some cyclophilin A was found to be associated with the B50 mitochondrial fraction, and this was thus a possible mediator of CSA's effects. Although addition of small amounts of recombinant cyclophilin A had no effect on tBID-induced cytochrome c release, addition of large amounts inhibited release. Interestingly, the inhibitory effect was similar in extent and non-additive with that of CSA [CHAPTER 7]. The effects of CSA contrasted with those of a structurally similar analogue, DB25, which binds to and inhibits cyclophilins similarly to CSA, but does not permit interaction with downstream targets such as calcineurin. DB25 in fact

stimulated tBID-induced cytochrome c release [CHAPTER 8], via a stimulation of tBID-induced BAK conformational change.

Cyclophilin D pull-downs from mitochondrial extracts were unable to identify any proteins interacting with cyclophilin D in the presence only of CSA (and not DB25), as might be expected in order to explain the differing effects of these two compounds [CHAPTER 9]. However, the previously reported [29] interaction of cyclophilin D with an ANT-VDAC complex in a mitochondrial membrane extract was confirmed. Additionally, two novel interaction partners, of approximately 18 and 65 kD, were identified in a B50 mitochondrial extract. These proteins interacted with cyclophilin D only in the absence of CSA and DB25. A protein of similar size to the larger of these was also pulled down from a rat heart mitochondrial extract, and identified by mass spectrometry. This previously uncharacterised 54 kD protein was analysed computationally.

Finally, ^{32}P labelling was used in an attempt to identify changes in mitochondrial phosphorylation patterns in response to tBID, CSA and DB25 [CHAPTER 10]. Although none of these compounds detectably altered phosphorylation, cyclophilin D overexpression was observed to increase phosphorylation of a 17 kD band, the identity of which remains unknown.

[11.2]The pathway of BID- and tBID- induced cytochrome c release

[11.2.1]tBID-induced BAK oligomerisation

Based on the work of Luo, Antonsson, Eskes, Pavlov, Guo, Kuwana, Terrones, Dejean and others [7,83-88,93], the following model of tBID-induced cytochrome c release has been proposed: BID is normally present in an inactive form in the cytosol. During apoptosis, an active form, tBID, is generated by caspase cleavage of BID. tBID translocates to the mitochondrial outer membrane, where it interacts with BAX or BAK to generate an activated 'open' conformer. 'Open' conformers can catalyse the conversion of further BAX/BAK molecules to the open state. These open conformers are able to self-assemble into a pore with transport activity specific for cytochrome c, through which this protein can pass into the cytosol.

The results presented here fully support this model. Firstly, BID was shown to be activated by caspase cleavage - whilst BID induced cytochrome c release at high concentrations [EC_{50} typically around 140 nM; Figure 40(**A**)], tBID was far more potent [EC_{50} typically around 10 nM; Figure 40(**B**)]. Secondly, from the dependence of tBID EC_{50} on the concentration of mitochondria, it was apparent that tBID binds tightly to mitochondria (presumably the outer membrane) [Figure 42]. As predicted, tBID induced a conformational change in mitochondrially resident BAK molecules, which preceded the release of mitochondrial cytochrome c stores [Figure 72]. Finally, the release of cytochrome c through BAK pores was indeed shown to be specific; another inter-membrane space protein (AIF) was not released during tBID-induced cytochrome c efflux [Figure 43]. (This said, there is some evidence that AIF is peripherally associated with the mitochondrial inner membrane [301], and may not be released under any circumstances until these interactions are disrupted following caspase activation, late in apoptosis [302]).

[11.2.2]An alternative mechanism of cytochrome c release induced by full-length BID?

Valentijn and co-workers [138] propose the existence of a second pathway of BID action, involving translocation of full-length BID to mitochondria. The authors suggest that full-length BID is able to induce cytochrome c release independently of BAX/BAK activation. The results of the present study suggest that the mechanism of action of full-length BID may be qualitatively different to that of tBID – i.e. that full-length BID does not simply act as a lower-affinity version of tBID. Thus whilst CSA was shown to inhibit tBID action [Figure 66], this inhibitor had no effect on the action of full-length BID [Figure 67]. Similarly, although addition of high concentrations of recombinant cyclophilin A inhibited tBID action [Figure 76], the same treatment had no effect on cytochrome c release induced by the full-length protein [Figure 77]. Since CSA and cyclophilin A are believed to act on the process of BAK oligomerisation (see below), full-length BID may therefore act independently of BAK. This could be checked by testing for conformational change of BAK induced by the full-length protein. If, as suspected, full-length BID was unable to induce BAK conformational change, the question of how, then, full-length BID is able to induce cytochrome c efflux would be an intriguing one. Is BID able to form autonomous pores, as suggested by some [80]? Or is BID able to induce membrane permeabilisation by interaction with other outer membrane systems – perhaps PT pore components, as suggested by others [111,123]?

[11.2.3]Involvement of the PT pore

In the literature, a popular model to explain the release of cytochrome c during apoptosis invokes opening of the PT pore as a mechanism of outer membrane permeabilisation [14]. Osmotic swelling of the mitochondrion following pore opening is predicted to rupture the outer membrane due to the far larger surface area of the convoluted inner membrane [52]. This model has received attention since it appeared to provide a simple explanation for the observed phenomenon of integration of multiple pro- and anti- apoptotic signals at the level of the mitochondrion, as well a providing a physiological role for the mysterious PT pore. There is, however, a substantial body of evidence indicating that the PT pore is unlikely to be involved; at least not necessarily so (reviewed above [1.3.6]). In a less controversial model [17], the PT pore is proposed to be involved not in outer membrane permeabilisation *per se*, but rather in a process of cytochrome c redistribution from sequestered stores within mitochondrial cristae to a more accessible pool, close to the outer membrane, thus 'priming' cytochrome c for release through outer membrane channels.

In the present study, the involvement of the PT pore in BID-induced cytochrome c release was conclusively ruled out, on several grounds: the lack of any stimulatory effect of calcium ions on BID action [Figure 47]; the *inhibition* of apoptosis by cyclophilin D overexpression (in contrast to the stimulation that would be expected to result in the case of PT pore involvement) [Figure 54]; and, categorically, by the lack of release of matrix-entrapped calcein during BID-induced cytochrome c release [Figure 48].

[11.3]Importance of the kinetic model

[11.3.1]Access to kinetic parameters

The kinetic model of cytochrome c efflux developed here [CHAPTER 6] allows information on previously inaccessible parameters to be derived from quantitative cytochrome c release data. The model makes distinct predictions concerning the effect of changes at each modelled stage – tBID-induced conformational change of BAK, BAK-induced conformational change of BAK (autocatalysis) and efflux of cytochrome c through BAK pores (relating to the value of the constants c, f and a respectively). Adjusting the values of these three parameters results in an excellent fit of predicted release to experimental release values, and thus the model can be used to derive values of these parameters under different experimental conditions. This information is normally inaccessible in cytochrome c release experiments - for instance there would ordinarily be no way to distinguish the effect of an increased rate of BAK autocatalysis of conformational change and an increased rate of cytochrome c transport through outer membrane pores (both resulting, as they would, in an apparently similar increase in the rate of cytochrome c release). The model is therefore a powerful tool in deconvoluting the changes in cytochrome c release observed under different conditions and therefore in determining the effect of experimental changes, as demonstrated by the use of the model to analyse the effects of CSA [CHAPTER 7].

[11.3.2]Use of the model in determining the effect of CSA

In the case of CSA, cytochrome c release experiments had shown that CSA inhibits tBID-induced cytochrome c release [Figure 66]. Published data, discussed in more detail below [11.4.1] had attributed the effect of CSA to inhibition of cytochrome c redistribution within mitochondria, thereby restricting access of cytochrome c to the outer membrane. However, analysis of the cytochrome c release data in the presence and absence of CSA according to the kinetic model suggested that rather than altering the value of a (the apparent rate constant for cytochrome c efflux through pores in the membrane; as would be expected for an inhibition of cytochrome c redistribution), CSA lowered the value of c (the rate constant for tBID-induced conformational change of BAK) [Figure 68]. A direct assay of BAK conformation supported this view, confirming that CSA inhibited a step occurring at the outer face of mitochondria [Figure 73], rather than an internal process.

[11.4]The existence of distinct internal pools of cytochrome c

[11.4.1]Scorrano's model

Scorrano and co-workers [17] and others put forward a convincing picture of cytochrome c sequestration within mitochondrial cristae. According to their model, the cristae represent a distinct compartment, separated from the inter-membrane space by narrow cristae junctions [Figure 103]. These junctions present a barrier to diffusion of solutes, and especially to large molecules such as proteins. A necessary first step in mitochondrial cytochrome c release was thus proposed to be the opening of these junctions, allowing efflux of the cytochrome c stores sequestered within cristae.

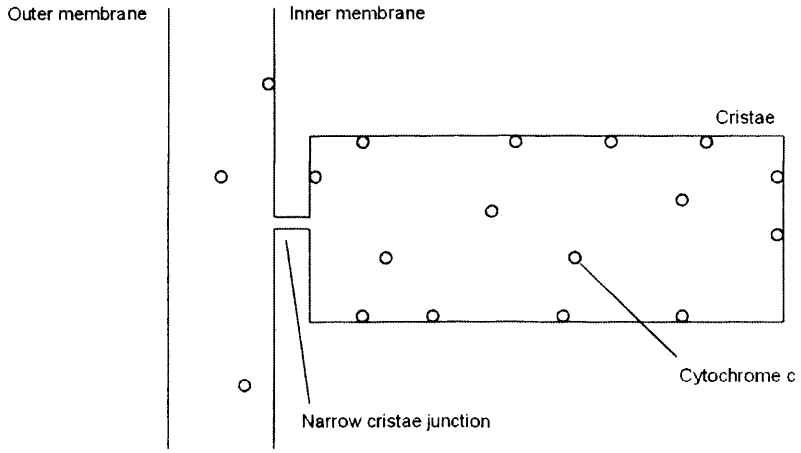

Figure 103 – Sequestration of mitochondrial cytochrome c stores within cristae. Recent models of mitochondrial substructure suggest that the cristae are separated from the intermembrane space by tight junctions, which prevent free diffusion of solutes and proteins [17,18]. Cytochrome c stores have been suggested to be sequestered in these spaces, so that they are unavailable for release during apoptosis prior to an active alteration of substructural state [20].

Scorrano's group measured the proportion of cytochrome c present in the intermembrane space and cristae compartments by comparing the rate of respiration driven by ascorbate (which can reach only the IMS store) with that of TMPD (which, being membrane-permeable, can reach all stores). Their value of around 15 % for cytochrome c present in the IMS compared well with the proportion (16 %) that could be released by digitonin solubilisation of the outer membrane. Whilst tBID could release all cytochrome c stores, the authors observed that tBID in the presence of CSA could only release 15 % of cytochrome c. They suggested that this amount represents the IMS store, and therefore that CSA inhibits a process of cytochrome c mobilisation from cristal spaces to the IMS (i.e. a widening of the cristae junctions). Based on calcein release experiments, they suggested that this process involves transient opening of the PT pore. Their work is supported by the observation that some IMS proteins (AIF and Smac) are indeed released earlier than the bulk of cytochrome c during apoptosis under some conditions [303,304].

In Scorrano's system, CSA did not inhibit tBID-induced oligomerisation of BAK, in contrast to the results of the present study [Figure 73]. Also, the effect of tBID on cristae organisation was shown by Scorrano to be independent of BAX and BAK, thus separating two functions of tBID – firstly, induction of BAK/BAX oligomerisation (investigated in this study) and secondly, a possible reorganisation of mitochondrial substructure. Indeed, the authors showed that a BH3 mutant of BID, unable to induce BAX/BAK conformational change, remained competent at inducing calcein release (indicative of PT pore opening) and cristae reorganisation.

In the experiments presented in this study there is no evidence for the existence of a separate store of cytochrome c. Firstly, analysis of the time-course of release does not show a two-component efflux; rather, the release data is accurately modelled by assuming passive diffusion of a single pool of cytochrome c through efflux channels [CHAPTER 6]. Thus tBID-induced opening of cristae junctions, if it does occur, must be an extremely rapid early process, so that it would not affect the observed efflux across the outer membrane. Secondly, although CSA does indeed inhibit tBID-induced cytochrome c release, there is no evidence that it inhibits the maximum amount of release, but only the speed of release of a single pool [7.3]. Finally, regarding the proposed mechanism of CSA inhibition, tBID is shown not to induce even transient PT pore opening in this system [5.3].

[11.4.2]Existence of a two-component cytochrome c store

The lack of any apparent effect of tBID on intermembrane space compartmentalisation in this study presumably reflects either the source of mitochondria (B50 cells as opposed to mouse liver), or the compositions of the assay media used. Scorrano attempted to address the problem of the effect of un-physiological buffers by recapitulating some of the effects on mitochondrial morphology in whole cells. Nevertheless, the generality of Scorrano's model has been questioned; for example von Ahsen and co-workers, using electron microscopy, detected no change in the internal structure of *Xenopus* mitochondria during BID-induced cytochrome c release [54]. Also a number of other groups have previously been unable to demonstrate any evidence of a two-component model in intact cells [258,269].

This said, it should be noted that the results of the present study do not conclusively rule out an effect of CSA on cytochrome c redistribution. As stated above (page 127), the value of *a* describes efflux across the outer membrane of a single *or functionally single* pool of cytochrome c. There may still be two (or more than two) distinct pools of cytochrome c within mitochondria, but if the rate of cytochrome c redistribution amongst these pools is rapid with respect to the rate of movement across the outer membrane, then the entire cytochrome c store will behave kinetically as a single pool. Figure 104(**A**) shows a hypothetical model of mitochondrial cytochrome c sequestration within mitochondria. The majority of cytochrome c is held in a large internal pool (Store 2; e.g. cristal spaces), but tBID-induced release occurs from a second, smaller pool (Store 1; e.g. intermembrane space). Release occurs with a rate constant k_1. Cytochrome c can move between these pools, and, specifically, can move by diffusion from Store 2 to Store 1 with rate constant k_3. If k_3 is of similar magnitude to k_1, then changes in k_3 (potentially induced by addition of an inhibitor such as CSA) will be reflected by a change in the kinetics of release [Figure 104(**B**)]. Conversely, if k_3 is large compared to k_1, even a two-fold change in k_3 does not alter the kinetics of cytochrome c release from Store 1 [Figure 104(**C**)]. If this second scenario is in fact the case in the B50 system investigated here, then CSA may indeed alter cytochrome c redistribution, additionally to its effects on BAK oligomerisation (as predicted by Scorrano and co-workers), but this change would not be visible. Further experiments, directly investigating internal redistribution of cytochrome c stores, would be necessary to investigate this possibility.

[11.4.3]Communication between tBID and internal mitochondrial systems

One of the biggest challenges to Scorrano's model is the fact that tBID, acting at the external surface of mitochondria, is proposed to affect the *internal* structure of the organelle. A signal must somehow be transmitted across the outer membrane, to affect inner membrane dynamics. The demonstration that tBID does not insert into the outer membrane [144,145] showed that tBID cannot exert any effect via physical interaction with a system internal to mitochondria. Scorrano suggested that the mediator of tBID's effects on internal structure might be the PT pore, with tBID proposed to induce transient PT pore opening. The inhibition by CSA of the substructural changes and cytochrome c release induced by tBID was thus proposed to be as a result of PT pore inhibition. This possibility is conclusively ruled out in this study by the demonstration that transient PT pore opening does not occur in B50 cell mitochondria treated with tBID [Figure 48].

[11.5]The effect of CSA at the outer membrane

[11.5.1]Introduction

Previously the inhibitory effect of CSA on apoptotic cytochrome c release was assumed to result from inhibition of the PT pore via cyclophilin D in the mitochondrial matrix [305]; since cyclophilin D is the mitochondrial cyclophilin isoform, this was the obvious target of CSA. The discovery that CSA exerts its effect at the *outer* mitochondrial membrane was therefore significant.

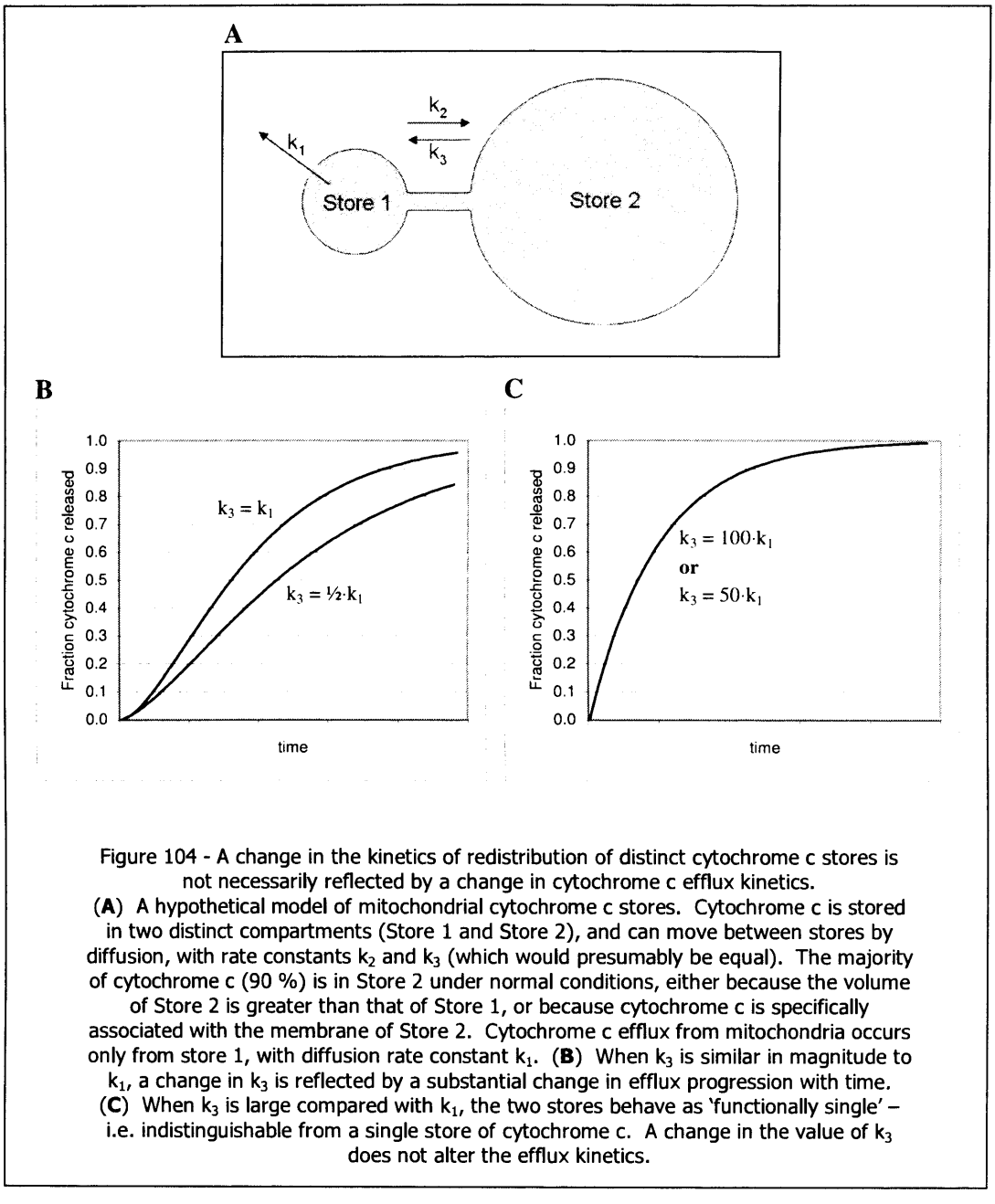

Figure 104 - A change in the kinetics of redistribution of distinct cytochrome c stores is not necessarily reflected by a change in cytochrome c efflux kinetics.
(**A**) A hypothetical model of mitochondrial cytochrome c stores. Cytochrome c is stored in two distinct compartments (Store 1 and Store 2), and can move between stores by diffusion, with rate constants k_2 and k_3 (which would presumably be equal). The majority of cytochrome c (90 %) is in Store 2 under normal conditions, either because the volume of Store 2 is greater than that of Store 1, or because cytochrome c is specifically associated with the membrane of Store 2. Cytochrome c efflux from mitochondria occurs only from store 1, with diffusion rate constant k_1. (**B**) When k_3 is similar in magnitude to k_1, a change in k_3 is reflected by a substantial change in efflux progression with time. (**C**) When k_3 is large compared with k_1, the two stores behave as 'functionally single' – i.e. indistinguishable from a single store of cytochrome c. A change in the value of k_3 does not alter the efflux kinetics.

Two possibilities thus existed : Firstly, CSA might indeed by exerting its effects via interaction with cyclophilin D in the matrix; this would require some signal to be transmitted from the matrix to an outer membrane system (BAK), allowing the effect of CSA to be observed at this site. Or, alternatively, CSA might be acting via an altogether different (non-cyclophilin D) pathway, the components of which were present at the outer membrane.

[11.5.2]Communication between matrix and outer membrane

If CSA's target is indeed matrix cyclophilin D, then how might an effect of inhibition of this enzyme be transmitted to the outer membrane? One possibility is that BID binding might be affected. This would fit with the observation that CSA decreases the value of the constant *c* (rate constant for tBID-catalysed BAK conformational change) - inhibition of binding would result in a lower effective concentration of tBID, which is equivalent to a decrease in *c*, since:

Equation 15

$$Rate \propto c \cdot [tBID]$$

CSA binding to cyclophilin D might have some effect on contact site dynamics, via an effect on cyclophilin D-associated ANT at these sites. It has been proposed that tBID binds to the outer membrane at contact sites [139], possibly by targeting cardiolipin [140] (which is enriched at these sites) or by targeting a specific membrane conformation [306]. Thus a CSA-induced disruption of contact site structure and/or function through an effect on cyclophilin D might conceivably result in a diminution of tBID-binding potential at the outer membrane.

[11.5.3]Cyclophilin A-catalysed BAK conformational change

In relation to this second possibility above, cyclophilin A was found to be associated with the mitochondrial fraction, thereby presenting a further potential target for CSA in this system. Cyclophilin A, being a cytosolic enzyme, would be associated with the mitochondrial outer membrane, and so would be correctly located to exert an effect on BAK oligomerisation. In fact, the amount of cyclophilin A present (around 1 μg/mg mitochondrial protein; Figure 74) was much greater than the amount of cyclophilin D previously observed in B50 mitochondria (60 ng/mg mitochondrial protein; [157]).

The role of proline isomerisation in native state conformational change has been considered previously as a method of protein regulation. Pappenberger and co-workers have shown the process to be energetically feasible, in some systems at least and, although a substantial kinetic barrier exists, kinetically feasible in the presence of catalysis by cyclophilins [159]. Proteins potentially regulated by this mechanism include the prolactin receptor [160], diphtheria toxin [161], the protein tyrosine kinase Itk [307] and the human immunodeficiency virus accessory protein Vpr [308]. Interestingly, Schinzel and co-workers have identified a proline residue (Pro168) in an unstructured loop of BAX which they propose to be involved in regulation of apoptotic activity [75]. The authors suggest that this residue somehow regulates release of the C-terminal trans-membrane domain from an internal binding pocket, thus directing BAX activation and targeting of the normally cytosolic protein to the mitochondrial outer membrane. Mutagenesis showed that BAX(ΔP168), BAX(P168A), BAX(P168G), and BAX(P168E)

were unable to release their transmembrane domain in response to apoptotic stimuli, and thus remained cytosolic following apoptotic stimuli. A similar residue, Pro185, is present in the BAK protein (which has 24 % sequence identity and 43 % sequence similarity with BAX). Unlike BAX, BAK is constitutively mitochondrial [Figure 71, page 148]; its C-terminal transmembrane domain is exposed without activation after translation. In keeping with this, the above authors were unable to detect any changes in BAK association with the mitochondrial outer membrane as a result of mutation of Pro185. Nevertheless it is tempting to speculate that the same proline residue might be involved in regulation of conformational change of BAK as well as BAX; in the case of BAK though, the relevant change would be conversion of membrane-integrated BAK to the 'open' conformer during activation by tBID, or by self-catalysis. Might this change be regulated by cyclophilins, and in particular by cyclophilin A? Further experiments using recombinant BAK and cyclophilin A are necessary to investigate this possibility. Additionally, further studies using cyclophilin A and D knockouts to probe the involvement of each might conclusively show which cyclophilin isoform is responsible for the effects of CSA on tBID-induced cytochrome c release.

[11.5.4]Differences between endogenous and recombinant cyclophilin A

Arguing against cyclophilin A-catalysed BAK conformational change is the lack of any stimulatory effect on tBID-induced cytochrome c release of addition of physiological levels of recombinant cyclophilin A. Nevertheless, recombinant cyclophilin A, whilst certainly retaining PPIase activity [Figure 84], might be somehow different to the endogenous protein, and thus unable to substitute functionally in the assays carried out above. For example, the cyclophilin A detected in the mitochondrial preparation here [Figure 74, page 151] is presumably membrane-associated (perhaps through interaction with other membrane proteins) and so may behave functionally differently to added cyclophilin A, which would remain free in solution. Additionally, cyclophilin A has been shown to be a substrate for glutathionylation under some conditions [309], and this modification was shown by circular dichroism significantly to affect cyclophilin A's secondary structure. Furthermore, Fratelli and co-workers have shown cyclophilin A to be heavily glutathionylated even under basal conditions [310], suggesting that this may be the predominant active form of the enzyme in normal cells. Recombinant, non-glutathionylated enzyme might behave functionally differently. Analysis of mitochondrially-associated cyclophilin A by mass spectroscopy to investigate the presence or absence of the glutathione moiety might help to resolve this issue.

[11.6]The effect of DB25

[11.6.1]Gain-of-function effects of cyclophilin A

Whilst addition of small amounts of recombinant cyclophilin A did not affect tBID-induced cytochrome c release, a larger amount of exogenous cyclophilin A had an inhibitory effect, identical in magnitude to that of CSA. This result suggested cyclophilin A might be the target of CSA, via a 'gain-of-function' calcineurin-type mechanism. Whilst the affinity of free cyclophilin A for downstream targets would be low in the absence of CSA, a higher concentration of cyclophilin A might nevertheless be able to substitute functionally for the presence of this compound. The involvement of

calcineurin itself in CSA action was ruled out by the absence of any external Ca^{2+} (required for calcineurin activation) in the cytochrome c release experiments (conducted in the presence of EGTA). However the existence of other interaction partners is a possibility; pull-down assays using recombinant cyclophilin A in the presence of CSA might be used in the future to identify any such proteins.

[11.6.2]DB25 as a non-calcineurin-interacting CSA analogue

Experiments with the CSA derivative DB25 allowed the mechanism of CSA inhibition to be investigated further [CHAPTER 8]. DB25 has modifications in the 3 and 4 positions of its ring structure when compared with CSA. The calcineurin binding surface when CSA is complexed with cyclophilin A comprises residues 4 – 8 [311]; the substitution at the 4 position disrupts the binding surface and prevents calcineurin interaction. This has been demonstrated previously for a number of other 4-substituted derivatives; for example MeVal-4-CSA was shown to retain the ability to inhibit the PT pore, but not that of inhibiting calcineurin [312]. The cyclophilin binding sites on CSA comprise residues 1 – 3 and 9 – 11, and the substitution in DB25 at position 3 enhances cyclophilin binding relative to CSA. This is desirable because 4-substituted derivates frequently display a lower affinity for cyclophilins: for example 4[(E)-2-butenyl]-4,4,*N*-trimethyl-L-threonine ($MeBm_2t$)-CSA shows only 1 % of CSA's affinity for cyclophilin D [313]. The mechanism explaining the increased apparent affinity of the 3-substituted compounds is likely to be partly kinetic. Cyclophilins recognise and bind a specific CSA conformational state, populated only by a small proportion of CSA molecules in aqueous solution; the rate-limiting step in complex formation between CSA and cyclophilins is the rate of *cis-trans* isomerisation of CSA at positions 9 and 10 [275]. 3-position-substituted derivatives increase the population of this state, thus accelerating cyclophilin binding, which can otherwise occur extremely slowly (minutes to hr). Thus although the extent of cyclophilin binding at equilibrium is not affected, the observed K_d is frequently higher in the absence of 3-position substituents since true equilibrium is not attained over the course of typical binding experiments.

In contrast to CSA, DB25 did not inhibit tBID-induced cytochrome c release, but instead stimulated release via a stimulation of tBID-induced BAK conformational change [Figure 80]. This result suggested that CSA was indeed acting via a 'gain-of-function' calcineurin-type mechanism, since DB25 retained cyclophilin inhibitory activity [Figure 82]. Since cyclophilin D was shown to inhibit tBID-induced cytochrome c release [Figure 54], the stimulatory effect of DB25 might be as a result of cyclophilin D inhibition (i.e. removal of cyclophilin D's inhibitory effect). This stimulatory effect of cyclophilin D inhibition would presumably also be present with CSA, but would be counteracted by CSA's stronger inhibitory effect (not present with DB25). This possibility would imply communication between matrix and outer membrane, as discussed above [11.5.2], since the effect of DB25 is mediated via BAK at the outer membrane.

[11.7]Identification of a novel cyclophilin D interaction partner

[11.7.1]Domain structure

In attempting to find a protein responsible for the effects of cyclophilins and CSA on tBID-induced cytochrome c release, a novel cyclophilin D interaction partner was identified. This 54 kD proline- and glutamine-rich protein (p54), present in the mitochondrial matrix, was found to associate with cyclophilin D in a CSA- and DB25- inhibitable manner. p54 has a short-chain dehydrogenase domain and a sterol binding domain, and shows significant homology to a number of hydroxysteroid dehydrogenases, for example estradiol 17β-dehydrogenase. p54 also has four low-complexity regions, rich in proline and glutamine residues, the largest of these being a 107 residue stretch from amino acids 298 – 404. Although this region may have functional significance (see below) it may also derive from polymerase slippage during DNA replication resulting in expansion of CAG (glutamine) codons and subsequent mutation [294], as discussed above [9.6.4].

[11.7.2]The role of p54 in steroidogenesis

On the basis of its domain structure and its mitochondrial localisation, p54 is likely to have a role in steroid processing in the mitochondrial matrix. The first step of steroidogenesis is the transfer of cholesterol from the outer mitochondrial membrane to the inner membrane - this process is thought to occur at contact sites between the inner and outer membrane [314]. The presence of a proline-rich tract in the centre of p54 could potentially serve to anchor the protein close to the site of steroid import via interaction with cyclophilin D associated with ANT at contact sites, thus maximising its catalytic activity. Since p54 appeared to bind to cyclophilin D's active site (p54 being dissociated from cyclophilin D by CSA [Figure 96]), and since cyclophilin D also interacts with ANT via its active site [36,166], this mechanism would require at least two cyclophilin D molecules, tethered together via a non-active site region, with one bound to p54 and one bound to ANT. Dimerisation of cyclophilin D via non-active site regions is in fact observed in this study [Figure 90].

Interestingly, CSA can inhibit sterol processing in mitochondria (e.g. 27-hydroxylation of cholesterol [173,174], and 25-hydroxylation of vitamin D3 [175]). This fact would fit with a model in which cyclophilin D serves to anchor p54 to a membrane site at which it is required for a stage of steroid processing, since CSA disrupts the p54-cyclophilin D interaction [Figure 96] and would thus dissociate p54 from this site.

[11.7.3]The role of p54 in transglutaminase-catalysed cross-linking reactions

There is an emerging link between poly-glutamine containing proteins, transglutaminases and apoptosis. Rodolfo and co-workers report that tissue transglutaminase (TG2) has a functional BH3 domain, and interacts with BAX at the outer mitochondrial membrane during apoptosis [315]. TG2 selectively accumulates to high levels during cell death, and cross-links BAK, possibly being responsible for the appearance of the high molecular weight BAX aggregates observed late in apoptosis [109]. This process might represent a stabilisation of BAX channels in the outer membrane. TG2 is also responsible for cross-linking of other cytosolic proteins during apoptosis; based on its sensitive regulation and limited substrate specificity, this activity is proposed to be mechanistically involved in

apoptotic progression, and not simply a means of preventing leakage of cellular components prior to phagocytosis, as was previously assumed [316]. The possibility that the 54 kD protein identified here might be cross-linked by mitochondrial transglutaminases as part of a regulatory mechanism in apoptosis is intriguing, and merits further investigation.

[11.8]Binding partners of mitochondrial cyclophilin D

In the course of this study, cyclophilin D has been found to form at least three types of multimeric structure [Figure 105]. Firstly, the interaction of cyclophilin D with ANT was confirmed [Figure 97]. Secondly, cyclophilin D was found to interact with the novel p54 protein [Figure 92]. Both of these interactions were disrupted by either CSA or DB25. Finally, overexpressed mitochondrial cyclophilin D was found to oligomerise *in vivo* [Figure 89]. The oligomers were not disrupted in the presence of CSA [Figure 90] and, since CSA occludes the enzyme's active site, this suggests that oligomerisation occurs via non-active site regions. Further work is necessary to investigate the relative population of these cyclophilin D interaction states in intact mitochondria and their functional significance. Are complexes formed between ANT and p54 in order to tether the latter to sites of steroid import, as suggested above? Is homo-oligomerisation a means of enabling this process? How does oligomer formation affect the PPIase catalytic function of the enzyme? Does cyclophilin A also oligomerise, and if so, how might this relate to its functions at the outer mitochondrial membrane?

[11.9]Phosphorylation of mitochondrial proteins

[11.9.1]Importance of protein phosphorylation in apoptosis

Phosphorylation is a key method of regulation of cellular protein activity, and no less so in apoptosis. For example BAD is activated by dephosphorylation by calcineurin [201,202]; BID is protected from cleavage by phosphorylation by casein I and II [135]; the induction of apoptosis by p53 is regulated both positively and negatively by its phosphorylation [317]; and induction of apoptosis by staurosporine is by a kinase inhibition mechanism [267]. CSA is known to influence protein phosphorylation through interactions with the calcineurin pathway [178], and the profile of CSA's effects on tBID-induced cytochrome c release raised the suspicion that CSA might be acting here via a similar mechanism. Clearly calcineurin itself was not involved, since tBID-induced cytochrome c release experiments were carried out in the absence of calcium. However a number of internal mitochondrial proteins are regulated by phosphorylation [209,212,213], and the existence of a mitochondrial calcineurin homologue is a possiblity. Regulation of this phosphatase by a mechansim analagous to that of CSA and calcineurin might fit with the observed effects of CSA.

To investigate whether the mechanism of action of tBID and CSA might indeed involve changes in phosphorylation state of mitochondrial proteins, proteins were labelled with ^{32}P in the presence or absence of tBID, CSA and DB25. Although no changes in phosphorylation state were observed under any of these conditions, it remains possible that the changes induced were below the detection limit of this assay. During the experiments carried out in this study, protein labelling had not reached steady state [Figure 99].

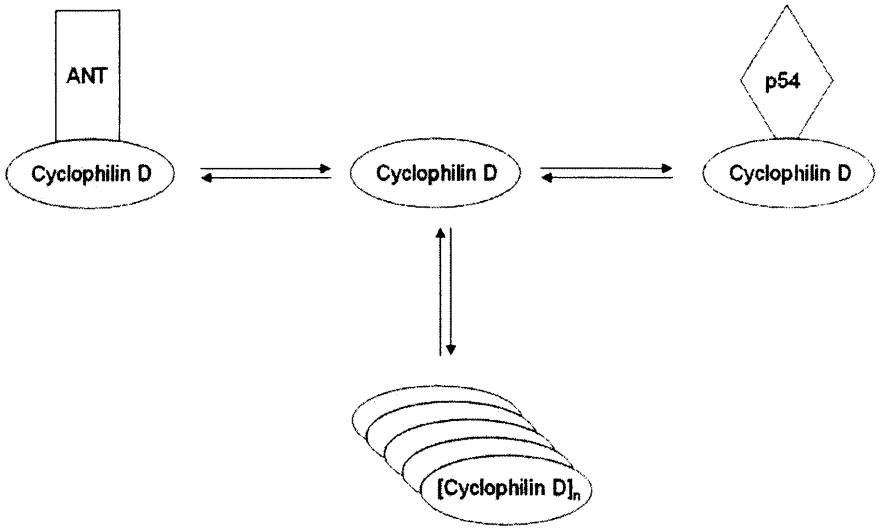

Figure 105 - Cyclophilin D interaction partners
Mitochondrial cyclophilin D can interact to form at least three multimeric structures. Cyclophilin D is able to dimerise with ANT (left) or with a novel mitochondrial protein, p54 (right). Cyclophilin D can also homo-oligomerise (bottom).

Under these conditions inhibition of phosphatase activity has two effects – firstly an increase in labelling, due to an inhibition of removal of ^{32}P label; but secondly a decrease in labelling due to an inhibition of P_i turnover (i.e. inhibition of removal of unlabelled P_i). Thus, depending on the kinetics of the relevant kinases and phosphatases, changes in phosphatase activity can in fact have no effect whatsoever on ^{32}P labelling. Isolation of mitochondrial phosphatase activity and investigation of its CSA sensitivity in a more well-defined *in vitro* system is required to further probe the involvement of CSA on this aspect of mitochondrial apoptosis signalling.

[11.9.2]Phosphorylation of a 17 kD mitochondrial protein

Despite the absence of any effect of tBID, CSA and DB25, it was observed that phosphorylation of a 17 kD protein was increased in cyclophilin D overexpressing mitochondria, compared to wild-type mitochondria. The phosphorylated band was shown to run as a lower molecular weight specie than cyclophilin D [Figure 101]. However it is possible that it may still correspond to a phosphorylated form of cyclophilin D, since phosphorylation may affect mobility on SDS-PAGE. If so, this would represent a previously unknown mechanism of regulation of the mitochondrial cyclophilin isoform, and this possibility deserves further study.

CHAPTER 12 :APPENDIX

[12.1]Molecular weight standards

[12.1.1]SDS-PAGE

Precision-Plus Dual Colour Protein Standards (Biorad)

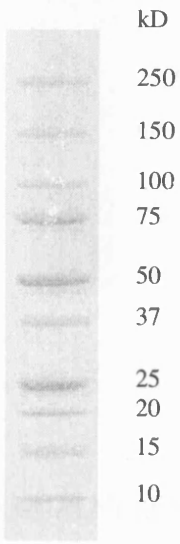

Odyssey Molecular Weight Marker (LiCor)

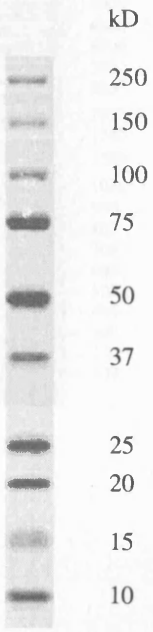

Low-Range Rainbow™ Molecular Weight Markers (Amersham)

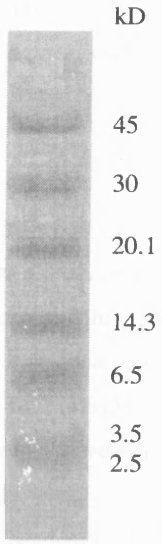

[12.1.2]DNA

GeneRuler DNA Ladder Mix (Fermentas)

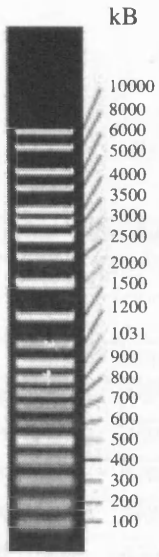

[12.2]Mass spectrometry data

The data displayed below derives from peptide mass matching of LC-MS-MS data against the NCBI database, carried out using the Mascot search engine (Matrix Science) [318]. The columns are as follows:

Query	Fragment number
Observed	Experimental m/z value (mass:charge ratio)
MW(exp)	Experimental m/z transformed to a relative molecular mass
Delta	Difference (error) between the experimental and calculated (predicted) masses
Score	Score assigned to the peptide match, based on sequence length and delta value
Start	Inclusive residue number of the first residue of the matched sequence (starting with 1 for the N-terminal residue of the intact protein)
Sequence	Sequence of the peptide in 1-letter code
End	Inclusive residue number of the last residue of the matched sequence

The ion score is $-10 \cdot \log_{10}(P)$, where P is the probability that the observed match is a random event. Individual ion scores > 37 indicate identity or extensive homology ($p<0.05$). (This cut-off depends on the database size). Protein score ('total score') is derived from ion scores as a non-probabilistic basis for ranking protein hits.

[12.2.1]Band 1 – 280 kD Protein

Tax_Id=10116 Erythroid spectrin alpha

Accession No.	Mass (Da)	pI	Total Score	No. Peptides matched	Total Coverage%
IPI00560498	280395.87	4.94	221	10	4

Query	Observed	z	MW(exp)	Delta	Score	Start	Sequence	End
10	486.78099	2+	971.547428	-0.017666	10.34	1478	TQLLAELGK	1486
12	516.28674	2+	1030.558928	-0.006898	19.85	1631	DLTSAGNLLK	1640
15	538.76938	2+	1075.524208	-0.026695	8.77	1230	VTTLGETAER	1239
17	549.80279	2+	1097.591028	-0.028219	41.46	709	GLADVQNLLR	718
19	552.8045	2+	1103.594448	-0.012928	3.33	523	IITLDETATK	532
21	563.80243	2+	1125.590308	-0.016641	30.14	2169	AYFLDGSLLK	2178
22	598.7981	2+	1195.581648	-0.042009	40.95	973	VIALYDFEAR	982
26	662.82134	2+	1323.628128	-0.050095	0.19	9	VLETAEEIQHR	19
27	738.85324	2+	1475.691928	-0.054776	21.18	1838	GDSGDTLAATQSLLK	1852
28	883.37849	2+	1764.742428	-0.085392	21.06	1961	QDTLDASLQSFQQER	1975

[12.2.2]Band 2 – 275 kD Protein

Tax_Id=10116 Non-erythroid spectrin beta

Accession No.	Mass (Da)	pI	Total Score	No. Peptides matched	Total Coverage%
IPI00555287	274328.49	5.5	772	22	9

Query	Observed	z	MW(exp)	Delta	Score	Start	Sequence	End
1	394.2068	2+	786.399048	-0.02446	12.08	824	LAGIEER	830
2	395.72432	2+	789.434088	-0.015589	14.44	1695	LFQLNR	1700
6	413.2136	2+	824.412648	-0.016612	4.16	1735	FREFAR	1740
13	446.20208	2+	890.389608	-0.044856	11.01	1055	EASLGEASK	1063
14	454.22072	2+	906.426888	-0.017768	19.02	1536	IDDIFER	1542
15	456.77608	2+	911.537608	-0.017568	32.54	478	VQAVVAVAR	486
16	465.71684	2+	929.419128	-0.037491	40	1857	QLQEDAAR	1864
18	495.22504	2+	988.435528	-0.021808	43.83	1741	DTGNIGQER	1749
21	525.77435	2+	1049.534148	-0.016359	24.07	1902	LVDTGDKFR	1910
22	529.19933	2+	1056.384108	-0.034059	5.36	682	AFEDEMSGR	690
23	555.27991	2+	1108.545268	-0.031148	39.23	75	ITDLYTDLR	83
25	573.25977	2+	1144.504988	-0.022752	23.38	2094	RPPSPEPSAK	2103
26	593.83282	2+	1185.651088	-0.04575	84.35	2074	LTTLELLEVR	2083
28	621.3326	2+	1240.650648	-0.042101	31.24	2010	LILEVHQFSR	2019
30	632.32545	2+	1262.636348	-0.050664	41.12	843	QALQDTLALYK	853
31	632.84974	2+	1263.684928	-0.0337	45.16	559	HLLGVEDLLQK	569
33	655.802	2+	1309.589448	-0.036742	7.6	1652	ALVADSHPESER	1663
34	677.359	2+	1352.703448	-0.037717	52.53	2172	SALPAQSAATLPAR	2185
36	703.83132	2+	1405.648088	-0.042998	28.4	1462	FMELLEPLNER	1472
37	731.39107	2+	1460.767588	-0.056219	45	360	GNLEVLLFTIQSK	372
38	574.59139	3+	1720.752342	-0.063179	16.01	250	LLDPEDISVDHPDEK	264
39	909.9287	2+	1817.842848	-0.069017	91.29	1543	SQNIITDSSSLNAEAIR	1559

[12.2.3]Band 3 – 225 kD Protein

Tax_Id=10116 Myosin heavy chain, cardiac muscle alpha isoform

Accession No.	Mass (Da)	pI	Total Score	No. Peptides matched	Total Coverage%
IPI00189809	224168.95	5.58	997	32	17

Query	Observed	z	MW(exp)	Delta	Score	Start	Sequence	End
3	415.7185	2+	829.422448	-0.022132	4.91	251	IHFGATGK	258
8	430.74164	2+	859.468728	-0.018806	19.07	1137	LRSDLTR	1143
9	434.71881	2+	867.423068	-0.021909	12.68	1524	NVHELEK	1530
12	442.21907	2+	882.423588	-0.036312	31.43	715	ILYGDFR	721
13	445.19887	2+	888.383188	-0.10842	35.63	444	INATLETK	451
14	455.22701	2+	908.439468	-0.020813	40.85	407	VGNEYVTK	414
15	462.7314	2+	923.448248	-0.048105	14.9	1478	SLSTELFK	1485
16	464.70812	2+	927.401688	-0.021545	4.37	1340	HDCDLLR	1346
17	466.2574	2+	930.500248	-0.013134	14.32	872	RKELEEK	878
18	480.24375	2+	958.472948	-0.014235	25.79	553	LYDNHLGK	560
19	486.773	2+	971.531448	-0.008484	38.22	1263	VKLEEAQR	1270
20	495.75039	2+	989.486228	-0.017999	36.98	561	SNNFQKPR	568
21	507.74954	2+	1013.484528	-0.018356	19.75	1320	QLEEEGKAK	1328
24	541.25826	2+	1080.501968	-0.01799	27.35	1271	SLNDFTTQR	1279
26	568.79834	2+	1135.582128	-0.041514	4.62	405	VKVGNEYVTK	414
27	576.29987	2+	1150.585188	-0.035463	15.48	1329	NALAHALQSAR	1339
28	593.25774	2+	1184.500928	-0.041217	28.05	1774	EQDTSAHLER	1783
30	612.79408	2+	1223.573608	-0.04097	21.9	1375	TKYETDAIQR	1384
31	619.7738	2+	1237.533048	-0.024401	31.99	1253	TLEDQANEYR	1262
32	623.32441	2+	1244.634268	-0.015695	23.5	955	DIDDLELTLAK	965
35	656.87985	2+	1311.745148	-0.031006	85.53	1866	LQDLVDKLQLK	1876
38	733.37372	2+	1464.732888	-0.03823	52.18	259	LASADIETYLLEK	271
39	743.85712	2+	1485.699688	-0.03133	69.47	1399	LQDAEEAVEAVNAK	1412
40	744.83434	2+	1487.654128	-0.044923	45.98	1117	IEELEEELEAER	1128
42	767.37491	2+	1532.735268	-0.032905	72.82	1595	VVDSLQTSLDAETR	1608
46	553.29136	3+	1656.852252	-0.052335	6.3	1292	QLEEKEALISQLTR	1305
47	831.89118	2+	1661.767808	-0.050322	24.76	979	NLTEEMAGLDEIIAK	993
48	856.41803	2+	1710.821508	-0.072489	59.83	415	GQSVQQVYYSIGALAK	430
49	859.88446	2+	1717.754368	-0.064831	23.75	1423	LQNEIEDLMVDVER	1436
52	870.93981	2+	1739.865068	-0.055495	0.83	726	ILNPAAIPEGQFIDSR	741
53	613.63385	3+	1837.879722	-0.037224	22.88	1179	DLEEATLQHEATAAALR	1195
54	976.41025	2+	1950.805948	-0.082068	1.69	617	LMATLFSTYASADTGDSGK	635

[12.2.4]Band 4 – 225 kD Protein

Tax_Id=10116 Myosin heavy chain, cardiac muscle beta isoform

Accession No.	Mass (Da)	pI	Total Score	No. Peptides matched	Total Coverage%
IPI00189811	223742.95	5.64	753	22	11

Query	Observed	z	MW(exp)	Delta	Score	Start	Sequence	End
3	415.7185	2+	829.422448	-0.022132	4.91	250	IHFGATGK	257
12	442.21907	2+	882.423588	-0.036312	31.43	713	ILYGDFR	719
13	445.19887	2+	888.383188	-0.10842	35.63	443	INATLETK	450
14	455.22701	2+	908.439468	-0.020813	40.85	406	VGNEYVTK	413
15	462.7314	2+	923.448248	-0.048105	14.9	1476	SLSTELFK	1483
16	464.70812	2+	927.401688	-0.021545	4.37	1338	HDCDLLR	1344
17	466.2574	2+	930.500248	-0.013134	14.32	870	RKELEEK	876
18	480.24375	2+	958.472948	-0.014235	25.79	552	LYDNHLGK	559
20	495.75039	2+	989.486228	-0.017999	36.98	560	SNNFQKPR	567
26	568.79834	2+	1135.582128	-0.041514	4.62	404	VKVGNEYVTK	413
27	576.29987	2+	1150.585188	-0.035463	15.48	1327	NALAHALQSAR	1337
28	593.25774	2+	1184.500928	-0.041217	28.05	1772	EQDTSAHLER	1781
30	612.79408	2+	1223.573608	-0.04097	21.9	1373	TKYETDAIQR	1382
32	623.32441	2+	1244.634268	-0.015695	23.5	953	DIDDLELTLAK	963
35	656.87985	2+	1311.745148	-0.031006	85.53	1864	LQDLVDKLQLK	1874
38	733.37372	2+	1464.732888	-0.03823	52.18	258	LASADIETYLLEK	270
39	743.85712	2+	1485.699688	-0.03133	69.47	1397	LQDAEEAVEAVNAK	1410
40	744.83434	2+	1487.654128	-0.044923	45.98	1115	IEELEEELEAER	1126
42	767.37491	2+	1532.735268	-0.032905	72.82	1593	VVDSLQTSLDAETR	1606
49	859.88446	2+	1717.754368	-0.064831	23.75	1421	LQNEIEDLMVDVER	1434
52	870.93981	2+	1739.865068	-0.055495	0.83	724	ILNPAAIPEGQFIDSR	739
53	613.63385	3+	1837.879722	-0.037224	22.88	1177	DLEEATLQHEATAAALR	1193

[12.2.5]Band 5 – 54 kD Protein

Tax_Id=10116 54 kDa protein

Accession No.	Mass (Da)	pI	Total Score	No. Peptides matched	Total Coverage%
IPI00557984	53534.56	6.01	285	6	12

Query	Observed	z	MW(exp)	Delta	Score	Start	Sequence	End
10	486.26289	2+	970.511228	-0.03345	50.56	27	DGANIVIAAK	36
11	510.23824	2+	1018.461928	-0.031129	33.02	388	DSLSDEVVR	396
13	546.25185	2+	1090.489148	-0.033786	16.99	158	QHCAYTIAK	166
18	676.83386	2+	1351.653168	-0.038589	55.31	2	LAGCTVFITGASR	14
19	680.35244	2+	1358.690328	-0.050151	39.26	385	IVKDSLSDEVVR	396
20	903.94952	2+	1805.884488	-0.056506	61.15	44	LLGTIYTAAEEIEAAGGK	61

[12.3]Derivation of kinetic analysis equations

[12.3.1]Formation of open channels with time

We begin with:

Equation 16

$$\frac{d[Open]}{dt} = -\frac{d[Closed]}{dt} = (c + f \cdot [Open]_t) \cdot [Closed]_t$$
$$\therefore -\frac{d[Closed]}{dt} = (c + f \cdot \{1 - [Closed]_t\}) \cdot [Closed]_t$$

Using the general result:

Equation 17

$$\int \frac{dx}{x(vx + w)} = \frac{-1}{w} \cdot \ln\left|\frac{vx + w}{x}\right|$$

it follows that:

Equation 18

$$\int \frac{d[Closed]}{(c + f \cdot \{1 - [Closed]_t\}) \cdot [Closed]_t} = -\int dt$$
$$\therefore \int \frac{d[Closed]}{[Closed]_t(-f \cdot [Closed]_t + \{c + f\})} = -\int dt$$
$$\therefore \frac{-1}{c + f} \cdot \ln\left|\frac{-f \cdot [Closed]_t + \{c + f\}}{[Closed]_t}\right| = -t + g$$
$$\therefore \ln\left|\frac{-f \cdot [Closed]_t + \{c + f\}}{[Closed]_t}\right| = (c + f) \cdot t + h$$
$$\therefore \frac{-f \cdot [Closed]_t + \{c + f\}}{[Closed]_t} = k \cdot e^{(c+f)t}$$
$$\therefore [Closed]_t \left[k \cdot e^{(c+f)t} + f\right] = c + f$$
$$\therefore [Closed]_t = \frac{c + f}{k \cdot e^{(c+f)t} + f}$$

Since at t=0, [Closed]=1 (by definition), it follows that $k = c$, and so:

Equation 19

$$[Closed]_t = \frac{c + f}{c \cdot e^{(c+f)t} + f}$$

or alternatively:

Equation 20

$$[Open]_t = 1 - \frac{c + f}{c \cdot e^{(c+f)t} + f}$$

[12.3.2]Rate of cytochrome c efflux

We begin with:

Equation 21

$$-\frac{d[Cytc]}{dt}=\left(1-\frac{c+f}{c\cdot e^{(c+f)t}+f}\right)\cdot a\cdot[Cytc]_t$$

Thus:

Equation 22

$$\int\frac{d[Cytc]}{[Cytc]_t}=-a\cdot\int\left(1-\frac{c+f}{c\cdot e^{(c+f)t}+f}\right)dt$$

Using the general result:

Equation 23

$$\int\frac{1}{u+v\cdot e^{w\cdot x}}=\frac{x}{u}-\frac{1}{u\cdot w}\cdot\ln\left(u+v\cdot e^{w\cdot x}\right)$$

we can integrate Equation 22 as follows:

Equation 24

$$\ln([Cytc]_t)=a\cdot\left(-t+(c+f)\left[\frac{t}{f}-\frac{1}{f\cdot(c+f)}\cdot\ln\left(c\cdot e^{(c+f)t}+f\right)\right]+m\right)$$

$$\therefore[Cytc]_t=n\cdot\exp\left[a\cdot\left(-t+(c+f)\left[\frac{t}{f}-\frac{1}{f\cdot(c+f)}\cdot\ln\left(c\cdot e^{(c+f)t}+f\right)\right]\right)\right]$$

Since at t=0, [Cytc]=1 it follows that:

Equation 25

$$n=\frac{1}{\exp\left[\frac{-a\cdot\ln(c+f)}{f}\right]}$$

and so:

Equation 26

$$[Cytc]_t=\frac{\exp\left[a\left(-t+(c+f)\left[\frac{t}{f}-\frac{1}{f\cdot(c+f)}\cdot\ln\left(c\cdot e^{(c+f)t}+f\right)\right]\right)\right]}{\exp\left[\frac{-a\cdot\ln(c+f)}{f}\right]}$$

[12.4]Derivation of equations for PPIase inhibition

In the case of a loose-binding inhibitor, the approximation $[I]_{free} \approx [I]_{total}$ holds, and so the following relationship can be used to derive a value for K_d by fitting of predicted values of I to experimental values, using $[I]_{total}$ for the value of [I] :

Equation 27

$$K_d = \frac{[I]\cdot([E]_0 - [EI])}{[EI]}$$

$$\therefore \frac{K_d}{[I]} = \frac{[E]_0}{[EI]} - 1$$

$$\therefore \frac{K_d}{[I]} + 1 = \frac{1}{P}$$

$$\therefore P = \frac{1}{\frac{K_d}{[I]} + 1} = \frac{[I]}{K_d + [I]}$$

where K_d is the dissociation complex for the cyclophilin-inhibitor complex, P is proportion inhibition, [I] is the concentration of free inhibitor, [E] is the concentration of free cyclophilin, [EI] is the concentration of cyclophilin-inhibitor complex and $[E]_0$ is the total concentration of cyclophilin (i.e. bound plus un-bound). However, in the case of CSA the binding of inhibitor to enzyme is extremely tight (in the low nanomolar range; Table 9). Thus $[I]_{free}$ is much lower than $[I]_{total}$, and Equation 27 cannot be used to derive a value of K_d (since $[I]_{free}$ is unknown). In this case we can proceed as follows:

Equation 28

$$K_d = \frac{[I]\cdot([E]_0 - [EI])}{[EI]}$$

At equilibrium, the proportion of total cyclophilin that is bound to inhibitor is P, and so the concentration of cyclophilin-inhibitor complex, [EI], is $P\cdot[E]_0$. Thus the concentration of free (unbound) cyclophilin, [E], will be $(1 - P) \cdot [E]_0$. Also, if $[I]_0$ is the total added concentration of inhibitor, the concentration of free inhibitor, [I] will be $[I]_0 - P\cdot [E]_0$. Thus:

Equation 29

$$K_d = \frac{(1-P)\cdot[E]_0\cdot([I]_0 - P\cdot[E]_0)}{[P]\cdot[E]_0}$$

$$K_d = \frac{(1-P)\cdot([I]_0 - P\cdot[E]_0)}{[P]}$$

Expanding and simplifying, this leaves us with a quadratic in P:

Equation 30

$$P^2 \cdot ([E]_0) + P \cdot (-[I]_0 - [E]_0 - K_d) + [I]_0 = 0$$

Thus:

Equation 31

$$P = \frac{[I]_0 + [E]_0 + K_d - \sqrt{(-[I]_0 - [E]_0 - K_d)^2 - 4 \cdot [E]_0 \cdot [I]_0}}{2 \cdot [E]_0}$$

CHAPTER 13 : REFERENCES

1. Ellis, R. E., Yuan, J. Y., and Horvitz, H. R. (1991) Mechanisms and functions of cell death, *Annu Rev Cell Biol* **7,** 663-698.

2. Kerr, J. F., Wyllie, A. H., and Currie, A. R. (1972) Apoptosis: a basic biological phenomenon with wide-ranging implications in tissue kinetics, *Br. J Cancer* **26,** 239-257.

3. Thornberry, N. A. and Lazebnik, Y. (1998) Caspases: enemies within, *Science* **281,** 1312-1316.

4. Scaffidi, C., Fulda, S., Srinivasan, A., Friesen, C., Li, F., Tomaselli, K. J., Debatin, K. M., Krammer, P. H., and Peter, M. E. (1998) Two CD95 (APO-1/Fas) signaling pathways, *EMBO J.* **17,** 1675-1687.

5. Zou, H., Li, Y., Liu, X., and Wang, X. (1999) An APAF-1.cytochrome c multimeric complex is a functional apoptosome that activates procaspase-**9,** *J Biol Chem* **274,** 11549-11556.

6. Van Loo, G., Demol, H., van Gurp, M., Hoorelbeke, B., Schotte, P., Beyaert, R., Zhivotovsky, B., Gevaert, K., Declercq, W., Vandekerckhove, J., and Vandenabeele, P. (2002) A matrix-assisted laser desorption ionization post-source decay (MALDI-PSD) analysis of proteins released from isolated liver mitochondria treated with recombinant truncated Bid, *Cell Death Differ* **9,** 301-308.

7. Antonsson, B., Conti, F., Ciavatta, A., Montessuit, S., Lewis, S., Martinou, I., Bernasconi, L., Bernard, A., Mermod, J. J., Mazzei, G., Maundrell, K., Gambale, F., Sadoul, R., and Martinou, J. C. (1997) Inhibition of Bax channel-forming activity by Bcl-**2,** *Science* **277,** 370-372.

8. Korsmeyer, S. J., Wei, M. C., Saito, M., Weiler, S., Oh, K. J., and Schlesinger, P. H. (2000) Pro-apoptotic cascade activates BID, which oligomerizes BAK or BAX into pores that result in the release of cytochrome c, *Cell Death Differ* **7,** 1166-1173.

9. Shimizu, S., Narita, M., and Tsujimoto, Y. (1999) Bcl-2 family proteins regulate the release of apoptogenic cytochrome c by the mitochondrial channel VDAC, *Nature* **399,** 483-487.

10. Marzo, I., Brenner, C., Zamzami, N., Jurgensmeier, J. M., Susin, S. A., Vieira, H. L., Prevost, M. C., Xie, Z., Matsuyama, S., Reed, J. C., and Kroemer, G. (1998) Bax and adenine nucleotide translocator cooperate in the mitochondrial control of apoptosis, *Science.* **281,** 2027-2031.

11. He, L. and Lemasters, J. J. (2002) Regulated and unregulated mitochondrial permeability transition pores: a new paradigm of pore structure and function?, *FEBS Lett.* **512,** 1-7.

12. Vander Heiden, M. G., Chandel, N. S., Schumacker, P. T., and Thompson, C. B. (1999) Bcl-xL prevents cell death following growth factor withdrawal by facilitating mitochondrial ATP/ADP exchange, *Mol. Cell.* **3,** 159-167.

13. Basanez, G., Nechushtan, A., Drozhinin, O., Chanturiya, A., Choe, E., Tutt, S., Wood, K. A., Hsu, Y., Zimmerberg, J., and Youle, R. J. (1999) Bax, but not Bcl-xL, decreases the lifetime of planar phospholipid bilayer membranes at subnanomolar concentrations, *Proc Natl Acad Sci U S A* **96,** 5492-5497.

14. Kroemer, G., Zamzami, N., and Susin, S. A. (1997) Mitochondrial control of apoptosis, *Immunol. Today.* **18,** 44-51.

15. Desagher, S. and Martinou, J. C. (2000) Mitochondria as the central control point of apoptosis, *Trends Cell Biol* **10,** 369-377.

16. MacFarlane, M. and Williams, A. C. (2004) Apoptosis and disease: a life or death decision, *EMBO Rep.* **5,** 674-678.

17. Scorrano, L., Ashiya, M., Buttle, K., Weiler, S., Oakes, S. A., Mannella, C. A., and Korsmeyer, S. J. (2002) A distinct pathway remodels mitochondrial cristae and mobilizes cytochrome c during apoptosis, *Dev Cell* **2,** 55-67.

18. Perkins, G., Renken, C., Martone, M. E., Young, S. J., Ellisman, M., and Frey, T. (1997) Electron tomography of neuronal mitochondria: three-dimensional structure and organization of cristae and membrane contacts, *J Struct Biol* **119,** 260-272.

19. Mannella, C. A., Pfeiffer, D. R., Bradshaw, P. C., Moraru, I. I., Slepchenko, B., Loew, L. M., Hsieh, C. E., Buttle, K., and Marko, M. (2001) Topology of the mitochondrial inner membrane: dynamics and bioenergetic implications, *IUBMB. Life* **52,** 93-100.

20. Scorrano, L. (2005) Proteins that fuse and fragment mitochondria in apoptosis: con-fissing a deadly con-fusion?, *J. Bioenerg. Biomembr.* **37,** 165-170.

21. Bernardi, P. and Azzone, G. F. (1981) Cytochrome c as an electron shuttle between the outer and inner mitochondrial membranes, *J Biol Chem* **256,** 7187-7192.

22. Tuominen, E. K., Wallace, C. J., and Kinnunen, P. K. (2002) Phospholipid-cytochrome c interaction: evidence for the extended lipid anchorage, *J Biol Chem* **277,** 8822-8826.

23. Zucchi, M. R., Nascimento, O. R., Faljoni-Alario, A., Prieto, T., and Nantes, I. L. (2003) Modulation of cytochrome c spin states by lipid acyl chains: a continuous-wave electron paramagnetic resonance (CW-EPR) study of haem iron, *Biochem J* **370,** 671-678.

24. Ott, M., Robertson, J. D., Gogvadze, V., Zhivotovsky, B., and Orrenius, S. (2002) Cytochrome c release from mitochondria proceeds by a two-step process, *Proc Natl Acad Sci U S A* **99,** 1259-1263.

25. Lehninger, A. L., Carafoli, E., and Rossi, C. S. (1967) Energy-linked ion movements in mitochondrial systems, *Adv. Enzymol. Relat Areas Mol Biol.* **29,** 259-320.

26. Hunter, D. R., Haworth, R. A., and Southard, J. H. (1976) Relationship between configuration, function, and permeability in calcium-treated mitochondria, *J Biol Chem* **251,** 5069-5077.

27. Haworth, R. A. and Hunter, D. R. (1979) The Ca2+-induced membrane transition in mitochondria. II. Nature of the Ca2+ trigger site, *Arch Biochem Biophys* **195,** 460-467.

28. Crompton, M. and Costi, A. (1990) A heart mitochondrial Ca2(+)-dependent pore of possible relevance to re-perfusion-induced injury. Evidence that ADP facilitates pore interconversion between the closed and open states, *Biochem J* **266,** 33-39.

29. Crompton, M., Virji, S., and Ward, J. M. (1998) Cyclophilin-D binds strongly to complexes of the voltage-dependent anion channel and the adenine nucleotide translocase to form the permeability transition pore, *Eur J Biochem.* **258,** 729-735.

30. Brustovetsky, N. and Klingenberg, M. (1996) Mitochondrial ADP/ATP carrier can be reversibly converted into a large channel by Ca2+, *Biochemistry.* **35,** 8483-8488.

31. Crompton, M. (2000) Mitochondrial intermembrane junctional complexes and their role in cell death, *J Physiol* **529** *Pt* **1,** 11-21.

32. Kokoszka, J. E., Waymire, K. G., Levy, S. E., Sligh, J. E., Cai, J., Jones, D. P., MacGregor, G. R., and Wallace, D. C. (2004) The ADP/ATP translocator is not essential for the mitochondrial permeability transition pore, *Nature* **427,** 461-465.

33. Nicholls, D. G. and Crompton, M. (1980) Mitochondrial calcium transport, *FEBS Lett* **111,** 261-268.

34. McStay, G. P., Clarke, S. J., and Halestrap, A. P. (2002) Role of critical thiol groups on the matrix surface of the adenine nucleotide translocase in the mechanism of the mitochondrial permeability transition pore, *Biochem J* **367,** 541-548.

35. Costantini, P., Belzacq, A. S., Vieira, H. L., Larochette, N., de Pablo, M. A., Zamzami, N., Susin, S. A., Brenner, C., and Kroemer, G. (2000) Oxidation of a critical thiol residue of the adenine nucleotide translocator enforces Bcl-2-independent permeability transition pore opening and apoptosis, *Oncogene* **19,** 307-314.

36. Clarke, S. J., McStay, G. P., and Halestrap, A. P. (2002) Sanglifehrin A acts as a potent inhibitor of the mitochondrial permeability transition and reperfusion injury of the heart by binding to cyclophilin-D at a different site from cyclosporin A, *J Biol Chem* **277,** 34793-34799.

37. Takuma, K., Phuagphong, P., Lee, E., Mori, K., Baba, A., and Matsuda, T. (2001) Anti-apoptotic effect of cGMP in cultured astrocytes: inhibition by cGMP-dependent protein kinase of mitochondrial permeable transition pore, *J Biol Chem* **276,** 48093-48099.

38. Halestrap, A. P., McStay, G. P., and Clarke, S. J. (2002) The permeability transition pore complex: another view, *Biochimie* **84,** 153-166.

39. Novgorodov, S. A., Gudz, T. I., Brierley, G. P., and Pfeiffer, D. R. (1994) Magnesium ion modulates the sensitivity of the mitochondrial permeability transition pore to cyclosporin A and ADP, *Arch Biochem Biophys* **311,** 219-228.

40. Fontaine, E., Ichas, F., and Bernardi, P. (1998) A ubiquinone-binding site regulates the mitochondrial permeability transition pore, *J Biol Chem* **273,** 25734-25740.

41. Walter, L., Nogueira, V., Leverve, X., Heitz, M. P., Bernardi, P., and Fontaine, E. (2000) Three classes of ubiquinone analogs regulate the mitochondrial permeability transition pore through a common site, *J Biol Chem* **275,** 29521-29527.

42. Huang, X., Zhai, D., and Huang, Y. (2001) Dependence of permeability transition pore opening and cytochrome C release from mitochondria on mitochondria energetic status, *Mol Cell Biochem* **224,** 1-7.

43. Isenberg, J. S. and Klaunig, J. E. (2000) Role of the mitochondrial membrane permeability transition (MPT) in rotenone-induced apoptosis in liver cells, *Toxicol. Sci* **53,** 340-351.

44. Chauvin, C., De Oliveira, F., Ronot, X., Mousseau, M., Leverve, X., and Fontaine, E. (2001) Rotenone inhibits the mitochondrial permeability transition-induced cell death in U937 and KB cells, *J Biol Chem* **276,** 41394-41398.

45. Crompton, M. and Costi, A. (1988) Kinetic evidence for a heart mitochondrial pore activated by Ca2+, inorganic phosphate and oxidative stress. A potential mechanism for mitochondrial dysfunction during cellular Ca2+ overload, *Eur. J. Biochem.* **178,** 489-501.

46. Bernardi, P. and Petronilli, V. (1996) The permeability transition pore as a mitochondrial calcium release channel: A critical appraisal, *Journal of Bioenergetics and Biomembranes* **28,** 131-138.

47. Ichas, F., Jouaville, L. S., and Mazat, J. P. (1997) Mitochondria are excitable organelles capable of generating and conveying electrical and calcium signals, *Cell* **89,** 1145-1153.

48. Al Nasser, I. and Crompton, M. (1986) The entrapment of the Ca2+ indicator arsenazo III in the matrix space of rat liver mitochondria by permeabilization and resealing. Na+-dependent and -independent effluxes of Ca2+ in arsenazo III-loaded mitochondria, *Biochem J* **239,** 31-40.

49. Al Nasser, I. and Crompton, M. (1986) The reversible Ca2+-induced permeabilization of rat liver mitochondria, *Biochem J* **239,** 19-29.

50. Crompton, M. (1999) The mitochondrial permeability transition pore and its role in cell death, *Biochem J* **341** *(Pt 2)*, 233-249.

51. Skulachev, V. P. (1996) Why are mitochondria involved in apoptosis? Permeability transition pores and apoptosis as selective mechanisms to eliminate superoxide-producing mitochondria and cell, *FEBS Lett* **397,** 7-10.

52. Zamzami, N. and Kroemer, G. (2001) The mitochondrion in apoptosis: how Pandora's box opens, *Nat Rev Mol Cell Biol.* **2,** 67-71.

53. Wigdal, S. S., Kirkland, R. A., Franklin, J. L., and Haak-Frendscho, M. (2002) Cytochrome c release precedes mitochondrial membrane potential loss in cerebellar granule neuron apoptosis: lack of mitochondrial swelling, *J Neurochem* **82,** 1029-1038.

54. von Ahsen, O., Renken, C., Perkins, G., Kluck, R. M., Bossy-Wetzel, E., and Newmeyer, D. D. (2000) Preservation of mitochondrial structure and function after Bid- or Bax-mediated cytochrome c release, *J Cell Biol* **150,** 1027-1036.

55. Kluck, R. M., Bossy-Wetzel, E., Green, D. R., and Newmeyer, D. D. (1997) The release of cytochrome c from mitochondria: a primary site for Bcl-2 regulation of apoptosis, *Science* **275,** 1132-1136.

56. Shimizu, S. and Tsujimoto, Y. (2000) Proapoptotic BH3-only Bcl-2 family members induce cytochrome c release, but not mitochondrial membrane potential loss, and do not directly modulate voltage-dependent anion channel activity, *Proc Natl Acad Sci U S A* **97,** 577-582.

57. Kim, T. H., Zhao, Y., Barber, M. J., Kuharsky, D. K., and Yin, X. M. (2000) Bid-induced cytochrome c release is mediated by a pathway independent of mitochondrial permeability transition pore and Bax, *J Biol Chem* **275,** 39474-39481.

58. Gogvadze, V., Robertson, J. D., Enoksson, M., Zhivotovsky, B., and Orrenius, S. (2004) Mitochondrial cytochrome c release may occur by volume-dependent mechanisms not involving permeability transition, *Biochem J* **378,** 213-217.

59. Nakagawa, T., Shimizu, S., Watanabe, T., Yamaguchi, O., Otsu, K., Yamagata, H., Inohara, H., Kubo, T., and Tsujimoto, Y. (2005) Cyclophilin D-dependent mitochondrial permeability transition regulates some necrotic but not apoptotic cell death, *Nature* **434,** 652-658.

60. Baines, C. P., Kaiser, R. A., Purcell, N. H., Blair, N. S., Osinska, H., Hambleton, M. A., Brunskill, E. W., Sayen, M. R., Gottlieb, R. A., Dorn, G. W., Robbins, J., and Molkentin, J. D. (2005) Loss of cyclophilin D reveals a critical role for mitochondrial permeability transition in cell death, *Nature* **434,** 658-662.

61. Vyssokikh, M. Y. and Brdiczka, D. (2003) The function of complexes between the outer mitochondrial membrane pore (VDAC) and the adenine nucleotide translocase in regulation of energy metabolism and apoptosis, *Acta Biochim Pol.* **50,** 389-404.

62. Vyssokikh, M., Zorova, L., Zorov, D., Heimlich, G., Jurgensmeier, J., Schreiner, D., and Brdiczka, D. (2004) The intra-mitochondrial cytochrome c distribution varies correlated to the formation of a complex between VDAC and the adenine nucleotide translocase: this affects Bax-dependent cytochrome c release, *Biochim Biophys Acta 1644,* 27-36.

63. Tsujimoto, Y., Cossman, J., Jaffe, E., and Croce, C. M. (1985) Involvement of the bcl-2 gene in human follicular lymphoma, *Science* **228,** 1440-1443.

64. Strasser, A., Connor, L., and Dixit, V. M. (2000) APOPTOSIS SIGNALING, *Annual Review of Biochemistry* **69,** 217-245.

65. Zha, H., Aime-Sempe, C., Sato, T., and Reed, J. C. (1996) Proapoptotic protein Bax heterodimerizes with Bcl-2 and homodimerizes with Bax via a novel domain (BH3) distinct from BH1 and BH2, *J Biol Chem* **271,** 7440-7444.

66. Simonen, M., Keller, H., and Heim, J. (1997) The BH3 domain of Bax is sufficient for interaction of Bax with itself and with other family members and it is required for induction of apoptosis, *Eur J Biochem* **249,** 85-91.

67. Yin, X. M., Oltvai, Z. N., and Korsmeyer, S. J. (1994) BH1 and BH2 domains of Bcl-2 are required for inhibition of apoptosis and heterodimerization with Bax, *Nature* **369,** 321-323.

68. Huang, D. C., Adams, J. M., and Cory, S. (1998) The conserved N-terminal BH4 domain of Bcl-2 homologues is essential for inhibition of apoptosis and interaction with CED-4, *Embo J* **17,** 1029-1039.

69. Rosse, T., Olivier, R., Monney, L., Rager, M., Conus, S., Fellay, I., Jansen, B., and Borner, C. (1998) Bcl-2 prolongs cell survival after Bax-induced release of cytochrome c, *Nature* **391,** 496-499.

70. Oltvai, Z. N., Milliman, C. L., and Korsmeyer, S. J. (1993) Bcl-2 heterodimerizes in vivo with a conserved homolog, Bax, that accelerates programmed cell death, *Cell* **74,** 609-619.

71. Degterev, A., Lugovskoy, A., Cardone, M., Mulley, B., Wagner, G., Mitchison, T., and Yuan, J. (2001) Identification of small-molecule inhibitors of interaction between the BH3 domain and Bcl-xL, *Nat Cell Biol* **3,** 173-182.

72. Korsmeyer, S. J., Shutter, J. R., Veis, D. J., Merry, D. E., and Oltvai, Z. N. (1993) Bcl-2/Bax: a rheostat that regulates an anti-oxidant pathway and cell death, *Semin. Cancer Biol.* **4,** 327-332.

73. Kaufmann, T., Schlipf, S., Sanz, J., Neubert, K., Stein, R., and Borner, C. (2003) Characterization of the signal that directs Bcl-x(L), but not Bcl-**2,** to the mitochondrial outer membrane, *J Cell Biol* **160,** 53-64.

74. Griffiths, G. J., Dubrez, L., Morgan, C. P., Jones, N. A., Whitehouse, J., Corfe, B. M., Dive, C., and Hickman, J. A. (1999) Cell damage-induced conformational changes of the pro-apoptotic protein Bak in vivo precede the onset of apoptosis, *J Cell Biol* **144,** 903-914.

75. Schinzel, A., Kaufmann, T., Schuler, M., Martinalbo, J., Grubb, D., and Borner, C. (2004) Conformational control of Bax localization and apoptotic activity by Pro168, *J Cell Biol* **164,** 1021-1032.

76. Muchmore, S. W., Sattler, M., Liang, H., Meadows, R. P., Harlan, J. E., Yoon, H. S., Nettesheim, D., Chang, B. S., Thompson, C. B., Wong, S. L., Ng, S. L., and Fesik, S. W. (1996) X-ray and NMR structure of human Bcl-xL, an inhibitor of programmed cell death, *Nature* **381,** 335-341.

77. Schendel, S. L., Xie, Z., Montal, M. O., Matsuyama, S., Montal, M., and Reed, J. C. (1997) Channel formation by antiapoptotic protein Bcl-2, *Proc Natl Acad Sci U S A* **94,** 5113-5118.

78. Minn, A. J., Velez, P., Schendel, S. L., Liang, H., Muchmore, S. W., Fesik, S. W., Fill, M., and Thompson, C. B. (1997) Bcl-x(L) forms an ion channel in synthetic lipid membranes, *Nature* **385,** 353-357.

79. Schlesinger, P. H., Gross, A., Yin, X. M., Yamamoto, K., Saito, M., Waksman, G., and Korsmeyer, S. J. (1997) Comparison of the ion channel characteristics of proapoptotic BAX and antiapoptotic BCL-2, *Proc Natl Acad Sci U S A* **94,** 11357-11362.

80. Schendel, S. L., Azimov, R., Pawlowski, K., Godzik, A., Kagan, B. L., and Reed, J. C. (1999) Ion channel activity of the BH3 only Bcl-2 family member, BID, *J Biol Chem* **274,** 21932-21936.

81. Schendel, S. L., Montal, M., and Reed, J. C. (1998) Bcl-2 family proteins as ion-channels, *Cell Death Differ* **5,** 372-380.

82. Nechushtan, A., Smith, C. L., Lamensdorf, I., Yoon, S. H., and Youle, R. J. (2001) Bax and Bak coalesce into novel mitochondria-associated clusters during apoptosis, *J Cell Biol* **153,** 1265-1276.

83. Eskes, R., Antonsson, B., Osen-Sand, A., Montessuit, S., Richter, C., Sadoul, R., Mazzei, G., Nichols, A., and Martinou, J. C. (1998) Bax-induced cytochrome C release from mitochondria is independent of the permeability transition pore but highly dependent on Mg2+ ions, *J Cell Biol* **143,** 217-224.

84. Pavlov, E. V., Priault, M., Pietkiewicz, D., Cheng, E. H., Antonsson, B., Manon, S., Korsmeyer, S. J., Mannella, C. A., and Kinnally, K. W. (2001) A novel, high conductance channel of mitochondria linked to apoptosis in mammalian cells and Bax expression in yeast, *J Cell Biol* **155,** 725-731.

85. Guo, L., Pietkiewicz, D., Pavlov, E. V., Grigoriev, S. M., Kasianowicz, J. J., Dejean, L. M., Korsmeyer, S. J., Antonsson, B., and Kinnally, K. W. (2004) Effects of cytochrome c on the mitochondrial apoptosis-induced channel MAC, *Am J Physiol Cell Physiol* **286,** C1109-C1117.

86. Kuwana, T., Mackey, M. R., Perkins, G., Ellisman, M. H., Latterich, M., Schneiter, R., Green, D. R., and Newmeyer, D. D. (2002) Bid, Bax, and lipids cooperate to form supramolecular openings in the outer mitochondrial membrane, *Cell* **111,** 331-342.

87. Terrones, O., Antonsson, B., Yamaguchi, H., Wang, H. G., Liu, J., Lee, R. M., Herrmann, A., and Basanez, G. (2004) Lipidic Pore Formation by the Concerted Action of Proapoptotic BAX and tBID, *J Biol Chem* **279,** 30081-30091.

88. Dejean, L. M., Martinez-Caballero, S., Guo, L., Hughes, C., Teijido, O., Ducret, T., Ichas, F., Korsmeyer, S. J., Antonsson, B., Jonas, E. A., and Kinnally, K. W. (2005) Oligomeric Bax Is a Component of the Putative Cytochrome c Release Channel MAC, Mitochondrial Apoptosis-induced Channel, *Mol Biol Cell* **16,** 2424-2432.

89. Wei, M. C., Zong, W. X., Cheng, E. H., Lindsten, T., Panoutsakopoulou, V., Ross, A. J., Roth, K. A., MacGregor, G. R., Thompson, C. B., and Korsmeyer, S. J. (2001) Proapoptotic BAX and BAK: a requisite gateway to mitochondrial dysfunction and death, *Science* **292,** 727-730.

90. Zong, W. X., Lindsten, T., Ross, A. J., MacGregor, G. R., and Thompson, C. B. (2001) BH3-only proteins that bind pro-survival Bcl-2 family members fail to induce apoptosis in the absence of Bax and Bak, *Genes Dev* **15,** 1481-1486.

91. Heimlich, G., McKinnon, A. D., Bernardo, K., Brdiczka, D., Reed, J. C., Kain, R., Kronke, M., and Jurgensmeier, J. M. (2004) Bax-induced cytochrome c release from mitochondria depends on alpha-helices-5 and -6, *Biochem J* **378,** 247-255.

92. Chandra, D., Choy, G., Daniel, P. T., and Tang, D. G. (2005) Bax-dependent Regulation of Bak by Voltage-dependent Anion Channel 2, *J Biol Chem* **280,** 19051-19061.

93. Luo, X., Budihardjo, I., Zou, H., Slaughter, C., and Wang, X. (1998) Bid, a Bcl2 interacting protein, mediates cytochrome c release from mitochondria in response to activation of cell surface death receptors, *Cell* **94,** 481-490.

94. Datta, S. R., Dudek, H., Tao, X., Masters, S., Fu, H., Gotoh, Y., and Greenberg, M. E. (1997) Akt phosphorylation of BAD couples survival signals to the cell-intrinsic death machinery, *Cell* **91,** 231-241.

95. Sax, J. K., Fei, P., Murphy, M. E., Bernhard, E., Korsmeyer, S. J., and El Deiry, W. S. (2002) BID regulation by p53 contributes to chemosensitivity, *Nat Cell Biol* **4,** 842-849.

96. Oda, E., Ohki, R., Murasawa, H., Nemoto, J., Shibue, T., Yamashita, T., Tokino, T., Taniguchi, T., and Tanaka, N. (2000) Noxa, a BH3-only member of the Bcl-2 family and candidate mediator of p53-induced apoptosis, *Science* **288,** 1053-1058.

97. Yu, J., Zhang, L., Hwang, P. M., Kinzler, K. W., and Vogelstein, B. (2001) PUMA induces the rapid apoptosis of colorectal cancer cells, *Mol Cell* **7,** 673-682.

98. Nakano, K. and Vousden, K. H. (2001) PUMA, a novel proapoptotic gene, is induced by p**53,** *Mol Cell* **7,** 683-694.

99. Desagher, S., Osen-Sand, A., Nichols, A., Eskes, R., Montessuit, S., Lauper, S., Maundrell, K., Antonsson, B., and Martinou, J. C. (1999) Bid-induced conformational change of Bax is responsible for mitochondrial cytochrome c release during apoptosis, *J Cell Biol* **144,** 891-901.

100. Ruffolo, S. C. and Shore, G. C. (2003) BCL-2 selectively interacts with the BID-induced open conformer of BAK, inhibiting BAK auto-oligomerization, *J Biol Chem* **278,** 25039-25045.

101. Cheng, E. H., Wei, M. C., Weiler, S., Flavell, R. A., Mak, T. W., Lindsten, T., and Korsmeyer, S. J. (2001) BCL-**2,** BCL-X(L) sequester BH3 domain-only molecules preventing BAX- and BAK-mediated mitochondrial apoptosis, *Mol Cell* **8,** 705-711.

102. Wei, M. C., Lindsten, T., Mootha, V. K., Weiler, S., Gross, A., Ashiya, M., Thompson, C. B., and Korsmeyer, S. J. (2000) tBID, a membrane-targeted death ligand, oligomerizes BAK to release cytochrome c, *Genes Dev* **14,** 2060-2071.

103. Grinberg, M., Sarig, R., Zaltsman, Y., Frumkin, D., Grammatikakis, N., Reuveny, E., and Gross, A. (2002) tBID Homooligomerizes in the mitochondrial membrane to induce apoptosis, *J Biol Chem* **277,** 12237-12245.

104. Terradillos, O., Montessuit, S., Huang, D. C., and Martinou, J. C. (2002) Direct addition of BimL to mitochondria does not lead to cytochrome c release, *FEBS Lett* **522,** 29-34.

105. Letai, A., Bassik, M. C., Walensky, L. D., Sorcinelli, M. D., Weiler, S., and Korsmeyer, S. J. (2002) Distinct BH3 domains either sensitize or activate mitochondrial apoptosis, serving as prototype cancer therapeutics, *Cancer Cell* **2,** 183-192.

106. Moreau, C., Cartron, P. F., Hunt, A., Meflah, K., Green, D. R., Evan, G., Vallette, F. M., and Juin, P. (2003) Minimal BH3 peptides promote cell death by antagonizing anti-apoptotic proteins, *J Biol Chem* **278,** 19426-19435.

107. Kuwana, T., Bouchier-Hayes, L., Chipuk, J. E., Bonzon, C., Sullivan, B. A., Green, D. R., and Newmeyer, D. D. (2005) BH3 domains of BH3-only proteins differentially regulate Bax-mediated mitochondrial membrane permeabilization both directly and indirectly, *Mol Cell* **17,** 525-535.

108. Sugiyama, T., Shimizu, S., Matsuoka, Y., Yoneda, Y., and Tsujimoto, Y. (2002) Activation of mitochondrial voltage-dependent anion channel by apro-apoptotic BH3-only protein Bim, *Oncogene* **21,** 4944-4956.

109. Capano, M. and Crompton, M. (2002) Biphasic translocation of Bax to mitochondria, *Biochem J* **367,** 169-178.

110. Shimizu, S., Matsuoka, Y., Shinohara, Y., Yoneda, Y., and Tsujimoto, Y. (2001) Essential role of voltage-dependent anion channel in various forms of apoptosis in mammalian cells, *J Cell Biol* **152,** 237-250.

111. Rostovtseva, T. K., Antonsson, B., Suzuki, M., Youle, R. J., Colombini, M., and Bezrukov, S. M. (2004) Bid, but not Bax, regulates VDAC channels, *J Biol Chem* **279,** 13575-13583.

112. Cheng, E. H., Sheiko, T. V., Fisher, J. K., Craigen, W. J., and Korsmeyer, S. J. (2003) VDAC2 inhibits BAK activation and mitochondrial apoptosis, *Science* **301,** 513-517.

113. Vyssokikh, M. Y., Katz, A., Rueck, A., Wuensch, C., Dorner, A., Zorov, D. B., and Brdiczka, D. (2001) Adenine nucleotide translocator isoforms 1 and 2 are differently distributed in the mitochondrial inner membrane and have distinct affinities to cyclophilin D, *Biochem J* **358,** 349-358.

114. Bauer, M. K., Schubert, A., Rocks, O., and Grimm, S. (1999) Adenine nucleotide translocase-1, a component of the permeability transition pore, can dominantly induce apoptosis, *J Cell Biol* **147,** 1493-1502.

115. Machida, K., Hayashi, Y., and Osada, H. (2002) A novel adenine nucleotide translocase inhibitor, MT-21, induces cytochrome c release by a mitochondrial permeability transition-independent mechanism, *J Biol Chem* **277,** 31243-31248.

116. De Giorgi, F., Lartigue, L., Bauer, M. K., Schubert, A., Grimm, S., Hanson, G. T., Remington, S. J., Youle, R. J., and Ichas, F. (2002) The permeability transition pore signals apoptosis by directing Bax translocation and multimerization, *Faseb J* **16,** 607-609.

117. Hardie, D. G. and Carling, D. (1997) The AMP-activated protein kinase--fuel gauge of the mammalian cell?, *Eur. J. Biochem.* **246,** 259-273.

118. Capano, M. and Crompton, M. (2006) Bax translocates to mitochondria of heart cells during simulated ischaemia: involvement of AMP-activated and p38 mitogen-activated protein kinases, *Biochem. J.* **395,** 57-64.

119. Narita, M., Shimizu, S., Ito, T., Chittenden, T., Lutz, R. J., Matsuda, H., and Tsujimoto, Y. (1998) Bax interacts with the permeability transition pore to induce permeability transition and cytochrome c release in isolated mitochondria, *Proc Natl Acad Sci U S A* **95,** 14681-14686.

120. Pastorino, J. G., Tafani, M., Rothman, R. J., Marcinkeviciute, A., Hoek, J. B., and Farber, J. L. (1999) Functional consequences of the sustained or transient activation by Bax of the mitochondrial permeability transition pore, *J Biol Chem* **274,** 31734-31739.

121. Pastorino, J. G., Chen, S. T., Tafani, M., Snyder, J. W., and Farber, J. L. (1998) The overexpression of Bax produces cell death upon induction of the mitochondrial permeability transition, *J Biol Chem* **273,** 7770-7775.

122. Wieckowski, M. R., Vyssokikh, M., Dymkowska, D., Antonsson, B., Brdiczka, D., and Wojtczak, L. (2001) Oligomeric C-terminal truncated Bax preferentially releases cytochrome c but not adenylate kinase from mitochondria, outer membrane vesicles and proteoliposomes, *FEBS Lett* **505,** 453-459.

123. Zamzami, N., El Hamel, C., Maisse, C., Brenner, C., Munoz-Pinedo, C., Belzacq, A. S., Costantini, P., Vieira, H., Loeffler, M., Molle, G., and Kroemer, G. (2000) Bid acts on the permeability transition pore complex to induce apoptosis, *Oncogene* **19,** 6342-6350.

124. Wang, K., Yin, X. M., Chao, D. T., Milliman, C. L., and Korsmeyer, S. J. (1996) BID: a novel BH3 domain-only death agonist, *Genes Dev* **10,** 2859-2869.

125. Chou, J. J., Li, H., Salvesen, G. S., Yuan, J., and Wagner, G. (1999) Solution structure of BID, an intracellular amplifier of apoptotic signaling, *Cell* **96,** 615-624.

126. Esposti, M. D. (2002) The roles of Bid, *Apoptosis* **7,** 433-440.

127. Krajewska, M., Zapata, J. M., Meinhold-Heerlein, I., Hedayat, H., Monks, A., Bettendorf, H., Shabaik, A., Bubendorf, L., Kallioniemi, O. P., Kim, H., Reifenberger, G., Reed, J. C., and Krajewski, S. (2002) Expression of Bcl-2 family member Bid in normal and malignant tissues, *Neoplasia* **4,** 129-140.

128. Footz, T. K., Birren, B., Minoshima, S., Asakawa, S., Shimizu, N., Riazi, M. A., and McDermid, H. E. (1998) The gene for death agonist BID maps to the region of human 22q11.2 duplicated in cat eye syndrome chromosomes and to mouse chromosome 6, *Genomics.* **51,** 472-475.

129. Lee, J. H., Soung, Y. H., Lee, J. W., Park, W. S., Kim, S. Y., Cho, Y. G., Kim, C. J., Seo, S. H., Kim, H. S., Nam, S. W., Yoo, N. J., Lee, S. H., and Lee, J. Y. (2004) Inactivating mutation of the pro-apoptotic gene BID in gastric cancer, *J Pathol.* **202,** 439-445.

130. Li, H., Zhu, H., Xu, C. J., and Yuan, J. (1998) Cleavage of BID by caspase 8 mediates the mitochondrial damage in the Fas pathway of apoptosis, *Cell* **94,** 491-501.

131. Esposti, M. D., Erler, J. T., Hickman, J. A., and Dive, C. (2001) Bid, a widely expressed proapoptotic protein of the Bcl-2 family, displays lipid transfer activity, *Mol Cell Biol* **21,** 7268-7276.

132. Tafani, M., Karpinich, N. O., Hurster, K. A., Pastorino, J. G., Schneider, T., Russo, M. A., and Farber, J. L. (2002) Cytochrome c release upon Fas receptor activation depends on translocation of full-length bid and the induction of the mitochondrial permeability transition, *J Biol Chem* **277,** 10073-10082.

133. Zha, J., Weiler, S., Oh, K. J., Wei, M. C., and Korsmeyer, S. J. (2000) Posttranslational N-myristoylation of BID as a molecular switch for targeting mitochondria and apoptosis, *Science* **290,** 1761-1765.

134. Tan, K. O., Tan, K. M., and Yu, V. C. (1999) A novel BH3-like domain in BID is required for intramolecular interaction and autoinhibition of pro-apoptotic activity, *J Biol Chem* **274,** 23687-23690.

135. Desagher, S., Osen-Sand, A., Montessuit, S., Magnenat, E., Vilbois, F., Hochmann, A., Journot, L., Antonsson, B., and Martinou, J. C. (2001) Phosphorylation of bid by casein kinases I and II regulates its cleavage by caspase 8, *Mol Cell* **8,** 601-611.

136. McDonnell, J. M., Fushman, D., Milliman, C. L., Korsmeyer, S. J., and Cowburn, D. (1999) Solution structure of the proapoptotic molecule BID: a structural basis for apoptotic agonists and antagonists, *Cell* **96,** 625-634.

137. Slee, E. A., Keogh, S. A., and Martin, S. J. (2000) Cleavage of BID during cytotoxic drug and UV radiation-induced apoptosis occurs downstream of the point of Bcl-2 action and is catalysed by caspase-3: a potential feedback loop for amplification of apoptosis-associated mitochondrial cytochrome c release, *Cell Death Differ* **7,** 556-565.

138. Valentijn, A. J. and Gilmore, A. P. (2004) Translocation of full-length Bid to mitochondria during anoikis, *J Biol Chem* **279,** 32848-32857.

139. Lutter, M., Perkins, G. A., and Wang, X. (2001) The pro-apoptotic Bcl-2 family member tBid localizes to mitochondrial contact sites, *BMC Cell Biol* **2,** 22.

140. Kim, T. H., Zhao, Y., Ding, W. X., Shin, J. N., He, X., Seo, Y. W., Chen, J., Rabinowich, H., Amoscato, A. A., and Yin, X. M. (2004) Bid-cardiolipin interaction at mitochondrial contact site contributes to mitochondrial cristae reorganization and cytochrome C release, *Mol Biol Cell* **15,** 3061-3072.

141. Hu, X., Han, Z., Wyche, J. H., and Hendrickson, E. A. (2003) Helix 6 of tBid is necessary but not sufficient for mitochondrial binding activity, *Apoptosis* **8,** 277-289.

142. Liu, J., Durrant, D., Yang, H. S., He, Y., Whitby, F. G., Myszka, D. G., and Lee, R. M. (2005) The interaction between tBid and cardiolipin or monolysocardiolipin, *Biochem Biophys Res Commun* **330,** 865-870.

143. Yan, L., Miao, Q., Sun, Y., and Yang, F. (2003) tBid forms a pore in the liposome membrane, *FEBS Lett* **555,** 545-550.

144. Gong, X. M., Choi, J., Franzin, C. M., Zhai, D., Reed, J. C., and Marassi, F. M. (2004) Conformation of Membrane-associated Proapoptotic tBid, *J Biol Chem* **279,** 28954-28960.

145. Oh, K. J., Barbuto, S., Meyer, N., Kim, R. S., Collier, R. J., and Korsmeyer, S. J. (2005) Conformational Changes in BID, a Pro-apoptotic BCL-2 Family Member, upon Membrane Binding: A SITE-DIRECTED SPIN LABELING STUDY, *J Biol Chem* **280,** 753-767.

146. Degli Esposti, M. (2002) Sequence and functional similarities between pro-apoptotic Bid and plant lipid transfer proteins, *Biochim Biophys Acta* **1553,** 331-340.

147. Goonesinghe, A., Mundy, E. S., Smith, M., Khosravi-Far, R., Martinou, J. C., and Esposti, M. D. (2005) Pro-apoptotic Bid induces membrane perturbation by inserting selected lysolipids into the bilayer, *Biochem J* **387,** 109-118.

148. Handschumacher, R. E., Harding, M. W., Rice, J., Drugge, R. J., and Speicher, D. W. (1984) Cyclophilin: a specific cytosolic binding protein for cyclosporin A, *Science.* **226,** 544-547.

149. Fischer, G., Bang, H., and Mech, C. (1984) [Determination of enzymatic catalysis for the cis-trans-isomerization of peptide binding in proline-containing peptides], *Biomed. Biochim Acta.* **43,** 1101-1111.

150. Galat, A. (1999) Variations of sequences and amino acid compositions of proteins that sustain their biological functions: An analysis of the cyclophilin family of proteins, *Arch. Biochem. Biophys.* **371,** 149-162.

151. Yao, Q., Li, M., Yang, H., Chai, H., Fisher, W., and Chen, C. (2005) Roles of cyclophilins in cancers and other organ systems, *World J. Surg.* **29,** 276-280.

152. Halestrap, A. P. and Davidson, A. M. (1990) Inhibition of Ca2(+)-induced large-amplitude swelling of liver and heart mitochondria by cyclosporin is probably caused by the inhibitor binding to mitochondrial-matrix peptidyl-prolyl cis-trans isomerase and preventing it interacting with the adenine nucleotide translocase, *Biochem J* **268,** 153-160.

153. McGuinness, O., Yafei, N., Costi, A., and Crompton, M. (1990) The presence of two classes of high-affinity cyclosporin A binding sites in mitochondria. Evidence that the minor component is involved in the opening of an inner-membrane Ca(2+)-dependent pore, *Eur J Biochem* **194,** 671-679.

154. Scorrano, L., Nicolli, A., Basso, E., Petronilli, V., and Bernardi, P. (1997) Two modes of activation of the permeability transition pore: the role of mitochondrial cyclophilin, *Mol Cell Biochem* **174,** 181-184.

155. Lin, D. T. and Lechleiter, J. D. (2002) Mitochondrial targeted cyclophilin D protects cells from cell death by peptidyl prolyl isomerization, *J Biol Chem* **277,** 31134-31141.

156. Schubert, A. and Grimm, S. (2004) Cyclophilin D, a component of the permeability transition-pore, is an apoptosis repressor, *Cancer Res* **64,** 85-93.

157. Li, Y., Johnson, N., Capano, M., Edwards, M., and Crompton, M. (2004) Cyclophilin-D promotes the mitochondrial permeability transition but has opposite effects on apoptosis and necrosis, *Biochem J* **383,** 101-109.

158. Schinzel, A. C., Takeuchi, O., Huang, Z., Fisher, J. K., Zhou, Z., Rubens, J., Hetz, C., Danial, N. N., Moskowitz, M. A., and Korsmeyer, S. J. (2005) Cyclophilin D is a component of mitochondrial permeability transition and mediates neuronal cell death after focal cerebral ischemia, *Proc Natl Acad Sci U S A* **102,** 12005-12010.

159. Pappenberger, G., Bachmann, A., Muller, R., Aygun, H., Engels, J. W., and Kiefhaber, T. (2003) Kinetic mechanism and catalysis of a native-state prolyl isomerization reaction, *J Mol Biol* **326,** 235-246.

160. O'Neal, K. D., Chari, M. V., McDonald, C. H., Cook, R. G., Yu-Lee, L. Y., Morrisett, J. D., and Shearer, W. T. (1996) Multiple cis-trans conformers of the prolactin receptor proline-rich motif (PRM) peptide detected by reverse-phase HPLC, CD and NMR spectroscopy, *Biochem J 315 (Pt 3)*, 833-844.

161. Johnson, V. G., Nicholls, P. J., Habig, W. H., and Youle, R. J. (1993) The role of proline 345 in diphtheria toxin translocation, *J Biol Chem* **268,** 3514-3519.

162. Borel, J. F. (1989) Pharmacology of cyclosporin (Sandimmune). Pharmacological properties *in vivo Pharmacol.Rev.* **41,** pp 259-371

163. Wang, M. Z., Shetty, J. T., Howard, B. A., Campa, M. J., Patz, E. F., Jr., and Fitzgerald, M. C. (2004) Thermodynamic analysis of cyclosporin a binding to cyclophilin a in a lung tumor tissue lysate, *Anal Chem* **76,** 4343-4348.

164. Waldmeier, P. C., Zimmermann, K., Qian, T., Tintelnot-Blomley, M., and Lemasters, J. J. (2003) Cyclophilin D as a drug target, *Curr Med Chem* **10,** 1485-1506.

165. Crompton, M., Ellinger, H., and Costi, A. (1988) Inhibition by cyclosporin A of a Ca2+-dependent pore in heart mitochondria activated by inorganic phosphate and oxidative stress, *Biochem J.* **255,** 357-360.

166. Woodfield, K., Ruck, A., Brdiczka, D., and Halestrap, A. P. (1998) Direct demonstration of a specific interaction between cyclophilin-D and the adenine nucleotide translocase confirms their role in the mitochondrial permeability transition, *Biochem J.* **336,** 287-290.

167. Krauskopf, A., Lhote, P., Mutter, M., Dufour, J. F., Ruegg, U. T., and Buetler, T. M. (2003) Vasopressin type 1A receptor up-regulation by cyclosporin A in vascular smooth muscle cells is mediated by superoxide, *J Biol Chem* **278,** 41685-41690.

168. Kimchi-Sarfaty, C., Kasir, J., Ambudkar, S. V., and Rahamimoff, H. (2002) Transport activity and surface expression of the Na+-Ca2+ exchanger NCX1 are inhibited by the immunosuppressive agent cyclosporin A and by the nonimmunosuppressive agent PSC**833,** *J Biol Chem* **277,** 2505-2510.

169. Montero, M., Lobaton, C. D., Gutierrez-Fernandez, S., Moreno, A., and Alvarez, J. (2004) Calcineurin-independent inhibition of mitochondrial Ca2+ uptake by cyclosporin A, *Br. J Pharmacol.* **141,** 263-268.

170. Smaili, S. S., Stellato, K. A., Burnett, P., Thomas, A. P., and Gaspers, L. D. (2001) Cyclosporin A inhibits inositol **1,4,**5-trisphosphate-dependent Ca2+ signals by enhancing Ca2+ uptake into the endoplasmic reticulum and mitochondria, *J Biol Chem* **276,** 23329-23340.

171. Zhong, Z., Li, X., Yamashina, S., von Frankenberg, M., Enomoto, N., Ikejima, K., Kolinsky, M., Raleigh, J. A., and Thurman, R. G. (2001) Cyclosporin A causes a hypermetabolic state and hypoxia in the liver: prevention by dietary glycine, *J Pharmacol. Exp Ther.* **299,** 858-865.

172. Hokanson, J. F., Mercier, J. G., and Brooks, G. A. (1995) Cyclosporine A decreases rat skeletal muscle mitochondrial respiration in vitro, *Am J Respir. Crit Care Med* **151,** 1848-1851.

173. Winegar, D. A., Salisbury, J. A., Sundseth, S. S., and Hawke, R. L. (1996) Effects of cyclosporin on cholesterol 27-hydroxylation and LDL receptor activity in HepG2 cells, *J Lipid Res* **37,** 179-191.

174. Princen, H. M., Meijer, P., Wolthers, B. G., Vonk, R. J., and Kuipers, F. (1991) Cyclosporin A blocks bile acid synthesis in cultured hepatocytes by specific inhibition of chenodeoxycholic acid synthesis, *Biochem J* **275,** 501-505.

175. Dahlback-Sjoberg, H., Bjorkhem, I., and Princen, H. M. (1993) Selective inhibition of mitochondrial 27-hydroxylation of bile acid intermediates and 25-hydroxylation of vitamin D3 by cyclosporin A, *Biochem J* **293,** 203-206.

176. Wu, J., Zhu, Y. H., and Patel, S. B. (1999) Cyclosporin-induced dyslipoproteinemia is associated with selective activation of SREBP-2, *Am J Physiol* **277,** E1087-E1094.

177. Epand, R. M., Epand, R. F., and McKenzie, R. C. (1987) Effects of viral chemotherapeutic agents on membrane properties. Studies of cyclosporin A, benzyloxycarbonyl-D-Phe-L-Phe-Gly and amantadine, *J Biol Chem* **262,** 1526-1529.

178. Matsuda, S. and Koyasu, S. (2000) Mechanisms of action of cyclosporine, *Immunopharmacology* **47,** 119-125.

179. Jurgensmeier, J. M., Xie, Z., Deveraux, Q., Ellerby, L., Bredesen, D., and Reed, J. C. (1998) Bax directly induces release of cytochrome c from isolated mitochondria, *Proc Natl Acad Sci U S A* **95,** 4997-5002.

180. Hales, K. G. and Fuller, M. T. (1997) Developmentally regulated mitochondrial fusion mediated by a conserved, novel, predicted GTPase, *Cell* **90,** 121-129.

181. Hermann, G. J., Thatcher, J. W., Mills, J. P., Hales, K. G., Fuller, M. T., Nunnari, J., and Shaw, J. M. (1998) Mitochondrial fusion in yeast requires the transmembrane GTPase Fzo1p, *J Cell Biol* **143,** 359-373.

182. Sesaki, H. and Jensen, R. E. (2001) UGO1 encodes an outer membrane protein required for mitochondrial fusion, *J Cell Biol* **152,** 1123-1134.

183. Wong, E. D., Wagner, J. A., Scott, S. V., Okreglak, V., Holewinske, T. J., Cassidy-Stone, A., and Nunnari, J. (2003) The intramitochondrial dynamin-related GTPase, Mgm1p, is a component of a protein complex that mediates mitochondrial fusion, *J Cell Biol* **160,** 303-311.

184. Chen, H., Detmer, S. A., Ewald, A. J., Griffin, E. E., Fraser, S. E., and Chan, D. C. (2003) Mitofusins Mfn1 and Mfn2 coordinately regulate mitochondrial fusion and are essential for embryonic development, *J Cell Biol* **160,** 189-200.

185. Shaw, J. M. and Nunnari, J. (2002) Mitochondrial dynamics and division in budding yeast, *Trends Cell Biol* **12,** 178-184.

186. Smirnova, E., Griparic, L., Shurland, D. L., and van der Bliek, A. M. (2001) Dynamin-related protein Drp1 is required for mitochondrial division in mammalian cells, *Mol Biol Cell* **12,** 2245-2256.

187. Hinshaw, J. E. (2000) Dynamin and its role in membrane fission, *Annu Rev Cell Dev Biol* **16,** 483-519.

188. Stowell, M. H., Marks, B., Wigge, P., and McMahon, H. T. (1999) Nucleotide-dependent conformational changes in dynamin: evidence for a mechanochemical molecular spring, *Nat Cell Biol* **1,** 27-32.

189. Sweitzer, S. M. and Hinshaw, J. E. (1998) Dynamin undergoes a GTP-dependent conformational change causing vesiculation, *Cell* **93,** 1021-1029.

190. Enriquez, J. A., Cabezas-Herrera, J., Bayona-Bafaluy, M. P., and Attardi, G. (2000) Very rare complementation between mitochondria carrying different mitochondrial DNA mutations points

to intrinsic genetic autonomy of the organelles in cultured human cells, *J Biol Chem* **275,** 11207-11215.

191. Frank, S., Gaume, B., Bergmann-Leitner, E. S., Leitner, W. W., Robert, E. G., Catez, F., Smith, C. L., and Youle, R. J. (2001) The role of dynamin-related protein 1, a mediator of mitochondrial fission, in apoptosis, *Dev Cell* **1,** 515-525.

192. Karbowski, M., Arnoult, D., Chen, H., Chan, D. C., Smith, C. L., and Youle, R. J. (2004) Quantitation of mitochondrial dynamics by photolabeling of individual organelles shows that mitochondrial fusion is blocked during the Bax activation phase of apoptosis, *J Cell Biol* **164,** 493-499.

193. Breckenridge, D. G., Stojanovic, M., Marcellus, R. C., and Shore, G. C. (2003) Caspase cleavage product of BAP31 induces mitochondrial fission through endoplasmic reticulum calcium signals, enhancing cytochrome c release to the cytosol, *J Cell Biol* **160,** 1115-1127.

194. Karbowski, M., Lee, Y. J., Gaume, B., Jeong, S. Y., Frank, S., Nechushtan, A., Santel, A., Fuller, M., Smith, C. L., and Youle, R. J. (2002) Spatial and temporal association of Bax with mitochondrial fission sites, Drp**1,** and Mfn2 during apoptosis, *J Cell Biol* **159,** 931-938.

195. Basanez, G. (2002) Membrane fusion: the process and its energy suppliers, *Cell Mol Life Sci* **59,** 1478-1490.

196. Scorrano, L. (2003) Divide et impera: Ca2+ signals, mitochondrial fission and sensitization to apoptosis, *Cell Death Differ* **10,** 1287-1289.

197. Amutha, B., Gordon, D. M., Gu, Y., and Pain, D. (2004) A novel role of Mgm1p, a dynamin-related GTPase, in ATP synthase assembly and cristae formation/maintenance, *Biochem J* **381,** 19-23.

198. Galigniana, M. D., Morishima, Y., Gallay, P. A., and Pratt, W. B. (2004) Cyclophilin-A is bound through its peptidylprolyl isomerase domain to the cytoplasmic dynein motor protein complex, *J Biol Chem* **279,** 55754-55759.

199. Tchaicheeyan, O. (2004) Is peptide bond cis/trans isomerization a key stage in the chemo-mechanical cycle of motor proteins?, *Faseb J* **18,** 783-789.

200. Simmen, T., Aslan, J. E., Blagoveshchenskaya, A. D., Thomas, L., Wan, L., Xiang, Y., Feliciangeli, S. F., Hung, C. H., Crump, C. M., and Thomas, G. (2005) PACS-2 controls endoplasmic reticulum-mitochondria communication and Bid-mediated apoptosis, *Embo J* **24,** 717-729.

201. Watabe, M. and Nakaki, T. (2004) Rotenone induces apoptosis via activation of bad in human dopaminergic SH-SY5Y cells, *J Pharmacol. Exp Ther.* **311,** 948-953.

202. Springer, J. E., Azbill, R. D., Nottingham, S. A., and Kennedy, S. E. (2000) Calcineurin-mediated BAD dephosphorylation activates the caspase-3 apoptotic cascade in traumatic spinal cord injury, *J Neurosci* **20,** 7246-7251.

203. Lewis, S., Bethell, S. S., Patel, S., Martinou, J. C., and Antonsson, B. (1998) Purification and biochemical properties of soluble recombinant human Bax, *Protein Expr Purif* **13,** 120-126.

204. Bradford, A. P. and Yedman, S. J. (1986) *Advances in Protein Phosphatase* **3,** pp 73-106

205. Sarrouilhe, D. and Baudry, M. (1996) Evidence of true protein kinase CKII activity in mitochondria and its spermine-mediated translocation to inner membrane, *Cell Mol Biol (Noisy. -le-grand)* **42,** 189-197.

206. Henriksson, T. and Jergil, B. (1979) Protein kinase activity and endogenous phosphorylation in subfractions of rat liver mitochondria, *Biochim Biophys Acta* **588,** 380-391.

207. Kitagawa, Y. and Racker, E. (1982) Purification and characterization of two protein kinases from bovine heart mitochondrial membrane, *J Biol Chem* **257,** 4547-4551.

208. Schwoch, G., Trinczek, B., and Bode, C. (1990) Localization of catalytic and regulatory subunits of cyclic AMP-dependent protein kinases in mitochondria from various rat tissues, *Biochem J* **270,** 181-188.

209. Technikova-Dobrova, Z., Sardanelli, A. M., Speranza, F., Scacco, S., Signorile, A., Lorusso, V., and Papa, S. (2001) Cyclic adenosine monophosphate-dependent phosphorylation of mammalian mitochondrial proteins: enzyme and substrate characterization and functional role, *Biochemistry* **40,** 13941-13947.

210. Verdanis, A. (1977) Protein kinase activity at the inner membrane of mammalian mitochondria, *J Biol Chem* **252,** 807-813.

211. Signorile, A., Sardanelli, A. M., Nuzzi, R., and Papa, S. (2002) Serine (threonine) phosphatase(s) acting on cAMP-dependent phosphoproteins in mammalian mitochondria, *FEBS Lett* **512,** 91-94.

212. Papa, S., Sardanelli, A. M., Scacco, S., and Technikova-Dobrova, Z. (1999) cAMP-dependent protein kinase and phosphoproteins in mammalian mitochondria. An extension of the cAMP-mediated intracellular signal transduction, *FEBS Lett* **444,** 245-249.

213. Sardanelli, A. M., Technikova-Dobrova, Z., Speranza, F., Mazzocca, A., Scacco, S., and Papa, S. (1996) Topology of the mitochondrial cAMP-dependent protein kinase and its substrates, *FEBS Lett* **396,** 276-278.

214. Azarashvili, T. S., Tyynela, J., Odinokova, I. V., Grigorjev, P. A., Baumann, M., Evtodienko, Y. V., and Saris, N. E. (2002) Phosphorylation of a peptide related to subunit c of the F0F1-ATPase/ATP synthase and relationship to permeability transition pore opening in mitochondria, *J Bioenerg. Biomembr.* **34,** 279-284.

215. Azarashvili, T., Krestinina, O., Odinokova, I., Evtodienko, Y., and Reiser, G. (2003) Physiological Ca2+ level and Ca2+-induced Permeability Transition Pore control protein phosphorylation in rat brain mitochondria, *Cell Calcium* **34,** 253-259.

216. Sanger, F., Nicklen, S., and Coulson, A. R. (1992) DNA sequencing with chain-terminating inhibitors. **1977,** *Biotechnology 24:104-8.*, 104-108.

217. Ruiz-Martinez, M. C., Berka, J., Belenkii, A., Foret, F., Miller, A. W., and Karger, B. L. (1993) DNA sequencing by capillary electrophoresis with replaceable linear polyacrylamide and laser-induced fluorescence detection, *Anal Chem* **65,** 2851-2858.

218. Laemmli, U. K. (1970) Cleavage of structural proteins during the assembly of the head of bacteriophage T4, *Nature* **227,** 680-685.

219. Kroger, A. and Klingenberg, M. (1966) On the role of ubiquinone in mitochondria. II. Redox reactions of ubiquinone under the control of oxidative phosphorylation, *Biochem Z* **344,** 317-336.

220. Harrington, C. R. (1990) Lowry protein assay containing sodium dodecyl sulfate in microtiter plates for protein determinations on fractions from brain tissue, *Anal Biochem* **186,** 285-287.

221. Folin, O. and Ciocalteu, V. (1927) On tyrosine and tryptophane determinations in proteins, *J. Biol. Chem.* **73,** 627-650.

222. Pedersen, P. L., Greenawalt, J. W., Reynafarje, B., Hullihen, J., Decker, G. L., Soper, J. W., and Bustamente, E. (1978) Preparation and characterization of mitochondria and submitochondrial particles of rat liver and liver-derived tissues, *Methods Cell Biol* **20**, 411-481.

223. Gordon, J. A. (1991) Use of vanadate as protein-phosphotyrosine phosphatase inhibitor, *Methods Enzymol.* **201**, 477-482.

224. Tanveer, A., Virji, S., Andreeva, L., Totty, N. F., Hsuan, J. J., Ward, J. M., and Crompton, M. (1996) Involvement of cyclophilin D in the activation of a mitochondrial pore by Ca2+ and oxidant stress, *Eur. J. Biochem.* **238,** 166-172.

225. Kamo, N., Muratsugu, M., Hongoh, R., and Kobatake, Y. (1979) Membrane potential of mitochondria measured with an electrode sensitive to tetraphenyl phosphonium and relationship between proton electrochemical potential and phosphorylation potential in steady state, *J. Membr. Biol.* **49,** 105-121.

226. Kofron, J. L., Kuzmic, P., Kishore, V., Colon-Bonilla, E., and Rich, D. H. (1991) Determination of kinetic constants for peptidyl prolyl cis-trans isomerases by an improved spectrophotometric assay, *Biochemistry.* **30,** 6127-6134.

227. O'Donohue, M. F., Burgess, A. W., Walkinshaw, M. D., and Treutlein, H. R. (1995) Modeling conformational changes in cyclosporin A, *Protein Sci* **4,** 2191-2202.

228. Zeder-Lutz, G., Wenger, R., Van Regenmortel, M. H., and Altschuh, D. (1993) Interaction of cyclosporin A with an Fab fragment or cyclophilin. Affinity measurements and time-dependent changes in binding, *FEBS Lett* **326,** 153-157.

229. Kozak, M. (1991) An analysis of vertebrate mRNA sequences: intimations of translational control, *J Cell Biol* **115,** 887-903.

230. Hernan, R., Heuermann, K., and Brizzard, B. (2000) Multiple epitope tagging of expressed proteins for enhanced detection, *Biotechniques* **28,** 789-793.

231. Johnson, N., Khan, A., Virji, S., Ward, J. M., and Crompton, M. (1999) Import and processing of heart mitochondrial cyclophilin D, *Eur J Biochem* **263,** 353-359.

232. Mertell, A. E. and Smith, R. M. (1975) Critical Stability Constants

233. Roucou, X., Montessuit, S., Antonsson, B., and Martinou, J. C. (2002) Bax oligomerization in mitochondrial membranes requires tBid (caspase-8-cleaved Bid) and a mitochondrial protein, *Biochem J* **368,** 915-921.

234. Roucou, X., Rostovtseva, T., Montessuit, S., Martinou, J. C., and Antonsson, B. (2002) Bid induces cytochrome c-impermeable Bax channels in liposomes, *Biochem J* **363,** 547-552.

235. Makalowski, W., Zhang, J., and Boguski, M. S. (1996) Comparative analysis of 1196 orthologous mouse and human full-length mRNA and protein sequences, *Genome Res* **6,** 846-857.

236. Thompson, J. D., Higgins, D. G., and Gibson, T. J. (1994) CLUSTAL W: improving the sensitivity of progressive multiple sequence alignment through sequence weighting, position-specific gap penalties and weight matrix choice, *Nucleic Acids Res* **22,** 4673-4680.

237. Esposti, M. D., Cristea, I. M., Gaskell, S. J., Nakao, Y., and Dive, C. (2003) Proapoptotic Bid binds to monolysocardiolipin, a new molecular connection between mitochondrial membranes and cell death, *Cell Death Differ* **10,** 1300-1309.

238. Kudla, G., Montessuit, S., Eskes, R., Berrier, C., Martinou, J. C., Ghazi, A., and Antonsson, B. (2000) The destabilization of lipid membranes induced by the C-terminal fragment of caspase 8-cleaved bid is inhibited by the N-terminal fragment, *J Biol Chem* **275,** 22713-22718.

239. Kaufmann, E., Geisler, N., and Weber, K. (1984) SDS-PAGE strongly overestimates the molecular masses of the neurofilament proteins, *FEBS Lett* **170,** 81-84.

240. Wang, X. (2001) The expanding role of mitochondria in apoptosis, *Genes Dev* **15,** 2922-2933.

241. Appaix, F., Minatchy, M., Riva-Lavieille, C., Olivares, J., Antonsson, B., and Saks, V. A. (2000) Rapid spectrophotometric method for quantitation of cytochrome c release from isolated mitochondria or permeabilized cells revisited, *Biochim Biophys Acta 1***457,** 175-181.

242. Zhai, D., Huang, X., Han, X., and Yang, F. (2000) Characterization of tBid-induced cytochrome c release from mitochondria and liposomes, *FEBS Lett* **472,** 293-296.

243. Arnoult, D., Parone, P., Martinou, J. C., Antonsson, B., Estaquier, J., and Ameisen, J. C. (2002) Mitochondrial release of apoptosis-inducing factor occurs downstream of cytochrome c release in response to several proapoptotic stimuli, *J Cell Biol* **159,** 923-929.

244. Eliseev, R. A., Salter, J. D., Gunter, K. K., and Gunter, T. E. (2003) Bcl-2 and tBid proteins counter-regulate mitochondrial potassium transport, *Biochim Biophys Acta 1***604,** 1-5.

245. Kluck, R. M., Esposti, M. D., Perkins, G., Renken, C., Kuwana, T., Bossy-Wetzel, E., Goldberg, M., Allen, T., Barber, M. J., Green, D. R., and Newmeyer, D. D. (1999) The pro-apoptotic proteins, Bid and Bax, cause a limited permeabilization of the mitochondrial outer membrane that is enhanced by cytosol, *J Cell Biol* **147,** 809-822.

246. Rodrigues, C. M., Sola, S., Sharpe, J. C., Moura, J. J., and Steer, C. J. (2003) Tauroursodeoxycholic acid prevents Bax-induced membrane perturbation and cytochrome C release in isolated mitochondria, *Biochemistry* **42,** 3070-3080.

247. Polster, B. M., Basanez, G., Young, M., Suzuki, M., and Fiskum, G. (2003) Inhibition of Bax-induced cytochrome c release from neural cell and brain mitochondria by dibucaine and propranolol, *J Neurosci* **23,** 2735-2743.

248. An, J., Chen, Y., and Huang, Z. (2004) Critical upstream signals of cytochrome C release induced by a novel Bcl-2 inhibitor, *J Biol Chem* **279,** 19133-19140.

249. Annis, M. G., Zamzami, N., Zhu, W., Penn, L. Z., Kroemer, G., Leber, B., and Andrews, D. W. (2001) Endoplasmic reticulum localized Bcl-2 prevents apoptosis when redistribution of cytochrome c is a late event, *Oncogene* **20,** 1939-1952.

250. Yamaguchi, H. and Wang, H. G. (2002) Bcl-XL protects BimEL-induced Bax conformational change and cytochrome C release independent of interacting with Bax or BimEL, *J Biol Chem* **277,** 41604-41612.

251. Pastorino, J. G., Shulga, N., and Hoek, J. B. (2002) Mitochondrial binding of hexokinase II inhibits Bax-induced cytochrome c release and apoptosis, *J Biol Chem* **277,** 7610-7618.

252. Liu, J., Weiss, A., Durrant, D., Chi, N. W., and Lee, R. M. (2004) The cardiolipin-binding domain of Bid affects mitochondrial respiration and enhances cytochrome c release, *Apoptosis* **9,** 533-541.

253. Eskes, R., Desagher, S., Antonsson, B., and Martinou, J. C. (2000) Bid induces the oligomerization and insertion of Bax into the outer mitochondrial membrane, *Mol Cell Biol* **20,** 929-935.

254. Boehning, D., Patterson, R. L., Sedaghat, L., Glebova, N. O., Kurosaki, T., and Snyder, S. H. (2003) Cytochrome c binds to inositol (1,4,5) trisphosphate receptors, amplifying calcium-dependent apoptosis, *Nat Cell Biol* ..

255. Iverson, S. L., Enoksson, M., Gogvadze, V., Ott, M., and Orrenius, S. (2004) Cardiolipin Is Not Required for Bax-mediated Cytochrome c Release from Yeast Mitochondria, *J Biol Chem* **279,** 1100-1107.

256. Petrosillo, G., Ruggiero, F. M., Pistolese, M., and Paradies, G. (2004) Ca2+-induced reactive oxygen species production promotes cytochrome c release from rat liver mitochondria via mitochondrial permeability transition (MPT)-dependent and MPT-independent mechanisms: role of cardiolipin, *J Biol Chem* **279,** 53103-53108.

257. Pallotti, F. and Lenaz, G. (2001) Isolation and subfractionation of mitochondria from animal cells and tissue culture lines *Methods Cell Biol* **65,** pp 1-35

258. Madesh, M., Antonsson, B., Srinivasula, S. M., Alnemri, E. S., and Hajnoczky, G. (2002) Rapid kinetics of tBid-induced cytochrome c and Smac/DIABLO release and mitochondrial depolarization, *J Biol Chem* **277,** 5651-5659.

259. Diaz, G. D., Li, Q., and Dashwood, R. H. (2003) Caspase-8 and apoptosis-inducing factor mediate a cytochrome c-independent pathway of apoptosis in human colon cancer cells induced by the dietary phytochemical chlorophyllin, *Cancer Res* **63,** 1254-1261.

260. de Kruijff, B. and Cullis, P. R. (1980) Cytochrome c specifically induces non-bilayer structures in cardiolipin-containing model membranes, *Biochim Biophys Acta* **602,** 477-490.

261. Hirsch, T., Marzo, I., and Kroemer, G. (1997) Role of the mitochondrial permeability transition pore in apoptosis, *Biosci. Rep* **17,** 67-76.

262. Hail, N., Jr. and Lotan, R. (2000) Mitochondrial permeability transition is a central coordinating event in N-(4-hydroxyphenyl)retinamide-induced apoptosis, *Cancer Epidemiol. Biomarkers Prev.* **9,** 1293-1301.

263. Nicotera, P. and Leist, M. (1997) Energy supply and the shape of death in neurons and lymphoid cells, *Cell Death and Differentiation* **4,** 435-442.

264. Crompton, M. (1990) The Role of Ca^{2+} in the Function and Dysfunction of Heart Mitochondria, in *Calcium and the Heart* (Langer, G. A., Ed.) pp 167-198, Raven Press.

265. Rodrigues, C. M., Fan, G., Wong, P. Y., Kren, B. T., and Steer, C. J. (1998) Ursodeoxycholic acid may inhibit deoxycholic acid-induced apoptosis by modulating mitochondrial transmembrane potential and reactive oxygen species production, *Mol Med* **4,** 165-178.

266. Bernardi, P. (1999) Mitochondrial transport of cations: channels, exchangers, and permeability transition, *Physiol Rev* **79,** 1127-1155.

267. Bertrand, R., Solary, E., O'Connor, P., Kohn, K. W., and Pommier, Y. (1994) Induction of a common pathway of apoptosis by staurosporine, *Exp Cell Res* **211,** 314-321.

268. Martinou, J. C., Desagher, S., and Antonsson, B. (2000) Cytochrome c release from mitochondria: all or nothing, *Nat Cell Biol* **2,** E41-E43.

269. Goldstein, J. C., Waterhouse, N. J., Juin, P., Evan, G. I., and Green, D. R. (2000) The coordinate release of cytochrome c during apoptosis is rapid, complete and kinetically invariant, *Nat Cell Biol* **2,** 156-162.

270. Minn, A. J., Kettlun, C. S., Liang, H., Kelekar, A., Vander Heiden, M. G., Chang, B. S., Fesik, S. W., Fill, M., and Thompson, C. B. (1999) Bcl-xL regulates apoptosis by heterodimerization-dependent and -independent mechanisms, *Embo J* **18,** 632-643.

271. Liu, J., Farmer, J. D., Jr., Lane, W. S., Friedman, J., Weissman, I., and Schreiber, S. L. (1991) Calcineurin is a common target of cyclophilin-cyclosporin A and FKBP-FK506 complexes, *Cell* **66,** 807-815.

272. Wang, H. G., Pathan, N., Ethell, I. M., Krajewski, S., Yamaguchi, Y., Shibasaki, F., McKeon, F., Bobo, T., Franke, T. F., and Reed, J. C. (1999) Ca2+-induced apoptosis through calcineurin dephosphorylation of BAD, *Science.* **284,** 339-343.

273. Nicolli, A., Basso, E., Petronilli, V., Wenger, R. M., and Bernardi, P. (1996) Interactions of cyclophilin with the mitochondrial inner membrane and regulation of the permeability transition pore, and cyclosporin A-sensitive channel, *J Biol Chem* **271,** 2185-2192.

274. Henderson, P. J. (1972) A linear equation that describes the steady-state kinetics of enzymes and subcellular particles interacting with tightly bound inhibitors, *Biochem. J.* **127,** 321-333.

275. Zeder-Lutz, G., Van Regenmortel, M. H., Wenger, R., and Altschuh, D. (1994) Interaction of cyclosporin A and two cyclosporin analogs with cyclophilin: relationship between structure and binding, *J. Chromatogr. B Biomed. Appl.* **662,** 301-306.

276. Ismailos, G., Reppas, C., Dressman, J. B., and Macheras, P. (1991) Unusual solubility behaviour of cyclosporin A in aqueous media, *J Pharm. Pharmacol.* **43,** 287-289.

277. Machida, K. and Osada, H. (2003) Molecular interaction between cyclophilin D and adenine nucleotide translocase in cytochrome c release: does it determine whether cytochrome c release is dependent on permeability transition or not?, *Ann. N. Y. Acad Sci* **1010**, 182-185.

278. MacGregor, G. R. and Caskey, C. T. (1989) Construction of plasmids that express E. coli beta-galactosidase in mammalian cells, *Nucleic Acids Res.* **17,** 2365.

279. Hernan, R., Heuermann, K., and Brizzard, B. (2000) Multiple epitope tagging of expressed proteins for enhanced detection, *Biotechniques.* **28,** 789-793.

280. Altschul, S. F., Madden, T. L., Schaffer, A. A., Zhang, J., Zhang, Z., Miller, W., and Lipman, D. J. (1997) Gapped BLAST and PSI-BLAST: a new generation of protein database search programs, *Nucleic Acids Res.* **25,** 3389-3402.

281. Henikoff, S. and Henikoff, J. G. (1994) Protein family classification based on searching a database of blocks, *Genomics.* **19,** 97-107.

282. Kiebler, M., Becker, K., Pfanner, N., and Neupert, W. (1993) Mitochondrial protein import: specific recognition and membrane translocation of preproteins, *J Membr Biol.* **135,** 191-207.

283. Claros, M. G. and Vincens, P. (1996) Computational method to predict mitochondrially imported proteins and their targeting sequences, *Eur J Biochem* **241,** 779-786.

284. Fuchs, M., Lammert, F., Wang, D. Q., Paigen, B., Carey, M. C., and Cohen, D. E. (1998) Sterol carrier protein 2 participates in hypersecretion of biliary cholesterol during gallstone formation in genetically gallstone-susceptible mice, *Biochem J.* **336,** 33-37.

285. van Amerongen, A., Demel, R. A., Westerman, J., and Wirtz, K. W. (1989) Transfer of cholesterol and oxysterol derivatives by the nonspecific lipid transfer protein (sterol carrier protein 2): a study on its mode of action, *Biochim Biophys Acta. 1004,* 36-43.

286. Nichols, J. W. (1987) Binding of fluorescent-labeled phosphatidylcholine to rat liver nonspecific lipid transfer protein, *J Biol Chem.* **262,** 14172-14177.

287. Gadella, T. W., Jr., Bastiaens, P. I., Visser, A. J., and Wirtz, K. W. (1991) Shape and lipid-binding site of the nonspecific lipid-transfer protein (sterol carrier protein 2): a steady-state and time-resolved fluorescence study, *Biochemistry.* **30,** 5555-5564.

288. Frolov, A., Cho, T. H., Billheimer, J. T., and Schroeder, F. (1996) Sterol carrier protein-**2,** a new fatty acyl coenzyme A-binding protein, *J Biol Chem.* **271,** 31878-31884.

289. Gadella, T. W., Jr. and Wirtz, K. W. (1994) Phospholipid binding and transfer by the nonspecific lipid-transfer protein (sterol carrier protein 2). A kinetic model, *Eur J Biochem.* **220,** 1019-1028.

290. Jornvall, H., Persson, B., Krook, M., Atrian, S., Gonzalez-Duarte, R., Jeffery, J., and Ghosh, D. (1995) Short-chain dehydrogenases/reductases (SDR), *Biochemistry.* **34,** 6003-6013.

291. Ward, J. J., McGuffin, L. J., Bryson, K., Buxton, B. F., and Jones, D. T. (2004) The DISOPRED server for the prediction of protein disorder, *Bioinformatics.* **20,** 2138-2139.

292. Folk, J. E. and Finlayson, J. S. (1977) The epsilon-(gamma-glutamyl)lysine crosslink and the catalytic role of transglutaminases, *Adv. Protein Chem. 31:1-133.*, 1-133.

293. Thacher, S. M. and Rice, R. H. (1985) Keratinocyte-specific transglutaminase of cultured human epidermal cells: relation to cross-linked envelope formation and terminal differentiation, *Cell.* **40,** 685-695.

294. Wells, R. D. (1996) Molecular basis of genetic instability of triplet repeats, *J Biol Chem.* **271,** 2875-2878.

295. Smith, G. K., Jie, J., Fox, G. E., and Gao, X. (1995) DNA CTG triplet repeats involved in dynamic mutations of neurologically related gene sequences form stable duplexes, *Nucleic Acids Res.* **23,** 4303-4311.

296. Ardail, D., Lerme, F., and Louisot, P. (1991) Involvement of contact sites in phosphatidylserine import into liver mitochondria, *J Biol Chem* **266,** 7978-7981.

297. Kerner, J. and Hoppel, C. (2000) Fatty acid import into mitochondria, *Biochim Biophys Acta.* **1486,** 1-17.

298. Tuller, G. and Daum, G. (1995) Import of sterols into mitochondria of the yeast Saccharomyces cerevisiae, *FEBS Lett.* **372,** 29-32.

299. Blom, N., Gammeltoft, S., and Brunak, S. (1999) Sequence and structure-based prediction of eukaryotic protein phosphorylation sites, *J. Mol. Biol.* **294,** 1351-1362.

300. Lehman, J. A., Calvo, V., and Gomez-Cambronero, J. (2003) Mechanism of ribosomal p70S6 kinase activation by granulocyte macrophage colony-stimulating factor in neutrophils: cooperation of a MEK-related, THR421/SER424 kinase and a rapamycin-sensitive, m-TOR-related THR389 kinase, *J. Biol. Chem.* **278,** 28130-28138.

301. Arnoult, D., Parone, P., Martinou, J. C., Antonsson, B., Estaquier, J., and Ameisen, J. C. (2002) Mitochondrial release of apoptosis-inducing factor occurs downstream of cytochrome c release in response to several proapoptotic stimuli, *J. Cell Biol.* **159,** 923-929.

302. Arnoult, D., Gaume, B., Karbowski, M., Sharpe, J. C., Cecconi, F., and Youle, R. J. (2003) Mitochondrial release of AIF and EndoG requires caspase activation downstream of Bax/Bak-mediated permeabilization, *EMBO J.* **22,** 4385-4399.

303. Chauhan, D., Hideshima, T., Rosen, S., Reed, J. C., Kharbanda, S., and Anderson, K. C. (2001) Apaf-1/cytochrome c-independent and Smac-dependent induction of apoptosis in multiple myeloma (MM) cells, *J. Biol. Chem.* **276,** 24453-24456.

304. Ferri, K. F., Jacotot, E., Blanco, J., Este, J. A., Zamzami, N., Susin, S. A., Xie, Z., Brothers, G., Reed, J. C., Penninger, J. M., and Kroemer, G. (2000) Apoptosis control in syncytia induced by the HIV type 1-envelope glycoprotein complex: role of mitochondria and caspases, *J. Exp. Med.* **192,** 1081-1092.

305. Soriano, M. E., Nicolosi, L., and Bernardi, P. (2004) Desensitization of the permeability transition pore by cyclosporin a prevents activation of the mitochondrial apoptotic pathway and liver damage by tumor necrosis factor-alpha, *J. Biol. Chem.* **279,** 36803-36808.

306. Epand, R. F., Martinou, J. C., Fornallaz-Mulhauser, M., Hughes, D. W., and Epand, R. M. (2002) The apoptotic protein tBid promotes leakage by altering membrane curvature, *J Biol Chem* **277,** 32632-32639.

307. Brazin, K. N., Mallis, R. J., Fulton, D. B., and Andreotti, A. H. (2002) Regulation of the tyrosine kinase Itk by the peptidyl-prolyl isomerase cyclophilin A, *Proc. Natl. Acad. Sci. U. S. A. %19;***99,** 1899-1904.

308. Bruns, K., Fossen, T., Wray, V., Henklein, P., Tessmer, U., and Schubert, U. (2003) Structural characterization of the HIV-1 Vpr N terminus: evidence of cis/trans-proline isomerism, *J. Biol. Chem.* **278,** 43188-43201.

309. Ghezzi, P., Casagrande, S., Massignan, T., Basso, M., Bellacchio, E., Mollica, L., Biasini, E., Tonelli, R., Eberini, I., Gianazza, E., Dai, W. W., Fratelli, M., Salmona, M., Sherry, B., and Bonetto, V. (2006) Redox regulation of cyclophilin A by glutathionylation, *Proteomics.* **6,** 817-825.

310. Fratelli, M., Demol, H., Puype, M., Casagrande, S., Eberini, I., Salmona, M., Bonetto, V., Mengozzi, M., Duffieux, F., Miclet, E., Bachi, A., Vandekerckhove, J., Gianazza, E., and Ghezzi, P. (2002) Identification by redox proteomics of glutathionylated proteins in oxidatively stressed human T lymphocytes, *Proc. Natl. Acad. Sci. U. S. A.* **99,** 3505-3510.

311. Papageorgiou, C., Florineth, A., and Mikol, V. (1994) Improved binding affinity for cyclophilin A by a cyclosporin derivative singly modified at its effector domain, *J. Med. Chem.* **37,** 3674-3676.

312. Schreier, M. H., Baumann, G., and Zenke, G. (1993) Inhibition of T-cell signaling pathways by immunophilin drug complexes: are side effects inherent to immunosuppressive properties?, *Transplant. Proc.* **25,** 502-507.

313. Mikol, V., Kallen, J., and Walkinshaw, M. D. (1994) The X-ray structure of (MeBm2t)1-cyclosporin complexed with cyclophilin A provides an explanation for its anomalously high immunosuppressive activity, *Protein Eng.* **7,** 597-603.

314. Thomson, M. (2003) Does cholesterol use the mitochondrial contact site as a conduit to the steroidogenic pathway?, *Bioessays* **25,** 252-258.

315. Rodolfo, C., Mormone, E., Matarrese, P., Ciccosanti, F., Farrace, M. G., Garofano, E., Piredda, L., Fimia, G. M., Malorni, W., and Piacentini, M. (2004) Tissue transglutaminase is a multifunctional BH3-only protein, *J. Biol. Chem.* **279,** 54783-54792.

316. Melino, G. and Piacentini, M. (1998) 'Tissue' transglutaminase in cell death: a downstream or a multifunctional upstream effector?, *FEBS Lett.* **430,** 59-63.

317. Haupt, S., Berger, M., Goldberg, Z., and Haupt, Y. (2003) Apoptosis - the p53 network, *J Cell Sci* **116,** 4077-4085.

318. Perkins, D. N., Pappin, D. J., Creasy, D. M., and Cottrell, J. S. (1999) Probability-based protein identification by searching sequence databases using mass spectrometry data, *Electrophoresis.* **20,** 3551-3567.